2002

Investigating spatio-temporal variability of hydrological components in the Canadian Rockies (Alberta)

Christopher Dennis Hopkinson
Wilfrid Laurier University

Investigating spatio-temporal variability of hydrological components in the Canadian Rockies

by

Christopher Hopkinson

B.Sc., Manchester University, 1995
M.E.S., Wilfrid Laurier University, 1997

Thesis

Submitted to the Department of Geography
in partial fulfillment of the requirements for
the Doctor of Philosophy degree
Wilfrid Laurier University
2002

Abstract

This thesis addresses two questions related to the broad topic of mountain hydrology:

1) How do interannual hydrological balance and pathway components vary in complex temperate high mountain environments at various spatio-temporal scales?
2) a) Is it possible, using dedicated hydrological models, for significant errors in simulated runoff components despite good hydrograph recreations (i.e. right results for wrong reasons)? b) If so, what kinds of errors are encountered?

The first question was addressed by undertaking a hydrological tracer and hydrometric study at three basin scales (Banff ~2200 km^2, Lake Louise ~400 km^2 and the headwaters ~30 km^2) within the Bow Valley of the Canadian Rockies from 1996 to 1999. To address question two, hydrometeorological basin properties learned from question one were used to perform two runs of the University of British Columbia watershed model for the Bow River at Banff during hydrological years 1996 – 1999. Simulations were evaluated using a conceptual $\delta^{18}O$ model of the hydrological balance.

Seasonal geochemical patterns in runoff were similar for all basins, indicating that interannual hydrometeorological conditions play the dominant role in controlling hydrological contributions to runoff. In both seasonal baseflow and event runoff from all basins, snow was the dominant component with rainfall contributing little, even during large rainfall events. Higher rainfall contributions were evident in the runoff from glacierised basins, suggesting that impervious surfaces lead to rapid runoff but in non-glacierised basins a large volume of rainwater is probably lost to evapotranspiration. In addition, it was considered that rainfall may have *appeared* to be absent from the hydrograph during the large rainfall event studied as it may have shunted out older snowmelt from karst storage in the headwaters, thus masking the actual rainfall signature.

For all model runs it was found that the snowmelt component of the hydrological balance was underestimated. This was generally compensated for by an overestimation of rain inputs. From the findings that rainfall was generally a minor component of annual runoff despite hydrometric observations (and phenomenological intuition) that might indicate otherwise, it was concluded that there may be a conceptual misunderstanding of the importance of rainfall contributions to runoff in glacierised high mountain basins.

Rainfall occurs during summer months and is the most susceptible flow component to evaporative loss. However, rain, snow and ice are not discriminated in many model evaporation routines, and this could lead to overestimations of rainfall in the balance. In addition, orographic enhancement of precipitation varies seasonally but this is often not accounted for in models. Using a single value to represent annual conditions likely leads to overestimations of rainfall at high elevations. Automated optimisation of a model containing such process-based conceptual flaws will ultimately force the model to overestimate certain parameters (rainfall in this case) and compensate with an underestimation of hydrologically more important components (namely snow).

Acknowledgements

In the Universal scheme of everything and all those wonderful picnics we call life, the writings presented here on in are no more than a speck of academic dust submitted in a self-indulgent pursuit of "greener grass". Time will tell regarding the greenness of grass but I do hope that the scribblings here add another pebble or two to our collective pyramid of knowledge. However, whilst on this brief academic sojourn, my path has become entwined with many others and I must make note of the helping hands, kindness and support offered to me.

The following organisations have contributed funding, data and/or logistical support to this project: Alberta Environmental Protection, Meteorological Service of Canada (CRYSYS), Water Survey of Canada, Parks Canada, National Water Research Institute, Geological Survey of Canada (National Glaciology Program), University of Waterloo Environmental Isotope Laboratory.

I am also compelled to acknowledge the friendship, guidance and assistance provided by the following people: Mom and dad (Eileen and Gordon) for setting me off on this path and allowing me to find my own direction; Mike English; Gordon Young; Scott Munro; Chris Smart; Jim Buttle; Jim Hamilton; Sherry Schiff; Martin Sharp; Mike Demuth; Peter and Barbara Duck; Alexi Zawadzki and Andrew Lowe for greatly assisting with UBC model calibration and runs; Alex Maclean; "teeth to the wind" Mike Sitar; Nadia Lausellet; Stella Heenan; Johnny "Barfly" Barlow; Barry Goodison; Ross Brown; Hugh Howe; Dick Allison; Tony Chatham; Charlie Pacas; the staff at Mineral Springs Hospital for repairing my legs – without a credit card this time!; mon amigo Bryan Mark; Hamish the Kiwi; Brad Thomas; Jules Blais; Melissa Lafreniere; Mary Ellen Patton; Bob Drimmie and Lois; Tim Davis; Dave Cable; Stephen Grasby; Masaki Hayashi; Corinne Schuster and Alistair "Krusty" Wallace; Ailsa for your everlasting devotion and "wags"; Ron, Pam and Ryan for making the path easier for me over recent months. And finally, my beloved Laura for joining me on our shared journey.

Dedicated to the memory of my grandfather, Dennis.
More than he knew was he responsible for
the direction I choose on this journey.

Table of Contents

List of Tables

List of Figures

Chapter 1 Introduction

1.1 Problem Statement

Mountain environments are undergoing gradual change resulting from a warming climate (Intergovernmental Panel on Climate Change, 2001). Evidence for a changing climate in temperate regions includes the relatively rapid glacial retreat and a coinciding but slow change of vegetation cover since leaving the Little Ice Age. Landcover changes alter the hydrological balance and flow routing pathways within a basin and it has been calculated that the recent warming observed in local records from the mountains of British Columbia has led to earlier spring melt and lower autumnal runoff (Leith and Whitfield, 1998). Of particular interest is that the loss of glacial mass during warm and dry years leads to higher river basin yields than would otherwise be expected (Meier, 1969; Fountain and Tangborn, 1985). Continued glacial recession and potential reductions in flow augmentation is of concern to water resource managers, and the need to predict future water availability in a scenario of changed climate and groundcover is clear.

There is also a need to understand the interactions between hydrological balance and pathway components within these environments and, further, to be able to model them adequately at an appropriate time step. It is known that hydrological models can be calibrated to recreate past hydrographs with high statistical efficiency. Even in large hydrometeorologically complex mountainous basins, Nash-Sutcliffe efficiencies (*e!* - indicating volumetric and temporal model hydrograph accuracy) greater than 90% can be obtained over several seasons (e.g. Kite and Kouwen, 1992). Despite potentially high overall efficiencies, questions remain regarding the temporal and volumetric accuracy of

the hydrological balance and routing predicted. When models are used for long-term forecasting or evaluating the implications of changed landcover, it is essential that their initial calibrations recreate the true hydrological balance and NOT just the overall hydrograph.

The thesis will address two specific questions that arise from the preceding statement:

1) How do annual hydrological balance and pathway components vary in complex temperate high mountain environments at various spatio-temporal scales?
2) a) Is it possible, using dedicated hydrological models, for significant errors in the predicted hydrological balance for a high mountain basin despite obtaining good recreations of past hydrographs? b) If so, what kinds of errors are encountered and how are they compensated?

1.2 Aims and Objectives

The overall aim of this thesis is to address the questions outlined above. However, it is apparent that these questions (particularly the first) are broad in scope and could not be adequately answered in a single thesis. Therefore, the approach taken in this study follows more of an inductive *observation, description, explanation* procedure rather than a more deductive *hypothetical* method. However, in the course of observation and description it frequently occurs that explanation cannot be immediately provided. In such instances hypotheses will be formulated and assessment will be attempted (if possible) using available data and information. Appropriate field and laboratory methods will be chosen to focus on the dual (but not exclusive) objectives of:

1) Gaining further insight into the spatio-temporal interaction of hydrological processes in mountainous basins;

2) Developing a method to evaluate the calibration of a hydrological model by evaluating its breakdown of the hydrological balance rather than simply the coefficient of determination (or Nash-Sutcliffe efficiency: *e.f*) between observed and simulated hydrographs.

An integrated "multi-tool" approach will be taken in this thesis, and the mountain hydrological system will be investigated from the input and the output sides simultaneously. On the input side, hydrometeorological, landcover and hypsometric data will be used in simple mass balance calculations, and for the calibration and running of a hydrological model. On the output side of the system, discharge and geochemical data will be collected in an attempt to "trace" contributing sources of water. Together, these tools will assist in fulfilling both objectives.

A problem faced in a project of this kind, and indeed in any efforts to model hydrological systems, is that input, storage and transfer processes change with time, differ from place to place and the dominance of certain processes changes with the scale of interest. Attempts have been made, therefore, to investigate the effect of basin size and elevation by conducting the study at three different spatial scales: 1) headwater or micro-scale (< 50 km^2); 2) intermediate or small meso-scale (< 500 km^2); 3) basin or large meso-scale (> 2000 km^2). At the headwater and intermediate scales, paired catchments of generally similar basins, apart from differing glacial cover, will be compared.

1.3 Study Area

1.3.1 Basin Overview

The Bow River Basin upstream of Banff, Alberta (2207 km^2, 2280 m a.s.l. average basin elevation) (Figures 1.1 and 1.2) was chosen for this study. It is largely undeveloped, is

the source of an important managed river basin supplying farmers across Southern Alberta and is relatively rich in hydrometeorological data. In addition, aspects of the hydrological regime of this basin have been investigated in two recent studies: Hopkinson and Young (1998) discerned the proportional contributions of inter-annual glacier wastage to river flow; and Zawadzki (1997) used the UBC Watershed Model to forecast changes to the river's flow regime in a situation of possible future climatic change. A further study by Grasby (1997), investigated controls on the geochemistry of the Bow River from Lake Louise (Figure 1.1) to the confluence with the Oldman River approximately 550 km downstream. Many earlier papers have also researched the effect of glacier cover to water resources in this region; notably Meek (1948), Collier (1958), Henoch (1971) and Young (1982 and 1991).

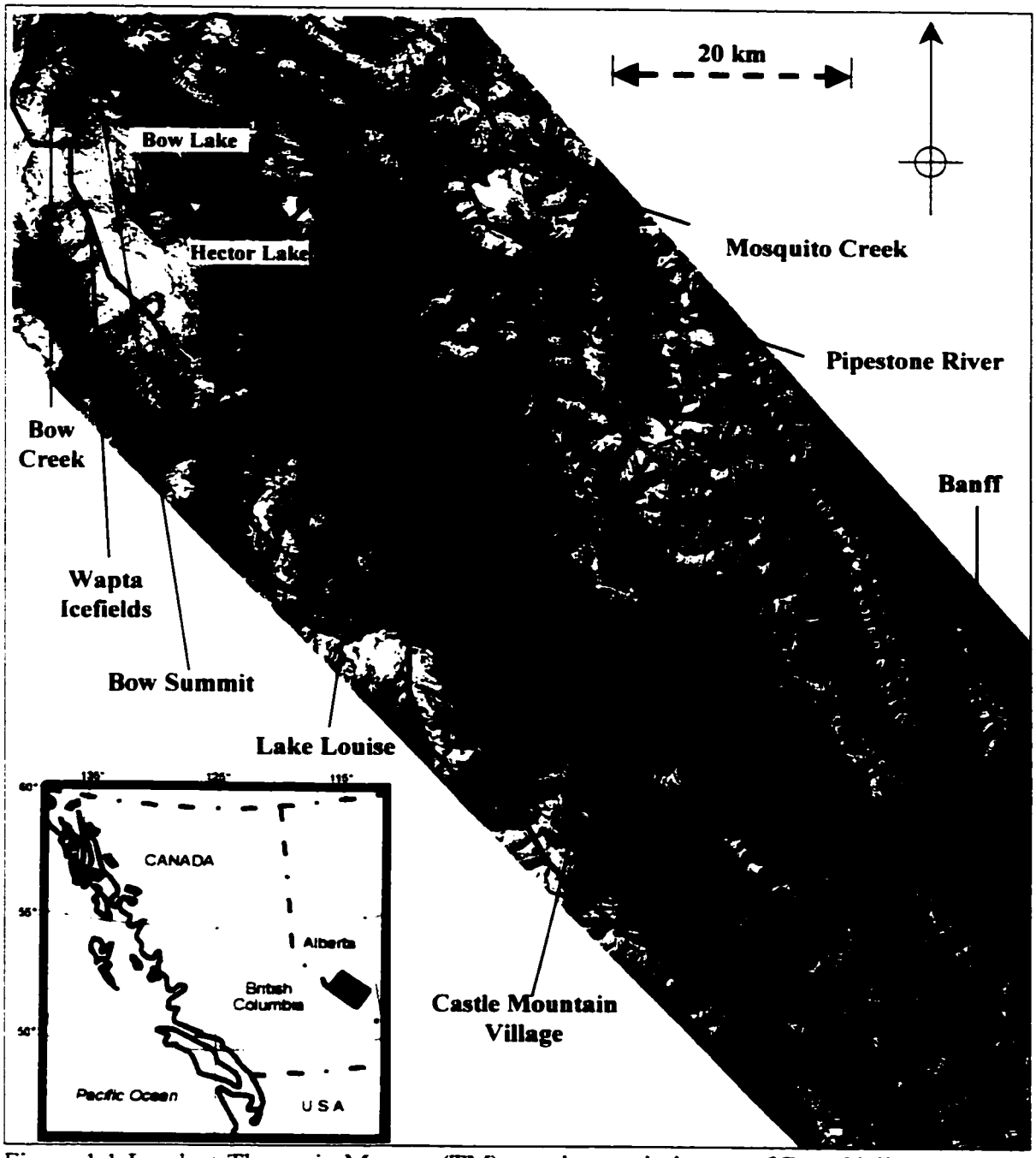

Figure 1.1 Landsat Thematic Mapper (TM) panchromatic image of Bow Valley upstream of Banff. September 1998. Important valley locations and sub-basins are indicated.

The Bow Valley above Banff ranges in elevation from 1350 – 3500 m a.s.l and drains the eastern side of the Canadian Rocky Mountains between latitudes 51 and 52° (N). It is largely underlain by carbonate rocks and deep valley tills, has about 38% natural forest coverage, is 2.3% (~51 km^2) glacierised and has a combined trellis and dendritic river

network containing many small lakes (See Table 1.1 and Figure 1.3 for a breakdown of basin hypsometry). A characteristic of the Bow Valley is the marked difference in glacier cover between the two sides of the basin. The west side has areas of ice sheets, particularly in the Waputik Mountains to the north, whereas in the east there is generally very little glacier cover. Upstream of Banff, there are several major tributaries, the most significant of these being the Pipestone River (309 km^2, 2425 m a.s.l. average basin elevation), which drains the northeastern slopes and joins the Bow at Lake Louise (426 km^2, 2365 m a.s.l. average basin elevation).

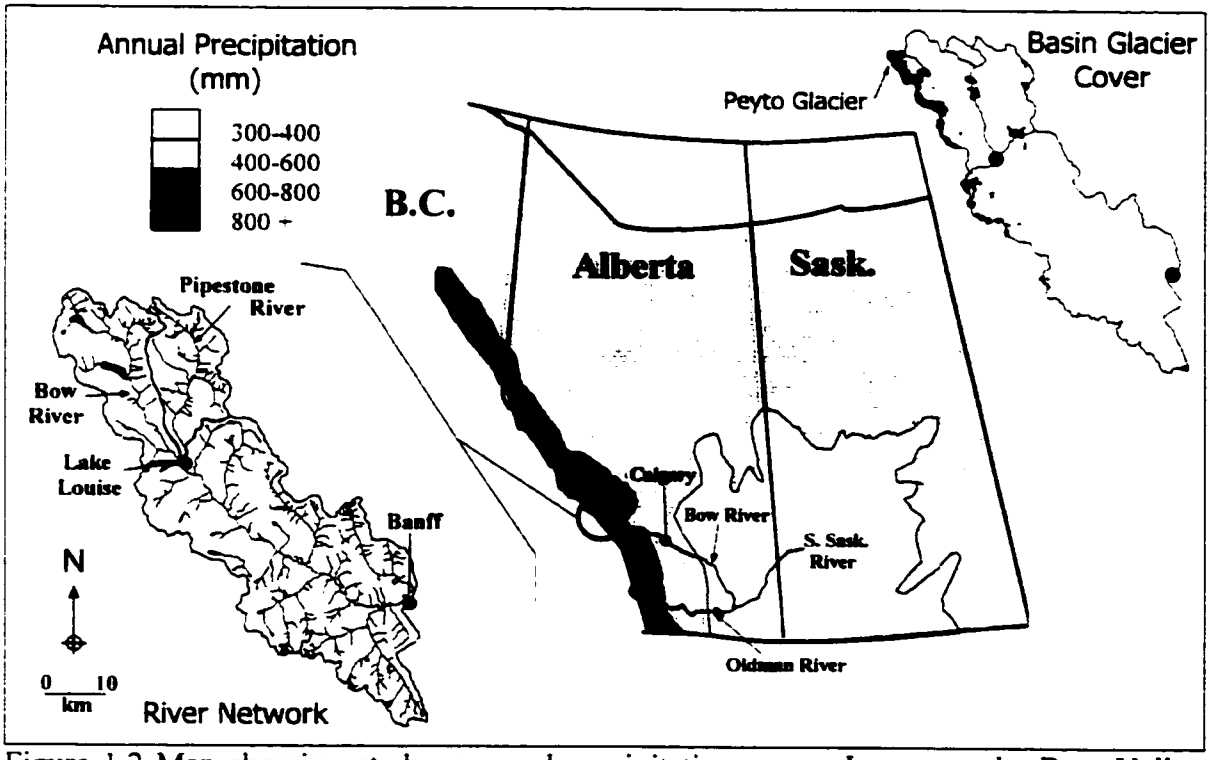

Figure 1.2 Map showing study area and precipitation zones. Insets are the Bow Valley above Banff showing river network, glacier coverage and location of Peyto Glacier.

The average annual temperature at Banff is approximately +3°C (meteorological data supplied by Environment Canada), which puts the average annual 0°C isotherm somewhere between 1800 and 2000 m a.s.l. (assuming an environmental lapse rate of around -0.6 °C per 100 m rise in elevation). In addition, temperatures in this part of the

Rockies can dip down to as low as -35°C in winter and rise up to +35°C in summer (Gadd. 1995).

Elevation Band	Landcover (m^2)						
(midpoint m.a.s.l.)	Water	Snow	Glacier Ice & Firn	Forest	Grass & Shrubs	Bare Ground	Sum (km^2)
1350	2319300			8748900	12534300	2320200	25.92
1450	1542600			46623600	18872100	3276000	70.31
1550	1262700			81928800	16936200	2181600	102.31
1650	887400			95775300	14975100	1970100	113.61
1750	7229700			123788700	33279300	3558600	167.86
1850	874800			110013300	29296800	5007600	145.19
1950	4710600			116344800	43708500	10542600	175.31
2050	603000			109381500	51102000	21010500	182.10
2150	873900	4500	55800	89272800	76835700	40419900	207.46
2250	1898100	13500	666900	39996900	110166300	78732000	231.47
2350	1278000	126900	1378800	4974300	90948600	125806500	224.51
2450	277200	154800	2723400	228600	26682300	149985000	180.05
2550	79200	910800	7191000	32400	3441600	135126900	146.78
2650	85500	2434500	9015300	7200	457200	91730700	103.73
2750	12600	3511800	5931000	3600	14400	56767500	66.24
2850	3600	3370500	3310200	2700		25954200	32.64
2950		3683700	2169900	900		12376800	18.23
3050	1800	1662300	770400			4911300	7.35
3150		760500	555300			1857600	3.17
3250		343800	269100			997200	1.61
3350		104400	157500			540000	0.80
3450		84600				115200	0.20
Sum (km^2)	23.9	17.2	34.2	827.1	529.3	775.2	2206.9
% Landcover	1.1%	0.8%	1.6%	37.5%	24.0%	35.1%	100%

Table 1.1 Landcover hypsometry for Bow Basin above Banff (see appendix 2 for satellite image analysis and GIS operations used to calculate hypsometric proportions).

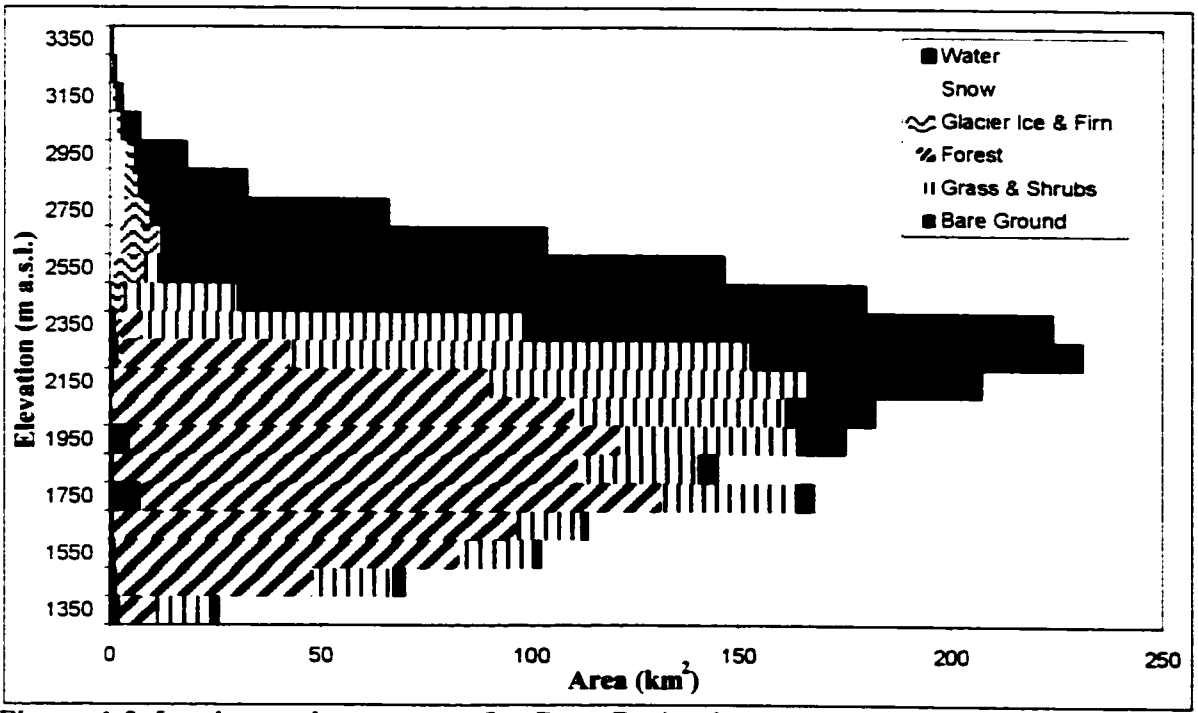

Figure 1.3 Landcover hypsometry for Bow Basin above Banff. (Landcovers classified from Landsat Thematic Mapper image, September 1998.)

Precipitation yields can be over 500 mm higher in the mountainous headwaters than in the heavily farmed and irrigated prairie lands downstream (Figure 1.2). Combining this with the knowledge that potential evaporation is below 300 mm per year in the headwater areas but over 450 mm per year downstream of Calgary (Environment Canada, 1978), the importance of the mountain hydrological system to water resource managers and planners is apparent. In fact, the average flow volume for the Bow at Banff is approximately 44% of the average flow of the River at the Oldman confluence (Environment Canada, 1990). This is despite an order of magnitude difference in basin size at these two locations.

The hydrological process that tends to dominate timing and volume of annual runoff at Banff is spring snowmelt. The average basin yield for June, taken from the 82-year discharge record at Banff, is 26 % (± 6.5 %) of the average annual yield. July and August show declining contributions of 23 % (± 5.6 %) and 14 % (± 2.7 %), respectively. However, it is known that during the later summer months, the small glacier cover within the basin can be a significant contributor to flow, particularly during warm and dry years when management decisions can be critical. For example, Hopkinson and Young (1998) estimated that for the record low flow year of 1970 glacial wastage contributed over 50% of basin yield during the month of August. It is important to note here that "wastage" only refers to a theoretical proportion of the glacier that is lost from long-term storage. It is likely that for the month in question the total contribution from glacial melt was much higher than suggested above. However, these figures refer only to the flow components of the hydrological balance and say nothing of flow routing. Based upon chemical activity ratios of samples collected monthly from 1978 to 1991, Grasby *et al.* (1999) suggested that almost all river water at Lake Louise and Banff was groundwater derived.

1.3.2 The Headwaters

About 50 km upstream of Banff (mid way between Banff and the northern headwaters) at an elevation of 1600 m a.s.l., is the village of Lake Louise. Here, two major tributaries meet: the Pipestone and the headwaters of the Bow. The Bow River at this point has a basin size of 426 km^2, is around 35% forested, 10% glacierised, 2% lake covered with the remaining ground cover being largely bare rock exposures in high alpine areas. The Pipestone watershed is 309 km^2 with similar proportions of forest and bare ground, around 3% glacier cover and minimal lake coverage. Both rivers are gauged by the Water Survey of Canada and were considered ideal basins to assist in linking the study of hydrological processes from the high headwaters down to Banff.

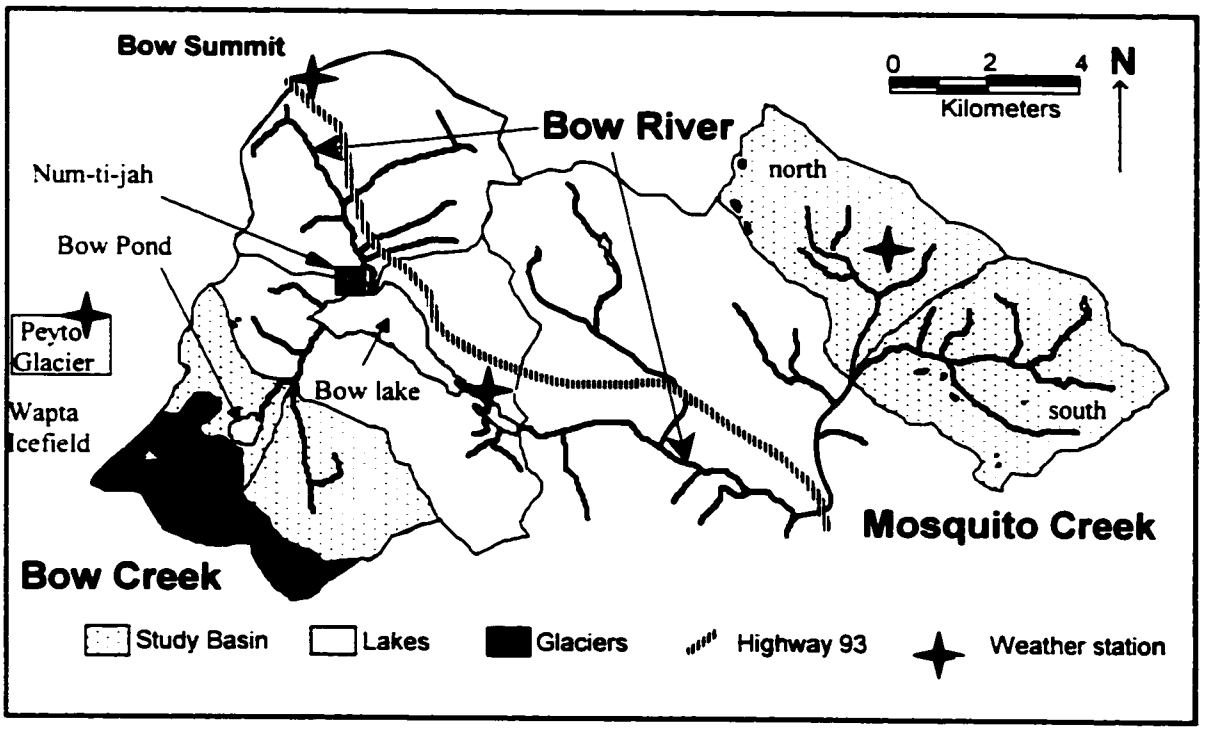

Figure 1.4 Bow Valley headwaters and important locations noted in the text.

The two basins chosen for the headwater study shall be referred to as Bow Creek and Mosquito Creek (see Figure 1.4). They both lie at the northern end of the Bow Valley at

latitude 51°40' N, range in elevation from 1900 m a.s.l. to over 3000 m a.s.l. and are largely alpine in character with some forest cover in the valley bottom below around 2100 m a.s.l. They were chosen as they are near to one another, access is relatively easy, there is minimal human disturbance and they were considered representative of two major "end-member" basin types within the Bow Valley; glacierised and non-glacierised.

1.3.2.1 Mosquito Creek

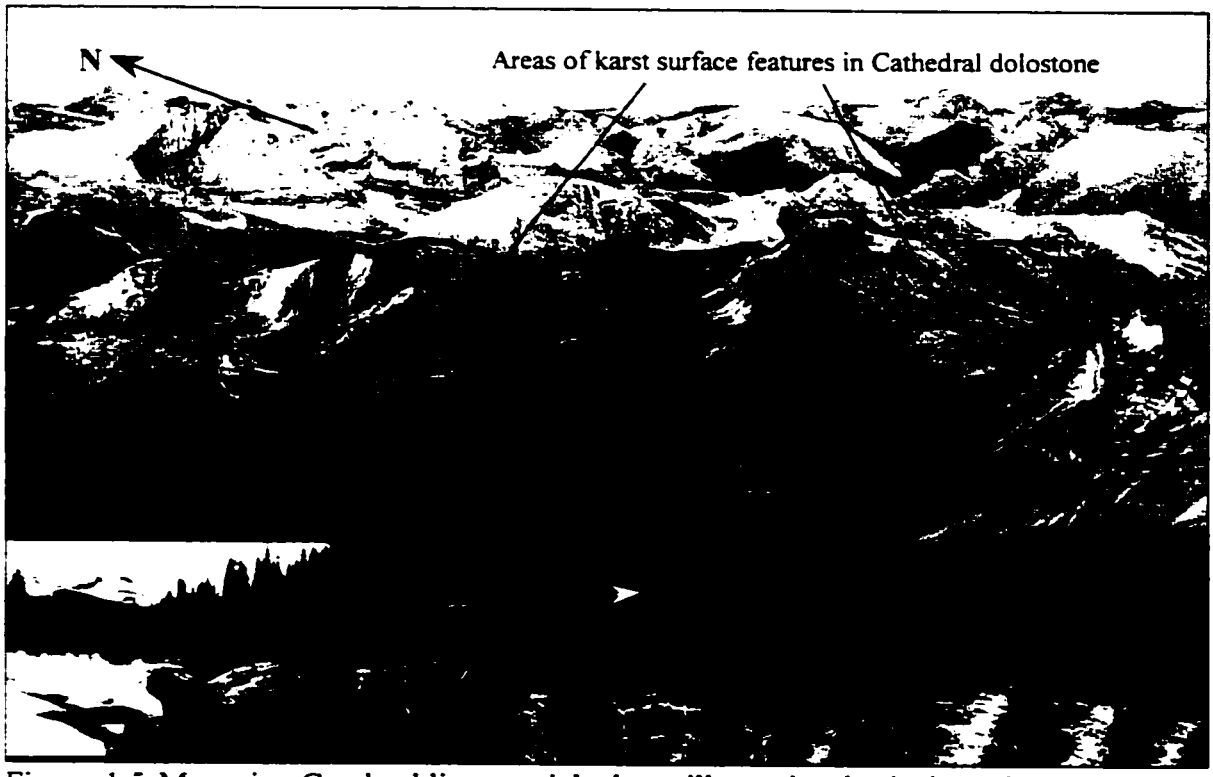

Figure 1.5 Mosquito Creek oblique aerial photo illustrating basin boundary. Inset is a photo taken at the confluence of the north and south basin creeks.

Mosquito Creek (Figure 1.4 and 1.5) lies at an average elevation of 2500 m a.s.l. and has a small number of high elevation hanging glaciers on northeast facing slopes. In total, this coverage is 1 - 2% of the 35 km^2 basin area and ice only becomes exposed in late summer during warm dry years. In this respect it is typical of eastern and southern basins within the Bow Valley. The forested lower elevations of the basin have a thin veneer of

organic soils ($\leq$ 0.25 m) with total forest coverage around 20%. The upper eastern slopes of Mosquito Creek are largely bare rock exposures of the *Cathedral* dolostone formation (see Gadd, 1995 for an overview of Rockies geology) with some areas of alpine meadow. There is no surface water retention and little surface drainage associated with this area of karst bedrock, and deeply incised drainage gulleys cut into the massive dolostone beds. One of the gulleys was observed to be largely nourished by spring water issuing from the bedrock through tills and detritus from the upper slopes. The dolostone bedrock dips down into Mosquito Creek in a southwesterly direction and most subsurface drainage from this formation would be expected to remain within the basin.

On the lower western side of the basin (southwest of the main north and south sub-basin tributaries) quartzitic rocks of the *Gog* Group underlie forest and glacial tills. The dolomite beds of the Cathedral formation are of more recent origin than those of the Gog and are geologically separated by shales of the Mount Whyte formation. However, the two geological areas of the basin just described lie adjacent to one another along a line running NW to SE through the basin due to a major thrust fault. This thrust fault and the upper karst region appear to exert a strong influence on the surface drainage topology within the basin. No known studies have investigated the lithology, glacial covers or the hydrological regime within the basin but the hydrological function of a nearby alpine karst aquifer within the Cathedral formation has been studied (Smart and Ford, 1986).

1.3.2.2 Bow Creek

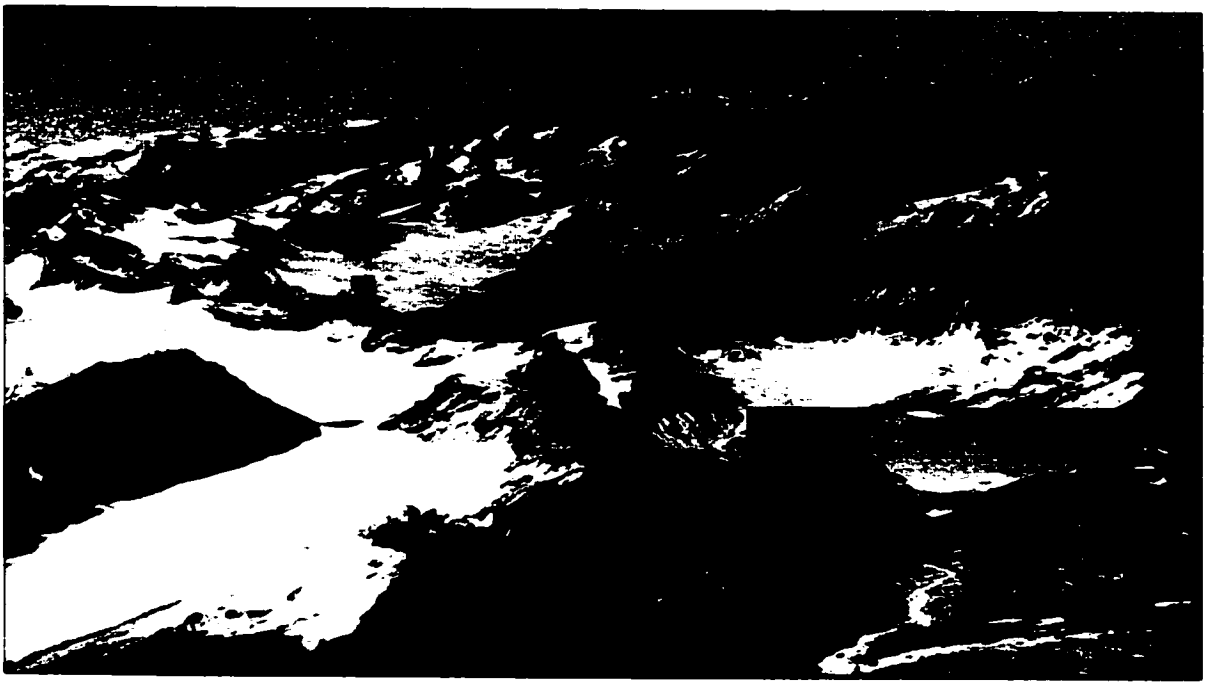

Figure 1.6 Oblique aerial photo of the Wapta Icefields in the northwestern corner of the Bow Valley. Inset is Bow Creek Basin at the confluence of "Bow Hut" (left) and "Bow Waterfall" Creeks.

Bow Creek Basin (Figure 1.4 and 1.6) is approximately 25 km^2, has an average elevation of 2600 m a.s.l., is approximately 32% glacierised and drainage from the Wapta Icefield dominates the annual and diurnal hydrographs. Below the Icefield, the basin surface cover is largely exposures of interbedded dolomites and shales, tills and a small forest (around 5% basin coverage) in a sheltered gorge on the south side. A small lake (about 700 m in diameter), known as "Bow Pond", lies below the Icefield on the main north tributary (Bow Waterfall Creek ~ 50 % glacierised). The lake acts to dampen the diurnal hydrograph and reduce sediment levels downstream (Smith, 1981). Drainage on the south side (Bow Hut Creek – 20% glacierised) flows through the gorge and is very heavily sediment laden in summer.

1.4 Basin Hydroclimatology

1.4.1 The Study Period

Field data collection for this study was carried out from 1996 to 1999. During the first two years from 1996 to 1997 the study was concentrated at the Bow River above Banff with occasional basin-wide sampling of major tributary inputs to the Bow River. However, during 1998 and the earlier part of 1999, the study focused more on the headwaters of the Bow Valley. In this section an overview of the meteorological conditions during the study period will be provided.

This sequence of years proved to be an interesting time period for such a hydrological study, as 1998 and 1999 experienced *El Niño* and *La Nina* conditions, respectively. The years 1996, 1997 and 1999 generally displayed similar conditions with slightly deeper than average winter snowpacks (Alberta Environmental Protection, 2000) (see appendix 1 for recent Bow Basin snow survey reports). In fact, 1996 was of interest in glaciological terms, as it was the first year in twenty that the local Peyto glacier displayed a net positive mass balance (Mike Demuth, pers. comm.). However, 1998 was an unusual year due to: a) the extremely shallow winter snowpack (50 – 70 % of the other three years – see appendix 1 and Table 1.2); b) relatively low annual precipitation (less than 40 % that of any of the other three years at the Bow Summit weather station – Figure 1.7); and c) higher than average annual temperatures (over 1.5 °C warmer than the other years studied - see Figure 1.7). Conditions in 1998 were similar to those of 1970 when high elevation snowpack almost completely disappeared and glacier wastage contributed over 10% of the annual basin runoff above Banff (Hopkinson and Young, 1998). The annual Bow River Basin hydrological yields for 1996, 1997, 1998 and 1999 reflected the

changes in meteorological conditions and were, respectively, 1312, 1292, 1094 and 1343 x 10^6 m^3. The long-term average yield from 1951 to 1999 (data courtesy of Water Survey of Canada) was 1249 x 10^6 m^3.

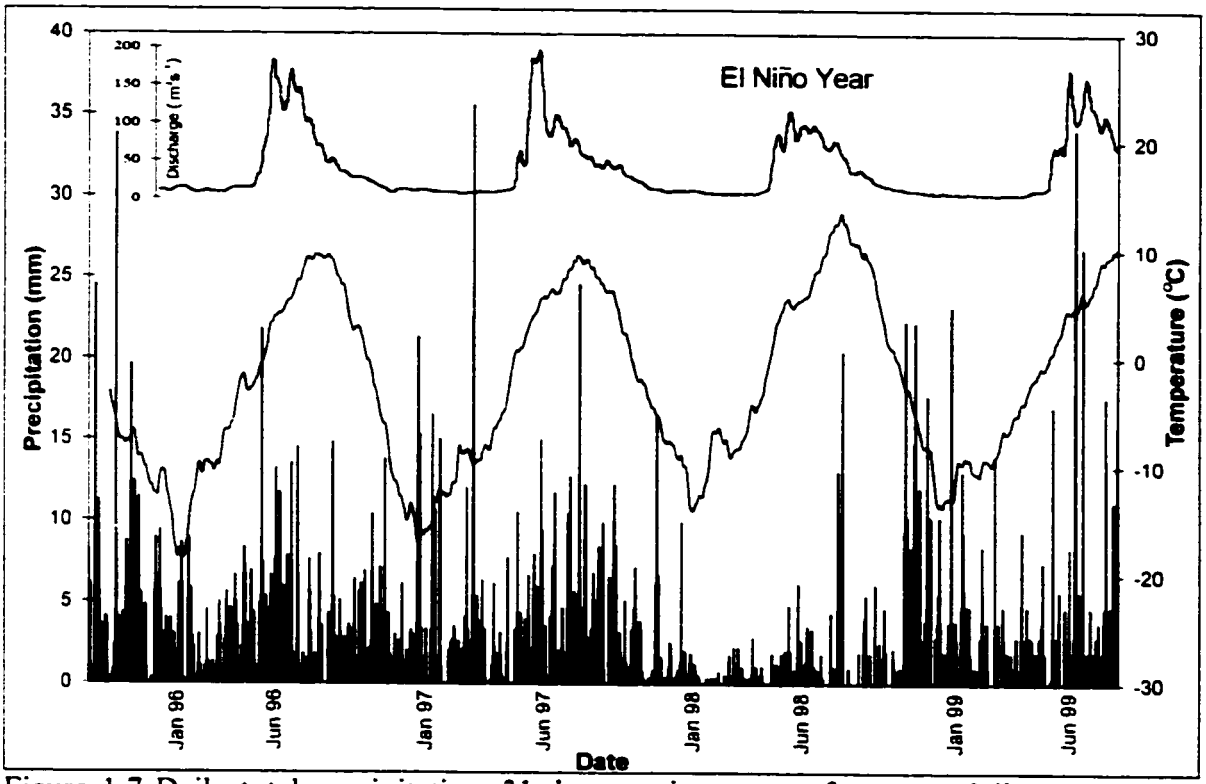

Figure 1.7 Daily total precipitation, 31 day running mean of average daily temperature for Bow Summit (2030 m a.s.l.) and average weekly discharge of Bow River at Banff from October 1995 to September, 1999.

Such contrasting years of deep to shallow snowpack or dry to wet conditions should be susceptible to different landcover and lithological controls which would manifest themselves in the basin hydrograph (volume, shape and timing) and runoff geochemistry. As an illustration of this point, the timing of the onset of basin-wide melt (observed in the runoff at Banff – Figure 1.7) reflected the interannual differences in meteorological forcings: 1996 = 14th May; 1997 = 9th May; 1998 = 24th April; 1999 = 18th May. In addition, years of high yield will ultimately lead to the activation of basin storages that

may otherwise remain dormant during years of low yield. Therefore, comparing basin hydrographs and runoff geochemistry over years of extremely different hydroclimatic conditions should provide a greater insight into the controlling mechanisms.

1.4.2 Basin Precipitation

In the Bow Basin, only two meteorological stations collect precipitation data year-round: one at Castle Mountain Village (1500 m a.s.l.) and another at Bow Summit (2030 m a.s.l.). Both of these stations are located within the main Bow Valley at opposite ends of the basin and are approximately 63 km apart (see Figure 1.1). From the records for 1996 to 1999 (hydrological years), it was found that totals of 2173 mm and 2681 mm were recorded at Castle Mountain and Bow Summit stations, respectively (see Table 1.2). This represents an average increase of 4.5 % per 100 m over the 530 m range studied. During the El Niño conditions of 1998, however, the recorded annual precipitation totals at Castle Mountain and Bow Summit gauges were 450 and 299 mm, respectively (Table 1.2). This constitutes a dramatic reduction in precipitation with height between these two sites. In general, however, the precipitation levels for 1998 were significantly lower than any other year in the study period, with the relative proportion being somewhere between 38 % and 77 % of the mean for the remaining three years (see Table 1.2).

Station / Year	Castle Village (1500 m a.s.l.)	Bow Summit (2030 m a.s.l.)	Basin SWE
1996	596	839	465
1997	569	785	437
1998 (*El Niño*)	450	299	276
1999 (*La Nina*)	559	762	450
Average	**544**	**672**	**407**

Table 1.2 Annual precipitation (mm) at Bow Summit and Castle Mountain Village weather stations and average late winter (April 1st) snowpack water equivalent (SWE) from Alberta Environmental Protection (AEP) snow course data for 1996 to 1999.

Precipitation data in the Bow Valley are currently collected automatically and do not discriminate between rainfall and snowfall. However, from archived long-term records collected at Banff (1350 m a.s.l.) and Lake Louise (1600 m a.s.l.) from 1961 to 1991 (obtained from the Meteorological Service of Canada), average annual snowfall proportions of 46% and 55% were respectively observed. Linear extrapolation of this elevational increase with height suggests about 74% snowfall at the average basin height of 2280 m a.s.l.

Due to a lack of discrimination between snow and rain in precipitation records, it is difficult to ascertain the seasonal and interannual variation in rainfall over the basin. In order to estimate the relative importance of rainfall from year to year and month to month within the Bow Basin, summertime precipitation totals were calculated for both Bow Summit and Castle Mountain weather stations (Table 1.3). The warmest months were chosen (June, July, August and September), as these were the least likely to contain any snowfall in the totals.

Station	Bow Summit (2030 m)					Castle Mountain Village (1500 m)				
Year	Jun	Jul	Aug	Sep	Total	Jun	Jul	Aug	Sep	Total
1996	77	64	42	55	238	46	47	30	60	183
1997	71	70	99	64	304	54	42	45	79	220
1998	29	15	47	18	109	107	39	34	21	201
1999	52	119	106	60	337	44	119	86	62	309
Average	**57**	**67**	**74**	**49**	**247**	**63**	**62**	**49**	**56**	**228**

Table 1.3 Monthly precipitation totals (mm) for Bow Summit and Castle Mountain Village weather stations from 1996 to 1999

Table 1.3 shows substantial variability in the monthly rainfall totals for summers 1996 to 1999 but it does not appear that any month was more or less susceptible to rainfall. Comparing the average total summer precipitation values for Bow Summit and

Castle Mountain Village from Table 1.3 the average increase in rainfall with height was approximately 1.6 % per 100 m. This is significantly smaller than the 4.5% per 100 m calculated for the entire time period and suggests that orographic enhancement of precipitation in this area is greatest during winter months. However, these precipitation gradients apply to a relatively limited range of basin elevations and most of the basin is above the elevation of Bow Summit.

Above 2030 m a.s.l. the only precipitation related records available in the Bow Basin were 10 winter snow courses collected by Alberta Environmental Protection (appendix 1), which ranged from 1580 m a.s.l. to 2380 m a.s.l., and Peyto Glacier specific mass balance data (courtesy of Mike Demuth, National Glaciology Program, Geological Survey of Canada), which ranged from 2150 m a.s.l. to 3150 m a.s.l. Figure 1.8 plots the average end of winter snow pack water equivalent for 1996 to 1999 of both the AEP snow courses (Table 1.2) and long-term average specific mass balance data. The average basin-wide increase in snow course water equivalence with elevation was approximately 8 % and 20 % per 100 m for the eastern and western sides of the basin, respectively with a basin-wide average of 15 % (calculated upwards from lowest S.W.E. measurement in the basin). This is illustrated in the high elevation snow course data, where western slope measurements exceed those of the eastern slopes due to rain shadow effects (Figure 1.8). It should be cautioned, however, that end of winter snow course data cannot be directly related to the complete winter precipitation record, as there are likely to be sublimation induced losses of snowpack, which may vary with space and elevation.

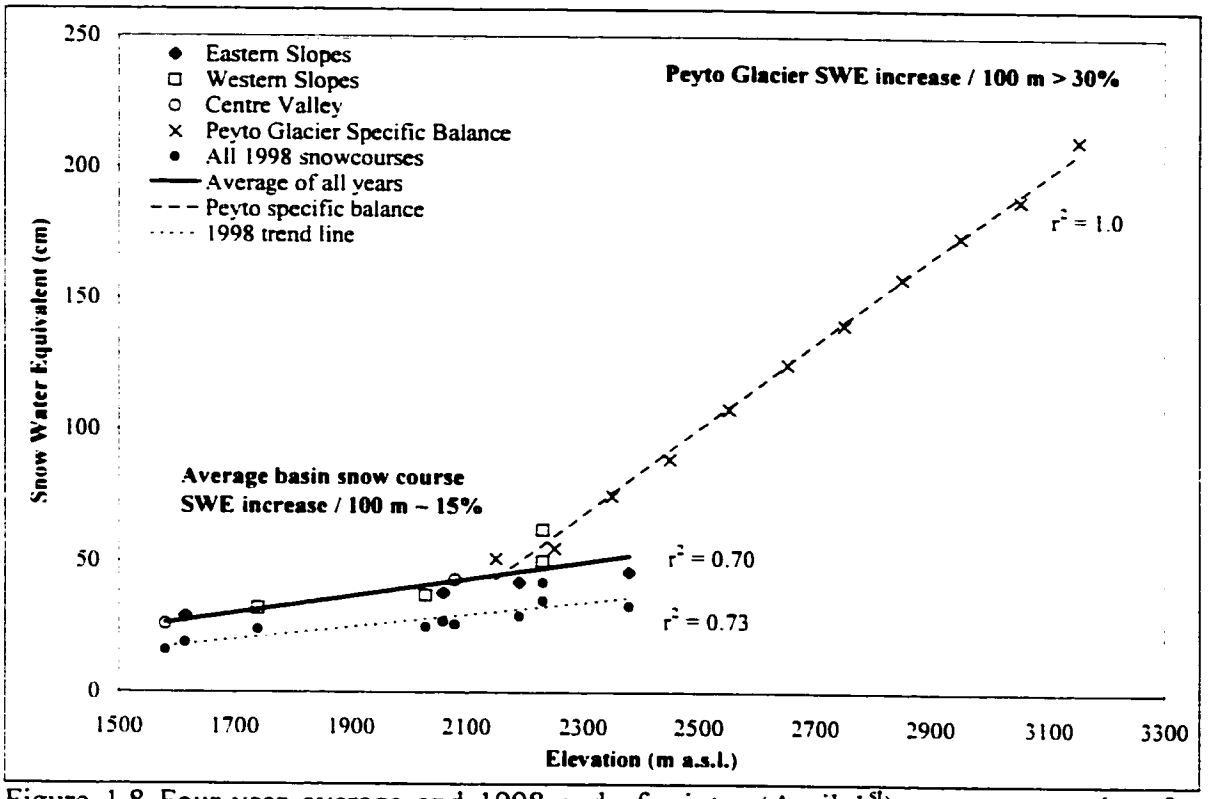

Figure 1.8 Four-year average and 1998 end of winter (April 1st) snow course data for Bow Valley, and average specific winter mass balance from Peyto Glacier (1966 – 1999).

The basin-wide snow course measurements for 1998 did not display reduced depths with height. This suggests that the reduced levels of annual precipitation observed in the Bow Summit record (Table 1.2) were mostly due to a localised reduction in summertime rainfall over the northern parts of the basin. Further evidence of localised shifts in precipitation patterns during this anomalous year was found in the east to west pattern of snowpack distribution across the basin. Snowpack water equivalent (S.W.E.) in the main Bow Valley during 1998 appeared to be smaller than at similar elevations on the eastern slopes (appendix 1). This is contrary to the other three years, where evidence for a reduction in S.W.E. east of the western slopes was observed in Figure 1.8.

The specific winter balance data for Peyto Glacier indicated an enhanced increase of S.W.E. with height above 2200 m a.s.l. of over 30 % per 100 m. These observations

suggest that with increasing elevation, the rate of precipitation enhancement increases. However, it would be inappropriate to assume that such high levels of precipitation enhancement occur across the entire basin. The specific winter mass balance record will naturally be greater than the average basin-wide S.W.E. for any particular elevation due to the preferential accumulation of snow in the depressions of glacial basins. The Peyto balance data, therefore, cannot provide a representative indication of increases in precipitation with height at upper basin elevations, but they do illustrate that a great depth of snow does fall over the western slopes of the basin in winter.

1.4.3 Environmental Temperature Lapse Rates

Daily average temperature records during 1996 to 1999 were collected at three locations within or near to the Bow Basin (see Figures 1.1 and 1.4): the two weather stations noted before (Castle Mountain and Bow Summit) and a third near the terminus of Peyto Glacier at approximately 2400 m a.s.l. (courtesy of Dr. Scott Munro, University of Toronto). The stations at Peyto and Bow Summit are 7 km apart with Peyto in the headwaters of the western slopes and Bow Summit down in the main valley. The average environmental temperature lapse rate between the two lower locations was approximately -0.46 °C per 100 m rise in elevation. However, the upper two stations displayed a temperature lapse rate of +0.42 °C per 100 m, indicating that inversion conditions may be common in this headwater area. Average summertime temperatures for Peyto and the main valley do not appear to be significantly different (Figure 1.9). However, during winter, inversions appear common with icefield air temperatures elevated above those of the valley. Such conditions are likely the result of katabatic airflow off the icefields.

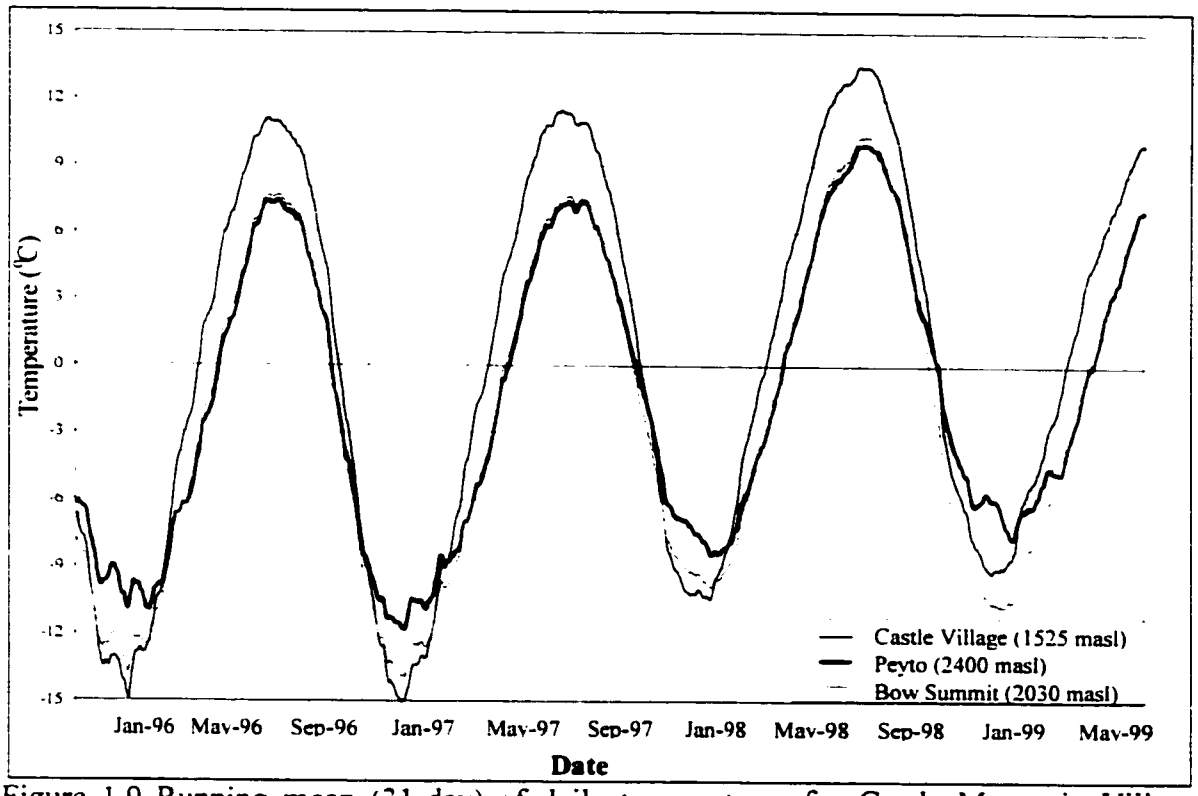

Figure 1.9 Running mean (31-day) of daily temperatures for Castle Mountain Village Bow Summit and Peyto Glacier from October 1995 to September, 1999.

It is inappropriate to assume Peyto data would be representative of all upper elevations within the basin (particularly on the eastern slopes) due to its proximity to the icefields (Figure 1.2), which constitute less than 2% of basin-wide coverage. In addition, although it may be true that inversion conditions occur in the basin headwaters, from Figure 1.9 it is apparent that these conditions occur mainly in the winter when temperatures are well below freezing and of little hydrological consequence. Further temperature data were collected within the Bow Valley headwaters during summer of 1998 and were used to assess conditions away from the icefields. One weather station was set up near Bow Lake at approximately 1900 m a.s.l. (data courtesy of Melissa Lafreniere, University of Alberta) and another near the eastern slope divide in Mosquito Creek (Figure 1.4) at the same elevation as the Peyto station (2400 m a.s.l). April to

September average temperatures were calculated and compared with those of the other three basin stations (Figure 1.10).

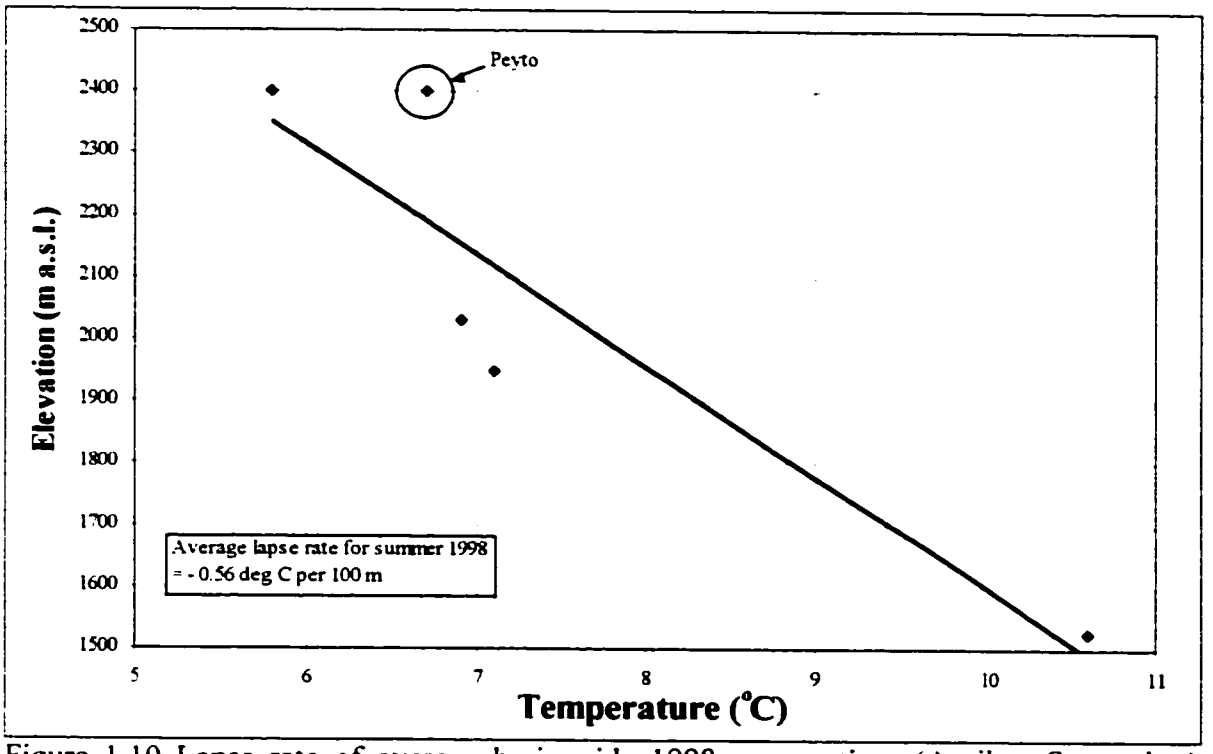

Figure 1.10 Lapse rate of average basin-wide 1998 summertime (April to September) temperatures in Bow Valley

From Figure 1.10, it is apparent that during the summer of 1998 there was an average lapse rate of approximately -0.56 °C per 100 m rise in elevation within the Bow Valley. The data point for Peyto Glacier weather station deviated from the rest of the basin trend by displaying temperatures that appeared to be slightly too high, particularly as it lies immediately down wind of a large ice mass (relatively warm temperatures might be the result of localised air mass subsidence off the icefield leading to subsequent adiabatic warming). The average temperature for Mosquito Creek at the same elevation but on the other side of the main valley was approximately 1 °C cooler. Without the Peyto data point, the lapse rate changed only very slightly to -0.62 °C per 100 m rise in elevation.

Therefore a lapse rate of 0.6 °C is thought to approximate the average conditions within the Bow Basin and is typical of global environmental lapse rates (Barry. 1992).

1.5 Thesis Layout

This thesis is divided into eight chapters plus references and appendices. In the following chapter, a review of hydrological processes in mountainous and hilly regions is provided. In addition, some of the tools used in mountain hydrological research, models appropriate to this environment and relevant issues regarding geochemistry and tracers are investigated. The purpose of the review chapter is to put the current research in context. Following the literature review, there are no chapters dedicated to methods, results and discussion but rather the thesis is divided into topics, where one chapter builds on the last. In all sections of the thesis there is a tendency to start with a broad overview of the process or system under investigation and then proceed towards more detailed analysis and discussion. The hierarchical approach taken is summarised in Figure 1.11.

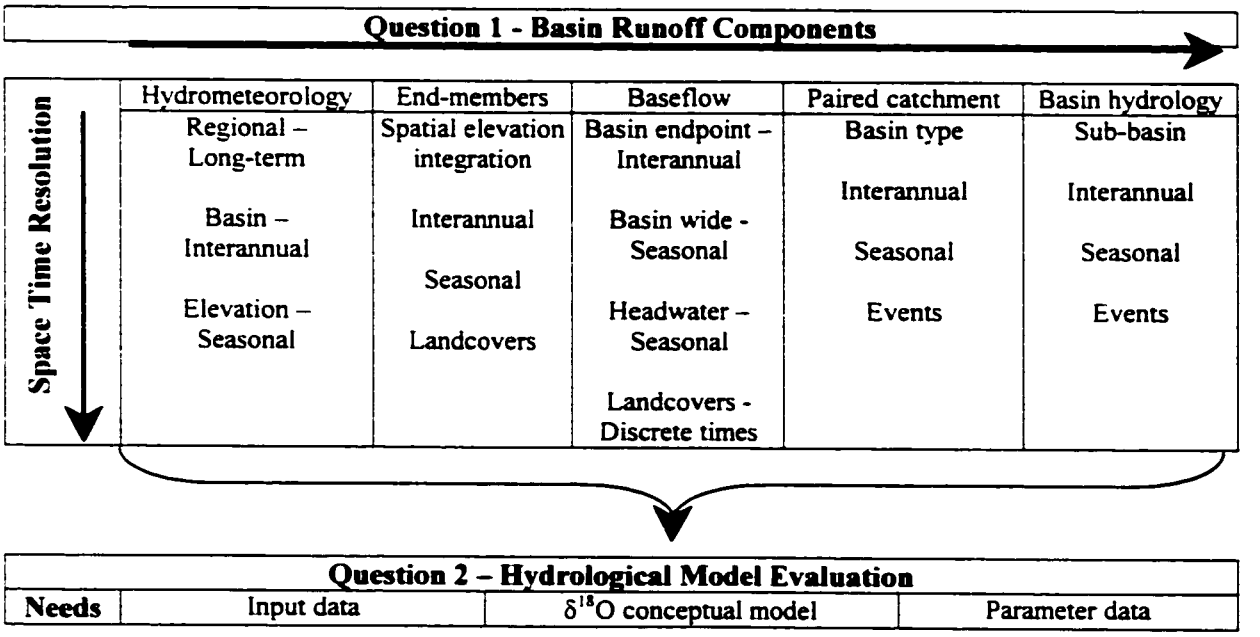

Figure 1.11 Methodological hierarchy adopted in this thesis.

Chapters Three and Four focus on hydrological balance end-members (snow, glacier ice and rain) and basin-wide baseflow characteristics, respectively. In Chapters Five and Six, the hydrological balance and flow pathways associated with events and the seasons within the Bow Valley are explored for the headwaters and the entire basin above Banff, respectively. In all of these topic-oriented chapters, influences of landcover, basin size and elevation are investigated. Analysis of relative areal yields, geochemical tracers and temporal discharge data filtering are used for much of the interpretation in these sections of the thesis. The seventh chapter details an attempt to evaluate and optimise the calibration of a hydrological model using geochemical tracers. Potential flaws with the model calibrations are highlighted. The concluding chapter brings together the main points raised in the study and discusses issues of scale, land cover, temporal variability and potential difficulties associated with modelling the mountain hydrological system.

Chapter 2 Literature Review

2.1 Introduction

This review chapter overviews recent progress made in hydrological interactions research carried out within northern mid-latitude mountainous regions containing alpine and glacial components. Many hydrological processes acting in these environments have similar characteristics to equivalent processes in more lowland hilly regions. As such, abundant literature exists concerning such processes and investigation techniques but not necessarily directly related to high-relief mountains. Where possible, relevant studies in mountainous areas will be cited. The purpose of this review is to illustrate the diverse body of literature from which the current research in the Bow Valley of the Canadian Rockies draws.

The chapter will begin with an overview of the environment in question with reference to climatic and landscape complexity. Following these introductory comments, hydrological processes in temperate mountainous environments and various measurement and tracer techniques will be highlighted using the hydrological cycle as a logical discussion framework. Finally, efforts to recreate these processes in a hydrological model developed and operationally used in these environments will be investigated.

2.2 The Mountain Environment

Climate and geology are the major determinants of weathering mechanisms, ground cover and vegetation types in any region of the world. In mountain regions, both geology and climate can vary over short distances and, in the case of local meteorological conditions, short time spans.

Orogenic uplift generally occurs along plate margins, and rock type and structure in mountain regions varies both spatially and altitudinally. For example, the Canadian Rockies comprise predominantly sedimentary rocks from an ancient continental shelf. Typical of these sedimentary deposits are layers of carbonate limestones, gritstone and shale beds of differing geochemical properties sometimes in complex fold and thrust structures with varying degrees of fracturation. In temperate regions, the surficial geology and geomorphology of all high mountain ranges has been reworked by prior glaciations to leave behind the steep "U" shaped valleys, deep tills and moraines typical of glaciated landscapes. Valley bottom tills in the Rockies can exceed 100 m in depth (Gadd, 1995).

The Earth's orbital tilt and rotation control seasonal and diurnal variations of solar radiation input. However, due to higher elevations and reduced overlying atmosphere, mountains receive more solar energy than at sea level. From data collected in the European Alps (Barry, 1979) this increase with height is approximately 5 – 10 % per 1000 m. However, ambient air temperatures decrease with increasing height at around 6 ^{o}C per 1000 m; the environmental lapse rate. This is because the atmosphere is predominantly heated from terrestrial infrared radiation (Barry, 1992). Further elevational cooling results from airflow across mountains, which is forced upward and expands due to lower pressures (Barry, 1992). This leads to temperature reduction at the dry adiabatic lapse rate of approximately 9.8 ^{o}C per 1000 m until the condensation level is reached and the air mass becomes saturated. Clouds then begin to form and the rate of cooling drops.

The resultant orographic cloudiness of mountain regions leads to higher precipitation than over adjacent lowlands. Rain and snowfall volumes tend to increase at higher altitudes (Barry, 1992). The Combination of temperature lapse rates and increased

precipitation with height results in greater potential for snow accumulation higher in the basin. The snowline altitude in a basin varies with season and continentality. In winter, temperate mountains tend to have continuous snowpack coverage even in valley bottoms, whereas during summer the regional snowline may be above mountaintops. The tendency for increased precipitation in maritime regions leads to lower snowlines. Conversely, the relatively arid climate experienced further inland leads to higher snowlines. The average end of ablation season snowline for a number of years within a region is known as the "climatic snowline" and a continued interannual accumulation of snow above this elevation leads to glaciation (Østrem, 1966). According to Østrem (1966), the glaciation limit (approximately the lowest height of mountains that can sustain glacier cover) can be 1000 m higher in the continental ranges of the Canadian Rockies than nearer the coast.

Steep terrain, rock exposures of varying geological structure and a wide range of climatic conditions lead to high rates of weathering and erosion (e.g. Hewitt, 1989). Weathered rock material accumulates at the base of slopes, often in the form of talus. In high altitude alpine zones (above treeline) soils are sparse and vegetation cover is minimal. At lower elevations where the climate is less harsh, chemical and biological activity breaks the regolith down to form shallow soil. Despite relatively shallow soils, extensive forest cover can be sustained in lower montane valleys. On high slopes within the sub-alpine zone, various trees and shrubs may be evident. In the alpine zone, relatively sheltered easy angled slopes may hold "alpine meadows" of grasses and hardy plants. The ecological zones of "montane", "sub-alpine" and "alpine" cannot be defined in terms of elevation as they vary regionally and with local climatic conditions.

2.3 Hydrological Cycling in Temperate Mountains

This section is divided into "input", "storage" and "output" components of the hydrological cycle in a mountainous watershed. The components discussed can be considered elements of a hydrological balance:

$$Q = P - E - \Delta S \qquad (2.1)$$

Where the river discharge (Q) equals the inputs of precipitation (P) minus losses from evapotranspiration (E) and changes in storage (S) in a unit of time. Discussion will focus on processes involved, aspects of geochemistry relevant to hydrological tracer studies and measurement techniques.

2.3.1 Hydrological Inputs

2.3.1.1 Precipitation

Dynamics and Measurement

The topography of mountainous basins introduces high spatio-temporal heterogeneity into precipitation characteristics. A large frontal system moving across a mountain chain may precipitate across the entire region at roughly the same time. Within this storm, however, the volume and type of precipitation may vary. Also, the system track relative to basin orientation can result in a lag between occurrences of the storm in different parts of the basin. Smaller orographic systems tend to precipitate greater quantities on the windward side of mountains causing a *rain shadow* effect on the lee side. Shower bearing cumulus clouds generated by thermal convection and valley winds (Barry, 1992) may be relatively isolated and only precipitate over small areas and for short time periods. Their

potentially rapid movement in windy mountain environments can lead to short intense cloudbursts of a few seconds duration at one location.

Precipitation is difficult to measure accurately. Many instruments are available to measure precipitation either in the form of rain or snow or both; e.g. the manual Tretyakov Gauge (Yang *et al.*, 1995). Dual instruments are frequently used to determine precipitation inputs in remote regions such as the Rockies but only provide information about conditions at one point. Point measures of precipitation may cause problems when representing large domains, as errors due to shading, splashing in and wind turbulence can be large and variable (Linacre, 1992).

Geochemistry

Hydrogen and oxygen isotope concentrations within atmospheric water vapour vary with temperature and distance from the original moisture source. Stable isotope concentrations within terrestrial water samples are expressed in $\delta^{18}O$ (or $\delta^{2}H$) ratio notation in per mil ($^{o}/_{oo}$) as the difference from standard mean ocean water (SMOW):

$$\delta^{18}O = \frac{(^{18}O/^{16}O)_{sample} - (^{18}O/^{16}O)_{SMOW}}{(^{18}O/^{16}O)_{SMOW}} \times 1000\ ^{o}/_{oo} \qquad (2.2)$$

Moisture near its oceanic source has an isotopic signature close to that of SMOW but as it rises and cools or travels inland, the heavier hydrogen (^{2}H) and oxygen (^{18}O) isotopes and are preferentially condensed over the lighter ^{1}H and ^{16}O isotopes (Dansgaard, 1964). This results in a depletion of heavy isotopes in continental precipitation and at higher elevations. There is also a temperature effect in isotope variations, which in temperate regions leads to a noticeable seasonality in isotope concentrations, with lighter values in winter. During the phase change from liquid to solid, differences between snow and rain

δ values can be experienced during the same event (Shanley *et al.*, 1995). The spatial and temporal variability of these values during a single storm event can be high (Kendall and McDonnell, 1993). The $\delta^{18}O$ / $\delta^{2}H$ relationship is largely controlled by evaporative processes (Dansgaard, 1964).

In addition to stable isotopes, there are other geochemical signatures in precipitation of interest to the hydrologist. During the 1950s and 60s, nuclear bomb testing released high concentrations of the radioactive isotope ^{3}H (tritium) into the atmosphere. Tritium has a half-life of over twelve years and atmospheric tritium unit (TU) levels are now close to background. Variations in TUs are related to latitude, continentality and seasonality. Concentrations are highest in inland precipitation at high northern latitudes and during summer (Gaspar, 1987).

In general, ionic concentrations in precipitation are low compared to surface waters and reflect their maritime origin with usually only Na^{+} (sodium) and Cl^{-} (chloride) displaying relatively high concentrations. However, further inland other ionic concentrations can be elevated from anthropogenic and aeolian inputs to the atmosphere.

2.3.1.2 Other Hydrological Inputs

The precipitation of moisture from fog or clouds can amount to a significant proportion of the hydrological budget. In the European Alps, wire mesh fog traps have been observed to record up to 150% of precipitation gauge totals during winter months (Grunow and Tollner, 1969, cited in Barry, 1992). Ion concentrations are generally found to be higher in fog than rain or snowfall with the highest levels near cloud base (Walmsley *et al.*, 1996). Other hydrological inputs from groundwater occur across the

surface watershed but quantifying the volumes involved is problematic (discussion of groundwater processes will be presented in section 2.3.2.4).

2.3.2 Storage and Transfer Processes

Before most precipitation enters the stream network it is intercepted by rock, soil, ice, snow, grass, shrubs or trees where it goes into temporary storage. Depending on the type of precipitation, location, groundcover and climatic conditions at the time, the duration of this storage may be from seconds to millennia.

2.3.2.1 Interception by Vegetation

Dynamics and measurement

In montane and into sub-alpine regions, the dominant natural ground cover is usually forest. Trees intercept incoming rainfall, snow and fog and store moisture on their surfaces. When sufficiently wetted, *stemflow* and *canopy drip* transfer excess moisture to the ground. *Throughfall* is the rain proportion that passes through the canopy and reaches the ground. Canopy storage is a function of the area and nature of the leaf surfaces and therefore varies between species (e.g. Aston, 1979). The great variety of species makes it difficult to characterise the relative efficiencies of deciduous and coniferous trees but the propensity for conifers not to defoliate combined with their long and often upward pointing needles result in a high annual storage capacity (Yunnian, 1990). As with precipitation, scaling measurements from one tree to the entire stand is problematic due to changing properties within the canopy (Pomeroy and Gray, 1995).

Geochemistry

Trees have a noticeable effect on the geochemistry of precipitation water reaching the ground. In general, the evaporation of intercepted water leads to an increase in ionic (e.g.

Barrie and Hales, 1984; Djorovic *et al.* 1997) and a slight enrichment of isotope (e.g. Holko, 1997) concentrations over open-air rainfall.

2.3.2.2 Snowpack

Accumulation, redistribution and measurement

In meso and macro-scale temperate mountain basins, the dominant annual hydrological event is usually spring snowmelt. Therefore, knowledge of the snow water equivalent (S.W.E.) and spatial distribution of the snowpack is important if the hydrological balance is to be determined or models used to forecast runoff.

At macro-scales, prevailing meteorological patterns and the location of mountain ranges control snowpack accumulation. Orographic controls lead to deeper snowpack with elevation and on the windward side of mountains. At smaller scales wind redistributes snow preferentially into hollows, gullies and the leeward side of slopes. Unstable accumulations on steep slopes can lead to catastrophic downward relocation from avalanching if there is insufficient tree cover density to bind the snowpack (Gubler and Rychetnik, 1991). Snowpack volumes within forests are largely dependent upon tree spacing and species, and are generally lower than in open areas but enhanced at the treeline (Gray and Male, 1981).

To determine S.W.E. over wide areas, snow surveys are usually undertaken. This entails dividing a watershed into zones of characteristic accumulation patterns and assessing snow depth and density within each zone either by digging snow pits or taking bulk samples using long snow tubes. Snow depth soundings are taken along transects between depth and density sample locations. The depth and density information is then averaged to determine the snowpack water content of the entire watershed.

Snowmelt

Snowmelt is controlled by the energy balance:

$$H_m = H_s + H_l + H_c + H_e + H_r + H_g \qquad (2.3)$$

where H_m is total heat energy available for melting; H_s is net short-wave solar radiation; H_l is net long-wave radiation; H_c is sensible heat transfer from the atmosphere; H_e is latent heat transfer from phase changes due to evaporation, sublimation, melting, condensation and freezing within the snowpack; H_r is heat input from rain; and H_g is heat from the ground (Nakawo and Hayakawa, 1998).

Solar radiation is usually the most important energy input to alpine snowpacks during the melt season (Cline, 1995). Slope angle and aspect, weather conditions, surface albedo and obstacle shading determine the amount of solar radiation conveyed to the snowpack. Radiant energy encountering the snow surface can be absorbed, transmitted or reflected and the albedo determines how much energy is available for absorption and transmission. Albedo varies with solar altitude and condition of snow. At low sun angles surface reflectance is enhanced (Oke, 1995). Maximum albedos of around 90% have been reported when the snow is fresh with a seasonal minimum (ignoring the effect of debris) of approximately 60% following snowpack ripening (Cline, 1995). In alpine areas the seasonal minimum albedo may correspond to the timing of highest energy inputs leading to a strong diurnal melt cycle (Cline, 1995).

Heterogeneity of groundcover and topography leads to irregular patterns of snowmelt. In general, melting begins at lower elevations and the snowline rises over the season. This progression may be slow and fairly uniform on a glacier surface but on surrounding slopes snowline can rise at faster more irregular rates (Young, 1982). However, in

montane zones tree cover can lead to an insulation effect reducing the amount of incident solar radiation to the snowpack, retarding melt.

Geochemistry

Studies of snowpack geochemistry during accumulation show that the isotopic concentrations of subsequent layers, although displaying the signature of their respective precipitation events, are relatively similar (Suzuki, 1995) with lightest values around mid winter (Shanley *et al.*, 1995). As with precipitation, there tends to be an isotopic depletion of snowpack with height. In the European Alps, this has been calculated at around -0.5 $^{o}/_{oo}$ 1000 m^{-1} (Moser and Stichler, 1974). The ionic chemistry of a mountain snowpack generally reflects that of the falling precipitation and atmospheric dry deposition (Clow and Mast, 1995).

Following the onset of spring, snow ripens and bulk snowpack tends to become isotopically enriched. There are two processes that lead to this enrichment: the first is the addition of isotopically heavy rainfall (Shanley *et al.*, 1995); and the second is the preferential loss of lighter ^{16}O isotopes from the snowpack due to the slightly different melting temperatures of ^{16}O and ^{18}O (Maule and Stein, 1990). In addition to this isotopic transformation, it is found that shortly after the onset of melt, ions within the snow pack are preferentially eluted (Johannessen and Henriksen, 1978). Davies *et al.* (1982) discovered that some ions were preferentially eluted over others and Brimblecombe *et al.* (1985) suggested the following sequence:

$$SO_4 > NO_3 > NH_4 > K > Ca > Mg > H > Na > Cl \qquad (2.4)$$

It has been found, however, that the snowpack goes through cycles of isotopic (Suzuki, 1995) and ionic (Hudson and Golding, 1998) enrichment and depletion during each rain or melt event. Therefore, snow pack and melt chemistry are not homogeneous, either through space or time once melt has commenced.

2.3.2.3 Glaciers

Glacial dynamics

Glaciation occurs in regions where snowpack persists throughout the melt season and further annual snowfalls accumulate. In temperate mountain regions the process of firnification may take only a few years (Sugden and John, 1993). An ice mass of sufficient weight moves down slope by processes of internal ice deformation (Glen, 1955; and Nye, 1957) and basal sliding (Weertman, 1957). A study carried out on Gornergletscher in Switzerland by Iken (1977) revealed summertime surface velocities between 2 and 5 $mmhr^{-1}$ and it was suggested that velocity variations reflected basal water pressures. This slow downward transfer removes ice from the *accumulation* zone and gradually deposits it into the *ablation* zone where it gradually melts away. Over a year, the net accumulation or ablation at a glacier surface can be quantified by measuring the mass balance of winter snow input (b_w) and summer melt (b_s):

$$b_n = b_w + b_s \qquad (2.5)$$

where b_n is the net annual balance. The elevation at which $b_n = 0$ at the end of the melt season is termed the *equilibrium line altitude* (ELA).

Glacial melt and routing

Glacial melt is controlled by the same energy balance components as snow. However, when glacial ice becomes exposed its lower albedo, typically 20 - 40% (Sugden and John, 1993), leads to greater absorption and transmission of radiation and a commensurate increase in melt. Debris on the ice surface can either enhance melting from a lowering of albedo or, if thick enough, impede it due to insulation (Østrem, 1959). Rainfall events tend to correlate with a reduction in glacial melt, and as the proportion of basin glacier cover increases the inverse relationship between rainfall and melt production increases (Meier, 1973). However, there is evidence to suggest that rainfall induced slush-flows originating from saturated snowpacks can lead to ice surface melting in excess of standard energy balance estimates (Smart *et al.*, 2000). In northern temperate regions maximum input of radiation is in June; however, the greater efficiency for meltwater production with rising snowline on a glacier leads to maximum melt in July or August (Meier, 1973). Glacial meltwater production therefore has an underlying seasonality on top of which is superimposed a diurnal regime of gradually increasing amplitude (Elliston, 1973).

Meltwater at the glacier surface flows along streams on the ice until crevasses or moulins intercept it and the water disappears into englacial passages on its way to the bed. Drainage through and beneath the glacier poses a *black box* problem to the glacial hydrologist; it is possible to observe inputs and outputs but to study the internal system requires remote, invasive or tracer techniques. Multiple tracer tests using rhodamine B and uranine on Findelengletscher in the Swiss Alps during winter and summer illustrated that drainage and discharge patterns at the glacier bed vary over short distances and that

winter flow through velocities (from glacier surface to portal) may be 100 times slower than during the summer (Moeri and Leibundgut, 1986).

Glacial melt geochemistry

Following spring melt, the remaining snow, firn and ice entering the glacial system are relatively free of solutes (Fountain, 1996). The preferential melting and evaporation of lighter isotopes during firnification (e.g. Sommerfield *et al.*, 1991) and mixture with rain should lead to a more enriched ice signature relative to snow. In ice that predates bomb testing there should be negligible tritium levels contrasting markedly to more recent snow and firn. Melt water entering the englacial system is generally ionically dilute and should have isotopic compositions determined partly by age, phase prior to melt (i.e. snow or ice) and elevational distribution.

Upon reaching the glacier bed, melt water usually encounters a sediment rich environment. Processes of dissolution and ion exchange following contact with these sediments elevate ionic concentrations in glacial meltwater (Souchez and Lemmens, 1987). Waters draining from beneath glaciers in temperate mountain regions are often found to be higher in solute loads, particularly calcium, than other surface waters (Souchez and Lemmens, 1987). Tranter *et al.* (1997a) investigated chemical compositions of waters sampled from boreholes on Arolla glacier, Switzerland, and suggested that subglacial water could be divided into three categories: 1) dilute and characteristic of supraglacial melt; 2) similar to but less concentrated than portal discharge, suggestive of main channel flow; 3) highly concentrated water draining slowly through a distributed hydraulic network. Strontium and sulphur isotope ratios, measured in the proglacial stream of the same glacier, show a seasonal variation consistent with an

expansion of the subglacial drainage network into areas of varying underlying bedrock lithology (Tranter *et al.*, 1997b).

2.3.2.4 Groundwater

Infiltration, the water table and ground water flow

During winter, cold temperatures and snow accumulation reduce the availability of surface water for groundwater recharge. At high elevations, permafrost (Furrer and Fitze, 1970) and seasonally frozen soil (Burn, 1991) hinder infiltration and percolation. Water tables generally reach their maximum depth just prior to spring when recharge begins. The depth and fluctuation of water tables in mountainous regions can be highly variable. In the Canadian Rockies, it is reported to be over 300 m below ground surface at some high elevation locations (Ozeray and Barnes, 1978) while at other valley locations it is observed to lie near the ground surface and fluctuate by up to 8 m between March and July (Gabert, 1986). (See appendix 4.2 for examples of seasonal groundwater level fluctuations in the Canadian Rockies.)

Groundwater characteristics measured at individual sites may be of little value at larger scales considering the great variety of ground composition, varying from thick impervious exposures of bedrock at high elevation to highly permeable thin forested soils in valley bottoms. In between these extremes are talus slopes and mass movement deposits, tills, moraines and other glacial debris, active ice surfaces and perennial snow packs, non forested soils of alpine meadows, alluvial deposits and, in areas of carbonate rock, karst terrain. Also, groundwater is routed through the soil zone of hill slopes via three major subsurface flow mechanisms; soil matrix, macropore and pipe flow (Anderson and Burt, 1990). Considering the wide variety of lithological units within

mountain environments and their individual heterogeneities, it is perhaps only possible to characterise the hydrogeology at either the small scale of an instrumented plot or the large scale of the mountain massif and upwards, where generalisations can be made based on topography, geology and climate (Forster and Smith, 1988). Assessing the spatial variability of groundwater hydrology at intermediate scales within mountainous environments is therefore quite a challenge to the river basin hydrologist.

At local scales (up to a few hectares), groundwater basins may vary by greater than 50% from surface watersheds (Hinton *et al.*, 1993). This can also be true in areas with well-developed karst drainage (common in the Rockies), where conduits can develop perpendicular to geological dip and bear no relationship to the surface watershed (Stringfield *et al.*, 1979). It is therefore important to note that in karst areas, large volumes of water can be transmitted over long distances relatively quickly. For example, Smart (1988) used the artificial tracer rhodamine WT to determine groundwater velocities of up to 840 m h^{-1} in the Maligne karst system of the Canadian Rockies. However, it is also important to note that such regions of karst bedrock are not always associated with rapid flow and may, conversely, act like storage reservoirs if main conduits are blocked or insufficiently developed (e.g. Smart and Ford, 1986). It should therefore be apparent that within mountainous basins, both peak runoff events and long-term baseflow discharges could be augmented by drainage from lithological units that are nourished outside of the surface watershed.

Geochemistry

A study of water chemistry in limestone areas of the Canadian Rocky Mountains by Ford (1971) illustrated that solute concentrations in springs draining high altitude alpine

sites were lower than in groundwaters from below treeline. The forest waters were enriched in solutes due to the greater CO_2 availability in forest soils. Infiltration of water with neutral pH into soil will induce leaching of some ions, with further dissolution facilitated by the formation of carbonic acid from equilibration with soil CO_2 (e.g. Tolgyessy, 1993). Hudson and Golding (1997) investigated the soil chemistry for a sub-alpine site in British Columbia and were able to distinguish four geographic site types based on chemical signature and groundwater head. Their four categories were hillslope, streamside (riparian), seepage zones, and forest. They found that within site chemistry varied significantly less than between sites (Hudson and Golding, 1997).

Isotope concentrations within soil water profiles display spatial and vertical patterns reflective of percolation rates and flow paths. For example, Gehrels *et al.* (1998) observed heterogeneous $\delta^{18}O$ profiles in the root zone of soils indicative of preferential flow paths. Also, Tsujimura *et al.* (1998) noted that $\delta^{18}O$ concentrations can differ in the same profile in local areas due to differing percolation vectors between hill slopes and flatter ground. In both of these studies it was found that the $\delta^{18}O$ profile homogenizes at depth, suggesting more diffuse flow with reduced influence from preferential flow paths. In addition, tritium levels in groundwater can be used to calculate residence times. Low tritium levels suggest the water predates H bomb testing but if higher concentrations are apparent then knowledge of the precipitation input values for the preceding years enables estimation of the recharge date (e.g. Clark and Fritz, 1997).

2.3.2.5 Mountain Lakes

Valley deepening and morainic deposits, typical of glaciated mountain areas, lead to a high number of lakes. Although lakes can store large quantities of water, not all of this

storage is effective at maintaining river runoff. Lakes tend to only effect storage within the range of water level above the outflow and, unlike large groundwater and glacial ice reservoirs, lakes only provide relatively short-term storage. However, lakes are an important component of the surface drainage network within mountain hydrological systems as they act to mix runoff from several different sources and introduce temporal lags between inputs and output.

Lake dynamics

Most deep lakes within temperate mountainous regions are dimictic (two mixing cycles per year). During winter, high elevation lakes are frozen over and any hydrological nourishment comes from groundwater. In spring, meltwater draining to lakes leads to melting at the fringes (Bilello, 1967) and solar heating of sediments in the littoral zone causes circulation, accentuating melt. Wind moves the ice around the surface leading to break up. As solar insolation increases, heating of deep lakes first leads to a period of isothermal conditions at 4 °C followed by summertime stratification of warm *epilimnetic* water overlying a cooler *hypolymnion*. During autumn, dropping temperatures and increased windiness act to breakdown the thermal stratification and as lake surfaces lose heat to the atmosphere a reverse gradient occurs with buoyant cold water approaching 0 °C at the surface. During the entire annual cycle, the bottom waters of deep lakes tend to remain at or near 4 °C.

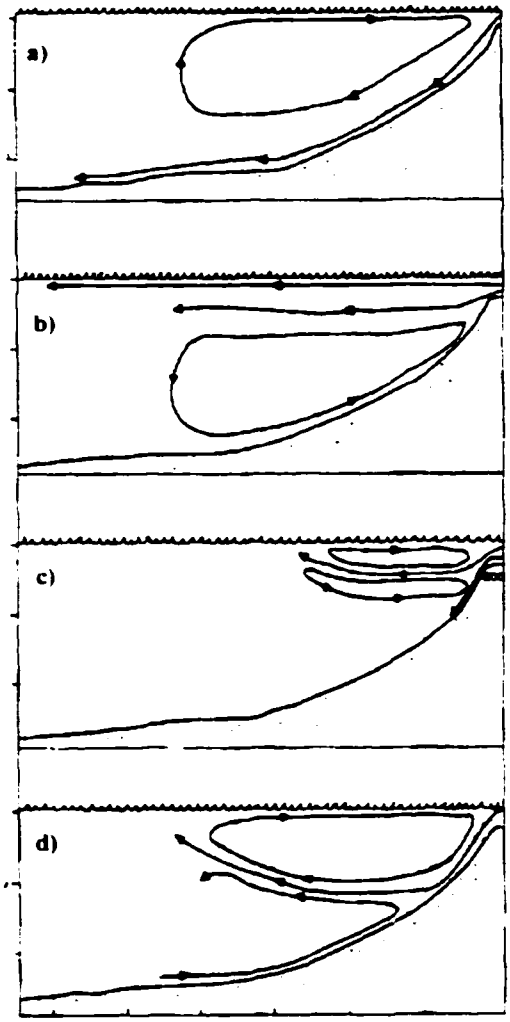

Figure 2.1 An example of variation of inflow patterns in a lake (adapted from Hutchinson, 1957): a) underflow; b) overflow; c) shallow interflow; d) deep interflow.

Smith (1982), using *drogues* to measure summertime currents within four glacier fed lakes in and near to the Upper Bow Valley, concluded that:

1) Relatively sediment free water of low density draining into Bow Lake led to *overflows*, i.e. the inflow skims the surface (see Figure 2.1);

2) Slightly higher sediment concentrations flowing into Hector Lake led to *interflows*, where the inflow drained through the lake near the thermocline;

3) At Peyto lake the inflow was very highly sediment laden and despite its cold temperature was denser than hypolimnetic water and sank, resulting in *underflows;*

4) The last lake studied, Waterfowl, was very shallow with no stratification and thus was considered *homopycnal* (full mixing).

Geochemistry

Lake storage and mixing patterns not only control the flow pathways of density currents through the water body but can also have a marked influence on lake chemistry. For example, the reduction of mixing between surface and deeper layers due to summer and winter stratification limits the exchange of oxygen from the atmosphere to the lake and can ultimately lead to reducing conditions at depth (Harrison *et al.*, 1993). Perhaps more importantly, from a hydrological tracer point of view, is that storage within lakes can lead to changes in both ionic and isotopic concentrations. Increased water temperatures and residence times within lakes can be expected to result in: a) enriched isotopic signatures as lighter ^{16}O and ^{1}H are preferentially evaporated from the lake surface (e.g. Gibson *et al.*, 1998); and b) higher solute levels than are present in upstream surface tributaries, as reactions have more time to reach equilibrium.

The ionic composition of many mountain lakes is similar to local groundwater for much of the year due to lake and groundwater exchanges (Williams *et al.*, 1990), and therefore the local geology and lithology exert a strong influence. In granitic basins, where weathering rates are low, acidic precipitation can have a detrimental impact on lake water quality. In a study of 200 lakes in the Southern Alps, Marchetto *et al.* (1994) found that many were acidic with 47% displaying alkalinities below 50 μ eq l^{-1}. In

carbonate regions like much of the Canadian Rockies, the buffering capacity of weathering materials is sufficient to prevent acidification.

2.3.3 Outputs

2.3.3.1 Sublimation and Evaporation

Losses by evaporation and sublimation of snow in a mountainous watershed are difficult to measure directly and are more commonly modelled from other more easily measured parameters. For example, the Turc equation (Turc, 1961) estimates annual potential evaporation from an empirical relationship based on temperature and precipitation data alone. It has been shown by Bailey *et al.* (1990) and Saunders and Bailey (1990) that windiness and solar input of radiation lead to estimates of potential evaporation that are higher than can be maintained in alpine environments. This is largely because bare rocks dry off relatively quickly following rainfall or snow melt and any surplus energy is converted to sensible heat in raising the rock temperatures rather than latent heat of evaporation. Due to difficulty ascertaining actual evaporation (AE), either by measurement or modelling, it is often inferred by measuring the other input and output components of the water balance and deeming the difference to be due to evaporation. This is problematic in mountains where difficulties in measuring precipitation and changes in storage from groundwater or glacial melt can invalidate the balance.

Tracer based techniques for the estimation of evaporation are being developed to address some of the difficulties associated with measuring or modelling this parameter. The knowledge that light oxygen isotopes are preferentially evaporated in the unsaturated soil zone has led to the development of a model that might be useful to monitor evaporation from soils (Barnes *et al.*, 1989). Solute concentrations have also been used to

estimate soil evaporation (Ullman, 1985) but such estimates are only valid if the water in the profile is fully equilibrated (Barnes *et al.*, 1989). Also, based upon earlier work by Gat (1981), Gibson *et al.* (1998) demonstrated that shallow lake evaporation estimates made using $\delta^{18}O$ data compare favourably with Penman and evaporation pan techniques.

2.3.3.2 River Runoff

The Hydrograph

The part of the hydrological balance often of most interest to the hydrologist is surface runoff yield (Q) and its variation through time for the basin of interest. Basin runoff is generally simple (although not always easy) to measure using area-velocity, volumetric and tracer dilution techniques to develop rating curves, which relate continuous measurements of stream depth (stage) to discharge. The temporal resolution of the hydrograph generated determines the level of detail that we can see in a hydrological *event*. In mountain regions, the slow upward progression of the snowline results in a seasonal prolongation of the snowmelt hydrograph, which at large basin scales can be characterised with daily runoff data. Individual storm or diurnal melt events in headwater basins require a finer temporal hydrograph resolution. There are various techniques available that enable *classification* of discharge hydrographs based upon their temporal and volumetric characteristics.

In a study of glacial melt runoff in the French Pyrénées, Hannah *et al.* (2000) developed an objective classification index system for the diurnal basin hydrograph. The index was derived from principle components and clustering analysis of the discharge time series based upon its properties of *shape* and *magnitude*. The hydrograph index could then be plotted through time to illustrate the seasonal distribution of event types

such as storm runoff, snow or ice melt, and recession flows (Hannah *et al.*, 2000). At a much broader spatio-temporal scale Smith *et al.* (1995) attempted a characterisation method for streamflow records collected from across the U.S.A. over interannual time periods. Their technique utilised a discrete wavelet transform of the individual discharge time series records to generate characteristic *scalogram* plots of periodic and stochastic time elements within the discharge records. Their results indicated that the wavelet scalograms (or wavelet variance plot) for each discharge record were a function of the regional hydroclimatic regime (Smith *et al.*, 1995).

Another potential hydrograph classification system that provides information about basin storage properties, which has not been fully developed, could be based on the hydrograph recession curve (Tallaksen, 1995). The recessional limb of any hydrograph demonstrates a decay rate (or rates) that is a function of the cumulative water transit time through the potentially large number of temporary storage "reservoirs" within a basin. Various mathematical expressions of this recession curve have been proposed, varying from simple linear reservoir functions to relatively complex non-linear or multiple reservoir functions (Hall, 1968; Tallaksen, 1995). The starting point for many hydrograph recession analyses is the simple linear reservoir (Hall, 1968):

$$Q_t = Q_0 \exp^{(-\alpha t)} \qquad (2.6)$$

where Q_0 and Q_t are discharge at the start of the recession curve and at time t after the start of the recession curve, respectively, and α is a coefficient of recession where α^{-1} is the time elapsed between discharge Q and Q/e. Therefore, α^{-1} can be considered an index of the temporal storage characteristics within a basin. Strictly speaking, however, basins

do not behave as simple linear reservoirs and so α^{-1} does not provide an absolute measure of basin recession flow characteristics.

At relatively small headwater scales, dual linear reservoirs have been found quite adequate for characterising recession flows from both forested (Moore, 1997) and glacierised (Collins, 1982) basins. In Moore's study (1997), the dual linear reservoirs were thought to be analogous to either: a) runoff draining footslope and upslope zones within the catchment; or b) drainage through the saturated through flow zone and the vadose zone. Collins (1982) *a priori* assumed that a dual linear reservoir system would represent the drainage characteristics of both the rapid moulin-conduit and slower firn aquifer systems within a glacierised basin in the Swiss Alps. From this simple assumption Collins (1982) was able to estimate the relative volumes of storage within each of these glacial storage reservoirs.

From the above (Moore, 1997; Collins, 1982) and many other studies (e.g. Hall, 1968; Gurnell, 1993; Wittenberg, 1999, etc.) it is clear that recession flows from individual basins cannot be accurately classified using the simple linear reservoir function in equation 2.6. However, for regional analyses where a number of basins are to be compared or where the scale of interest is variable, a realistic recession function that can be equally applied to all basins and scales does not exist. For this reason Tallaksen (1995) concluded that: "*a simple expression is preferable as the recession behaviour will vary considerably between the catchments.*" Therefore, although the recession function illustrated in equation 2.6 is not strictly correct, the α^{-1} index provides a robust means for comparisons through space and time.

Geochemistry

Geochemical properties of surface waters reflect precipitation inputs, weathering transformations and the mixing of components that occurs during the transfer of water from the surface to the stream. Any water that does not fall onto the open channel directly is susceptible to a change in geochemical signature dependent on the time of delay and the environment the water encounters. Therefore, examination of stream water geochemistry can be indicative of the runoff generating mechanisms and hydrologically active parts of a basin during an event and can be used to assess changing sources of water contributing to the river. In the following sections, some theories regarding runoff generation and techniques used to separate hydrograph components will be discussed.

2.4 Runoff Generation and Hydrograph Separations

2.4.1 Runoff Generation

It has been suggested by Pearce *et al.* (1986) that transmission of precipitation to runoff in vegetated humid headwater catchments can be described by three *variable source area concepts:*

1) *Partial area Horton overland flow* - rainfall or snowmelt encounter an area of ground where the hydrological input exceeds the infiltration rate either due to surface saturation or low surface permeability.
2) *Saturation overland flow* - the water table in valley floors rises and meets the ground surface.
3) *Subsurface flow* - infiltrating water moves through the ground by slow soil matrix (Darcian) processes or rapidly through preferential flow paths (macropores or pipes).

Increases in rainfall or snowmelt enlarge the area of runoff contribution on a seasonal and event basis. It should be noted, however, that these concepts relate to soil covered hill

slope environments and therefore may not be applicable to many areas within high mountain basins. Although in a non-glacierised alpine basin in Austria it was found that runoff did vary with the changing area of saturated ground at a variety of scales consistent with the variable source area concept (Kirnbauer and Haas, 1998).

It can generally be said of alpine headwaters that the high surface gradients, large areas of exposed bedrock, shallow soils and potentially extensive karst networks result in rapid runoff responses. A quick response, however, does not necessarily provide much information about the transmission process or the origin of water actually entering the stream. In the case of exposed impermeable slopes, Hortonian overland flow may occur but the propensity for talus to accumulate at the base of such slopes can lead to a rapid percolation of water to depth. Alternatively, slow percolation into thin soils overlying tills or bedrock on steep slopes may be transmitted down slope rapidly by preferential flow at the base of the soil layer leading to return flow at lower elevations. In mountain basins, the mix of runoff generating mechanisms changes with scale and between locations (Peshke *et al.*, 1990) and there is still much debate about specific ground to channel transfer processes (e.g. Becker and McDonnell, 1998). Quantifying the relative contributions to stream runoff is the aim of hydrograph separations.

2.4.2 Hydrograph Separations

Sklash and Farvolden (1979) described three approaches to hydrograph separation termed *time*, *ultimate delivery* and *historical* aspects. The time aspect approach is concerned with separating an event hydrograph into *old* (pre-event) and *new* (event) water. The ultimate delivery mechanism approach is concerned with ascertaining flow paths and transfer processes of water to the channel. The historical approach is less

concerned with flow paths and more with where or in what state the hydrograph water originated prior to reaching the channel, e.g. rainfall, snowmelt or groundwater.

Prior to the use of tracers to identify the components of streamflow, it was common to use graphical techniques (e.g. Gray, 1970) or hydrograph recession curves (e.g. Hall, 1968) to separate the hydrograph into *baseflow*, *interflow* and *surface runoff*. These are simplistic techniques as they generally assume baseflow is maintained by deep groundwater and bank storage, interflow is event water traveling beneath the ground and surface runoff is event water traveling over the ground. Estimates of actual groundwater contribution to streamflow using these non tracer based methods tend to be small with runoff being dominated by rainfall or snowmelt traveling as overland flow or interflow (e.g. Meyboom, 1961). Given that many ionic and isotopic tracer studies have demonstrated that a high proportion of event runoff is derived from "pre-event" water already held in groundwater storage (e.g. Pinder and Jones, 1969; Rodhe, 1981) graphical and recession analysis based hydrograph separations can be unreliable.

A study by McDonnell *et al.* (1991), using deuterium isotope ratios to characterise new and old water in a New Zealand catchment, found that of 11 rainfall events studied only four showed signs of event water in the stream. Such studies use two-component mixing models:

$$Q_n = Q_t - Q_o \tag{2.7}$$

and

$$\frac{Q_o}{Q_t} = \left[\frac{(C_t - C_n)}{(C_o - C_n)}\right] \tag{2.8}$$

where Q_o, Q_n and Q_t are old, new and total discharge, respectively and C_o, C_n and C_t are old, new and total discharge solute or isotope concentration. In addition, the following assumptions must be met for two-component separations (Sklash and Farvolden, 1982):

1) The signature of the event component is significantly different from the pre-event component and the tracer used is conservative (i.e. will mix linearly);
2) The event component maintains a constant signature or its variations are documented;
3) Groundwater and event water are significantly different;
4) Water from the saturated and unsaturated zones have equivalent signatures or the contribution from the unsaturated zone is negligible;
5) Surface storage contributes minimally to the event.

McDonnell *et al.* (1991) also analysed chloride and electrical conductivity (EC) and obtained further samples from suction lysimeters to perform a three-component separation of groundwater, soil water and on-channel precipitation. Using a three-component mixing model (below) they found that between 12 - 16% of the event hydrograph was from soil water, <5% from on channel precipitation and the remaining 80% from groundwater.

$$Q_t = Q_{cp} + Q_s + Q_{gw} \tag{2.9}$$

and

$$\frac{Q_s}{Q_t} = \left[\frac{(C_t - C_{gw})}{(C_s - C_{gw})}\right] - \frac{Q_{cp}}{Q_t}\left[\frac{(C_{cp} - C_{gw})}{(C_s - C_{gw})}\right] \tag{2.10}$$

The subscripts s, t, gw, cp represent soil water, streamflow, groundwater and channel precipitation (McDonnell *et al.*, 1991).

A combined hydrometric and geochemical tracer study carried out by Sklash and Farvolden (1979) enabled the authors to develop an explanation for high proportions of groundwater in event hydrographs. They suggested that close to the stream channel the water table is usually near to the surface and infiltration of event water will cause the tension-saturated zone to become pressurised. A groundwater ridge forms, increasing the gradient from groundwater to the channel, thus enhancing the volume of groundwater discharge. In contrast, however, other geochemical hydrograph separation studies conducted over a variety of landscape lithologies (e.g. moorland headwaters (Chapman *et al.*, 1993), forested hillslopes (Peters and Ratcliffe, 1997) and peat wetlands (Sirin *et al.*, 1998)) have demonstrated that preferential pathways can lead to rapid soil matrix bypass flow and deliver event water rapidly to the stream. Geochemical hydrograph separations have thus provided valuable information regarding runoff generation processes and have demonstrated that processes differ between regions, landscape units and even in the same soil profiles (e.g Weiler *et al.*, 1998).

Another hydrograph separation technique is End Member Mixing Analysis (EMMA), and was introduced by Christopherson *et al.* (1990) after recognising that most hydrograph separation techniques assume groundwater has a homogeneous tracer signature throughout. The method allows the separation of discharge into any number n of end-members using m conservative chemical species provided $m > (n - 1)$. The end-members are defined according to soil horizons and therefore the technique provides information on flow routing through the ground. After testing the method at Plynlimon, Wales and Birkenes, Norway, Christopherson *et al.* (1990) suggested that even if some

event rainfall made it to the stream, its chemical composition was still controlled by terrestrial processes.

2.4.3 Longitudinal Streamflow Separations

The studies outlined above have dealt with individual events at one point along the stream profile. However, some tracer studies have attempted to investigate stream and groundwater interaction along the longitudinal profile of the channel. Although discharge measurements along a stream profile can indicate gaining and losing reaches and thus quantify groundwater credit and deficit, natural tracers can provide further information on the source. For example, measurements of EC taken along an alpine stream in Italy were found to change with contributing lithologies (Apello *et al.*, 1983). It was suggested that the method could be used to identify the response of sub areas to changing hydrological conditions and may therefore be useful to assess variable source area concepts. A study by Ellins *et al.* (1990) used discharge and ^{222}Rn measurements to investigate surface to groundwater interactions in a karst drainage basin. They were able to not only discern the magnitude of losses and gains to the stream but along one reach of unchanging discharge they demonstrated that there were indeed losses to and gains from groundwater but they happened to volumetrically cancel out.

2.4.4 Hydrograph Separations in Sub-alpine and Alpine Environments

Various studies have used tracer based hydrograph separation techniques to investigate the changing proportions of ground (subsurface) to overland (surface) routed contributions to streamflow in alpine and sub-alpine environments. Miller *et al.* (1995), using silica data and a two-component mixing model, calculated that during snowmelt in a sub-alpine site in the Adirondacks, New York, the subsurface contribution to runoff

was 95% for the first event, reducing to only 30% about a month later. In a study using sodium and chloride stream sample data carried out by Sueker (1995) for three alpine watersheds in Rocky Mountain National Park, Colorado, subsurface contributions during spring snow melt were estimated to be generally below 50% with maximum proportions early in the melt season.

Comparisons of runoff mechanisms using stable isotope traces of rain storms over sub-alpine and alpine sites in the coast mountains of British Columbia have shown that although both site types sometimes displayed up to 90% "pre-event" water in event hydrographs, the "new" water contributions in the alpine site were generally higher and more variable (Laudon and Slaymaker, 1997). The observations of Miller *et al.* (1995) and Sueker, (1995) suggest that increasing antecedent basin storage volumes were responsible for the increase in surface runoff contributions during the melt season. Also, from the results of Laudon and Slaymaker (1997) and by comparing the results of Sueker (1995) and Miller *et al.* (1995) it appears that alpine sites may be more prone to surface (overland) and new (event) water contributions to runoff than are sub-alpine sites.

Groundwater contributions to runoff in heavily glacierised alpine basins were investigated by Collins and Young (1979). At Gorner gletscher, overlying igneous and metamorphic bedrock in the Swiss Alps, an electrical conductivity (EC) based separation of surface melt and groundwater suggested that subglacial inputs were out of phase with portal discharge due to slow routing at the bedrock interface. At Peyto Glacier, overlying karst bedrock in the Canadian Rockies, subglacial inputs were in phase with portal discharge and this was thought due to rapid flow through karst solution channels. Collins

and Young (1979) suggested, therefore, that groundwater contributions to alpine glacier discharge during late summer were significantly influenced by bedrock geology.

The interactions of glacial melt, snow melt and groundwater in alpine basins over seasonal time scales can be investigated using combinations of isotopic and ionic tracers. For example, Behrens *et al.* (1975) used environmental isotopes and EC to separate snowmelt, icemelt and subglacial spring water in the Rofenach Basin of the Austrian Alps. They assumed snow and ice to have similar stable isotope values that differed from groundwater, and that old glacial ice would differ from snow and groundwater by having a zero tritium concentration. Further, they assumed the EC of glacial melt would differ from groundwater. Their results demonstrated that in late summer groundwater contributed little to runoff, and icemelt contributed more than snowmelt.

Over longer periods of time, several years for example, it is possible to investigate the storage potential and residence times within groundwater aquifers using tracers and modelling techniques. By inputting deuterium and tritium isotope, precipitation and groundwater data into simple flow routing models, Maloszewski *et al.* (1983) were able to estimate groundwater residence times in a 19 km^2 sub-alpine basin in Bavaria. They calculated that average groundwater residence time was approximately 2 years but using a model that divided groundwater routing into upper and lower reservoirs they estimated residence times of 0.8 and 7.5 years, respectively. In the same study, it was calculated that the basin storage depths were 0.6 and 1.9 m for upper and lower reservoirs, respectively. A later study by Maloszewski *et al.* (1992), carried out in a 33 km^2 alpine basin, using a similar technique with $\delta^{18}O$ and tritium isotope data, found that despite running the model separately for each tracer, the residence time estimations were both

just over 4 years. The longer average storage time than for the smaller sub-alpine site corresponded with a greater storage depth of 6.6 m (Maloszewski *et al.*, 1992).

2.4.5 Problems with Hydrograph Separation Techniques

Although the utility of geochemical hydrograph separations has been demonstrated, problems with the application of the technique often stem from violations of the assumptions listed earlier. Kendall and McDonnell (1993) have illustrated that care should be taken to address the issues of spatial and temporal heterogeneity in stable isotopic signatures of components used in mixing models. It was shown that the compositions of rainfall, soil and groundwater vary both spatially and temporally; groundwater and soil water differ from each other and throughfall is usually enriched relative to open-air rainfall. In addition, if open water bodies are evident, it was suggested that three-component models are needed to account for their presence (Kendall and McDonnell, 1993). In addition, the preferential melting of light ^{16}O isotopes during snowmelt could potentially lead to slight hydrograph separation errors if the bulk snowpack signature is used (Maule and Stein, 1990).

Similar concerns were raised regarding the use of ionic tracers for hydrograph separations. For example, it was suggested by Caine (1989) that it is impossible to conduct accurate snowmelt hydrograph separations on the rising limb due to preferential elution of ions from the snowpack. In glacierised basins, where diurnal fluctuations in discharge are marked, the use of EC for seasonal hydrograph separations was questioned by Brown and Tranter (1990). Also, the use of EMMA for certain hydrograph separation applications has recently come into question. Ball and Trudgill (1997) used EMMA to trace source waters for a 10-ha plot at the Panola Mountain Research Watershed and

found that the constant chemical signatures in soil horizons necessary for the technique to work were not evident. In addition, it has been reported (Hooper *et al.*, 1998) that earlier success using the technique may have been due to unrepresentative sampling in the riparian zone, which it is now thought may dominate stream water chemistry. If this is the case, then basin-wide flow paths cannot adequately be inferred using EMMA. Given the potential errors associated with hydrograph separation techniques, it is important that care is taken to ensure that the assumptions implicit in tracer based hydrograph separations (Sklash and Farvolden, 1982) are met, and that some form of error analysis be performed to quantify the level of confidence in the result.

A relatively simple but rigorous method for quantifying the level of uncertainty (W_f) in tracer based hydrograph separations was demonstrated by Genereux (1998). For a two-component mixing model the uncertainty in the first mixing fraction (W_{f1}) can be described as a function of the uncertainties in each of the tracer concentrations (W_c) used in the mixing model:

$$W_{f_1} = \sqrt{\left[\frac{c_2 - c_s}{(c_2 - c_1)^2} W_{c_1}\right]^2 + \left[\frac{c_s - c_1}{(c_2 - c_1)^2} W_{c_2}\right]^2 + \left[\frac{-1}{(c_2 - c_1)^2} W_{c_s}\right]^2} \qquad (2.11)$$

where the subscripts 1 and 2 refer to the first and second flow components, respectively, and s refers to the samples taken from the stream. The uncertainty function *W* may be any user-defined type of uncertainty (e.g. mean error, standard deviation, 95% confidence limits, etc.) but it is important for quantification purposes that the same type of error is used consistently (Genereux, 1998).

2.5 Modelling the Hydrograph

2.5.1 Introduction

There are many empirical or *black box* models that can adequately predict basin yields for the short-term, based upon regressions between hydrological input and river flow output data. However, when changes occur within the *black box* these relationships tend to break down. To predict river flow in a circumstance of changed climate and landcover for basins dominated by snow and glacier melt, it is first necessary that current modelled hydrographs are adequately explained by present hydrometeorological conditions, particularly spatio-temporal variations in snow and ice cover and the energy budget (Kuhn, 1993). Therefore, models used for such purposes must physically represent (both functionally and spatially) the major components within the mountain hydrological system. The term used for such models is *Physical Distributed.* Despite the existence of many models that fall into this category, it is often difficult to determine their suitability for long-term forecasting. This is because good results obtained between modelled and archived observed data may occur when a deficiency in one modelled component is compensated for by another (Braun and Aellen, 1990).

In this section an introduction to a model that has been designed specifically for use in mountainous areas will be given. The model chosen for this discussion and subsequent analysis was the UBC Watershed Model.

2.5.2 UBC Watershed Model

The UBC Watershed Model (UBCWM) was designed to provide a quantitative description of watershed behaviour in mountainous areas. Unlike other spatially distributed models, the UBCWM divides the basin being modelled into elevation bands

to account better for the elevational dependence of key input data and transfer algorithms. To accommodate the general scarcity of meteorological data in remote mountain areas, the model requires only maximum and minimum temperature and daily precipitation. From these input data, the model delivers daily outputs of the following:

1) Total flow at the basin endpoint;
2) Snowpack growth or depletion per elevation band;
3) Soil moisture budget;
4) A breakdown of surface runoff (fast), interflow (medium), upper (slow) and lower groundwater (very slow) routing pathways (see Figure 2.2);
5) A hydrological balance of snow, ice and rainfall for the three upper flow reservoirs.

Within each elevation band, further landcover distribution is facilitated by specifying basin proportions of forest, glacier, bare ground and lake coverages. Orientation of forest and glacier cover proportions can also be factored into the model routine to take account of slope aspect and shading. Model parameter values for balance, storage and routing algorithms can be user specified based on experience with the model and "real world" values or calculated by the model using an optimisation routine to give the best overall model performance. See Quick and Pipes (1977 and 1996) for further details.

The algorithm for glacial melt input (important in climate and landcover change studies) assumes that glacierised areas are simply infinitely deep snowpacks with a low albedo. The lack of a glacial storage algorithm (such as suggested by Moore, 1993), however, was earlier thought (Fountain and Tangborn, 1985) to lead to a mis-representation of flow peaks in the hydrograph, particularly later in the melt season when flow through glaciers is most prone to storage lags.

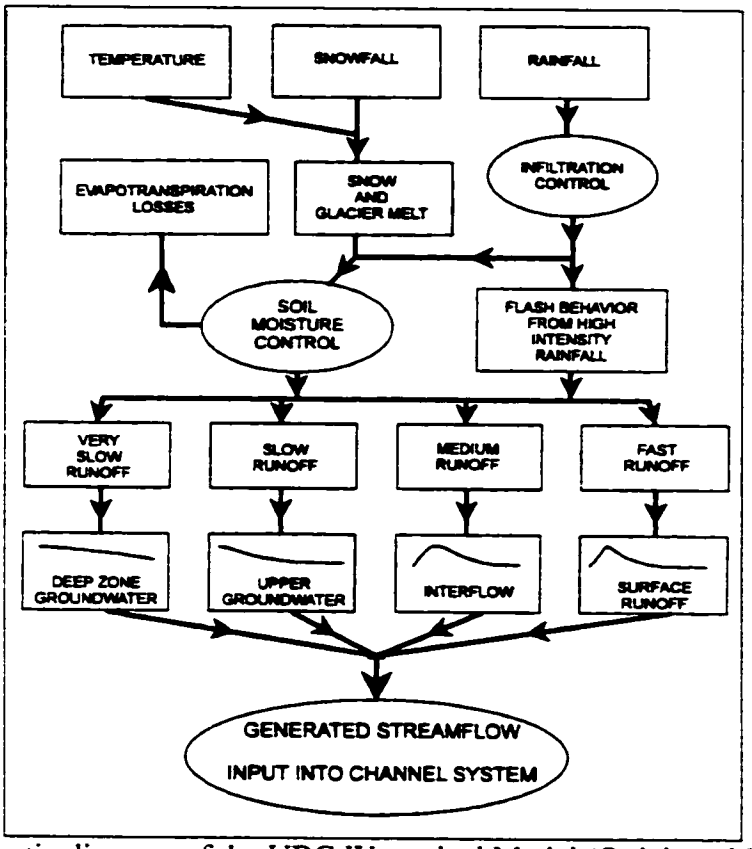

Figure 2.2 Schematic diagram of the UBC Watershed Model (Quick and Pipes, 1996)

For many years, the UBCWM has been successfully used by BC Hydro for runoff and reservoir level forecasting. The model's ability to fully utilise the low density of limited meteorological data in the Rockies of British Columbia is the reason for its adoption and continued use. The UBCWM has also been used in an attempt to predict future flow patterns in the Bow River above Banff, Alberta resulting from possible CO_2 induced climatic change (Zawadzki, 1997). A further utility of the UBCWM is as a flow component based chemistry simulator (Hudson and Quick, 1997). By assigning chemical signatures to each of the flow path components (surface, interflow, upper and lower groundwater) simulated within the model and then mixing each of these components, Hudson and Quick (1997) were able to construct a stream water chemograph. Their results compared favourably with observations.

2.6 Concluding Remarks

The preceding discussion has investigated our state of knowledge in the area of hydrological processes in mid-latitude mountainous environments, some of the methodological techniques, and an example of our ability to model these processes. The literature presented in this review deals with several individual studies taken from a broad range of: a) global locations; b) landcover and geomorphological site types; and c) spatio-temporal scales. Within this limited mountainous context, hydrometeorological processes vary widely in space and time, and with landcover types. It is also evident that most studies are focused on narrow ranges of spatio-temporal scale. Due to pragmatic limitations most publications deal with processes at the hill slope, small paired-catchment or regional spatial scale, and either the event, seasonal or interannual temporal scale.

Hydrological models are generally developed and improved upon from the knowledge and data presented in the global literature covering hydrological processes. Given that the literature is geographically incomplete, and covers disparate global locations and scales, it is likely that many algorithms or "default" parameters within models may not be appropriate for the geographic context for which a model is being developed. Similarly, when we parameterize hydrological models we generally do not have all the appropriate information for the basin in question, and so again resort to the literature for examples. Inevitably, therefore, all model calibrations are a compromise and even though we are able to achieve good correspondence between archived and simulated runoff, we may often achieve the right results for the wrong reasons.

From this overview of the literature, it is felt that there is a need for mountain hydrological research to be conducted in a more integrated manner than has traditionally been the case. Specifically, there is a need to link process studies from headwater and

event scales to larger basin and interannual scales, and to assess the changing influence of landcovers at these various scales. By then using the information collected from such an integrated hydrological processes study for model calibration and evaluation, it is believed that more could be learned about basin hydrological linkages and our ability to model them, than would be from a wide variety of smaller scale studies that are spatio-temporally fragmented.

Chapter 3 Spatio-temporal Variation of Hydrological End-member Geochemistry

3.1 Introduction

This chapter investigates patterns of and controls on spatio-temporal variability in stable oxygen isotope signatures of hydrological balance components in the Bow valley above Banff from 1996 to 1999. In addition, radioactive tritium isotopes and ionic signatures have been investigated to a lesser degree and the results are presented here to supplement the findings from the $\delta^{18}O$ isotope analysis. The hydrological components discussed will be those that make up the input side of a hydrological balance; i.e. for a mountainous river basin such as the Bow Valley these would be snowmelt, rainfall and glacial icemelt. Evaporation is a very important balance end-member but constitutes a loss of water and thus does not have a unique signature. However, it can influence the signature of other balance components and this will be noted when appropriate.

There are three objectives of this chapter:

1) To investigate spatio-temporal variations in hydrological end-member geochemistry to aid in interpreting hydrograph signatures presented in Chapters Five and Six;
2) To elucidate some of the controls on these geochemical patterns;
3) To generate a basin-wide model of monthly end-member (snow, glacial ice and rain) $\delta^{18}O$ patterns for the 1996 - 1999 study period to be used in the subsequent hydrological model evaluation presented in Chapter Seven.

Following this brief introduction is a summary of the common methods used in the end-member geochemistry characterisations. More specific methods relating to individual end-members are outlined in subsequent sections. The first end-member to be

investigated is snowpack, followed by glacial ice and then rainfall. The spatio-temporal and elevational controls on the geochemical signatures of each end-member are explored within separate sections of this chapter. The geochemical parameter of most interest here is that of $\delta^{18}O$ due to it being generally conservative and potential use of this tracer to separate out components of a hydrological balance. The chapter ends with a conceptual model of basin-wide $\delta^{18}O$ end-member signatures.

3.2 Methods Summary

End-member samples of bulk snowpack, composite rainfall and surface glacial ice were collected from various locations within the Bow River Basin (Figure 3.1) from 1996 to 1999. Several samples were also collected from Peyto Glacier Basin, which is part of the Wapta Icefield and adjacent to the headwaters of the Bow (Figure 1.2). Collecting samples from all locations within the basin at all times was logistically impossible, and although efforts were made to represent the entire elevation range and major landcover types, samples had to be collected where and when convenient. Specific methods and sampling strategies adopted for each balance component are outlined in subsequent sub-sections (raw sample data are tabulated in appendix 3).

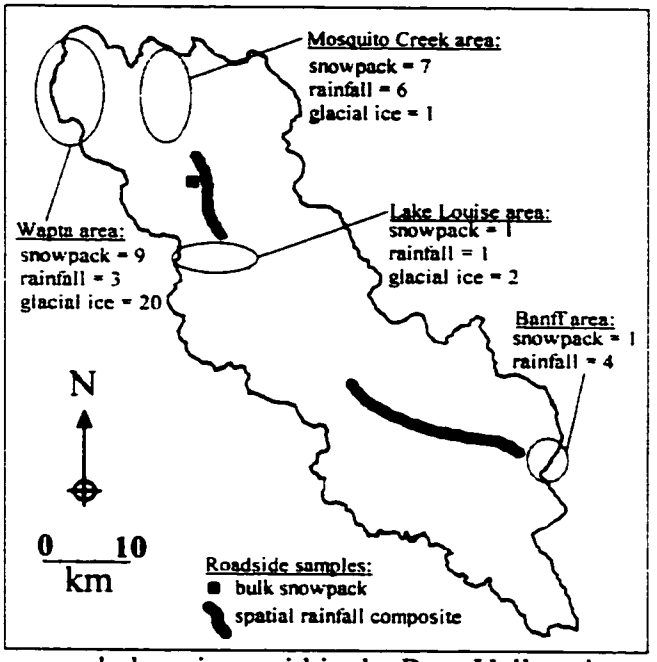

Figure 3.1 End-member sample locations within the Bow Valley above Banff.

All water samples were stored in gas capped scintillation vials. $\delta^{18}O$ analysis was carried out on a Varian Mass Spectrophotometer at the Environmental Isotope Laboratory at the University of Waterloo. Raw $\delta^{18}O$ data were provided to two decimal places but after conducting repeat $\delta^{18}O$ analyses on 191 samples, a mean analytical reproducibility of $\pm$ 0.10 $^{o}/_{oo}$ (σ = 0.08 $^{o}/_{oo}$) was calculated with an analytical precision of $\pm$ 0.16 $^{o}/_{oo}$ at the 95% confidence level (error bars on figures). Enriched tritium analysis was performed in the same laboratory using a liquid scintillation technique with a Hewlett Packard scintillation counter with an analytical detection limit of approximately $\pm$ 1 TU (Tritium Unit). Electrical conductivity (EC), pH (both temperature compensated and calibrated with known standards, EC $\pm$ 2 μScm^{-1} and pH $\pm$ 0.1 units) and alkalinity (standard titration technique, $\pm$ 2 mgl^{-1}) were all measured in the field when possible to do so.

3.3 Snowpack Geochemistry

3.3.1 Snowpack $\delta^{18}O$ Signature

3.3.1.1 Elevational Patterns

From 1996 to 1999, 19 bulk snowpack samples were collected from snow pits and snow coring tubes within the Bow Basin (Figure 3.2) during the time of maximum snowpack accumulation in spring. Each sample represented the entire snowpack profile at an individual location. Samples were temporarily stored in large ziplock bags and allowed to melt naturally (without artificial heating) before being transferred to sample bottles. The range of elevations sampled was 1400 to 2900 m a.s.l (virtually the entire basin range) and the average sample elevation was approximately 2290 m a.s.l. (the elevation of maximum ground cover). $\delta^{18}O$ values ranged between -20.0 $^{o}/_{oo}$ to -24.1 $^{o}/_{oo}$ with an average of -22.2 $^{o}/_{oo}$ and a standard deviation (σ) of 1.2 $^{o}/_{oo}$. The samples were collected from several different locations and when all are plotted together there appears no evidence of any elevational dependence.

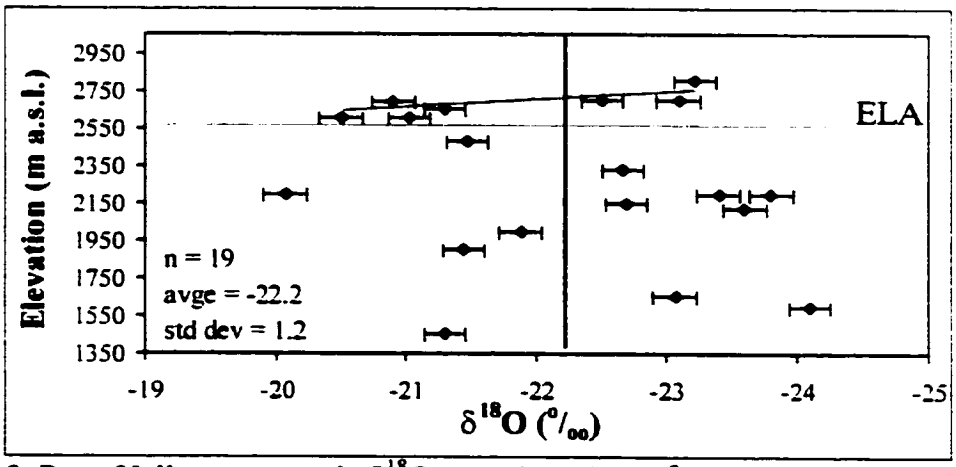

Figure 3.2 Bow Valley snowpack $\delta^{18}O$ sample values ($^{o}/_{oo}$) with elevation (m a.s.l). Vertical line = average isotopic composition.

From the literature on isotopes in precipitation within mountainous regions (e.g. Yurtsever and Araguas, 1993; Schotterer *et al.*, 1996) depletion in snowpack $\delta^{18}O$ with elevation would be expected. The disagreement between the observations noted here (Figure 3.2) and other studies may be linked to the turbulent atmospheric conditions often experienced in mountainous environments during winter. Such conditions could preferentially redistribute a high proportion of the light mid-winter high-elevation snowpack downwards where vegetation cover near the treeline would capture it. In addition, snowpack metamorphosis processes resulting from radiation melt, wind packing and possible sublimation, would vary widely with space, elevation and landcover, and could potentially alter localised snowpack $\delta^{18}O$ signatures. Regardless of the specific mechanism, it is probably safe to assume that meteorological and landcover effects play a large role in altering the basin-wide snowpack $\delta^{18}O$ signature and therefore minimise the influence of elevation.

Due to the complexity of topography and landcover within the Bow Basin it is impossible to characterise truly the spatial variability of snowpack signature with the small sample set collected. Although there is no apparent trend in basin-wide snowpack samples, the data suggest that there might be localised patterns. In the alpine zone it is impossible to model the snowpack $\delta^{18}O$ signature for any specific location but a general trend of depleting snowpack $\delta^{18}O$ signature with height appears to occur in the upper parts of the basin (Figure 3.2). Indeed, if all data from above 2600 m a.sl. (the long-term glacial equilibrium line and approximate tree-line) are plotted together, there is a noticeable elevational trend of 1 $^{o}/_{oo}$ depletion per 100 m rise in elevation ($n = 7$, $r^2 =$

0.67, significance level = 0.025). However, at elevations near and below treeline, where most of the summer time melt occurs, the $\delta^{18}O$ / elevation trend breaks down.

3.3.1.2 Snowpit Stratigraphy

It has already been highlighted that the spatial variability of sample locations within the Bow Valley above Banff was relatively limited due to logistical sampling difficulties. The wide variety of landcovers and elevations within the basin were represented within the sample data but systematic differences in spatial snowpack signatures related to shifting weather patterns over the basin during the winter may not be accounted for. For example, if major snowpack accumulations within different parts of the basin were associated with localised precipitation events with unique $\delta^{18}O$ signatures, then the spatial variability of bulk snowpack would be linked to the temporal variability in $\delta^{18}O$ in winter precipitation. Therefore, if it is found that temporal variability of the winter precipitation signature at any location exceeds that of the variability within the basin sample data, then a spatial bias in the data could exist. Given that $\delta^{18}O$ is known to vary seasonally with changing temperature and precipitation source zones (Dansgaard, 1964; Schotterer *et al.*, 1996), it is felt that the temporal variability within winter precipitation would place an upper limit on the potential spatial variability within an area susceptible to the same weather systems. However, if the temporal variability in winter precipitation were below that of the basin sample data, then a spatial bias would be less likely.

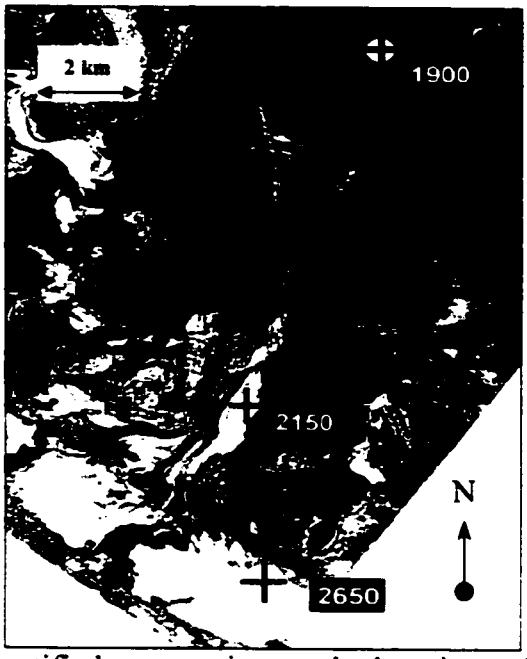

Figure 3.3 Peyto Basin stratified snow pit sample locations shown on Landsat TM summertime panchromatic image.

It was not possible to sample precipitation throughout any of the winter periods, and so a surrogate record had to be chosen. It was thought that stratified snow samples taken from high elevation snowpits at the end of winter prior to melt would provide a reasonable representation of the variability throughout the winter precipitation record. Snow samples of $\delta^{18}O$ were collected from visibly distinct snow layers within a snowpit near the terminus of Peyto Glacier. Additional stratified samples were collected from two more snow pits (one high in the accumulation zone of Peyto Glacier, and another lower down beside Peyto Lake) but these samples were taken from approximately equal depths within the pits rather than distinct layers within the snowpit profile. The stratified snowpit samples were collected in early May 1999, and the locations are illustrated in Figure 3.3. See Figure 3.4 for the stratified snow pit $\delta^{18}O$ profiles.

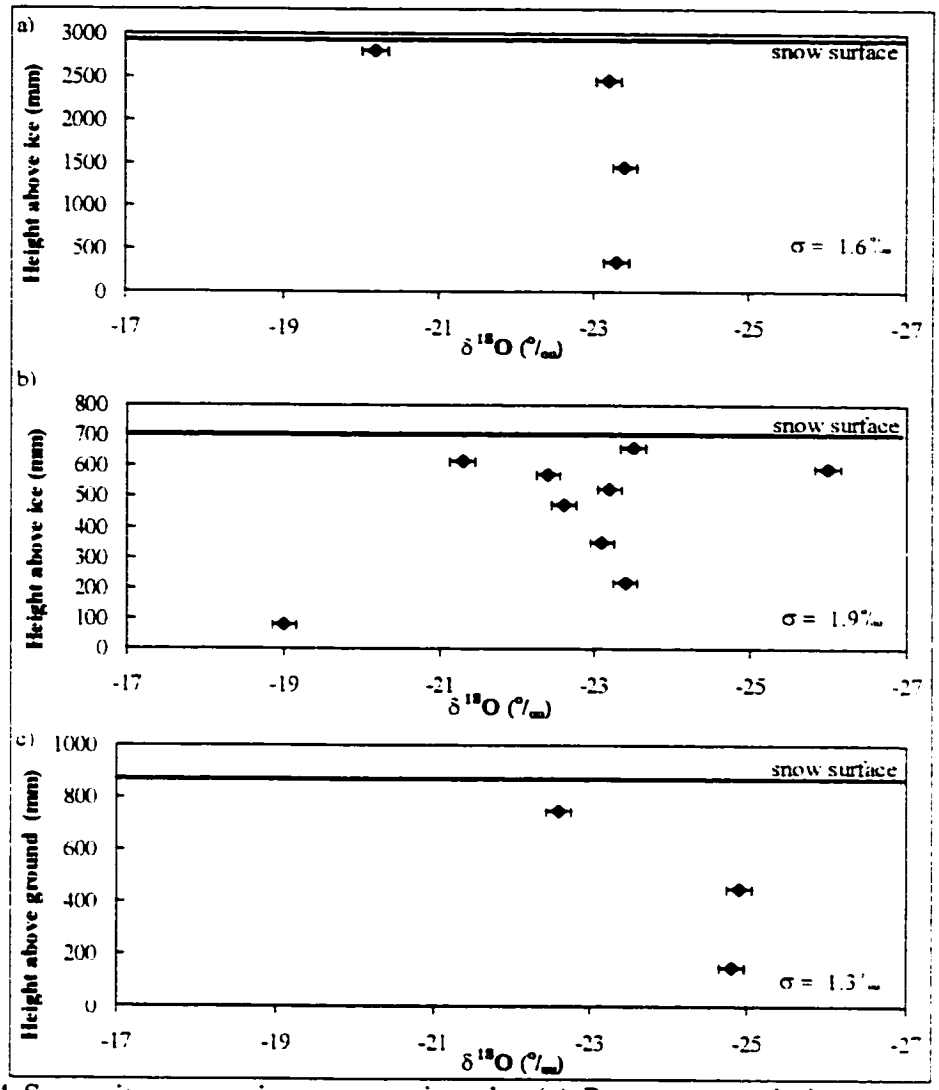

Figure 3.4 Snowpit oxygen isotope stratigraphy (a) Peyto accumulation area at 2650 m a.s.l. (b) Peyto Glacier terminus at 2150 m a.s.l. (c) Near Peyto Lake at 1900 m a.s.l.

In general, the three snow pits display $\delta^{18}O$ sample standard deviations close to or slightly more than for the basin-wide bulk snowpack sample set (1.4 $^{o}/_{oo}$). Due to the low sample number within each of these snow pits, the relatively high standard deviations are probably more a function of individual outliers than overall variability within the snowpack. For example, enriched $\delta^{18}O$ signatures in the bottom layer of the glacier terminus snow pit (Figure 3.4b) and in the surface layers of the two remaining snowpits (Figure 3.4a and 3.4c) may be linked to warmer temperatures (and possibly rainfall

mixing) at the start and end of the winter season, respectively. Therefore, if the snowpack in other parts of the basin contained a different proportion of the snow type that corresponded to these "outlying" snowpack layers, then it is possible that a spatial bias could exist within the raw basin sample data. For this reason, the maximum snowpit standard deviation of 1.9 $^{o}/_{oo}$ will be assumed to also represent the approximate level of spatial variability within the basin-wide samples.

Given the difficulty in establishing a model of the seasonal and spatial variability of basin-wide snowpack oxygen isotope signature it is thought fair to assume that the average snowpack value of -22.2 $^{o}/_{oo}$ (95 % confidence limits ±3.8 $^{o}/_{oo}$) is a reasonable approximation of the Bow Valley snowpack signature for 1996 to 1999. However, it has to be recognised that the average basin-wide snowpack signature may vary from year to year in response to climatic variability.

3.3.1.3 Interannual and Seasonal Snow Melt

In order to investigate inter-annual variability in the snowpack $\delta^{18}O$ signature, those years with sufficient bulk snowpack samples have been averaged and compared. It was found that samples collected from spatially diverse parts of the basin during the two deep snowpack years of 1996 and 1999, displayed average $\delta^{18}O$ values of -22.3 $^{o}/_{oo}$ ($n = 6$, σ = 1.5 $^{o}/_{oo}$) and -22.6 $^{o}/_{oo}$ ($n = 6$, $\sigma = 1.3$ $^{o}/_{oo}$) were respectively returned. For the shallow snowpack and warmer year of 1998 an isotopic weight of -21.6 $^{o}/_{oo}$ ($n = 6$, $\sigma = 1.0$ $^{o}/_{oo}$) was found. During 1997, an average could not be calculated from the single bulk snowpack sample collected from 1500 m a.s.l. near the basin endpoint (-21.3 $^{o}/_{oo}$) but it was assumed that the basin-wide signature would probably be close to that of 1996 due to

both years experiencing similar snowpack conditions (see section 1.4 for an overview of interannual climatic conditions and appendix 1 for snow survey reports).

These limited data suggest that during years of greater snowpack accumulation the overall isotopic signature may be more depleted than during years of little snowpack accumulation. This variation from year to year likely reflects the changes in atmospheric patterns during the winter months. For example, 1998 was an *El Niño* year experiencing very little snowfall as the polar branch of the jet stream was pushed to the north bringing in drier and warmer weather from the south (Woo, 2001). These air masses would have had a more enriched isotopic signature than normal. On the other hand, 1999 was a *La Nina* year with contrasting conditions to the prior year, which probably brought in more precipitation from northerly regions with a relatively depleted $\delta^{18}O$ signature.

Although the bulk winter snowpack for any year and any location may have a characteristic $\delta^{18}O$ signature, it is incorrect to assume that this signature will be the same as melt water draining from it. At the onset of melt, when the snowpack is still cold, melt-freeze cycles lead to small quantities of early melt waters having a depleted $\delta^{18}O$ signature relative to bulk snowpack (Maule and Stein, 1990). Later melt is not significantly enriched compared to the bulk snowpack signature, however, due to the much larger volumes involved (Chris Smart, pers. Comm.). There are no data available from the present study but a shift in $\delta^{18}O$ signature of around 1 $^{o}/_{oo}$ between initial and final snowpack melt water has been observed in similar mountainous environments (e.g. Raben and Theakstone, 1998). This observation is only of practical importance, however, if the volume of initially depleted melt water is significant compared to the bulk snowpack meltwater during the time step of interest.

For the inter-annual and seasonal study of basin hydrology and model evaluation presented in Chapter Seven, a monthly time step has been adopted. In most parts of the basin, the snowpack melt would be well under way within one month of localised melt initiation and, therefore, the slight depletion of small early melt volumes would likely not significantly alter the monthly melt signature at the larger basin scale. However, considering the complexities surrounding the temporal distribution of basin-wide snowmelt signature at a monthly time step, it is not feasible to characterise the true temporal variation of snowmelt $\delta^{18}O$ signature at the basin scale with the data available. Therefore it is felt that a robust approach to characterising the snowpack end-member $\delta^{18}O$ signature for subsequent hydrograph separation or hydrological model validation is to assume a constant value with uncertainty limits of $\pm$ 1 σ (70% confidence level).

3.3.2 Snowpack Tritium Signature

Five end of winter bulk snowpack samples taken in April 1998 and May 1999 were analysed for tritium content (all values $\pm$ 0.9 TU). The average value was 8.9 TUs, ranging from 6.1 to 10.7 (σ = 1.8). From the limited number of samples collected it is impossible to draw any conclusions about basin-wide spatio-temporal patterns but these data are included for use in future sections of the thesis.

3.3.3 Ionic Snowpack Signature

All field sampled snowpack samples were found to have a low dissolved solids content with a mean electrical conductivity of 10 $\mu S\ cm^{-1}$ (approximate total dissolved content of around 7 mg/l) with a range from 0 to 32 $\mu S\ cm^{-1}$. Virtually all snow samples were found to be slightly acidic with an average pH of 6.0 (near the atmospheric equilibrium pH of 5.7) ranging from 6.9 to 5.3. Total alkalinity concentrations reflected

the generally low dissolved ion content with an average value of 2.4 mg/l, ranging from 0 to 5 mg/l (see appendix 3 for raw data). These values are typical for the low ionic concentrations found in continental precipitation (Harrison *et al.*, 1993).

3.4 Glacial Ice Geochemistry

3.4.1 Glacial Ice $\delta^{18}O$ Signature

From 1996 to 1999, 23 glacial ice samples were collected during the time of ice exposure in the summer months (see Figure 3.5). All of the samples were collected in ziplock bags from below the ice weathering crust (~ 10 – 30 mm deep) on glacier surfaces from various locations on the Wapta Icefield and hanging glaciers on the eastern slopes of the Bow Valley. Ice was sampled directly as opposed to sampling surface melt runoff, as it was important to avoid contamination of the samples with snowmelt from higher elevations. The range of elevations sampled was 2100 to 2700 m a.s.l. (approximately 75% of the range of ice exposure for 1998 (see Table 1.1)) and the average sample elevation was approximately 2310 m a.s.l. (a little above the modal basin height). The average sample height was well into the summer time ablation zone but was below both the mean ice exposure height for 1998 of ~ 2550 m a.s.l. and the 30 year modal ELA at Peyto Glacier of ~ 2650 m a.s.l. (Demuth and Pietroniro, 1999).

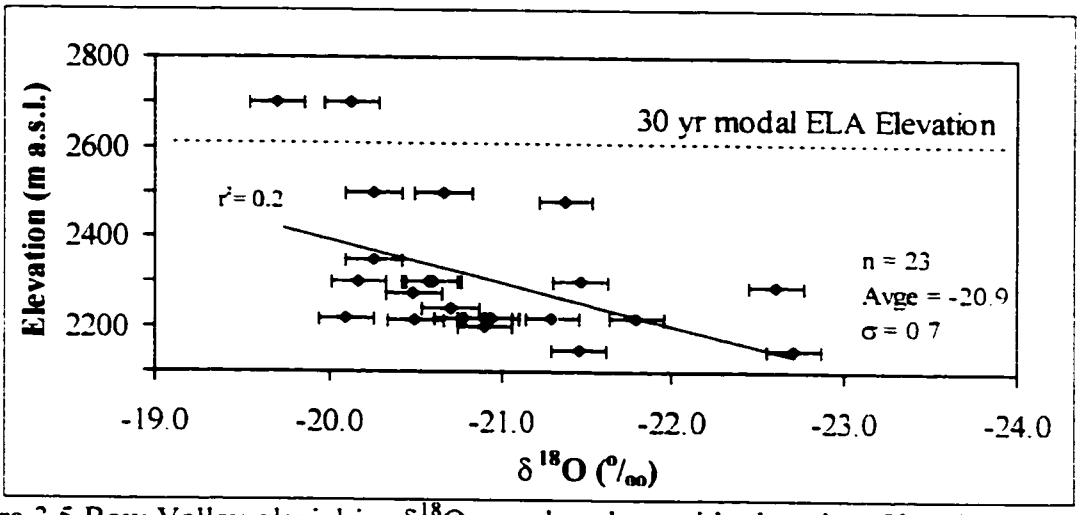

Figure 3.5 Bow Valley glacial ice $\delta^{18}O$ sample values with elevation. Showing long-term ELA height and a slight elevational trend in the data.

$\delta^{18}O$ values ranged between -19.7 °/oo to -22.7 °/oo with an average of -20.9 °/oo and a standard deviation of 0.7 °/oo. The average value was further corroborated by data collected by West (1972) in which a study of 86 ice samples taken from Peyto Glacier tongue revealed an average isotopic value of -20.7 °/oo. The average ice isotope signature was, therefore, more enriched than snow (-22.2 °/oo) and this was to be expected for the following reasons:

1) During firnification of the snowpack in the accumulation zone, any melting or evaporation leads to a preferential loss of lighter isotopes (e.g. Sommerfield *et al.*, 1991).

2) Any summertime rain events at high elevation mix isotopically enriched rain (see section 3.5.1) with snowpack, again leading to an enriched signature in firn at the end of summer.

The lower overall range and standard deviation in ice isotope values compared to those of snow could be partly the result of a mixed elevation and landcover effect. Basin-wide winter snowpack covers twice the elevational range of ice and encounters far more

different landcovers. The ranges of environmental conditions controlling melt and sublimation processes experienced by basin-wide snowpack are therefore greater than for high elevation ice. In addition, during firnification the variation of isotope values throughout the snowpack profile lessens and homogenisation occurs concurrent with gradual enrichment (e.g. Raben and Theakstone, 1998; Shanley *et al.*, 1995).

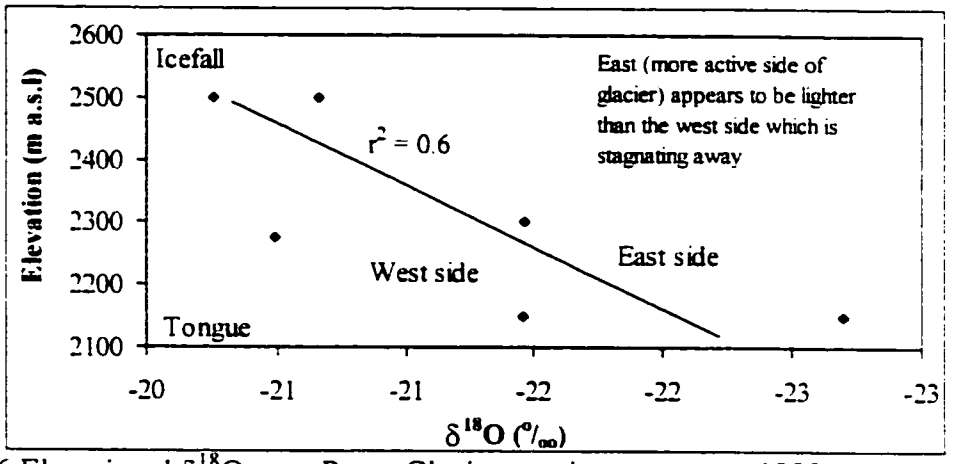

Figure 3.6 Elevational $\delta^{18}O$ over Peyto Glacier terminus, summer 1999.

All 23 ice samples were collected from different locations within the northern headwaters of the Bow Basin and when all were plotted together (Figure 3.5) there appeared a slight pattern of ^{18}O enrichment with elevation ($r^2 = 0.2$, significance level = 0.02). However, six samples taken from Peyto Glacier in the summer of 1999 (Figure 3.6) illustrated a relatively strong localised trend ($r^2 = 0.6$, significance level = 0.08). It can be seen that from the snout at 2150 m a.s.l. up to almost 2500 m a.s.l., there does appear to be an enrichment of the ^{18}O signature with elevation. The same pattern and approximately the same range of values were reported at these elevations on Peyto Glacier by West (1972). Therefore, there is confidence that this pattern is real and not coincidental. The reason given by West (1972) was due to a reverse elevation effect resulting from emergent ice at the snout originating high in the accumulation area and ice

emerging just below the ELA originating just above the ELA. Reid (1896) proposed this pattern of ice movement through a glacier and a reverse isotopic gradient in ice below the ELA is considered evidence for this.

It is generally assumed that at the highest elevations the snow that makes up glacial firn has the lightest $\delta^{18}O$ signature as a result of cooler temperatures during snowpack accumulation, and ultimately this is why an elevation effect is observed in ice below the ELA (West, 1972). Although this process may be partly responsible for the patterns observed in ice $\delta^{18}O$ patterns, the lack of a strong corroborating trend in high elevation snowpack samples collected in this study (section 3.3) suggests that other processes must also be acting. A slightly different but complementary hypothesis is proposed:

1) Snowpack at high elevations undergoes very little melt during the summer season and therefore likely preserves much of its depleted winter signature.
2) Snowpack persisting just above the ELA undergoes more melting during the summer, thus preferentially losing light isotopes and is mixed more with isotopically enriched summer time rainfall.

If high elevation winter snowpack did not possess an elevational isotope gradient at the end of the winter, the combined effect of the two processes noted above will very likely create such a gradient. Therefore, leading to heavier firn at lower elevations and ultimately heavier ice just below the ELA. In both West's (1972) and the current study the range of isotopic weight from Peyto's snout to ELA was approximately -22 $^{o}/_{oo}$ to -20 $^{o}/_{oo}$. Just above the ELA on Peyto two samples were obtained near the basin divide at over 2700 m a.s.l. during late summer of 1998. These samples were both around -20 $^{o}/_{oo}$ and are therefore similar in isotopic weight to those samples taken from below the ELA. This

observation corroborates the above hypothesis but the low number of samples collected precludes the possibility of drawing firm conclusions.

It should be borne in mind that patterns observed at Peyto may be localised and not representative of other local glacial covers. For example, from Figure 3.6 it can be seen that although the isotope signature appears to lighten with elevation on both sides of the glacier, the west side is consistently heavier. The west side of the Glacier is currently undergoing stagnation due to lack of upstream ice nourishment and this could be the reason for the disparity in $\delta^{18}O$ values. Over the Bow Basin as a whole, glacial ice in the ablation zone is likely to be a mixture of active and stagnating ice, and therefore applying an appropriate isotopic signature to any one location at any point in time through the melt season would be problematic.

It is possible, however, to apply a simple conceptual temporal/elevation $\delta^{18}O$ model to the entire basin. A simple approach that would account for the observations in the data, the rising TSL and increasing ice exposure throughout the season would be to start with an icemelt $\delta^{18}O$ signature of -21.5 $^{o}/_{oo}$ in May and gradually rise up to -20.5 $^{o}/_{oo}$ in September. During August, the time of maximum ice melt contribution, the modeled signature would be -20.8 $^{o}/_{oo}$, approximately the average ice value over the entire ablation zone.

3.4.2 Tritium

Three combined ice samples taken from various locations in three distinct elevation bands ranging from 2150 to 2500 m a.s.l. returned enriched TU values of 0, thus suggesting that all of the ice sampled pre-dated the bomb testing of the 1950s. No samples were taken from above the ELA where there could potentially be "younger" ice

with a higher TU value. However, most of the ice melt normally occurs below the ELA and should therefore be very old ice with a TU value of 0.

3.4.3 Ionic Glacial Ice Signature

Three ice samples taken from low down in the ablation zones of three different glaciers (Peyto, Bow and a hanging glacier in Mosquito Creek) were analysed in the field for EC, pH and alkalinity. The pH levels for these samples were between 7.8 and 8.0, with total alkalinity of 7, 14 and 5 mg/l, respectively. Electrical conductivity was variable with values of 9, 32 and 53 $\mu s\ cm^{-1}$, respectively. Although these concentrations are generally reflective of neutral water with a low ionic content, there is a slightly higher level of dissolved ion content in glacial ice than for snowpack. It is known that during firnification, ions within the snowpack are preferentially eluted early on in the melt process (Johannessen and Henriksen, 1978) and thus it may be logical to expect that the ionic content within ice would be lower. However, the glaciers in this temperate region contain a high and variable proportion of "dirty" ice from aeolian inputs during firnification.

3.5 Rainfall Geochemistry

3.5.1 Rainfall $\delta^{18}O$ Signature

From 1996 to 1999, 16 rain samples were collected during the summer months of May to September (see Figure 3.7). Composite samples were taken from a range of elevations during single storm events or several samples of different events were collected at one location and then combined. The range of sample elevations was 1400 to 2250 m a.s.l. but the true average sample elevation is difficult estimate accurately given

that each sample point in Figure 3.7 represents a different volume of rainfall. However, assuming that each sample is equally representative, then the average sample elevation is approximately 1900 m a.s.l. The average $\delta^{18}O$ signature of all samples was found to be -12.6 $^{o}/_{oo}$ with a standard deviation of 2.2 $^{o}/_{oo}$. Summertime rainfall was significantly more enriched than end of winter snowpack with the average difference being around 10 $^{o}/_{oo}$. This is in agreement with other similar studies of bulk snowpack and rainfall signatures (e.g. Mast *et al.*. 1995).

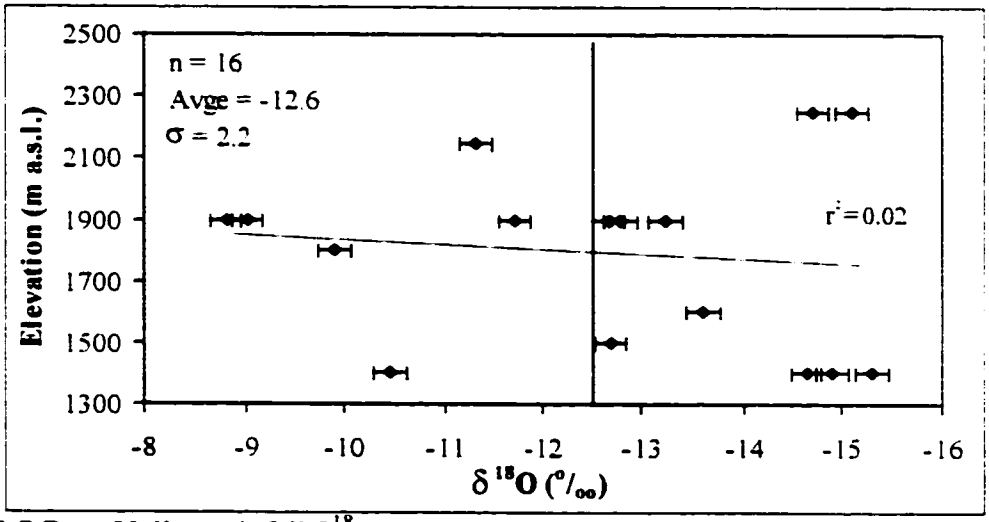

Figure 3.7 Bow Valley rainfall $\delta^{18}O$ sample values with elevation. Vertical line = average isotopic weight.

Rainfall should be significantly more enriched in ^{18}O than snow or ice for the following reasons:

1) Rainfall occurs mainly during the summer when temperatures are warmer and more enrichment of the atmospheric moisture will have taken place through evaporation:
2) The dominant weather patterns between winter and summer are different. In winter, most snowfall is precipitated from north and westerly air masses whereas during

summer. Idaho highs force warm southerly air masses into the region with have a heavier $\delta^{18}O$ signature (unpublished data compiled by Yonge in Grasby, 1997).

It should be noted that the average collection elevation of summer rainfall samples was lower than ice or end of winter snow. This is largely due to the logistical difficulties of sample collection but also reflects the spatial distribution of these hydrological end-members. Obviously, ice cannot be sampled below glacier termini and spring snowpack persists longer at higher elevations. However, it is recognised that rainfall occurs at all elevations and so the low range of altitudes sampled could bias the $\delta^{18}O$ signatures slightly if there is an elevational gradient. It was appropriate, therefore, to estimate the effect elevation might have on the rainfall $\delta^{18}O$ signature and quantify the level of potential bias.

$\delta^{18}O$ isotope gradients in precipitation are reported to generally deplete by between 0.15 and 0.35 $^{o}/_{oo}$ per 100 m rise in elevation (Yurtsever and Araguas, 1993). The range of elevation in the Bow Basin is approximately 1600 m and thus if the upper limit of 0.35 $^{o}/_{oo}$ per 100 m is adopted it is found that the range in $\delta^{18}O$ variation due to elevation alone could be up to 5.6 $^{o}/_{oo}$ Also, if the $\delta^{18}O$ composition for the average basin height of ~ 2200 m a.s.l. is calculated, using 0.35 $^{o}/_{oo}$ per 100 m, it is found that the rainfall signature becomes -13.7 $^{o}/_{oo}$ instead of -12.6 $^{o}/_{oo}$ (still significantly different from snow or ice). However, this calculation assumes that an elevational depletion of $\delta^{18}O$ composition exists in the Bow Valley and therefore any elevational trends in sample data need to be investigated.

From Figure 3.7, it is apparent that the bulk rainfall samples displayed no elevational trend ($r^2 = 0.02$, significance level = 0.62) within the 850 m range sampled. Although it is

possible that for individual events there are elevational gradients in the $\delta^{18}O$ composition of rainfall, these observations suggest such gradients may not be significant at the larger basin scale over the summer months. Air mass turbulence and spatial variability in rainfall $\delta^{18}O$ composition may mask widespread altitude effects, and as such no particular elevation would be more or less representative of the basin as a whole. However, the lack of a strong elevation effect does not preclude the possibility of a temporal variation in rainfall signature.

For this study, it was impossible to adequately investigate seasonal variations in rainfall signature due to the logistical difficulty of obtaining and paying for sufficient samples and analysis. However, from the few samples collected there was no evidence of a distinct seasonal signature. As with winter snowpack signatures, it was also considered appropriate to investigate the possible interannual variability in summertime rainfall signature due to changing atmospheric conditions. This is difficult given the limited number of samples for each year but it does appear that a pattern of year-to-year variability similar to the snowpack observations was evident. The years 1996 and 1997 displayed similar rainfall signatures of, respectively, -14.3 $^{o}/_{oo}$ ($n = 3$, $\sigma = 1.4$) and -14.9 $^{o}/_{oo}$ ($n = 2$, $\sigma = 0.3$) and were both depleted compared to the overall average rainfall signature. For the El Niño year of 1998 the most enriched signature was observed (as with snowpack) of -11.3 $^{o}/_{oo}$ ($n = 7$, $\sigma = 2$). For 1999 (La Nina), the rainfall signature lightened slightly to -12.3 $^{o}/_{oo}$ ($n = 4$, $\sigma = 1.8$). If each of these signatures is assumed to be representative of each individual year, then the average for the 4-year period becomes -13.2 $^{o}/_{oo}$. This is slightly lighter than the average of all the samples lumped together (-12.6 $^{o}/_{oo}$) but is probably a more appropriate value for the whole four year period as the

complete rainfall sample set is disproportionately biased towards the heavy El Niño year (n = 7 out of a total n of 16).

3.5.2 Rainfall Tritium Signature

Three bulk rainfall samples were collected for enriched tritium analysis. The first was an amalgamation of several rainfall events at 1850 m a.s.l. during July and August of 1998. The second and third samples were collected at two different elevations (1400 and 2150 m a.s.l., respectively) and were a combination of all rainfall events during the first two weeks of August 1999. TU values of 13.8, 16.8 and 14.1 were respectively recorded. Given the small number of samples it is impossible to say how representative they are of true summertime rainfall. However, it is assumed that the bulk sampling approach should increase the confidence in the results.

The first important observation is that the mean rainfall value of 14.9 TUs is higher than the average for bulk winter snowpack of 8.9 TUs. This reflects the seasonal variation in TU signature reported elsewhere (e.g. Gaspar, 1987 and Schotterer, 1996). In addition, the data from 1999 suggest that rainfall at lower elevations may have an increased TU value, reflective of enrichment from enhanced evaporative processes lower in the atmosphere. However, no conclusion can be formulated regarding the elevational trend in TU signature from these two samples as it has already been demonstrated from the $\delta^{18}O$ data that the elevational control on isotopic signature is complex.

3.5.3 Ionic Rainfall Signature

There were no ionic analyses of rainfall samples, either in the field or in the lab. However, it is to be expected that the range of values in rainfall precipitation would be similar to those in the snowpack, i.e. generally quite dilute and slightly acidic.

3.6 End-member Geochemistry Conclusions

3.6.1 End-member $\delta^{18}O$ Signatures

A summary of average and temporally variable $\delta^{18}O$ signatures for the hydrological balance components studied is provided in Table 3.1. The dynamic, or temporally variable, isotope signatures presented are best estimates based upon the data collected, and for the Bow Basin above Banff, these end-member characterisations provide an approximation of the patterns for each of the years in question. These $\delta^{18}O$ characterisations will assist with the definition of end-member signatures for subsequent geochemical hydrograph separations and the hydrological model evaluation analysis presented in Chapter Seven.

Static $\delta^{18}O$ signatures (‰)		Dynamic $\delta^{18}O$ signatures (‰)		
Snowpack	Avg = -22.2 σ = 1.9 n = 20	Hydrological years:	1996 =	-22.3 (σ = 1.5, n = 6)
			1997 =	-22.3 (estimated from 1996)
			1998 =	-21.6 (σ = 1.6, n = 7)
			1999 =	-22.6 (σ = 1.0, n = 6)
Icemelt	Avg = -20.9 σ = 0.7 n = 23	All years:	May =	-21.5
			June =	-21.3
			July =	-21.0
			August =	-20.8
			September =	-20.5
Rain	Avg = -13.2 σ = 2.2 n = 16	Hydrological years:	1996 =	-14.3 (σ = 1.4, n = 3)
			1997 =	-14.9 (σ = 0.3, n = 2)
			1998 =	-11.3 (σ = 2.0, n = 7)
			1999 =	-12.3 (σ = 1.8, n = 4)

Table 3.1 Average and estimated dynamic hydrological component isotope signatures within the Bow Valley above Banff, from 1996 – 1999.

End of winter snowpack tended to have a reasonably consistent $\delta^{18}O$ signature for the locations sampled but the variation from year-to-year likely reflected changes in atmospheric patterns associated with El Niño and La Nina. The level of variability in the basin-wide bulk snowpack data (expressed by σ) was thought to be under-estimated due to the possibility of spatial bias in the data. It was thought by assessing the temporal

variability associated with layers within individual deep snowpits, this would provide an upper limit on the potential spatial level of variability. Using this method, the basin-wide snowpack σ increased from 1.4 to 1.9 $^{o}/_{oo}$.

Glacial ice collected from various locations within the headwaters demonstrated a weak $\delta^{18}O$ trend of enrichment with elevation (significance level = 0.02). Localised data collected on Peyto Glacier (this study and West, 1972) corroborated the likelihood of a change in signature with height. The estimated dynamic signature associated with icemelt, therefore, begins light in the spring and becomes heavier as the transient snowline approaches the glacier equilibrium line. This pattern reflects the general enrichment of glacial ice with height up to the equilibrium line due to changing snow/rain ratios and elution of light isotopes during firnification in the accumulation zone.

Unfortunately, due to logistical limitations it was impossible to assess the true elevational and seasonal controls on rainfall signature for individual events and locations. However, the lack of any coherent trends in the composite data collected suggest that spatial and elevational mixing of air masses probably minimizes the effects of elevation and season in the $\delta^{18}O$ rainfall signature at the larger basin scale. As with snowpack, it was found that interannual variability in rainfall $\delta^{18}O$ signatures was likely linked to El Niño and La Nina conditions.

3.6.2 End-member Tritium Signatures

The tritium signatures for each of the three end-members of interest in this chapter were found to be markedly different. All ice samples returned zero concentrations of tritium, reflecting their pre 1950s origin. Snow and rainfall displayed values near current

background atmospheric levels but rain was about 50% higher due to the distinct seasonal pattern observed in tritium worldwide (Schotterer, 1996).

3.6.3 End-member Ionic Signatures

In general, all of the hydrological end-member samples investigated displayed low ionic concentrations. Snowpack samples tended to have dilute EC signatures and slightly acidic with pH values between 5.3 and 6.9. Glacial ice was generally more alkali with a slightly higher dissolved solids content than snowpack and was thought to reflect the entrapment of aeolian material during firnification.

3.6.4 Summary

This chapter has provided a spatio-temporal overview of hydrologically important geochemical signatures for the snow, rain and glacial ice end-members within the mountainous Bow Basin above Banff for the years 1996 to 1999. In addition to attempting to characterise the major patterns in end-member geochemistry, some of the potential controlling mechanisms influencing the observed patterns have been discussed. The next chapter will attempt a similar task but rather than investigating hydrological end-members, the focus will be directed towards elucidating the patterns and controls on basin-wide baseflow geochemistry.

Chapter 4 Spatio-temporal Variation of Baseflow Geochemistry

4.1 Introduction

The main objective of this chapter is to characterise the interannual and seasonal $\delta^{18}O$ signature of the basin-wide deep groundwater baseflow end-member for use in the evaluation of the UBC hydrological model presented in Chapter Seven. A complementary objective is to gain insight into basin groundwater and surface water interactions through the study of natural geochemical tracers and measurement of headwater baseflow discharge levels.

A difficulty associated with the first objective is that at interannual time periods, baseflow sources vary in magnitude and extent, and individual sources may have distinct time-variant geochemical signatures. This difficulty is addressed, however, by taking two complementary approaches:

1) The spatio-temporal variation of $\delta^{18}O$ in saturated zone groundwater and baseflow within the Bow River above Banff and headwater basins of varying landcover characteristics are investigated so that elevation, landcover and scale influences can be considered when characterising basin-wide baseflow;
2) Basin-wide baseflow is considered a single hydrological end-member with its own temporally changing signature. This "black box" approach means that individual groundwater baseflow components can be lumped together in the final characterisation rather than modelled individually.

In the UBC model, runoff is divided into four time-response based components (see section 2.5). The faster three components are approximately analogous to overland flow,

throughflow and shallow groundwater flow. Each of these "flow path" components can be divided up into volumetric proportions of "hydrological origin" sub-components; i.e. snow, ice or rain content. Deep groundwater maintained baseflow is the final component of the model, and it cannot be quantitatively divided into its hydrological origin sub-components. This model system grossly simplifies actual runoff generation mechanisms but is a convenient method of conceptualisation at the larger basin scale. For this reason, and for the analyses presented here to be applicable to the model evaluation in Chapter Seven, the component of baseflow that will ultimately be characterised in this chapter is that which is maintained by deep saturated zone groundwater.

The chapter focuses on the following:

1) Bow River at Banff baseflow – an investigation of the geochemical and hydrological composition of the interannual basin baseflow for the Bow River at Banff;
2) Basin-wide baseflow – an investigation of the elevational, seasonal and flow pathway controls on Bow River baseflow;
3) Headwater baseflow – an investigation of the spatio-temporal composition of headwater baseflow by scrutinising the geochemistry of first order streams and headwater basin longitudinal stream profiles. Areal yields of sub-basins and direct channel inputs from groundwater along the profiles are discussed to assess the influences of landcover on baseflow.
4) Groundwater wells – the temporal change in geochemical composition of well water in the headwaters is studied to gain insight into groundwater residence times, hydrological composition and flow pathways, and to provide an indicator of the

seasonal fluctuation in groundwater $\delta^{18}O$ during years of different hydrometeorological character.

5) Summary and conceptual basin $\delta^{18}O$ baseflow model – the main findings of the chapter are discussed and linked together. A characterisation of the interannual and seasonal variation in basin baseflow $\delta^{18}O$ is proposed.

This chapter investigates spatio-temporal variation in baseflow geochemistry by sampling dry period baseflow from various stream locations within the basin and storage from groundwater wells. The same geochemical parameters are investigated as in the previous chapter and the analytical methods are the same. Methods specific to any of the analyses outlined in this chapter are noted within the appropriate section. Raw basin profile discharge measurements and groundwater sample data are provided in appendix 4.

4.2 Bow River at Banff Baseflow

4.2.1 Baseflow Hydrological Composition

It is often assumed that interannual baseflow reflects the composition of mean annual precipitation for the location studied (e.g. Fritz, 1981 and Yonge *et al.*, 1989). From the Banff (1350 m a.s.l.) and Lake Louise (1600 m a.s.l.) meteorological records for 1961 to 1991 (see section 1.4.2) the proportions of precipitation falling as snow were 46% and 55%, respectively. Linear extrapolation of this elevational increase in snowfall proportion with height leads to about 74% snowfall at the basin average height of 2280 m a.s.l. The question to be answered here then is: does the annual basin baseflow at Banff reflect the proportional contributions of snow and rain precipitation reaching the ground?

A two-component hydrograph separation technique was employed to assess the contributing proportions of snow and rain to basin-wide baseflow at Banff. For the

purposes of the analysis presented in this chapter, interannual baseflow for the Bow River at Banff has been considered as any discharge below 20 m^3s^{-1}. This discharge was chosen as these flow conditions normally occur between late October and early May of the following year, when no melt or rain events would normally be expected. Ice melt from glaciers was not considered a significant contributor to basin-wide groundwater and therefore winter baseflow at Banff. At a localized scale in the basin headwaters, water from ice melt may contribute to groundwater in bedrock and tills beneath and surrounding ice covered areas but this is not thought to significantly impact the larger basin system for two main reasons:

1) Basin-wide glacial coverage is about 2% and is limited to headwater areas, which are distal to the basin endpoint of interest. The wintertime contributions from pressure melting at the glacier bed for a 50 km^2 glacier area (assuming 6 mm of melt per year (Sugden and John, 1993)) would result in a constant discharge of less than 0.01 m^3s^{-1};
2) Ice melt takes place during summer when water tables would be expected to be relatively high from spring snowmelt and the hydraulic potential would tend to be directed from the ground into surface streams. Thus any melt runoff leaving a glacier portal will likely travel along gaining watercourses and not be able to infiltrate to groundwater.

Assigning an isotopic signature to interannual baseflow was straightforward, as this could be sampled in-stream during winter when there were no events and the only flow contributor was deep groundwater. Baseflow samples collected at Banff each year from 1996 to 1999 indicated that this signature was relatively constant from year to year and had an oxygen isotope weight of -20.5 $‰$ ($n = 15$, $\sigma = 0.17$). Using the interannual

average $\delta^{18}O$ values of -22.2 ‰ and -13.2 ‰ for snow and rain, respectively, proportions of 81% snow and 19% rain were calculated. The maximum and minimum possible proportions for snow contribution are 97% and 62%, respectively, based on the same calculation using 1 standard deviation from the mean for each of the components.

The geochemical and hydrometeorological estimations of basin-wide snow melt contribution to interannual baseflow are similar at 81% and 74%, respectively and well within the bounds of error. However, a slightly higher estimate of the snow proportion using the $\delta^{18}O$ separation technique could occur for the following reasons:

1) The hydrometeorological estimate of snow/rain ratio may have been underestimated because if both total precipitation and snowfall ratio increase with elevation then the basin-wide representative snowfall accumulation would occur above the average altitude of the basin.
2) Rainfall generally occurs during summer, when water tables, air temperatures and incident radiation tend to be highest; therefore disproportionately elevating the loss of the rainfall component over others to evaporation.
3) The $\delta^{18}O$ signatures chosen for the separation analysis may not have been truly representative of their respective flow components. For example, snow melt has a lighter $\delta^{18}O$ signature than bulk snowpack at melt onset, and it is this early melt that may preferentially recharge groundwater aquifers. Other potential biases are discussed earlier in Chapter Three.

Although there are several potential sources of error in such analyses it would appear that rainfall contributes ~20% to interannual baseflow in the Bow Basin above Banff.

Further discussion of the contribution of rainfall to river runoff will be provided later when investigating river isotope signatures in Chapters Five and Six.

4.2.2 Tritium Signature

During 1998 and 1999, four samples were collected and analysed for tritium from the Bow River at Banff during interannual baseflow conditions (defined by $Q < 20\ m^3s^{-1}$). The TU values returned were 14.9, 13.3, 16.1 and 13.8 and therefore have a mean TU value of 14.5, which is close to average rainfall (14.9 TUs). This may be for 2 reasons:

1) Rainfall is an important component of the balance during the winter months. This is unlikely, however, given that the $\delta^{18}O$ baseflow separation suggested that snow was the dominant end-member;
2) Groundwater contributing to baseflow is a mixture of recent and old water. From the limited data available, it is impossible to calculate the relative proportions of old and recent groundwater contribution as has been carried out in other studies (e.g. Maloszewski *et al.*, 1992). However, the observed signature could either be the result of a high proportion of groundwater that is less than ten years old (i.e. TU slightly above current background levels) or possibly a small contribution of water that dates back to the 1950s (i.e. very high TU).

It is likely, therefore, that the annual baseflow at Banff is noticeably influenced by groundwater that predates the preceding hydrological year.

4.2.3 Ionic Signatures

In total, nine Bow River samples were collected at Banff during baseflow conditions from 1996 to 1999 and a summary of EC, pH and total alkalinity is provided in Table 4.1. Alkalinity and EC concentrations are generally an order of magnitude greater than the

other hydrological end-member components of snow, ice and rain (see Chapter Three), with a buffered pH value of around 8. These signatures reflect the high weathering potential within this predominantly carbonate basin.

Statistics	Q (m^3s^{-1})	EC (μScm^{-1})	pH	Alk (mgl^{-1})
mean	14.1	356	8.2	112
std. dev.	3.8	61	0.4	7
number	9	9	6	6

Table 4.1 Summary of Bow River at Banff baseflow hydrochemistry

4.3 Basin-wide Baseflow

4.3.1 Basin $\delta^{18}O$ Signatures Profiles

The Bow Basin is physiographically complex and hydrological end-members cannot be characterised from samples that do not take into account elevational and spatio-temporal variations. From a catchment balance point of view, the deep groundwater that maintains long-term baseflow can be considered a dynamic storage component that is isotopically characterised by the origin of its hydrological inputs in a similar fashion to river runoff. The major differences are that deep groundwater $\delta^{18}O$ signatures are generally less susceptible to rapid fluctuation due to large potential storage volumes, and, unlike in-channel stream flow, groundwater is present throughout the basin.

Although groundwater is generally the main source of baseflow, much water may still be ground routed but reach the stream quickly following events (e.g. McDonnell *et al.*, 1991). In this region, work by Grasby (1997) has shown that a high proportion of all Bow River flow is probably routed through the ground. Although a high proportion of water in the river may have, at some time, been routed through the ground, baseflow and ground-

routed event water often have different $\delta^{18}O$ signatures, thus facilitating hydrograph separations of "new" and "old" water. Therefore, if it is assumed that all ground-routed "new" water throughout the year reaches the river with its input end-member isotopic signature intact, then the baseflow end-member component of interest here is the seasonally changing "old" groundwater $\delta^{18}O$ signature throughout the basin.

For a basin with a large altitudinal range such as the Bow Valley above Banff, it might be expected that elevation would exert a strong influence on the deep groundwater baseflow $\delta^{18}O$ signature. This pattern has been observed in this region and is generally attributed to similar gradients in precipitation and reductions in temperature with elevation (Yonge *et al.*, 1989). However, in this study there has been little evidence for strong $\delta^{18}O$/elevation gradients in winter snowpack or summertime basin-wide rainfall and it is thought that within the Bow Valley as a whole, atmospheric mixing and precipitation redistribution tend to homogenise the elevational signature. The objectives of this section are to investigate the elevational and interannual variability in groundwater maintained baseflow $\delta^{18}O$ signature within the Bow River Basin.

The elevational and temporal variation of river baseflow geochemistry (or the changing "old" water signature) was investigated by collecting samples during winter and summer baseflow conditions along the Bow River and accessible major tributaries for which samples could be obtained. For this part of the investigation, all winter baseflow samples were collected at least one week prior to initiation of spring melt ($Q < 20$ m^3s^{-1} at Banff) conditions. Late summer baseflow samples were collected on the Bow at Banff recessional limb during cool dry periods at least three days after a major rainfall event ($Q = 40 - 80$ m^3s^{-1} at Banff). In total, six longitudinal profiles of river and tributary samples

were collected: three during August and three at the end of winter for each of the years from 1997 to 1999. For the summertime tributary samples, only basins with zero or minimal glacier cover were visited due to the possibility of glacier melt contributions to runoff. The Bow River is quite difficult to access from the highway between 1550 m a.s.l. and 1800 m a.s.l., and so during August 1998 in-river samples between these elevations were collected by canoeing down the river itself. The river and tributary $\delta^{18}O$ signature profiles are plotted in Figure 4.1.

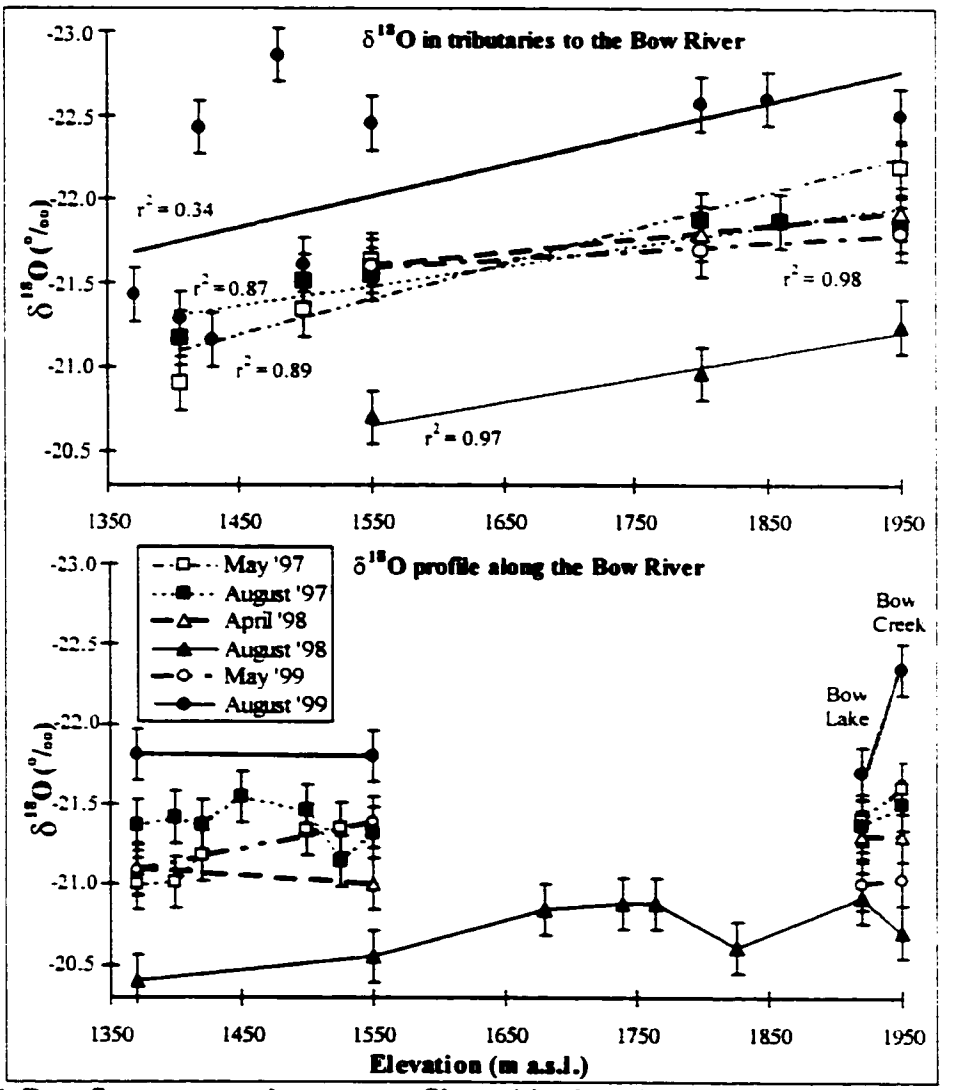

Figure 4.1 Baseflow oxygen isotope profiles with elevation along Bow River and major tributaries from Banff up to the headwaters. (Error bars = 0.16 $^{o}/_{oo}$ analytical precision.) (Lines are for illustrative purposes only and do not imply statistically significant trends.)

Along the Bow River profiles there were generally no appreciable differences in $\delta^{18}O$ from basin headwaters to endpoint, and the only evidence of any elevational patterns were localised: between 1550 – 1800 m a.s.l. during August 1998; and from Bow Creek (glacierised headwater) to Bow Lake during August 1999 (discussed below). However, samples collected from major tributaries with minimal to no glacier cover indicated an approximate depletion of 0.15 $^{o}/_{oo}$ per 100 m (see Figure 4.1). Therefore, although tributary inputs tended to demonstrate an elevational depletion of groundwater baseflow, this pattern was not evident in the river signature. There are various possible reasons for the difference in observations between river and tributary signatures:

1) Lakes in the bottom of the main valley could be controlling the overall river signature through processes of damping (mixing) and or evaporation. There are more lakes at higher elevations and these are the surfaces most susceptible to evaporative enrichment of the isotope signature. This process could act to reduce the elevation pattern in the river profile. Lake influences on runoff and geochemistry in the headwaters will be explored further in section 5.4.
2) The main river could be exchanging water with regional aquifers or groundwater stored in the deeper tills of the main valley and thus the influence of tributary runoff on river geochemistry could be reduced. Deep groundwater isotope patterns in the main valley will be examined in section 4.5.
3) Tributaries from highly glacierised basins are not represented in the tributary data in Figure 4.1, as they were not required for the groundwater baseflow investigation and also because most of these basins are located in the north western headwaters of the Bow valley and are difficult to access. Volumetrically, these tributaries can be

expected to contribute a high proportion of the total headwater runoff during late summer, and the $\delta^{18}O$ signature of these tributaries could have a disproportionate effect on the river $\delta^{18}O$ signature. However, for headwater glacial tributaries to reduce the elevational depletion in the river signature, their runoff signatures would need to be relatively enriched compared to other tributaries. From the conceptual model in Table 3.1, basin-wide glacial ice, at least, might expected to have an enriched $\delta^{18}O$ signature of around -20.8 $^{o}/_{oo}$ at this time of the year.

Specific details relating to the four points raised above will be explored further in later parts of the thesis. The discussion here shall be restricted to the general changes in baseflow $\delta^{18}O$ from year to year and the observed depletion of $\delta^{18}O$ with elevation.

In Chapter Three no evidence for basin-wide $\delta^{18}O$ elevation effects in snowpack or rainfall were observed and so the depletion observed in tributary data is probably more related to a changing dominance of rain to snow with increasing elevation. A two-component separation calculated using the average snow and rain signatures of -22.2 $^{o}/_{oo}$ and -13.2 $^{o}/_{oo}$, respectively, and the average Bow River headwater tributary baseflow value of -21.4 $^{o}/_{oo}$ ($n = 6$, $\sigma = 0.4^{o}/_{oo}$), then an approximate snow melt contribution of 91% is returned. This proportion may seem high but the headwater sample elevation of 1950 m a.s.l. is around the same height as the average annual basin-wide 0°C isotherm and the stream water sampled would have originated above this elevation. However, these observations are based upon average interannual conditions and there is likely to be a significant seasonal or year-to-year variation in baseflow composition.

From Figure 4.1 it is apparent that the annual tributary and river profile data are closely grouped except for the summers of 1998 and 1999. Summer and winter of 1997

and the winters of 1998 and 1999 display generally similar baseflow values. To explain this, it is necessary to consider the hydrometeorological conditions in the Bow Basin during this time period (see section 1.4). The years 1996, 1997 and 1999 were all deep snowpack years and all displayed above average river basin yield (see Figure 1.7 and appendix 1). During the El Niño year of 1998, however, there was an extremely shallow winter snowpack, which melted out rapidly due to warmer temperatures, and the overall basin yield was 12% below the long-term average (section 1.4). The relatively enriched August baseflow for 1998 (compared to 1999, see Figure 4.1) may reflect the heavier than average rain and snow $\delta^{18}O$ signatures for that year or it could also be simply due to an increased ratio of rainfall to snow melt in baseflow.

4.3.2 Profile EC Signatures

To investigate variations in dissolved solids content in summertime baseflow during years of different hydrometeorological conditions, EC was measured during the 1998 and 1999 Bow River August baseflow profiles at convenient sites along the river and major tributaries with minimal glacier coverage (Figure 4.2). From Figure 4.2, it is apparent that comparative tributary and river dissolved ion concentrations were higher during the summer of August 1999. This is particularly interesting given that the recessional discharges for the Bow at Banff on the day of sampling for 1998 and 1999 were 56 and 80 m^3s^{-1}, respectively. Thus, the higher dissolved solids content in the river occurred during increased flow. Two processes that may lead to a higher concentration of dissolved solids in 1999 summer baseflow are considered:

1) In Chapter Three, snowpack was observed to be acidic (average pH of 6.0) with the potential, therefore, to weather the ubiquitous carbonate material in the Bow Basin.

The basin snowpack depths for 1999 were approximately two times those of 1998 and thus there was likely a greater weathering potential in the basin for this year;

2) Melt contributions from small glacier coverages within headwater basins, would have been more likely during August 1998 than 1999, and would have likely led to a dilution of the groundwater EC signature.

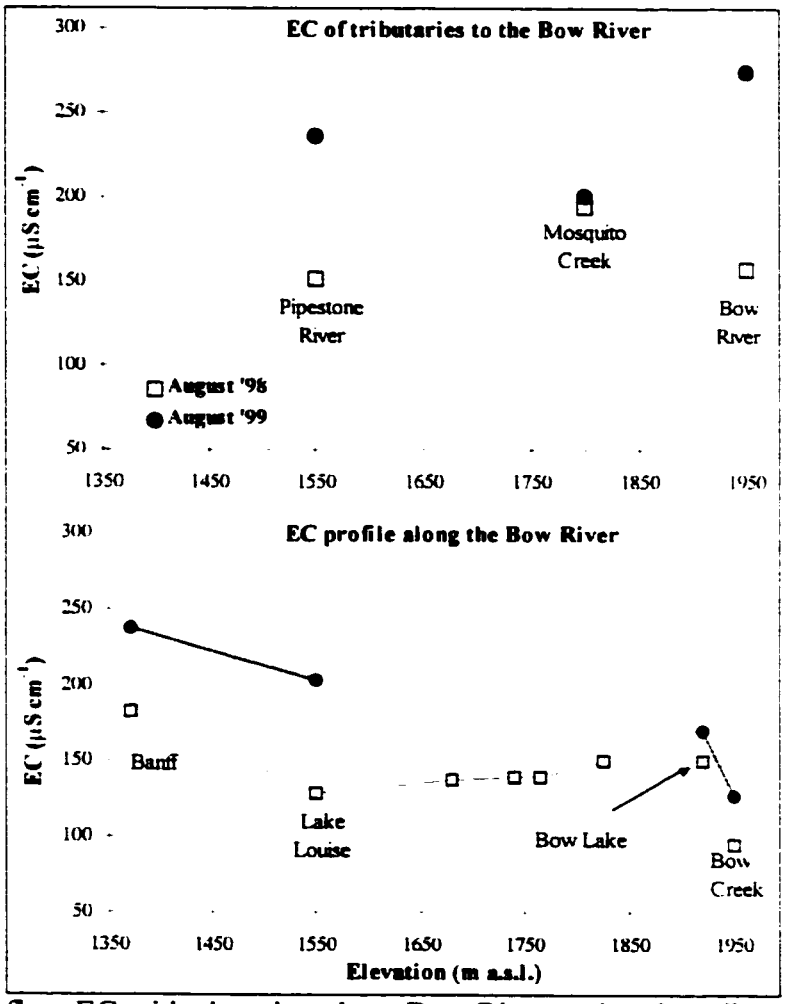

Figure 4.2 Baseflow EC with elevation along Bow River and major tributaries from Banff up to the headwaters. (Lines are for the purpose of illustration only.)

From the tributary EC data shown in Figure 4.2, there is no apparent elevational trend. However, in the river samples, it is clear that dissolved ion concentrations were greatest at the basin endpoint at Banff and lowest in the basin headwaters above Bow

Lake. However, it needs to be borne in mind that the headwater sample for the Bow River was taken from Bow Creek, a glacially fed stream with a strong melt signal and a relatively dilute dissolved solids content. The elevated baseflow EC for the basin endpoint at Banff was likely a function of longer groundwater and in-channel residence times, and reduced dilution from glacial melt inputs lower down in the basin.

The several in-channel samples taken between Bow Lake and Lake Louise during summer 1998 displayed a localised downstream dilution that appeared to disagree with the general basin-wide pattern of a downstream increase in EC. This was probably the result of dilute glacial melt contributions from the Wapta Icefields entering the river below the lake, thus reducing the dissolved concentration in the river. However, the reason for this initial high EC reading at the Bow Lake outflow (Figure 4.2) should be considered further, as lakes are an important hydrological feature within the Bow Basin.

The sample collected at Bow Lake outflow represents an amalgamation of several different water sources with a relatively long residence time in the lake (discussed in section 5.4). It is likely that a high proportion of the lake water is groundwater derived but some consideration of the dominant surface inputs must be made (see Figure 1.4 for a map of this area). The glacial stream flowing into the lake is typically heavily sediment laden and upon inflow loses energy leading to settling out of the sediment (there are other surface inputs to the lake but they are comparatively small and not gauged). The exact residence time from glacial inflow to outflow is unknown but a full turnover of the lake (given an average length, width, estimated depth and measured summer discharges of 4 km, 500 m, 40 m and 6 - 9 m^3s^{-1}) should take around 130 days. From a study by Smith (1981), it was found that during the summer, the cold glacial inflow (4 - 6 m^3s^{-1} during

summer) tended to flow across the thermally stratified lake as a shallow rightward-deflected interflow above the denser hypolimnion (at 4°C). Therefore the residence time of the dominant glacial inputs should be much less than 130 days, perhaps on the order of days to weeks. This time period is more than sufficient to allow a change in EC due to dissolution processes (e.g. Collins, 1995). Thus the rise in EC from dominant lake inflow (Bow Creek) to outflow is likely a function of surface inflow mixing with groundwater and continued dissolution of glacial melt water sediment content during transit.

4.4 Headwater Baseflow

4.4.1 Introduction

Thus far, some discussion of changing geochemical groundwater characteristics with elevation and season has been put forward but the influence of differing land covers has not been seriously addressed. For example, in the last section it was apparent that certain trends in geochemical signatures may exist at the larger basin scale, but over more localised areas the trends can be reversed; particularly in response to glacial melt inputs from small parts of the basin. In the Bow Basin, headwater geochemistry is thought to be largely influenced by the different landcover dominances from one side of the basin to the other: i.e. glacial on the west side and forest on the east side. In order to investigate the influence of land covers to groundwater and baseflow geochemistry two different sampling strategies were adopted. Firstly, samples were taken from headwater springs draining different land cover types. Secondly, longitudinal stream sample profiles were carried out along Mosquito Creek and Bow Creek during baseflow conditions (see Chapter One for a detailed overview of these sub-basins).

4.4.2 Geochemistry of Basin Springs

In the headwaters of the Bow Basin, summer baseflow is maintained either from glacial runoff (which will be investigated in the following section), direct input of groundwater along gaining water courses (including small lakes) or by springs issuing from a variety of landcovers and lithologies. The potential influence of landcover on baseflow geochemistry is investigated here by sampling groundwater springs from a variety of lithologies underlying the dominant landcover categories occurring in the lower reaches of headwater basins. Non-glacierised landcovers in the Bow Basin can be broadly lumped into two categories: bare ground and forest. This is a convenient (although not completely accurate) division of the landcover types, as the surface lithology from which such springs issue tends to vary from shallow organic soils in forested areas to mainly tills and rock material devoid of organics in areas of bare ground. It is thought the presence of organic soil structures combined with well-developed root systems and high biological demand for water in forest areas will result in significantly different hydrogeochemical properties than in areas devoid of vegetation.

During July of 1998, seven spring water samples draining till, soil, karst and talus lithologies were collected from forested and bare ground areas within the 1950 - 2150 m a.s.l. elevation band from Bow and Mosquito Creeks. There was difficulty controlling the timing of sample acquisition but at least all were collected prior to noon on the day of collection. These samples were analysed for EC, $\delta^{18}O$ and, in one case, tritium (see Table 4.2). Although this is a limited number of samples, this methodology enables a cursory examination of potential landcover influences on groundwater geochemistry.

location	Date	$\delta^{18}O$ (‰)	TU	EC ($\mu S\ cm^{-1}$)
Non-forested headwater spring water samples				
Bow Crk (till slope)				
	13-Jul-98	-19.4		176
Bow Crk (floodplain tills)				
	14-Jul-98	-19.1		224
Mosquito Crk (talus slope)				
	24-Jul-98	-19.9		88
Mosquito Crk (karst spring)				
	24-Jul-98	-20.4		176
Forested headwater spring water samples				
Bow Crk (soil and till slope)				
	13-Jul-98	-20.6		175
Bow Crk (talus slope)				
	31-Jul-98	-20.3		204
Mosquito Crk (karst spring)				
	12-Jul-98	-21.7	9.1	211

Table 4.2 Geochemistry of spring water samples from Mosquito and Bow Creek headwaters collected during July 1998.

From the EC data in Table 4.2, there is no evidence of a landcover influence to the dissolved ion content in groundwater issuing from springs. The highest and lowest EC levels in spring water were observed in floodplain tills of glaciogenic material and a talus slope, respectively. Of these two lithologies, the floodplain tills are associated with low hydraulic gradients and relatively low permeability thus leading to increased residence time. It is more likely, therefore, that varying lithology and residence times play a more important role in controlling the ionic chemistry of spring water.

From the $\delta^{18}O$ data in Table 4.2, springs issuing from forested areas tend to be relatively depleted (average = -20.9, σ = 0.7) compared to those discharging from open areas (average = -19.7, σ = 0.6). The sample populations are small and the difference between them of 1.2 ‰ is not significant at the 95% level (P = 0.08). However, if the data points are compared in terms of similar lithologies (i.e. tills, talus, karst), springs

issuing from forest areas are consistently more depleted. Perhaps suggesting that there may indeed be a land or vegetation cover influence to groundwater $\delta^{18}O$ signatures.

If it is assumed that summertime rain and spring snow melt are the major sources of groundwater recharge, then the simplest explanation of a systematic difference in the $\delta^{18}O$ signatures between landcovers would be a different mixing ratio of snow/rain in groundwater. Combining the observation in Chapter Three that summertime rain is generally enriched compared to snow, with the data in Table 4.2 suggests that the rainfall content in groundwater may be elevated in open areas and reduced in forest areas.

Forest canopies transfer rain to the ground by stemflow, canopy drip and throughfall. However, a potentially large proportion of rainfall tends to be intercepted and subsequently lost to evaporation. Exact figures on the relative proportions are not available for this region but values between 12% and 62% have been recorded from studies of upland conifer interception ratio (compiled by Newson, 1994). Therefore, the relative depth of rainfall reaching the ground surface during summer will probably be lower in forest areas. If the relative reduction in summertime rainfall reaching the ground in open areas is greater than the relative reduction in winter snowpack volume, then this process could lead to systematically heavier groundwater $\delta^{18}O$ signatures in open areas.

Another process that can lead to enrichment of the $\delta^{18}O$ signature in water is evaporation (e.g. Dansgaard, 1964). Evaporation in a soil profile can influence groundwater up to several metres below the ground surface (Hillel, 1982), and so it is plausible that evaporation could also influence the $\delta^{18}O$ signature of groundwater in some areas. Ground surface heating and turbulent boundary layer conditions will likely produce conditions more favourable for shallow soil moisture evaporation in open areas rather

than canopy covered areas (e.g. Oke, 1995). Although transpiration processes will inevitably be more active in forest areas (thus resulting in relatively high fluxes of groundwater loss) this process alone should not directly alter the isotopic signature of groundwater. However, direct evaporation of groundwater, either in the vadose zone or from a shallow water table, could lead to isotopic enrichment and, therefore, contribute to the observed difference in $\delta^{18}O$ signature between forest covered and open areas.

4.4.3 Headwater Stream Discharge Profiles

4.4.3.1 Introduction

To investigate the effect of landcover features on baseflow composition within each headwater basin, samples of basin endpoint, headwater and all surface tributaries and major groundwater sources were collected during summer baseflow conditions (details below). For each of these longitudinal stream profiles, discharge was measured in-stream either by dye dilution or area-velocity techniques. For the dye dilution measurements a 20% concentration of Rhodamine WT was continuously injected for at least one hour into the main headwater channel. Downstream flow samples were collected above and at least 50 m below surface tributaries to the channel, and were analysed for dye concentration on a Turner Designs field fluorometer within 24 hours of collection. Discharge was calculated as a function of volumetric dilution. Manual area-velocity measurements were undertaken using a Marsh McBirney electromagnetic flow meter, 30 m tape and a metre stick. Where two surface tributaries were close together, one discharge measurement would be made between the two. The catchment boundaries, major landcovers and geological features associated with each tributary were delineated so that areal hydrologic yield could be calculated and the influence of sub-basin characteristics on geochemical

signatures could be assessed. For a more in depth description of the two headwater basins see section 1.3.2.

As mentioned in Chapter One, Bow Creek and Mosquito Creek were chosen for study due to their differing landcover characteristics and because they are both representative of the two major basin type end-members; i.e. highly glacierised and virtually non-glacierised. Many of the reasons for investigating these two kinds of headwater basin have been outlined previously but here the differences in "baseflow" conditions will be assessed and quantified. "Baseflow" has been expressed in inverted commas because it is the baseflow at the larger scale of the Bow Basin at Banff that is of interest. It is obvious that when investigating end-member headwater basins of both non-glacierised and glacierised coverages that the baseflow conditions will differ and occur during different hydrometeorological conditions. In glacial basins, conditions that lead to baseflow elsewhere tend to result in high flow from melt inputs. For such basins, "baseflow" occurs, therefore, when melt is suppressed during cold periods or precipitation. In this section, relative contributions of these various baseflow components will be investigated.

4.4.3.2 Bow Creek

Only one longitudinal stream profile (Figure 4.3) was sampled on Bow Creek and this was on the south side of the basin, known as "Bow Hut Creek" (basin characteristics described in section 1.3.2.2). Sampling was carried out in the early morning of July 31st, 1998 during cool cloudy conditions and approximate minimum diurnal flow. Discharge measurements along the stream profile, using dye dilution, were made at the headwater, along Bow Hut Creek both upstream and downstream of all main surface tributaries, and at the basin endpoint so that the areal yield of each sub-basin could be calculated (stream

profile, tributaries, landcovers and stream discharges illustrated in Figure 4.3). Dye dilution techniques were used, as the stream was too steep and turbulent in parts for area-velocity techniques. In the centre of the basin the stream cut through a dolostone gorge that was difficult to access for much of its length and so discharge was measured at either end. All observed surface streams were also sampled for EC and subsequent $\delta^{18}O$ analyses. Thus, the hydrological yield and geochemical signatures for each sub-basin could be combined and then compared with the basin endpoint to assess the influence of hydrologically significant landcover features (see Table 4.3). (Landcover influences on basin hydrological yield will be discussed in section 4.4.3.4). Direct groundwater discharge to the channel could not be measured but could be inferred by summing up the surface inputs and subtracting from the basin endpoint discharge.

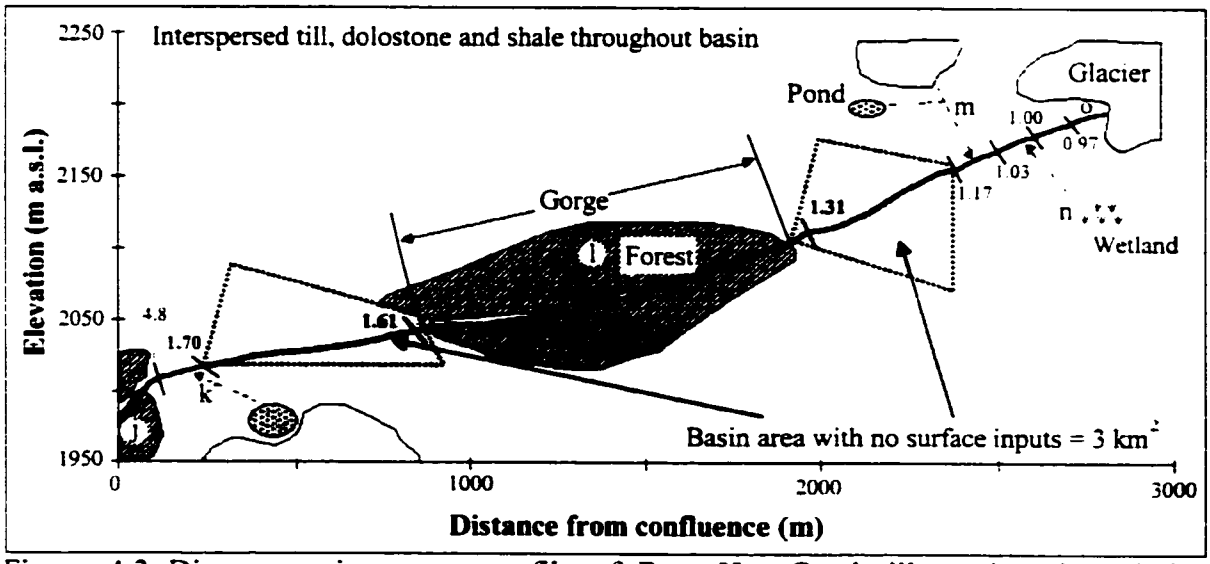

Figure 4.3 Diagrammatic stream profile of Bow Hut Creek illustrating the relative positions of major proximal landcovers, sampled tributary inputs (dashed arrows) and raw discharges. (Elevations only apply to the stream profile – thick black line.)

The EC data for each of the Bow Hut Creek tributaries (letters "k" to "o" in Figure 4.3), presented in Table 4.3, suggested that the streams could be divided into two

categories: those with ECs around 100 μS cm^{-1} and those around 200 μS cm^{-1}. It was clear from the glacier cover data that those tributaries displaying lower EC contained a significant snow and ice melt dilution signature. The higher EC category of surface input was dominated by relatively well-developed soils within the forest and alpine meadow areas. Therefore, this signature was indicative of groundwater that had not undergone melt dilution to the extent of the glacial streams.

The $\delta^{18}O$ signatures did not indicate any systematic landcover relationship and, in general, the values from all the locations were similar. Of note, however, is that the signatures tended to be enriched compared to snow or ice signatures measured in this area, which suggests that there was some mixing of summertime rainfall in baseflow draining from this headwater basin. (It was assumed that due to rapid melt water transit times and cold temperatures, evaporative enrichment of in-stream glacial melt water would have a minimal impact on $\delta^{18}O$ signature.) Given that all three end-member components of snow, ice and rain contribute to baseflow in this basin, no tracer-based separation of the relative proportions could be performed with the data available.

Bow Hut Creek Longitudinal Profile							
Summer - 31st July 1998	**Elev.**	**Basin area**	**Glac. Area**	**Discharge**	**Areal Yield**	**EC**	**$\delta^{18}O$**
Surface tributaries:	**(m a.s.l.)**	**(km^2)**	**(km^2)**	**(m^3s^{-1})**	**(mm d^{-1})**	**(μS cm^{-1})**	**(‰)**
o - Headwater below icefield	2195	4.8	2.2	0.97	18	99	-20.0
n - Alpine meadow & wetland	2179	1.2	0.1	0.03	2	205	-20.2
m - Glacial runoff and pond	2164	3.0	0.5	0.14	4	93	-19.9
l - Forest springs around gorge	2057	2.3	0.0	0.30	12	204	-20.3
k - Bow Waterfall Creek (glacial & pond)	2012	10.6	5.2	3.10	25	95	-20.4
j - Basin endpoint	**1981**	**24.9**	**8.0**	**4.80**	**17**	**109**	**-20.2**
Remaining non surface inputs - calculated		*3.0*		*0.3 (~0.7,-0.3)*	*8*	*201*	

Table 4.3 Sampled and calculated hydrogeochemistry for Bow Creek profile with hydrological yield and glacial coverage for each sample point sub-basin.

By summing the baseflow from each of the measurable tributary inputs and comparing to the basin endpoint, it was found that there was a shortfall of 0.26 m^3s^{-1}.

Performing an error analysis of individual profile discharges by assuming a measurement uncertainty level of ±10% suggests that the actual discharge shortfall lies in the range 0 to 1.0 m^3s^{-1}, and the 0.26 m^3s^{-1} is not significantly different from zero. However, applying a simple mixing model calculation to the tributary and basin endpoint discharges and ECs, and assuming that any missing discharge would have a characteristic groundwater signature of 200 $\mu S\ cm^{-1}$, returns a discharge of 0.3 m^3s^{-1}. The observation that this mixing model calculation for groundwater input matches that calculated from the raw stream discharge measurements, increases confidence in the profile discharges and yield data. Applying the estimation of direct groundwater contribution to the stream channel (0.3 m^3s^{-1}) to those basin areas lying between surface tributary inputs (3 km^2) suggests that the instantaneous yield for the remaining basin area was around 8 mmd^{-1}.

4.4.3.3 Mosquito Creek

For Mosquito Creek (section 1.3.2.1), four longitudinal stream tributary sample profiles were carried out (tributary locations on Figure 4.4). Three were conducted in 1998: one each during summer for the north and south branches of the main Mosquito Creek and a third on the north branch in the fall (discussed in section 4.4.3.4). Each sample set was collected following at least one full day without rain. The total rain depths collected at Bow Summit weather station (14 km away) during the prior three days were 0.3, 0.0 and 0.8 mm, respectively (average daily precipitation here is approximately 2 mm). The first discharge profile utilised a dye dilution technique with a continuous injection of 20% Rhodamine WT into the headwater stream of the north branch ("g" on Figure 4.4). Half an hour following the beginning of dye injection, flow sampling commenced at the headwaters with all downstream locations visited in turn (Figure 4.4).

Samples were collected at least 50 m downstream of tributary inputs, and the basin endpoint at "a" was reached two hours later. From observed average stream cross-section velocities of > 1 ms^{-1}, it was estimated that the average time of travel from headwater to confluence (~ 4.5 km) would not exceed 75 minutes, and so two hours was considered sufficient for full mixing of the dye along the stream profile.

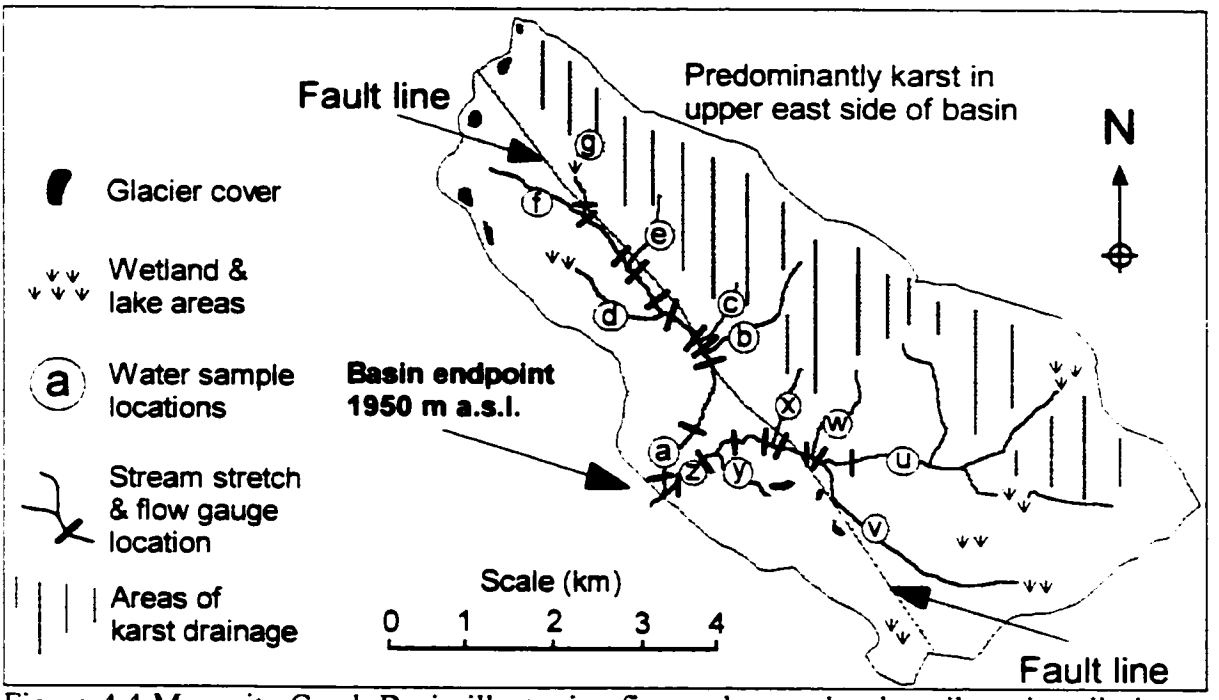

Figure 4.4 Mosquito Creek Basin illustrating first and second order tributaries, discharge measurement and sample locations, areas of karst, wetlands, glaciers, and a thrust fault.

For south branch summer and the north branch fall samples, area-velocity measurements were employed. The measurement technique was changed after the first run on the north branch, as dye dilution was thought not to be an appropriate technique for a headwater stream that may be susceptible to effluence or hyporheic flows. Tributary discharge was therefore estimated by measuring as close to the upstream and downstream side of the tributary inputs as possible. Stream profile discharges are illustrated in Figure 4.5. EC and $\delta^{18}O$ samples were taken directly from the first order tributary inputs and all

sub-basins were divided into the following categories based on their dominant surface hydrological characteristics: wetland, glacial, karst, mixed karst (a mixture of bedrock types) or combinations of the above (Figure 4.4 and Table 4.4).

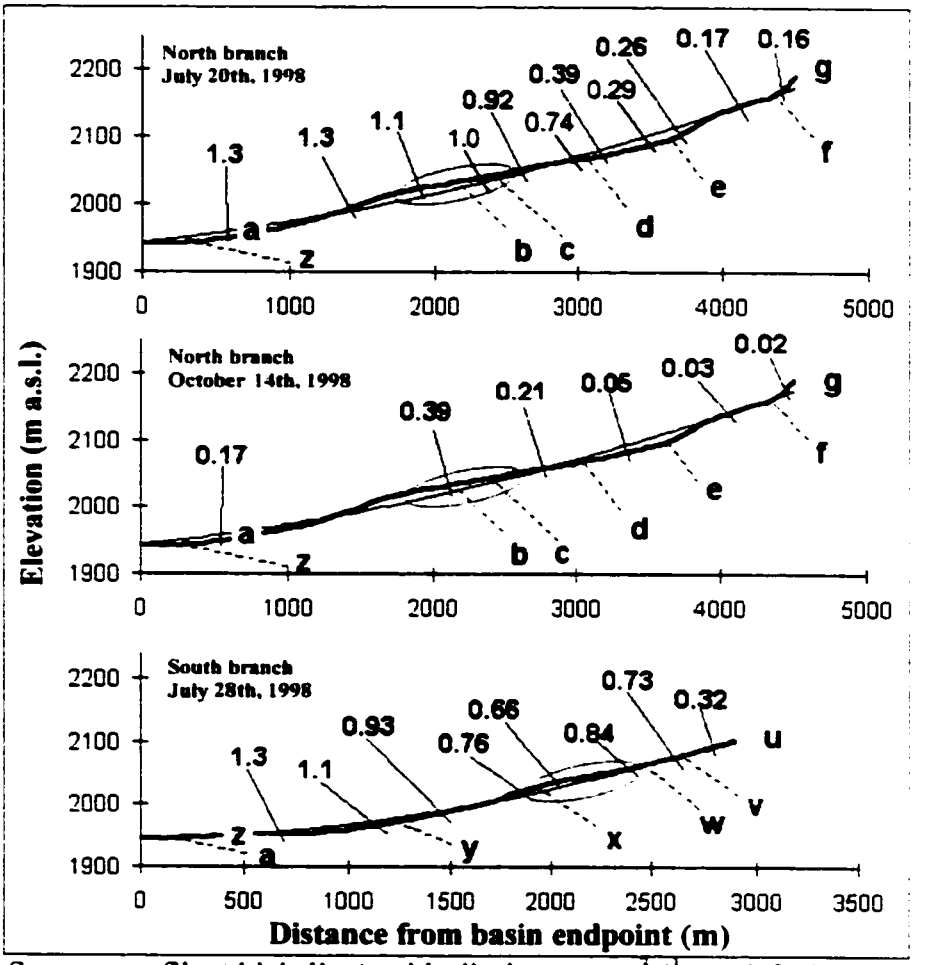

Figure 4.5 Stream profile (thick line) with discharges (m^3s^{-1}) and fault line intersection zone (circled). Thin line = quadratic regression curve to illustrate depressions and rises in the profile. (Elevations apply to the stream profile. Letters indicate sub-basin tributaries)

Mosquito Creek north branch stream tributaries were sampled again during late summer of 1999 to provide a comparison with the data collected in 1998. Unfortunately, these samples were collected one day following a rain event and thus did not constitute true basin baseflow. In addition, discharge for the longitudinal stream profile could not be measured and so only tributary EC and $\delta^{18}O$ have been presented (Table 4.5).

North Tributary Hydrochemistry						
Dominant surface hydrology of tributary sub-basins	**Elevation (m a.s.l.)**	**Basin area (km^2)**	**Sub-basin Q (m^3s^{-1})**	**Areal Yield (mmd^{-1})**	**EC (μScm^{-1})**	**$\delta^{18}O$ (‰)**
Summer - 20th July, 1998						
g - Wetland and glacial	2190	1.8	0.16	8	116	-20.3
f - Glacial	2190	0.6	0.01	1	288	-20.1
e - Karst	2092	2.8	0.03	1		
d - Wetland and glacial	2063	4.2	0.35	7	160	-20.2
c - Karst	2042	0.4	0.09	5		-21.5
b - Karst	2027	2.7	0.08		221	-21.5
a - North branch endpoint	**1950**	**16.5**	**1.3**	**7**	**170**	**-20.4**
Net groundwater input			*0.6 (± 0.5)*			
Fall - 14th October, 1998						
g - Wetland and glacial	2190	1.8	0.02	1	175	-20.2
f - Glacial	2190	0.6	0.01	1	242	-19.7
e - Karst	2092	2.8	0.02	1	224	-20.5
d - Wetland and glacial	2063	4.2	0.16	3	204	-20.2
c & b - Karst	2035	3.1	0.18	5	227	-20.0
Stretch of stream effluence	~ 2000		*-0.22*			
a - North branch endpoint	**1950**	**16.5**	**0.17**	**1**	**222**	**-20.7**
South Tributary Hydrochemistry						
Summer - 28th July, 1998						
u - Karst and wetland	2103	8.4	0.32	3	190	-20.7
v - Wetland and glacial	2057	5.1	0.41	7	145	-20.0
w - Mixed karst	2039	0.8	0.11	12	284	-20.9
Stretch of stream effluence	~ 2000		*-0.18*			
x - Mixed karst	1996	0.5	0.10	17		-21.7
y - Glacial	1960	0.8	0.18	19	191	-20.1
z - South branch endpoint	**1950**	**18.5**	**1.3**	**6**	**173**	**-20.5**
Net groundwater input			*0.4 (± 0.4)*			

Table 4.4 Sample hydrogeochemistry for 1998 Mosquito Creek longitudinal profiles. (Net groundwater input error assumes ±10% uncertainty in discharge measurements.)

Mosquito Creek's north and south branch endpoint baseflow discharge, EC and $\delta^{18}O$ readings collected during the July 1998 profiles were virtually identical (Table 4.4), suggesting that these two sub-basins are hydrologically similar. In general, the isotope ratios for Mosquito Creek are slightly depleted compared to Bow Creek with slightly higher EC readings. Higher EC readings for Mosquito Creek probably indicate a dominance of groundwater flow pathways in this basin, whereas a higher proportion of the runoff in Bow Creek is glacial melt dominated and thus comparatively dilute (in Table 4.3 baseflow EC was 100 $\mu S\ cm^{-1}$ lower on glacierised tributaries than non-glacierised).

The difference in $\delta^{18}O$ signature of 0.3 $^{o}/_{oo}$ between the endpoint baseflow samples at Bow and Mosquito Creeks could also be a function of glacier cover. For example, if all summertime baseflow signatures for glacierised and non-glacierised tributaries (Tables 4.3 and 4.4) are compared, it is found that the average $\delta^{18}O$ values of -20.1 $^{o}/_{oo}$ ($n = 8$, $\sigma = 0.2$) and -21.0 $^{o}/_{oo}$ ($n = 7$, $\sigma = 0.6$) are significantly different ($P = 0.009$). However, this observation may appear counter-intuitive, as glacial runoff, which would be expected to have a high snow and icemelt content is significantly more enriched than groundwater dominated runoff, which might be expected to contain a greater rainfall proportion. These observations suggest, therefore, that glacierised runoff during baseflow conditions probably contains an appreciable rainfall component, whereas groundwater baseflow in non-glacierised basins is dominated by snow melt (this issue will be revisited in the following chapter when investigating a rainfall event in more detail – section 5.2.6.).

The high elevation hanging glaciers in the headwaters of Mosquito Creek are very small and are almost permanently out of direct sunlight. However, during the summer of 1998, ice exposure was more extensive than during average years leading to increased glacier melt runoff in the eastern slope basins of minimal glacier coverage. Tributaries containing glacier cover were not always the highest yielding, however, and sub-basins containing karst and wetland areas often displayed comparable areal yields (Table 4.4). Water sampled from karst tributaries during the summer tended to be isotopically lighter than other stream tributaries (Tables 4.2, 4.4 and 4.5) indicating a greater snowmelt proportion or reduced enrichment through evaporation. Sub-basins containing wetland and glacial coverages, therefore, were likely more susceptible to evaporation processes or

increased contributions of rainfall. (Elevation ranges are similar for the sub-basins and so isotope/elevation effects would likely not cause the differences observed.)

Location of surface tributaries:	Elevation (m a.s.l.)	Basin area (km^2)	EC ($\mu S\ cm^{-1}$)	$\delta^{18}O$ ($^o/_{oo}$)
Headwaters (above "d")	2070	6.9	141	-22.4
d - Wetland and glacial	2063	4.2	122	-21.9
b - Karst	2027	2.7	178	-22.4
GW seep (forest spring)	1990		195	-22.1
a - Basin endpoint	*1950*	*16.5*	*146*	-22.2

Table 4.5 Sample geochemistry for Mosquito Creek north branch, 7th August 1999.

Another important observation regarding the karst tributary inputs to Mosquito Creek is that the difference in baseflow discharge from July to October was relatively low compared to direct groundwater and other surface inputs to the main channel (Table 4.4). For the Mosquito Creek north profiles, the baseflow runoff dropped by almost an order of magnitude from summer to winter. However, the runoff from the karst fed gulleys (b, c and e in Table 4.4) changed very little with almost identical areal yields and were also observed to be still flowing at the end of the following winter (May, 1999). The absolute discharges were not high and there may be some error in the measurements (perhaps 50% either way) but the fact that these tributaries displayed similar yields over three months apart despite large variations elsewhere demonstrates that fluctuations in runoff from these sub-basins is minimal. It may be, therefore, that such karst areas are responsible for maintaining a significant amount of the year round baseflow in such headwater basins.

The enrichment in the $\delta^{18}O$ signature on karst tributary "b" of 1.5 $^o/_{oo}$ from July to October (Table 4.4) indicates a contribution from summertime rainfall, and demonstrates that the signature does vary seasonally as a result of changing flow component proportions within the aquifer. From the observations of a depleted $\delta^{18}O$ signature in July following spring melt in April, and an enriched signature in October following

summertime rain, it is likely that the aquifer response time is at least three months. If this is the case, then the apparent stability in hydrological yield over a similar time period indicates that the storage potential within these aquifers must be large. These observations are somewhat concurred in a study by Smart and Ford (1986) conducted in the Castleguard Meadows karst aquifer about 100 km to the northwest and in the same geological formation. Their results indicated that flow from the "Red Spring" aquifer of the Castleguard system had an approximate storage capacity of 250 000 m^3 and a half-life of 55 days. The karst areas in Mosquito Creek Basin do not appear to have reached the level of development observed at Red Spring, and surficial deposits and landslide material probably cover many karst resurgences. It is likely, therefore, that the permeabilities of the Mosquito karst aquifers are lower and this may lead to longer residence times.

From Table 4.5, it is apparent that the stream EC values for summer 1999 on Mosquito Creek north are lower, and $\delta^{18}O$ more depleted than during the summer of 1998. Both of these observations reflect the greater snowpack in the basin during 1999, thus leading to increased dilution or reduced residence times and a greater proportional snowmelt contribution to baseflow runoff. Of note is that during the day prior to sampling, a rainstorm occurred (0.9 mm at Bow Summit) and the stream levels in Mosquito Creek during sample collection were noticeably swollen as a result. The $\delta^{18}O$ value of a bulk rainfall sample collected at the basin outlet was -12.8 $^{o}/_{oo}$, which is near the basin-wide average rainfall signature and significantly heavier than any of the samples in the stream the following day (~ -22 $^{o}/_{oo}$). The observation that runoff may be isotopically depleted during years of deep snowpack, even following rain events, could

be further evidence that in this highly forested basin, rainfall does not contribute much to baseflow or runoff. (Further discussion of this issue will be provided in the following chapter, where hydrological events will be investigated in more detail.)

4.4.3.4 Headwater Basin Areal Yields

Relative basin yields of groundwater and surface runoff contributions for Bow and Mosquito Creeks are presented in Table 4.6. The areal yield of groundwater contributing directly to the stream channel was calculated by combining the net groundwater discharge with the potential area of the basin from which this contribution could have originated. Net groundwater discharge was estimated from the longitudinal profile endpoint discharge minus the sum of all the other measured inputs. The area of direct groundwater contribution to main channel discharge was considered to occur in the areas between surface tributary inputs, and was therefore defined as the total basin area minus the tributary sub-basin areas. It should be noted that discussion of groundwater areal yield does not pertain to all groundwater inputs to runoff in the basin, only those occurring as direct input to the main drainage channel between discharge measurement locations.

The Bow Hut Creek Basin baseflow was dominated by surface inputs to the stream, with 88% of the flow volume entering the stream directly from tributaries. This is despite the measurements being taken in the morning when no melt or rainfall events were taking place. For the visible surface streams, draining sub-basin areas totalling 19.6 km^2, the areal yield was 19 mmd^{-1}. In contrast, the less obvious groundwater yield in areas other than surface tributaries (3.0 km^2) was 8 mmd^{-1}. Thus, for the highly glacierised Bow Hut Creek Basin, inputs to the stream during early morning summer baseflow were dominated both volumetrically and areally by surface runoff. Although a relatively high

groundwater areal yield was found in the forested gorge area (12 mmd^{-1}, Table 4.3), the general basin-wide dominance of surface runoff during baseflow is the result of glacial melt water storage (in both glacial and lacustrine systems) and subsequent release following the termination of melt.

Location & Date	Area (km^2)	Discharge (m^3s^{-1})	Areal Yield ($mm\ d^{-1}$)
Bow Hut Creek Areal Yield			
Summer - 31st July 1998			
Surface Tributaries	19.6	4.5 (+0.3, -0.7)	**20** (17 - 21)
Non surface inputs to channel	3.0	0.3 (+0.7, -0.3)	**8** (0 - 29)
Total	24.9	4.8 (±0.5)	17 (15 - 18)
Mosquito Creek North Areal Yield			
Summer - 20th July, 1998			
Surface Tributaries	12.5	0.8 (+0.5 -0.1)	**5** (5 - 9)
Non surface inputs to channel	4.0	0.6 (+0.2 -0.5)	12 (2 - 17)
Total	16.5	1.4 (±0.1)	7 (6 - 8)
Fall - 14th October, 1998			
Surface Tributaries	12.5	0.4 (±0.1)	2 (2 - 3)
Losses in area of fault line	2.6	-0.22 (±0.06)	
Total	16.5	0.17 (±0.02)	1
Mosquito Creek South Areal Yield			
Summer - 28th July 1998			
Surface Tributaries	15.6	1.1 (+0.3, -0.1)	**6** (6 - 8)
Non surface inputs to channel	2.4	0.4 (+0.1, -0.4)	**14** (0 - 18)
Losses in area of fault line	0.5	-0.18 (±0.15)	
Total	18.5	1.3 (±0.1)	6 (6 - 7)

Table 4.6 Relative headwater basin areal yields of surface and groundwater (non-surface) contributions to main channel. Maximum and minimum yields calculated assuming ± 10% uncertainty in raw profile discharge measurements.

In northern temperate mid-latitudes, the period around late July corresponds to high glacial melt storage and baseflow discharges (Sugden and John, 1993; and see section 5.3 for seasonal runoff data in this basin). Therefore, the low groundwater/surface water runoff ratio of 0.3/4.5 (or 7%) is no surprise and is a direct reflection of the high proportion of glacier cover in the Bow Creek Basin. At this time of the year, the baseflow areal yield for the entire Bow Basin above Banff was between 2 and 3 mmd^{-1}, with the annual maximum of approximately 6 mmd^{-1} during peak annual snowmelt runoff in late May. These values are low compared to the instantaneous glacierised headwater baseflow

yield of ~17 mmd^{-1}, indicating that during summer baseflow conditions at Banff, the glacierised headwaters may be disproportionately important in maintaining runoff (this issue will be returned to later when investigating seasonal areal yields in section 5.3.2). The groundwater yield also appeared to be high with a value (~ 8 mmd^{-1}, Table 4.6) close to that for the entire basin during peak annual runoff (~ 6 mmd^{-1}). This observation suggests that groundwater contributions from headwater regions without glacier cover may also be hydrologically important at the larger basin scale.

In Mosquito Creek Basin, the reduced glacial coverage was evident in the comparatively low July discharges and basin baseflow areal yields measured in both the north and south sub-basins. The overall basin baseflow yields for Mosquito Creek (~ 6 – 8 mmd^{-1}) were approximately 35% those measured on Bow Hut Creek (~ 17 mmd^{-1}). However, the summertime baseflow yield on Mosquito Creek was greater than that of the Bow Basin above Banff (~ 2 mmd^{-1}) despite similar landcover proportions. This difference between headwater baseflow yields and the Bow Basin baseflow yield suggests that the flux of direct groundwater contribution to flow along gaining watercourses was greater in the headwaters during the summer of 1998. This is likely a function of increased levels of precipitation (snow and rain) and reduced actual evapotranspiration losses in the headwaters.

The summertime baseflow yields from remaining headwater areas not contributing to Mosquito Creek's surface tributaries were estimated to be around 12 and 14 mmd^{-1} on the north and south tributaries, respectively (Table 4.6). These groundwater yields were very high and there is the possibility of error in these calculations (Table 4.6). If these high yields are reasonable, however, they suggest that these inputs to the stream may not have

originated from within the associated surface watershed. These high groundwater yields may provide evidence for a complex sub-surface drainage system, where groundwater is transported across surface watersheds. In the headwaters of Mosquito Creek, such drainage systems could be associated with karst, fault lines or the tendency for geological beds to dip downwards to the southwest. However, higher groundwater yields than observed at the basin endpoint could also indicate that at the larger basin scale, losses of stream flow to ground could be reducing overall basin yield.

From the raw profile discharge data displayed in Figure 4.5 it is apparent that in-channel discharge appeared to drop by approximately 0.2 m^3s^{-1} over short stream sections on both the south branch during July and on the north branch during October (see also Table 4.4 and 4.6). There was no evidence of a drop in discharge on the north branch during July but due to the dye dilution technique used, any reduction in flow could not have been detected. It is difficult to quantify the potential level of error in individual area-velocity measurements but given the less than ideal stream channel conditions for this technique, the error is likely larger than the 10% often assumed. However, considering that the apparent drops in discharge exceeded 20% on the south branch and 50% on the north branch, and that in both cases the two upstream measurements exceeded the downstream measurements, there is reasonable confidence that discharge actually did drop in the areas observed. These observations are particularly interesting, as the combined surface tributary inputs to the south branch stream during the summer were less than the endpoint discharge, indicating that there was a net input of groundwater to the channel: i.e. the stream channels experienced net influent (gaining) flow conditions (Tables 4.4 and 4.6).

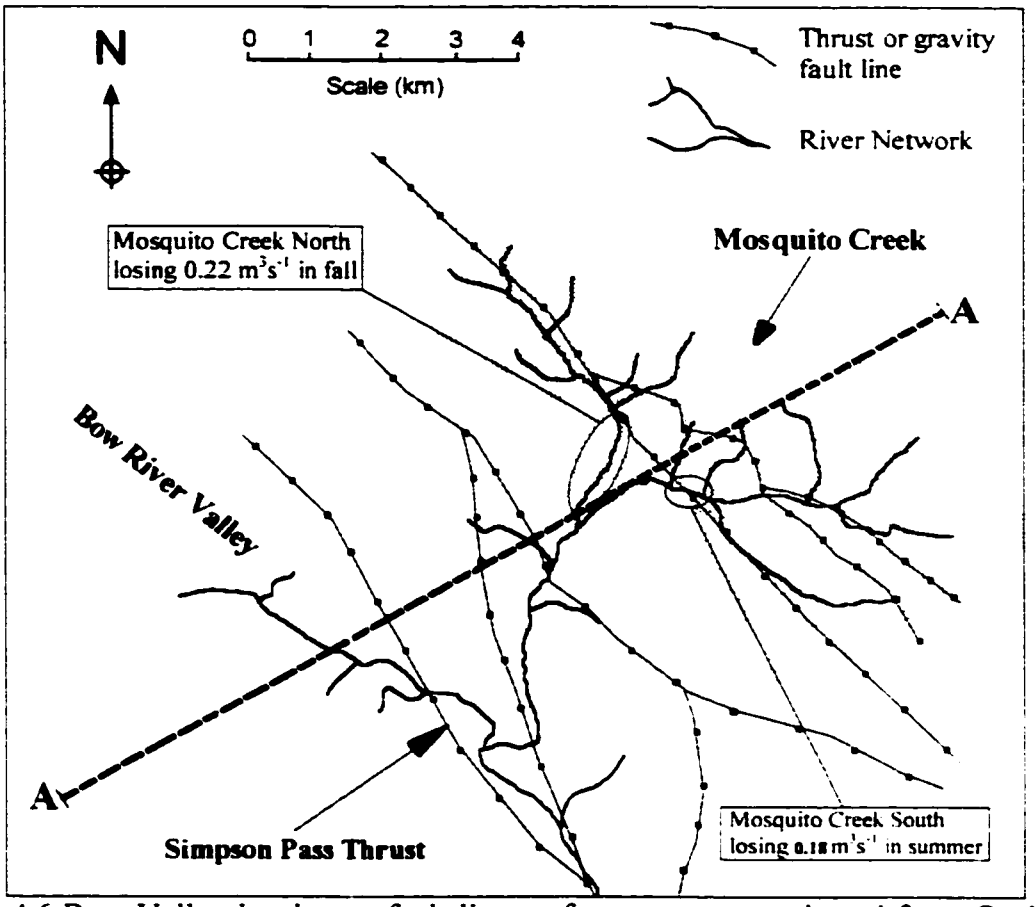

Figure 4.6 Bow Valley headwater fault line surface exposures, adapted from Geological Survey of Canada map 1464A (Hector Lake). (Cross-section A-A shown in Figure 4.7).

From Figures 4.5 and 4.6, it is apparent that the stretch of stream flow loss approximately coincided with a thrust fault and a localised convexity or "hump" in the stream profile. It is possible, therefore, that such fault line and stream intersections may be hydrologically important either in terms of: a) directly removing flow from the channel and transferring it elsewhere; b) causing the localised convexity within the valley profile and forcing the stream channel above the local water table; or c) altering the fabric of the local bedrock (perhaps increased fracturing) thus increasing local bedrock permeability resulting in increased groundwater infiltration, transient storage and hyporheic flow. It should be noted that this fault surfaces within a region dominated by massive quartzitic (Gog group) sandstone beds and is not associated with karst.

The simplest explanation for the stream water losses would probably be that the convexity in the stream profiles leads to a localised rise of the stream channel above the local water table. This could lead to a loss of flow from the stream channel to bypass flow in the hyporheic zone, which has been observed to occur in stream stretches of 10s of metres in small mountainous catchments (e.g. Harvey and Bencala, 1993) to several km in more lowland environments (e.g. Fernald *et al.*, 2001). It should be noted that the measured loss of discharge on Mosquito Creek in October occurred at the basin endpoint over 1 km downstream of the localised convexity in the profile, and therefore it cannot be ascertained if this discharge loss coincided exactly with the channel convexity. However, given that the observed discharge loss on the south branch during July occurred over a short stream stretch (< 500 m), it is thought likely that both north and south branch discharge losses were localised. For a channel length of 500 m with a wetted perimeter of 4 m (the approximate channel conditions on both branches in the area of effluence), a vertical infiltration of 0.2 m^3s^{-1} equates to a relatively high hydraulic conductivity (K) of approximately 10^{-4} ms^{-1}. Such a high K value during both summer and fall baseflow is suggestive of a permanent hydrological "sink" and could be due to losses of water to the upthrust fault intersecting the streams in the vicinity of the apparent flow losses.

The thrust fault running through Mosquito Creek basin eventually links up with other fault lines within Bow Valley (see Figures 4.6 and 4.7). Although no hydrogeological studies have been carried out to investigate the hydrological impact of fault lines in this area, faults are known to have the capacity to drain water from the surface and act as preferential conduits of groundwater flow (Stone, 1999). Intuitively, this is thought unlikely here due to the fault and stream intersections occurring at low points along the

fault's surface exposure, and therefore, if it were acting as a preferential flow conduit it would be thought more likely to discharge water into the stream rather than remove it. However, if fault line recharge is occurring, faults could act to drain water from the headwaters and transfer it down gradient ultimately to resurge at a lower fault line exposure at a much later date.

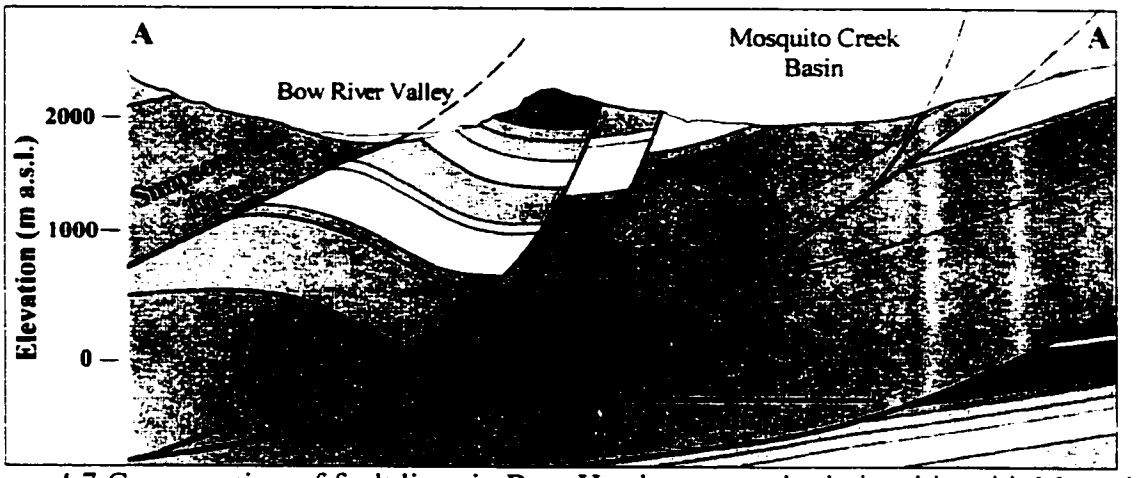

Figure 4.7 Cross section of fault lines in Bow Headwaters and relationship with Mosquito Creek (adapted from Geological Survey of Canada map 1464A section 7).

4.5 Groundwater Wells

4.5.1 Introduction

The baseflow of most interest in this study is that component which is maintained by saturated zone groundwater. Therefore, in order to corroborate or dismiss some of the above findings and suggestions, and provide greater insight into the seasonal geochemical characteristics of basin baseflow, it is necessary to investigate the groundwater that feeds it. For this purpose, three groundwater wells in the main valley of the Upper Bow Basin along with a perennial hard rock spring in Peyto Basin and a small soil water (MCSW) well in Mosquito Creek Basin were periodically sampled for $\delta^{18}O$, EC and Tritium (see Figure 4.8a).

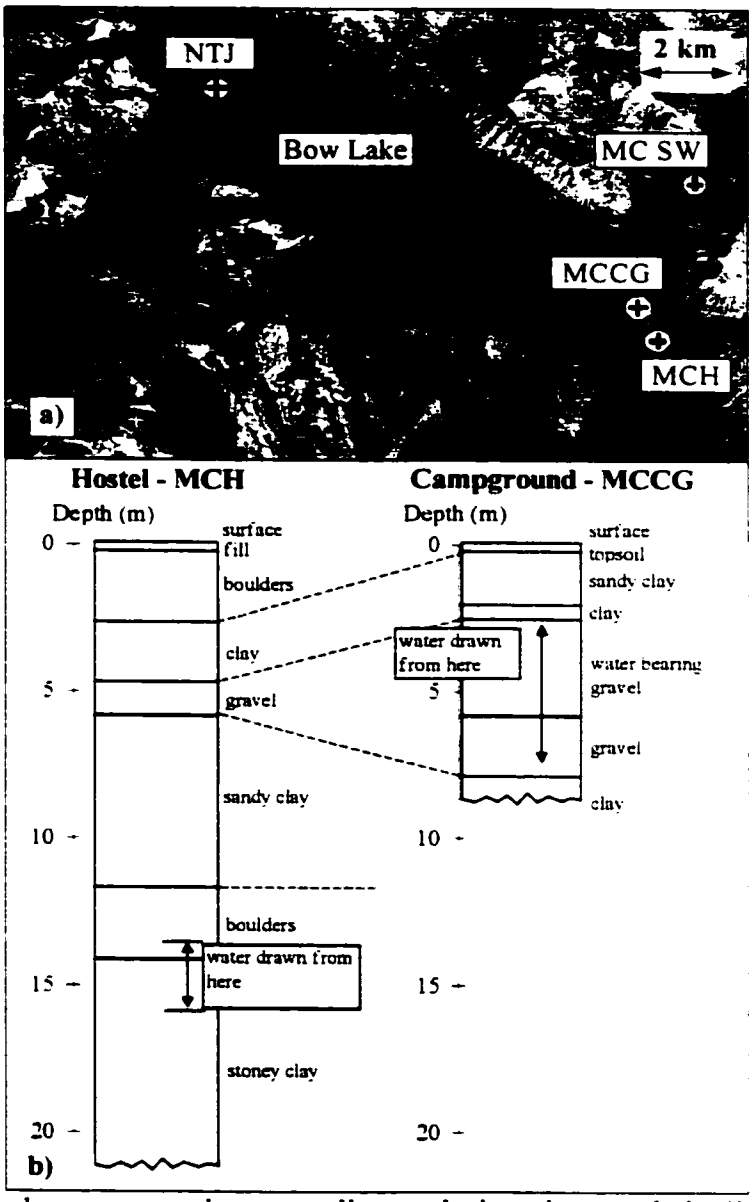

Figure 4.8 (a) Headwater groundwater well sample locations and (b) lithology for two wells near Mosquito Creek in the Bow Valley (lithological data provided by Alberta Environmental Protection well log reports).

Two of the wells were located near the Mosquito Creek confluence with the Bow River: one at Mosquito Creek Hostel (MCH) and one at a Banff National Park Campground (MCCG). These two wells were hand pump operated and approximately 100 m apart but tapped different depths and lithologies (Figure 4.8b). The third well was located at Num-ti-jah Lodge adjacent to Bow Lake at the confluence of Bow Creek and

the Bow River. Unfortunately, the well log records for this privately owned well were not available but it is known that deep glacial tills dominate the lithology in this area. All groundwater well samples were collected between 1800 and 2000 m a.s.l. and, therefore, no inferences about elevation patterns can be made.

4.5.2 Groundwater Well $\delta^{18}O$ Signatures

Seasonality in groundwater isotopic signatures is clearly demonstrated in Figure 4.9. During years of heavy snowpack, both deep groundwater (5 to 20 m) and perennial spring water have a seasonality that leads to the lightest signatures in mid to late summer. This is thought to be reflective of the infiltration of snowmelt that occurred approximately three months previously. From these observations, it would appear that groundwater maintained summertime baseflow in deep snowpack years would be isotopically most depleted during the month of August. This corroborates the observed depletion of $\delta^{18}O$ in the Bow Valley summertime baseflow profiles during 1999 (Figure 4.1a), and suggests that patterns observed in groundwater well and spring water may assist in characterising the river baseflow.

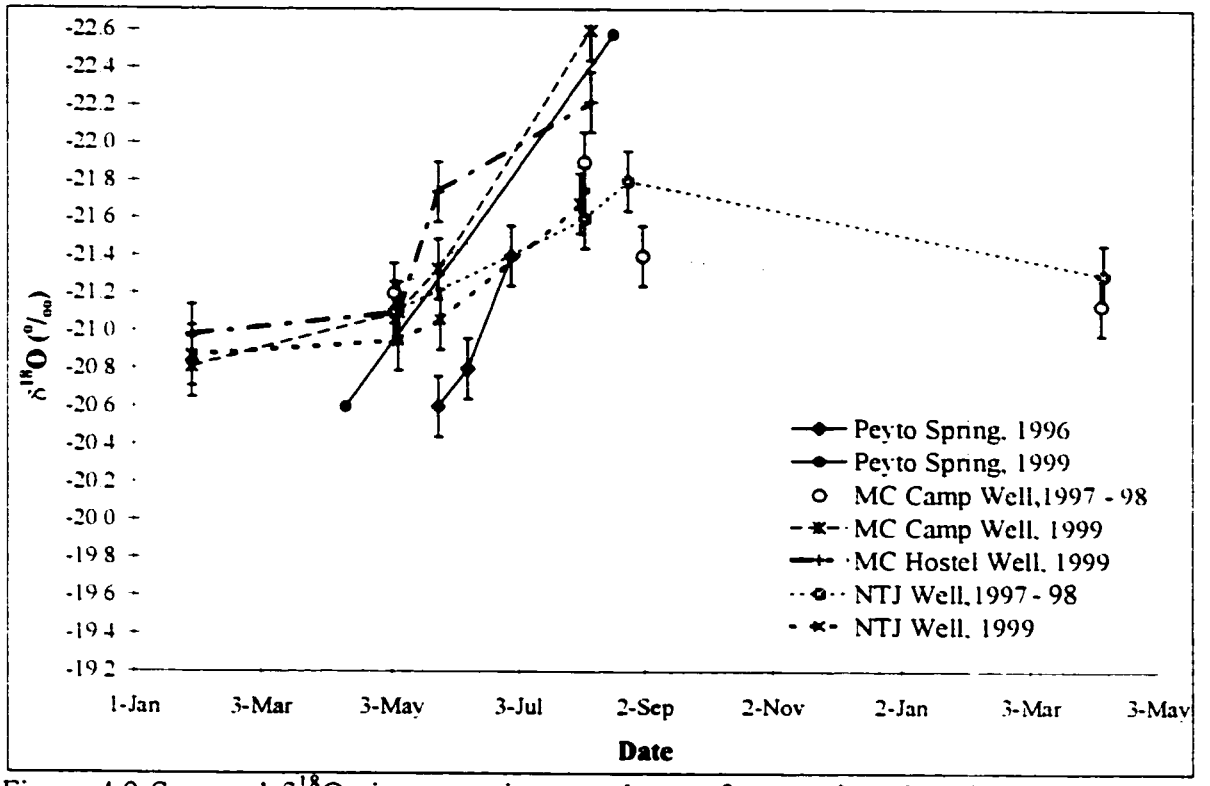

Figure 4.9 Seasonal $\delta^{18}O$ signatures in groundwater from various locations in the upper Bow Basin during high snow years (1996, 1997 and 1999).

Further evidence that the groundwater wells displayed a snow melt signature which was lagged by a few months is that, as with snowpack (Table 3.1), the groundwater $\delta^{18}O$ signatures for 1999 (Figure 4.9) were the lightest of all years sampled with August displaying signatures that were very close to that of average annual snowpack (-22.6 °/oo). In addition, 1998, the heaviest isotopic snowpack year (-21.6 °/oo), displayed the heaviest groundwater signatures (Figure 4.10). The observation that summertime spring and well samples during deep snowpack years (Figure 4.9) displayed $\delta^{18}O$ signatures close to that of snow (Table 3.1) suggests that these groundwater samples had not undergone significant enrichment from evaporation or mixing with rainfall infiltration.

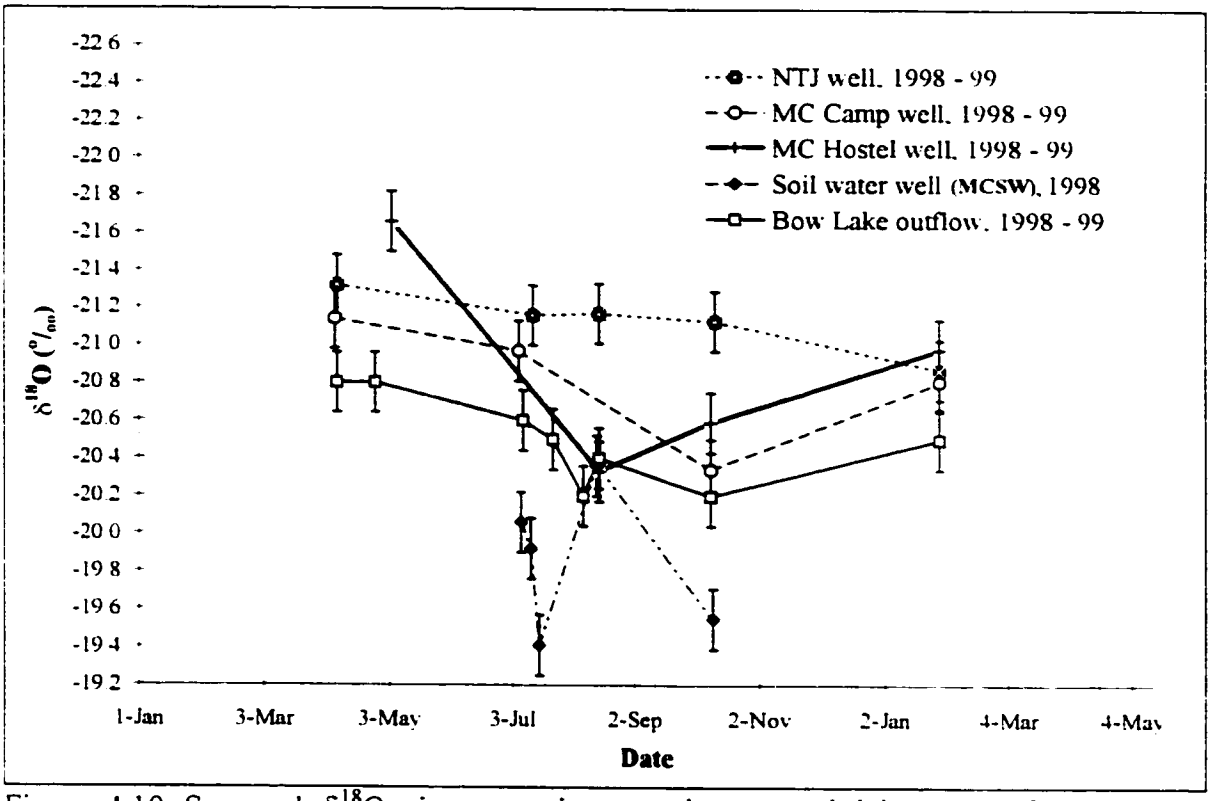

Figure 4.10 Seasonal $\delta^{18}O$ signatures in groundwater and lake water from various locations in the upper Bow Basin during the shallow snowpack year, 1998.

Groundwater well $\delta^{18}O$ data collected during the shallow snowpack year of 1998 is presented in Figure 4.10. Unfortunately, the hard rock spring sample site at Peyto was not visited during the dry year of 1998 but some soil water samples were taken from a shallow (0.3 m deep) soil well in Mosquito Basin (MCSW on Figure 4.8a), and these are also displayed in Figure 4.10. It can be seen that the distinct seasonality observed during years of deep snowpack was not in evidence during 1998. If anything, the seasonality was slightly reversed at the two wells near Mosquito Creek, with enriched isotope signatures during early summer becoming more depleted as winter approached.

Unfortunately, no local water table or flow pathway data exist but a hypothesis that fits the observations of summertime enrichment followed by a fall to winter depletion of

groundwater at the Mosquito Creek wells during 1998, and stresses the importance of antecedent groundwater conditions, follows:

1) The water table in the centre of the Bow Valley rises annually in response to spring melt infiltration and subsequently drops due to reduced recharge. [There are no deep groundwater level records in the Bow Valley but from records at similar elevations (1600 – 2000 m a.s.l.) in the Marmot Creek Basin (about 100 km to the south in the Kananaskis Mountains) such seasonal fluctuations are normal with annual water table elevations reflecting hydrometeorological conditions (data provided by Dave Cable, Alberta Environmental Protection – see appendix 4.3).]
2) Reduced snowpack in 1998 is assumed to have led to reduced recharge and lower than normal groundwater table levels in the main Bow Valley following spring melt.
3) Reduced groundwater tables following spring melt in 1998 may have allowed a higher proportion of rainfall to contribute to deep groundwater than normal, thus leading to the overall annual isotopic enrichment observed at all wells (Figure 4.10).
4) The relatively short period of isotopic depletion from summer to winter (1998 – 99) observed in both Mosquito Creek wells (Figure 4.10) may again reflect the generally low water table and subsequent increased inputs of groundwater from areas of higher ground. Groundwater flowing in from elevated areas would be expected to have a larger snow contribution and therefore a lighter isotopic signature. Using the elevational pattern of depletion observed in river tributary baseflow of approximately 0.15 $^{o}/_{oo}$ per 100 m (Figure 4.1a), the observed summer to winter depletion in deep groundwater of 0.4 to 0.6 $^{o}/_{oo}$ (Figure 4.10) suggests that the average groundwater source elevation would have been between 250 and 400 m above the main valley. The

closest possible source area that lies 250 - 400 m directly upslope from the wells of Mosquito Creek lie 2 km away. Combining this distance with the time from spring melt in April 1998 to the winter samples of January 1999 (approximately 270 days) gives a minimum flow rate of around 8 md^{-1}.

The groundwater well $\delta^{18}O$ data from Num-ti-jah Lodge (NTJ) during 1998 lacked the amplitude observed in the Mosquito Creek wells suggesting that there may have been some interchange of groundwater and lake water taking place. This well is close to Bow Lake (~ 50 - 100 m) and is located within an area of mixed deltaic gravels and till. As such it is unlikely that the groundwater table near the well could vary significantly from year-to-year as it may at other locations. Lake water followed a similar trend to the groundwater wells but was consistently heavier (compare Figures 4.9 and 4.10 with Figure 5.28) probably due to mixing with rainfall inputs from glacierised basins and perhaps evaporative enrichment. However, the lake water was much lighter than rainfall and a mixture of lake and local groundwater could explain why in 1998 Num-ti-jah well water was lighter and less variable than other headwater wells.

If the above hypothesis regarding the lake and groundwater interchange is correct, then this raises a question as to why the well isotope data do not display the same kind of fluctuation observed in the lake. The answer to this question likely lies in the relative hydraulic head gradients surrounding the lake following spring melt. During the winter, it can be assumed that the groundwater level immediately around the lake lies close to the lake water level. During spring melt, when lake water was isotopically light, the lake stage was observed to rise by at least 0.5 m above the winter level. At this time the hydraulic head and the transfer of water from the lake to the ground would theoretically

be maximised. If the water table stabilized over this shallow depth rapidly, then the lake to ground hydraulic gradient would reduce and the hydrologic interchange would diminish. This being the case then, the groundwater well would not follow the complete fluctuations of lake isotope signature but would instead remain relatively light reflecting the time of greatest lake to ground interchange (i.e. during spring melt).

The generally heavy isotope signature of shallow soil water in Figure 4.10 may reflect a higher proportion of rain content at this depth or indicate that evaporative enrichment takes place in the shallow (< 0.3 m) groundwater zone.

4.5.3 Groundwater Well Tritium Signature

Oxygen isotope data provide much information about the potential seasonality of snowmelt transcending groundwater aquifers but thus far little has been discerned about the potential age of water in headwater groundwater wells. From examination of tritium in the Bow River at Banff during winter (mean = 14.5 TU; see section 4.2.2) higher than average annual levels were observed (compare with sections 3.3.2 and 3.5.2), suggesting that baseflow had a noticeable level of "old" water (post 1950s) combined with more recent water. Therefore, by examining the seasonal variation of tritium signatures within groundwater well samples, it should be possible to discern if the groundwater was all of recent origin or whether it was mixed with water of a much longer residence time (several years). To this end, samples were collected at the Mosquito Creek campground well during 1998 and 1999 and analysed for tritium. The campground well was chosen for this analysis as it is the shallowest well that does not appear to interchange water with a local water body and is therefore probably the most likely to display a seasonal fluctuation (as demonstrated by the $\delta^{18}O$ data in Figures 4.9 and 4.10). Unfortunately,

there were insufficient data to facilitate quantitative estimations of groundwater age such as carried out by Maloszewski *et al.* (1992), but a qualitative discussion of the observations is provided.

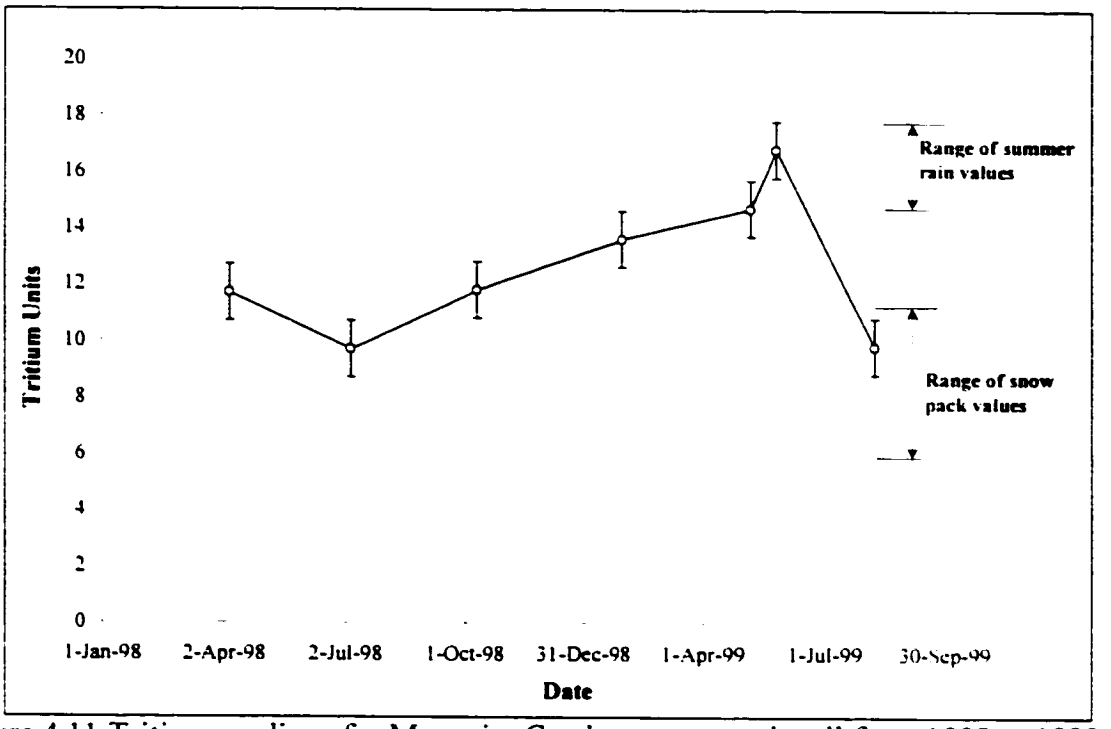

Figure 4.11 Tritium readings for Mosquito Creek campground well from 1998 to 1999.

From the observed tritium levels in the groundwater well at Mosquito Creek campground (Figure 4.11), it would appear that 1998 and 1999 displayed slightly different patterns during the spring to late summer period (April to August). During the shallow snowpack year of 1998, the groundwater tritium signature demonstrated limited fluctuation with an annual signature characteristic of mixed rain and snow. A simple two-component mixing model using average TU values of 8.9 for snow and 14.9 for rain, suggests that during the early baseflow period in 1998 (TU = 12) snow and rain each comprise about 50% of the volume. During summer (TU = 10), the snowmelt value increased to approximately 80%. These values disagree with the $\delta^{18}O$ data, which

suggested that rainfall did not contribute significantly to groundwater at any time. Therefore, it must be assumed that the high TU component of the balance during the baseflow period (and potentially low water table) of 1998 was not completely derived from rainfall. This being the case then, it should be concluded that there was probably a noticeable "old" water component in groundwater with an elevated TU signature mixing with recent water of a lower TU value.

Still examining the 1998 pattern, it would appear that the summertime drop in TU was probably associated with the snowmelt wave (discussed earlier) traversing the groundwater system. The subsequent rise in TU as winter approached may be partially associated with enrichment from summer rainfall but could also be the result of "old" water that has been resident in the ground for several years mixing with the more recent snowmelt. The hypothesis that old water was largely responsible for the continued enrichment in TU signature during winter 1998 to 1999 is corroborated by the $\delta^{18}O$ observations illustrated in Figure 4.10. After the well $\delta^{18}O$ signature enriched during the fall (probably responding to rain inputs) it then altered direction and began to deplete as the winter baseflow period progressed. This depletion in $\delta^{18}O$ occurred at the same time as the enrichment in TU and it is therefore unlikely that rain inputs from an up gradient location several months previously could have been the main cause. If rain inputs were responsible, continued enrichment in both $\delta^{18}O$ and TU would have been expected.

Of interest is that the TU signature continued to rise following the onset of spring melt in 1999 (TU = 15, May 6th and TU = 17, May 25th). From the $\delta^{18}O$ data, the May 25th sample point was still associated with winter baseflow (-21.3 $^{o}/_{oo}$) and it appeared to be several months before the snowmelt wave actually traversed this groundwater system.

Therefore, this rise in TU may have been associated with a shunt of older water (even more enriched in tritium than all rain samples) through the system as snowmelt started to flow through the unsaturated zone. Three to four months later, the TU level returned to a level closer to recent snowmelt, thereby corroborating the observations in the $\delta^{18}O$ data.

4.5.4 Groundwater Well Ionic Signatures

4.5.4.1 Electrical Conductivity in Groundwater Wells

Differences in the groundwater well geochemical patterns between 1998 and 1999 were also evident in the EC traces (Figure 4.12). For the campground well at Mosquito Creek, the winter signature for both years was approximately the same but following melt the patterns differed. In 1998, the EC increased, possibly in response to an early snowmelt acid shock, and then remained high for the rest of the summer. Minimal changes in the 1998 summertime geochemical signature were also evident in the traces for $\delta^{18}O$ (Figure 4.10) and tritium (Figure 4.11), and likely reflect the reduced flux of water through this system during this low yield year. In 1999, on the other hand, a more dynamic signature was observed at the Mosquito Campground well with an early rise in EC declining later in the summer. The reduced EC later in 1999 may have been due to volumetric dilution and shorter residence times compared to the groundwater of 1998 or possibly the result of a reduced hydrogen ion content in later melt waters.

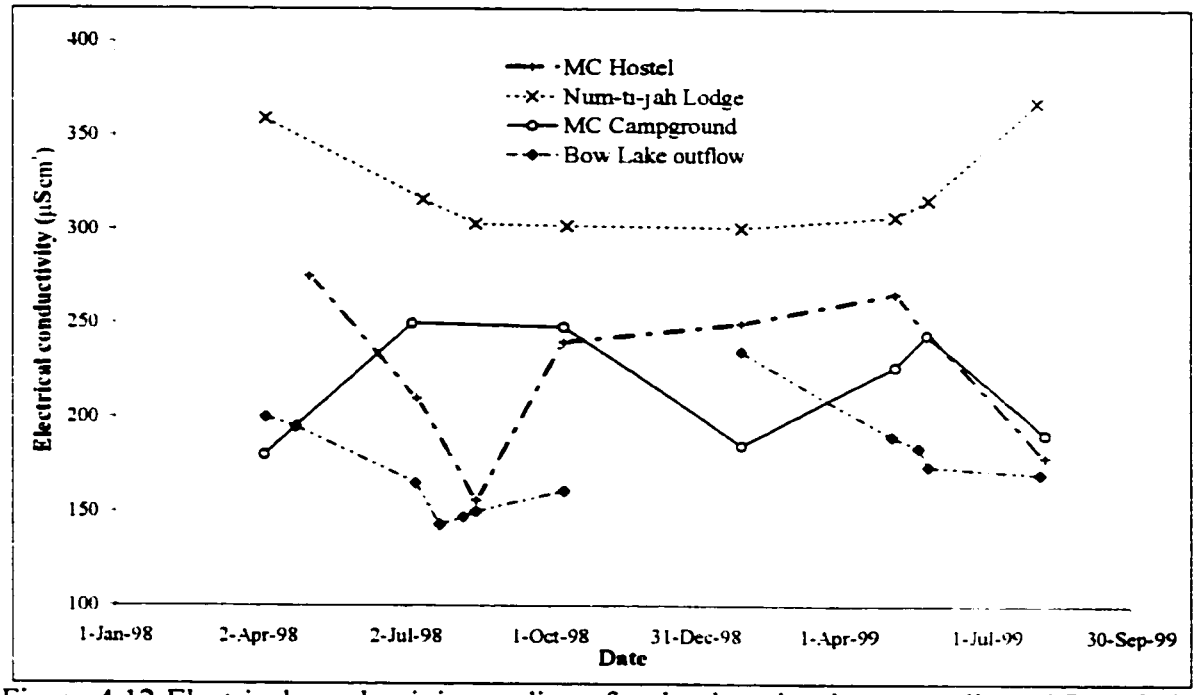

Figure 4.12 Electrical conductivity readings for the three headwater wells and Bow Lake during 1998 and 1999.

The patterns at Mosquito Creek hostel well are different from the campground, probably because the water is drawn from a much greater depth (15 m as opposed to 5 m) and the lithologies above the water bearing gravels of the wells are different. It would be expected that infiltrating water should take longer to reach this depth and may undergo different weathering reactions. However, the relatively rapid drop in EC following melt onset in 1998 is difficult to interpret and may potentially be linked to preferential flow through the boulder aquifer that the hostel well presumably taps (see Figure 4.8b). The $\delta^{18}O$ readings do suggest that the Mosquito Creek hostel well may indeed respond faster to the snowmelt wave than the campground well, despite the large difference in depth. Unfortunately, no tritium data were collected at this well and therefore it is difficult to make any inferences about groundwater age.

The EC pattern at Num-ti-jah Lodge groundwater well reverses from 1998 to 1999 (Figure 4.12). As with the earlier observations in $\delta^{18}O$ patterns, this may be related to groundwater lake water interchange. It has been suggested that during 1998, the groundwater levels around the lake may have been lower than normal due to minimal snowmelt infiltration. As a result the hydraulic gradient at the edge of the lake during the summer may have been directed from the lake to the ground, and it is possible that the groundwater source of Num-ti-jah well was being replenished partly by lake water and not just snowmelt, as would normally be the case.

The weathering potential of groundwater that originated as snowmelt may potentially be higher than that originating as lake water, due to relative hydrogen ion content and the flow paths taken. Snowpack always displayed a pH around 6 and Bow Lake outflow was consistently around 8.5. In addition, groundwater that originated as snowmelt would have passed through soil zones thus increasing its acidity. In 1998, when it is thought lake water may have infiltrated to ground, high pH water entering the ground via lateral flow pathways at the lake margin, could have resulted in a low weathering potential and commensurately low groundwater EC levels (lake water EC is displayed in Figure 4.12 for reference). In 1999, the deep snowpack and associated increase in melt likely raised water table levels (reversing the lake to ground hydraulic gradient), and the acidic soil routed snowmelt may have led to dissolution and higher EC levels in groundwater.

4.6 Concluding Remarks

4.6.1 Overview

Baseflow was a very complex component to characterise at the basin scale. Winter samples, river and tributary profiles and groundwater well samples were all collected and

analysed in order to elucidate groundwater processes and characterise the inter-annual basin-wide seasonal $\delta^{18}O$ baseflow signature. In general, annual river baseflow is characterised by a relatively constant signature during the winter months but gradually becomes isotopically depleted during summer in response to spring snowmelt and gradual percolation to deep groundwater. It was observed that groundwater wells begin to deplete their $\delta^{18}O$ signature in response to snowmelt onset within weeks, probably as a result of infiltration through gravels and boulders. However, the volumetric influence of snowmelt in deep groundwater is maximised around August. The signature then changes and could begin to reflect the input of summertime rainfall. However, tritium and EC traces at the headwater wells appear to suggest that a significant volume of old water (rather than purely rainfall) is more likely to be replacing the snowmelt wave. These observations are corroborated by the Bow River baseflow profiles that display the same summertime response to earlier snowmelt and also the high possibility of winter baseflow containing a significant but unquantifiable proportion of old water.

It was found that 1998 was different from other years, in that the shallow snowpack did not replenish the groundwater store as much as would normally be expected and the summertime baseflow $\delta^{18}O$ signature was slightly heavier than winter due to rainfall contributions. During 1999, however, the deep snowpack and an assumed low antecedent groundwater table led to a high volume of snowmelt infiltration, which probably caused an acceleration of groundwater fluxes. This early melt pulse during 1999 may have been responsible for a large flux of acidic water through the soil zone and into the groundwater system, thus elevating levels of dissolved solids later in the year. Such a process could also have been linked to the seasonal rise in groundwater EC adjacent to Bow Lake. The

"see-saw" in groundwater EC near the lake may, therefore, have been a function of changing hydraulic gradients, with 1998 having a low water table leading to losses of lake water to the ground, and the reverse in 1999.

Upstream of Bow Lake, it was found that summertime surface tributary inputs to the headwater stream baseflow were substantially greater than direct groundwater inputs to the main channel and were a result of the high glacial coverage on the western slopes of the Bow Valley. On the eastern slopes, however, the baseflow yields were found to be noticeably higher than for the Bow Basin above Banff. These observations exemplify the importance of the headwaters to overall basin hydrology.

Landcovers in these headwater environments were also found potentially to exert a strong influence on hydrologic yield. For example, forest covers lead to reduced rainfall volumes reaching the ground due to processes of interception by and evaporation from the canopy. Parallel to this finding, some open areas of landcover often displayed higher yields. Part of the explanation for this observation was thought related to areas of karst within dolostone beds in the upper reaches of Mosquito Creek. In these areas, snowmelt is able to drain rapidly to depth, where evaporative losses are reduced, and then subsequently re-enter the surface drainage system lower down in the valley by draining through tills and talus slopes. Discharges from these areas did not appear to vary significantly through the course of the year, which is in contrast to basin runoff that was observed to change by up to two orders of magnitude. This flow regulation suggests that the storage of water in these karst areas is probably large compared to the relatively small volume of discharge. Such karst areas, therefore, are important in maintaining year round runoff in some headwater areas and, due to the widespread occurrence of carbonate

bedrock in the Bow Valley, likely contribute a significant proportion of basin-wide baseflow.

An unexpected but interesting observation from the headwater profiles conducted in Mosquito Creek was that stream water was being lost to ground in the vicinity of a large thrust fault. Losses were observed during the summer and fall and were up to 50% of the natural flow of the Creek during annual baseflow conditions. It is not known what happens to the water after leaving the surface drainage system but it may be lost to local groundwater due to a localised drop in the water table; continue down-slope as hyporheic flow; or potentially enter the fault line and bypass the local surface drainage system. Of interest is that this fault line joins up with other major faults that run along the main Bow Valley and it is possible that such fault lines act as large-scale preferential flow conduits transferring water from headwaters to lower elevations in the basin.

4.6.2 Baseflow $\delta^{18}O$ signature for Bow River at Banff

A major objective of this chapter was to characterise the oxygen isotopic behaviour of groundwater maintained Bow River baseflow above Banff. This isotopic description (or model) is to be used as an input for the deep groundwater baseflow end-member geochemical signature used in the hydrological model evaluation presented in Chapter Seven. To this end, baseflow data collected during winter, and as part of the longitudinal Bow River profiles, were the main source of information for this characterisation. The headwater groundwater well data were used to assist with interpreting the magnitude of temporal variation in the deep groundwater baseflow signature. The observed $\delta^{18}O$ values for headwater wells were not used to characterise baseflow at Banff due to the wells being located high within the basin with disproportionately high snowmelt water content,

and being too deep to immediately influence river runoff. In addition, baseflow sampled during the longitudinal river profile experiments likely contained residual hydrological contributions from small melt and rain events that occurred earlier over small parts of the basin. Therefore, the winter groundwater baseflow component signature was estimated from the observed interannual baseflow signature at Banff, with the summer signature being calculated from the average isotopic displacement from winter conditions observed within both the Bow River and groundwater wells.

From the data presented throughout this chapter, a summary of the seasonal behaviour of baseflow $\delta^{18}O$ signature from 1996 to 1999 for the Bow River at Banff is possible. At Banff a value of approximately -20.5 $^{o}/_{oo}$ has been observed during each winter prior to spring melt (April-May) from 1996 to 1999. For the deep snowpack year of 1997 the groundwater signature from well data (Figure 4.9) depleted by about 0.6 $^{o}/_{oo}$ from winter to summer, with the lightest month being August (no data exist for 1996 but hydrological conditions were similar to 1997 and therefore the baseflow signatures were likely similar). For 1999, the level of isotopic depletion (Figure 4.9) appeared to increase to approximately 1.2 $^{o}/_{oo}$ (the higher level attributed to lighter snowpack and the potentially greater groundwater storage capacity from lower water tables at the start of the season). For both 1997 and 1999, however, the Bow River baseflow samples at Banff suggest a depletion of approximately only 0.4 $^{o}/_{oo}$ and 0.8 $^{o}/_{oo}$, respectively (Figure 4.1). Therefore, using the average amplitude of seasonal $\delta^{18}O$ depletion observed in the wells and the Bow River during 1997 and 1999, and adding this amplitude to the winter baseflow values of -20.5 $^{o}/_{oo}$, the actual August deep groundwater maintained baseflow signatures are estimated to be approximately -21.0 $^{o}/_{oo}$ and -21.5 $^{o}/_{oo}$, respectively.

During 1998, average groundwater well $\delta^{18}O$ signatures (not including Num-ti-jah due to lake proximity) were enriched by 1.1 $^{o}/_{oo}$ at the end of the year compared to the beginning (Figure 4.10). A similar observation was made for the Bow River baseflow with a level of enrichment around 0.7 $^{o}/_{oo}$ (Figure 4.1). The assumed average enrichment of groundwater baseflow for the shallow snowpack year of 1998 from winter to summer is, therefore, approximately 0.9 $^{o}/_{oo}$. This summertime enrichment is thought due to the relatively enriched El Niño snowpack of very limited basin-wide volume, and increased levels of summer rainfall infiltration to ground. A graphical summary of the conceptual groundwater baseflow $\delta^{18}O$ model for the years 1996 to 1999 is presented in Figure 4.13.

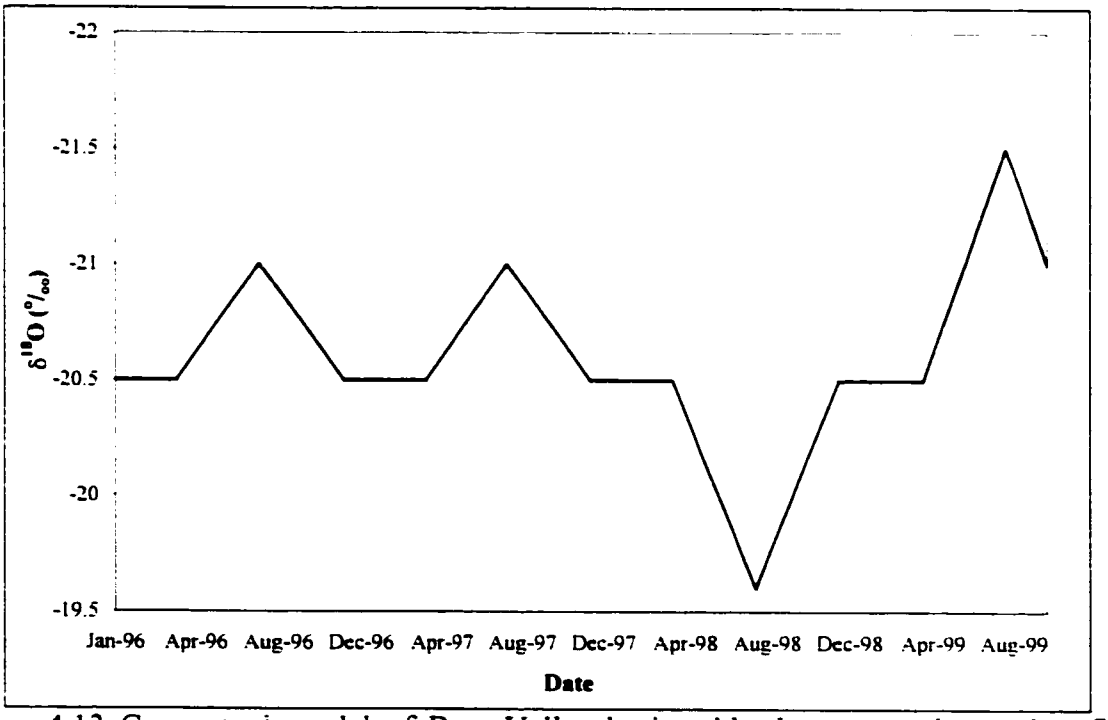

Figure 4.13 Conceptual model of Bow Valley basin-wide deep groundwater baseflow $\delta^{18}O$ signature from 1996 to 1999.

Chapter 5 Hydrological Flow Components in the Bow Valley Headwaters

5.1 Introduction

The current chapter investigates surface water discharge hydrographs, runoff yield, the water balance and geochemistry within the Bow Valley headwaters (Figure 1.4 and section 1.3.2) to elucidate some of the spatio-temporal patterns and varying flow component proportions within temperate mountainous areas. Headwater basins were studied to examine the influence of snowmelt, rainfall, basin glacier coverage and lakes on the surface runoff hydrograph. One basin, Mosquito Creek, has little glacier cover, is characteristic of the eastern slopes of the Bow Valley and field studies were undertaken here during 1998 and 1999. Another basin, Bow Creek, is highly glacierised and some hydrometric data were collected here from 1996 to 1999. Within these headwaters, both event and seasonal studies have been carried out. (The reader is referred back to Chapter One for detailed discussion of the physiography and climatic conditions within the Bow Basin and section 4.4 where baseflow conditions within these headwater basins were investigated.)

A difficulty linking headwater hydrogeochemical observations with those at the basin-wide scale above Banff is that river water may be stored and the geochemical signature altered during transit from headwaters to basin endpoint. Within the Bow Valley headwaters there are several lakes that could potentially alter the river hydrogeochemistry through processes of flow retardation and mixing. Directly downstream of Bow Creek and within the main Bow Valley is Bow Lake. Water samples were collected above and below this lake to investigate the effect of lake transit on river

$\delta^{18}O$ and whether or not the lake input signatures were simply amalgamated, lagged or modified. These analyses are reported near the end of this chapter in section 5.4.

Before investigating potential lake influences on river runoff, the spatio-temporal variability in basin hydrograph components has been studied using a variety of analytical steps where possible and appropriate to do so:

1) Quantitative runoff yield and basin water balance estimates.
2) Qualitative overview of seasonal hydrograph $\delta^{18}O$ patterns and hydrological balance.
3) Quantitative hydrograph separations into new and old components (equation 2.8) using isotopes where possible: snowmelt and rainfall events.
4) Qualitative overview of hydrograph EC patterns and hydrological flow pathways.
5) Quantitative hydrograph separations into new and old components by dilution using EC of glacial melt runoff.
6) Overview of hydrograph tritium patterns to qualitatively assess age and mixture of flow components.
7) A comparison of the approximate areal yields for Mosquito and Bow Creek Basins.
8) Wavelet filtering of hourly discharge data to investigate temporal patterns within basin hydrographs.

The methods, results and discussion of the analyses reported in this chapter are divided into three main sections and a concluding summary following this introduction:

1) Mosquito Creek - Investigation of basin water balance, hydrograph components, temporal patterns in the hydrograph and hydrological processes within a non-glacierised headwater basin (section 5.2);
2) Bow Creek – Similar techniques as above but applied to a glacierised headwater basin (section 5.3);

3) Lake modification - Investigation of headwater lake influence on the river $\delta^{18}O$ signature (section 5.4);

4) Concluding remarks - A summary and integration of the major findings from earlier sections of the chapter (section 5.5).

5.2 Mosquito Creek – Non-Glacierised Basin

5.2.1 Field Sampling and Data Acquisition

Measurements of stream discharge, EC and pH were taken at the basin endpoint (see Figure 1.4 for basin map) of the relatively low glacier cover basin containing Mosquito Creek from April 1998 to August 1999. Water samples were collected during each site visit and subsequently analysed for Tritium and $\delta^{18}O$ at the University of Waterloo Isotope Laboratory (analytical methods described in section 3.2). Two snowmelt and one rainfall event were investigated with frequent samples being taken several hours apart. For seasonal analyses, field measurements were taken approximately every 5 to 15 days during six short field campaigns:

1) 6th April to May 12th, 1998

2) 4th July to August 16th, 1998

3) 3rd October to 10th October, 1998

4) 25th January to 30th January, 1999

5) 4th May to 4th June, 1999

6) 9th August to 17th August, 1999

In addition to the data collected during site visits, an automatic weather station was installed on a high level plateau at 2400 m a.s.l. in Mosquito Creek Basin to monitor temperature, precipitation and short-wave radiation. Unfortunately, ground squirrel

activity led to both the complete loss of the precipitation record and disconnection of the solar panel resulting in total loss of data logger power during the winter of 1999. Fortunately, there is a Meteorological Service of Canada weather station collecting hourly temperature and precipitation just 14 km away on Bow Summit (Figure 1.4), near Num-ti-jah Lodge, and these data were used to supplement those that were lost.

Further problems were encountered installing a pressure transducer to monitor discharge on Mosquito Creek. Therefore, no long-term automatic discharge measurements were available for spring melt runoff or during an important rainfall runoff event in August on Mosquito Creek during 1998. However, a working Drucks 930 pressure transducer was available for the beginning of the 1999 melt season and was successfully installed in time to monitor spring melt runoff at an hourly interval before being dismantled at the end of June. The manual and automatic discharge data collected for 1998 and 1999 are illustrated in Figures 5.1 and 5.2, respectively.

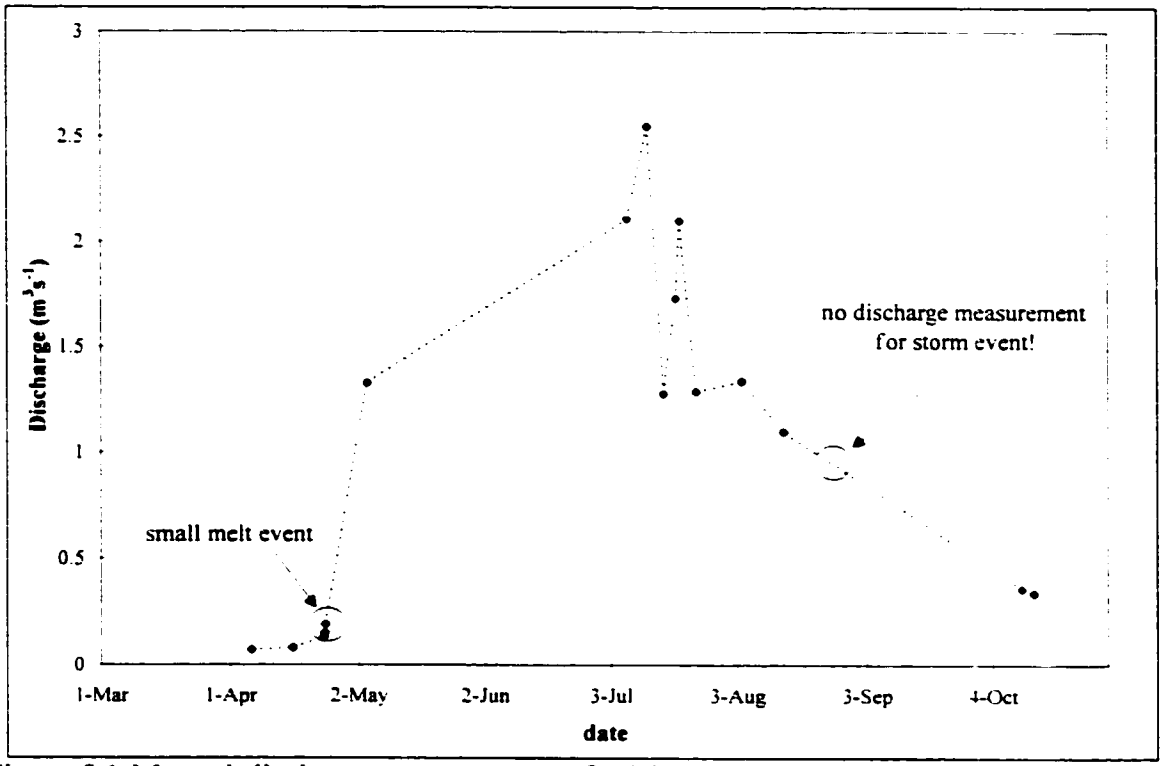

Figure 5.1 Manual discharge measurements for Mosquito Creek below the confluence of the north and south tributaries during 1998.

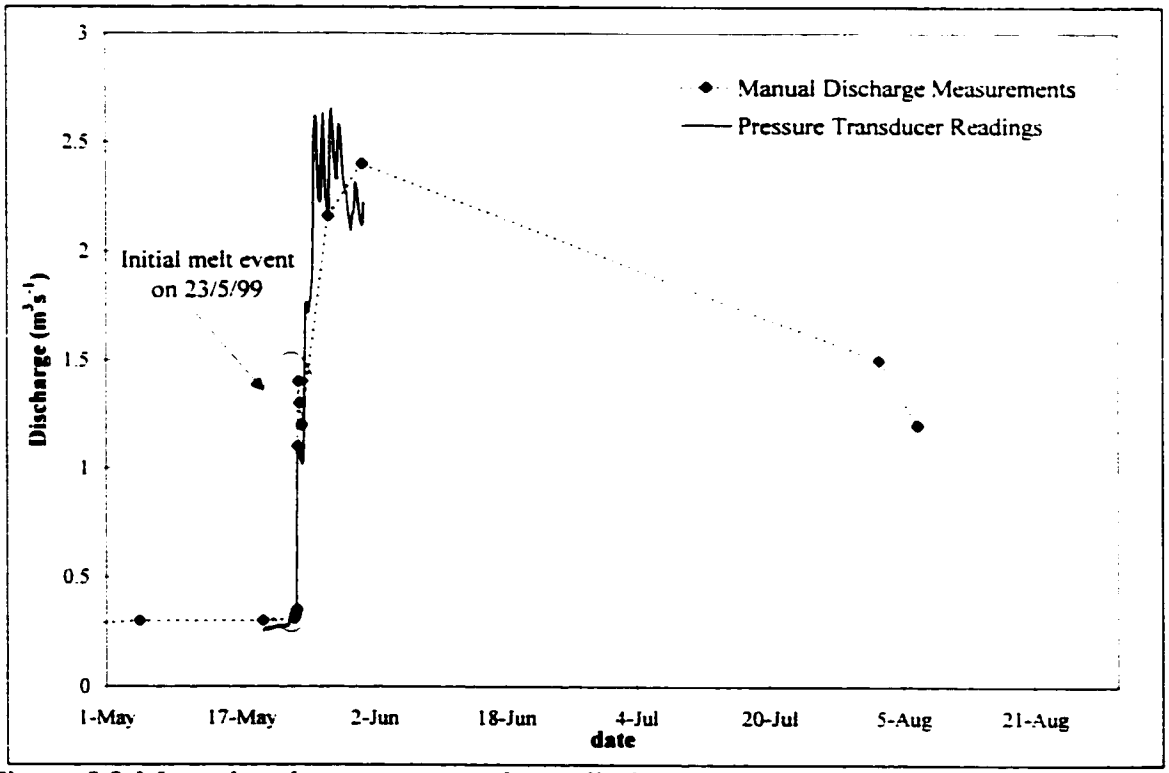

Figure 5.2 Manual and pressure transducer discharge measurements for Mosquito Creek below the confluence of the north and south tributaries during the 1999 melt period.

5.2.2 Annual Areal Yield and Hydrological Balance

For months with continuous automatic or at least two manual discharge measurements, approximate basin areal yield was calculated from the average of the measured discharges divided by the basin area. Annual baseflow (approximately the beginning of November to the start of observed spring melt) was assumed constant at 0.1 m^3s^{-1} (from field measurements during this period). For those summertime months with less than two measurements (May, June and September in 1998; and July, September and October in 1999), the areal yield was assumed to be the same as that at the adjacent Pipestone River (monitored by Water Survey of Canada) due to the two basins being similar in landcover distribution (see Chapter One) and observed similarities in yield during other times of the year (see section 6.4 and Table 6.1). This assumption is not completely appropriate as there could be differences in areal yield associated with basin elevation or size (see section 6.4). However, for the purpose of assessing the approximate differences in hydrological yields for 1998 and 1999 in Mosquito Creek, this methodology is considered adequate.

The estimated areal yields for Mosquito Creek during hydrological years 1998 and 1999, therefore, were 640 mm and 730 mm, respectively; an increase of 14%. Given the limited number of discharge measurements throughout the year and the need to "fill the gaps" with data from another basin, the statistical confidence in the basin yield values is low. However, a lower relative yield in 1998 was to be expected in this area due to the differences in annual weather conditions (see section 1.4). The year 1998 was generally low yielding due to *El Niño* conditions with reduced precipitation and warmer temperatures. The opposite occurred the following year, when *La Nina* led to increased winter precipitation and commensurately enhanced spring runoff.

For hydrological years 1998 and 1999, the recorded precipitation totals at Bow Summit less than 14 km away at 2030 m a.s.l. (Figures 1.4 and 1.7) were 300 mm and 830 mm, respectively; an increase of 177%. For further comparison, the average end of winter snow depth measured around the entire Bow Valley (see appendix 1 and section 1.4.2) increased by 77% from 260 mm in 1998 to 460 mm in 1999. In order to compare the annual Bow Summit precipitation with the Mosquito Creek runoff yield it was necessary to estimate the increase in precipitation from Bow Summit at 2030 m a.s.l. to the average elevation of Mosquito Creek Basin at 2500 m a.s.l. From observations of snow courses within this elevation range on the eastern slopes of the Bow Basin (section 1.4.2, Figure 1.8 and appendix 1), it was earlier found that the average precipitation enhancement gradient during 1996 to 1998 was 8% per 100 m rise in elevation. Therefore, the estimated annual precipitation totals over Mosquito Creek Basin for 1998 and 1999 were 410 mm and 1140 mm, respectively.

Before the losses or gains in basin storage for 1998 and 1999 could be estimated using a simple water balance approach, the losses due to evaporation needed to be discerned. Unfortunately, actual evaporation was not measured and could not be calculated. However, an upper limit on actual evaporation (in mm) could be estimated using the Turc calculation of potential basin evaporation (Turc, 1961):

$$E = P/\{0.90 + (P/[300 + 25T + 0.05T^3])^2\}^{0.5} \qquad (5.1)$$

where P = total annual precipitation and T = average annual temperature. It was possible to extrapolate the total precipitation and average temperature from the elevation at Bow Summit (2030 m a.s.l.) to the average elevation of Mosquito Creek (2500 m a.s.l.) using the elevational precipitation gradient (8% per 100 m) and lapse rate (-0.56 °C per 100 m)

established for this part of the basin in sections 1.4.2 and 1.4.3. From these calculations, it was estimated that the upper limits on basin evaporation were approximately 230 mm and 260 mm for 1998 and 1999, respectively (these values are considered reasonable given that average annual evaporation for the entire Cordillera region west of Calgary is given as < 350 mma^{-1} in the Atlas of Alberta (1969)).

A simple water balance was then performed to estimate the changes in storage within Mosquito Creek for both years:

$$Q = P - E - \Delta S \qquad (5.2)$$

where Q = runoff yield, P = precipitation, E = evaporation and ΔS = change in storage. From the above yield and precipitation estimations and the upper limit on evaporation, the estimated change in storage for 1998 was - 460 mm and for 1999 + 150 mm.

There are several questions surrounding the reliability of the water balance estimates and these numbers can only be considered a rough guide of the actual conditions within the basin for these two years. However, it does appear quite certain that 1998 experienced a loss of water from basin storage and 1999 a net gain. These observations corroborate earlier hypotheses in Chapter Four concerning interannual water table fluctuations with increased/decreased groundwater fluxes during deep/shallow snowpack years, and also the large apparent streamflow losses in the basin during 1998 (section 4.4).

If the individual estimates of runoff yield, basin precipitation and evaporation are reasonable, then a large change in basin storage for the apparently small change in basin runoff suggests that there may have been be a significant regulatory influence on the interannual hydrograph. Such flow regulation in these regions is often considered a function of glacier coverage (e.g. Hopkinson and Young, 1998). In most years, the

influence of glacier melt in Mosquito Creek basin would be negligible or non-existent but in 1998 the snowlines were at their highest in several decades during late summer, and small hanging glaciers in the headwaters of Mosquito Creek were observed to be snow free. However, during the summertime baseflow sampling profiles of Mosquito Creek's north and south tributaries (described in the last chapter) the yields for sub-basins with glacier covers were not necessarily higher than other landcovers. Landcovers (or lithological types) that did appear to demonstrate relatively high areal yields and a level of seasonal consistency were areas of karst (section 4.4.3), and it may be that some of the observed interannual flow regulation was related to storage in these groundwater zones.

1.2.3 Temporal Signals in the Hydrograph

5.2.3.1 Introduction

In this section of the thesis, Mosquito Creek's discharge hydrograph is investigated in a little more detail to elucidate some of its temporal characteristics. Hydrographs are known to contain various elements of periodicity or cyclicity associated with external forcing mechanisms. The most obvious examples are annual fluctuations associated with the tilt of the Earth on its axis whilst it orbits the sun, and the diurnal cycle due to global rotation. Both of these cycles can become strongly evident in hydrographs, especially in temperate mountainous regions, due to the recurrent changes in solar insolation and associated snowmelt pulses. In addition, hydrographs also contain temporal patterns associated with basin storage and accumulation effects (Klemeš, 2000 - Chapter 6.1). The characteristics to be investigated here are those of:

1) Dominant patterns of recurrent hydrograph "periodicity";

2) Timing of these recurrent patterns within the hydrograph;

3) The relative strength of these patterns.

By studying these characteristics, more will be learned about the composition of, and forcing mechanisms upon, basin runoff. The same analyses will be applied to the discharge data collected in the Glacierised Bow Creek Basin (section 5.3.3) to facilitate a comparison of interbasinal temporal runoff characteristics.

5.2.3.2 Wavelet analysis technique

There are various methods available to investigate time-frequency dominance in a time series signal such as a hydrograph. The most common and widely known technique is probably the Fourier transform (Polikar, 1996). However, although Fourier filter transforms can accurately discern *what* frequencies (periods or cycles) are dominant within a time series, the transform cannot indicate *when* these frequencies occur within the time series. A technique that was recently developed to overcome this shortcoming of the Fourier transform, and therefore can be used to meet the three objectives listed above, is that of continuous wavelet analysis (Torrence and Compo, 1998).

Wavelet analysis is a technique that is gaining popularity in geophysical applications where there is a need to assess temporal periodicity within time series data. The technique decomposes the data set into a time-frequency plot illustrating dominant modes of periodicity and the distribution of these modes through the time series (Torrence and Compo, 1998). The wavelet filter technique differs from the more widely used Fourier technique in that both amplitude and frequency of the windowing filter is variable. Wavelet analysis has been applied to several meteorological and oceanographic problems in an attempt to identify high-resolution temporal patterns in long time series data (e.g. Meyers *et al.*, 1993; Gamage and Blumen, 1993) and introductions to the topic are

provided by Polikar (1996), and Burrus *et al.* (1998). The use of wavelet analysis to assessment temporal river discharge variability has been demonstrated by Smith *et al.* (1998).

In order to carry out such analysis, it is normal to code the necessary algorithms in a programming environment or use a semi interactive programming 'tool kit' such as MatLab (e.g. Misiti *et al.*, 1997). However, a simple interactive wavelet graphical user interface is available on the World Wide Web (Research Systems Incorporated, 2001). This tool enables the user to enter up to 2000 consecutive data points and interactively alter the filter parameter settings. For the analysis presented here a "Morlet" wavelet filter was used, as it is relatively simple due to it being based a sine wave function, and it is commonly used for geophysical applications (Torrence and Compo, 1998). Parameter settings for the wavelet filter were all kept at the default values recommended in the web based software.

5.2.3.3 Results and discussion

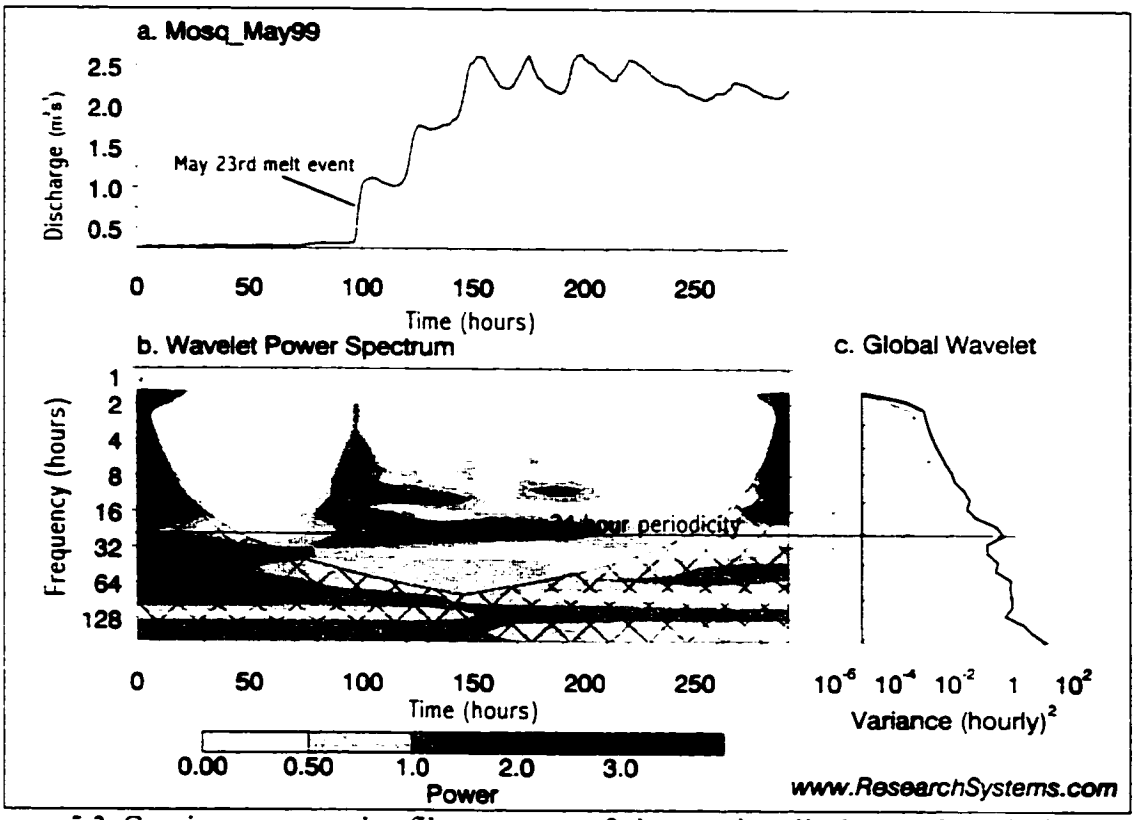

Figure 5.3 Continuous wavelet filter output of time series discharge data during 1999 early nival melt period for Mosquito Creek (Figure generated on World Wide Web courtesy of Research Systems Incorporated (2001)).

Unfortunately, Mosquito Creek only had continuous hourly discharge data from the 19th to the 31st of May 1999 (293 hours) and so the wavelet analysis could only be applied to this brief melt period (see Figure 5.3). Figure 5.3a (top left) is a graph of the raw hourly discharge data in m^3s^{-1}. A time frequency plot of the filtered discharge data is displayed in Figure 5.3b (bottom left). On the y axis of this graph is the time periodicity or frequency of recurring patterns. Along the bottom axis is the time (in hours) following the start point in the data. On this plot, time periods of recurring temporal periodicity have been illustrated. Darker tones (higher "powers" of variance) indicate strong correspondence between the wavelet template and the frequency of recurring patterns. The hatched area around the edge of the plot surrounds the "cone of influence", outside

of which "edge effects" in the data create false time frequency patterns (Torrence and Compo, 1998). Any time frequency patterns in the centre of the plot (outside of the hatchings) are significant at the 90% level. The line graph in Figure 5.3c (bottom right) is the sum of all the component wavelets or the frequency variance distribution of the global wavelet (also known as a wavelet scalogram), which illustrates (with horizontal data spikes) the most commonly recurring periodicities over the entire time series. Higher variance indicates that the "width" of the wavelet pattern template corresponds with actual patterns in the time series being analysed. The variance tends to be greatest for the longer time periodicities due to increased noise (or larger number of hydrological events) in the signal at these time periods. For shorter time periods the variance level within the hydrograph signal tends to reduce as there are less individual events recorded. The global wavelet output is almost identical to the frequency distribution plot generated using a Fourier transform based spectral analysis.

Much of the time series variance is associated with "edge effects" due to the data sets being relatively small with a high proportion of the data outside the "cone of influence". However, most of the variance plot area on the "half bell" shape curve shown in Figure 5.3c is associated with edge effects or "noise" (hatched) and only a small fraction (unhatched) is of interest here. Along the global wavelet curve, it is apparent that one time frequency was dominant during the short time period studied and this is reflected in the horizontal "spike" coinciding with the 24-hour period. Therefore, the wavelet analysis identified the diurnal cycle that was prominent during the spring snowmelt period.

In this case, the observation of a diurnal cycle within the hydrograph is rather trivial, given that this is readily apparent from visual inspection of the discharge time series.

However, the value of this tool will become apparent in later sections of the thesis, where longer time periods will be examined and the time frequency characteristics of various basins compared (see sections 5.3.3 and 6.5). This example from Mosquito Creek provides a clear illustration of the use of the wavelet filter technique to detect dominant cycles within the hydrograph.

5.2.4 Seasonal River Geochemistry

The two years 1998 and 1999 were hydrometeorologically distinct with 1998 being an *El Niño* year with relatively little basin-wide snowpack (at least 50% lower than most years), reduced annual precipitation and warmer than average temperatures (see section 1.4 for an overview of meteorological conditions). In addition, after reviewing the geochemical groundwater data provided in Chapter Four, it was thought likely that the reduced snowpack of 1998 led to lower than normal regional water table levels at the beginning of 1999. This interannual variation in meteorological and groundwater storage conditions would probably have had a significant impact upon basin runoff generation processes, flow pathways and hydrological balance components. If changes to the basin hydrological regime did occur, they would likely be manifested in the seasonal stream geochemistry. The purpose of this section, therefore, is to investigate seasonal runoff geochemistry during 1998 and 1999 on Mosquito Creek to assess whether there was any interannual variability, which could be attributable to changing hydrological conditions within the basin.

From the beginning of April 1998 to the middle of August 1999 (17 months), 24 stream samples were collected from Mosquito Creek basin endpoint (Figure 1.4) in order to analyse enriched tritium, EC and $\delta^{18}O$ (methods described in section 3.2), and

characterise the changing seasonal signatures. For both years, samples were collected during the main spring freshet period from baseflow to peak melt conditions and then again in late summer of both years. Interannual baseflow sampled during October 1998 and again in January 1999.

The seasonally changing TU, EC and $\delta^{18}O$ signatures in surface runoff from Mosquito Creek during 1998 and 1999 are illustrated in Figure 5.4. Tritium levels fluctuate between rainfall and snowpack concentrations but it would be incorrect to deduce that rain or snow inputs were responsible for these fluctuations due to the possibility of changing proportions of old water content with varying residence times. However, the seasonal tritium signature at Mosquito Creek is useful to characterise here as it provides a reference for comparison with that observed on the glacierised Bow Creek, which will be presented in section 5.3.4.

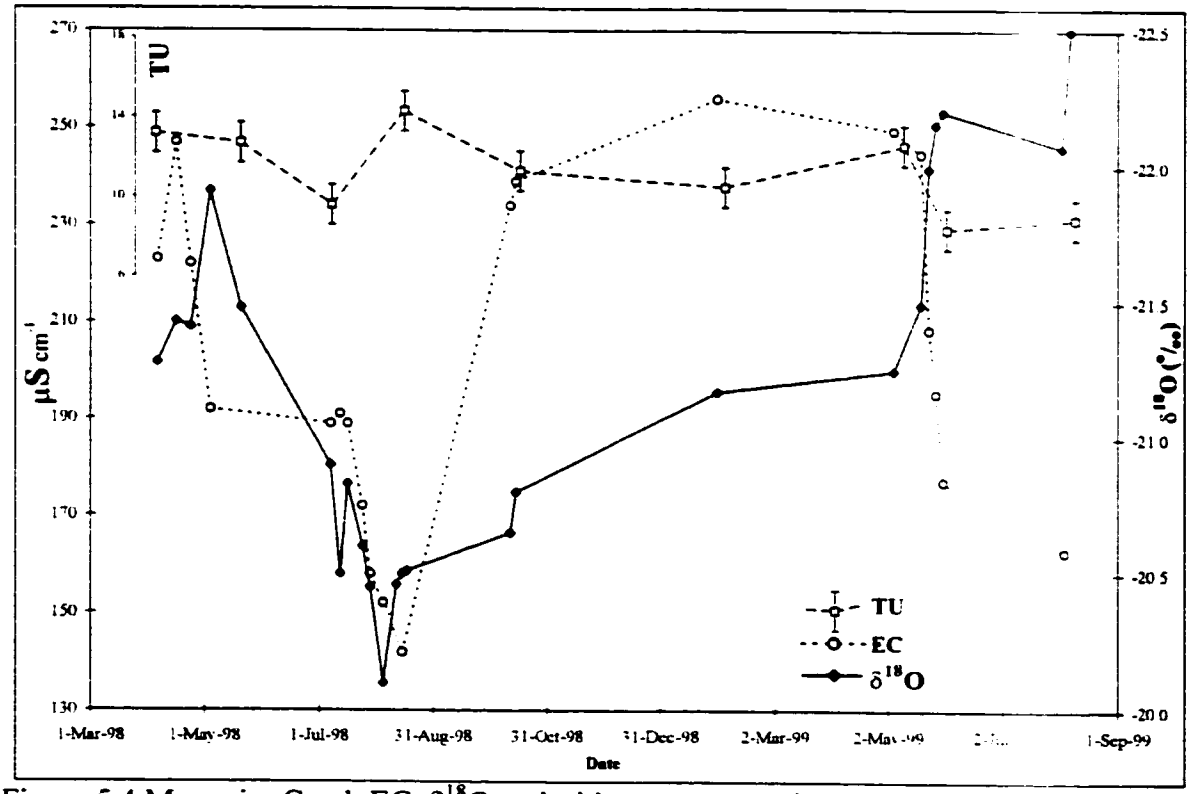

Figure 5.4 Mosquito Creek EC, $\delta^{18}O$ and tritium concentrations during 1998 and 1999.

For both years, the late winter baseflow $\delta^{18}O$ signature was around -21.2 to -21.3 $^{o}/_{oo}$ (n = 3), which suggests about 89% snow and 11% rain content using the average component signatures from Chapter Three and a simple two-component mixing model (equation 2.8). At the onset of snowmelt (April 23rd 1998 in Mosquito Creek), $\delta^{18}O$ began to deplete as the snowmelt proportion in the stream increased. In 1998, only a slight depletion was observed during the freshet with the lightest stream signature occurring in early May before it began to enrich during the summer. This pattern reflects the rapid melt out of the shallow snowpack within the basin followed by a subsequent influence of summertime rainfall on the hydrograph.

For 1999, the melt onset occurred a month later (May 23rd) due to the deeper snowpack and cooler temperatures (section 1.4). This led to greater depletion of the stream $\delta^{18}O$ signature than was observed in 1998 during the melt period. In addition, this depletion continued on into the summer indicating that snowmelt was still the dominant contributor to flow even in August. In fact, the stream sample taken in August 1999 had a $\delta^{18}O$ value of -22.5 $^{o}/_{oo}$, which was virtually the same as the average 1999 snowpack value of -22.6 $^{o}/_{oo}$ suggesting that the entire seasonal hydrograph was dominated by snowmelt. This relationship between $\delta^{18}O$ and discharge is illustrated in Figure 5.5.

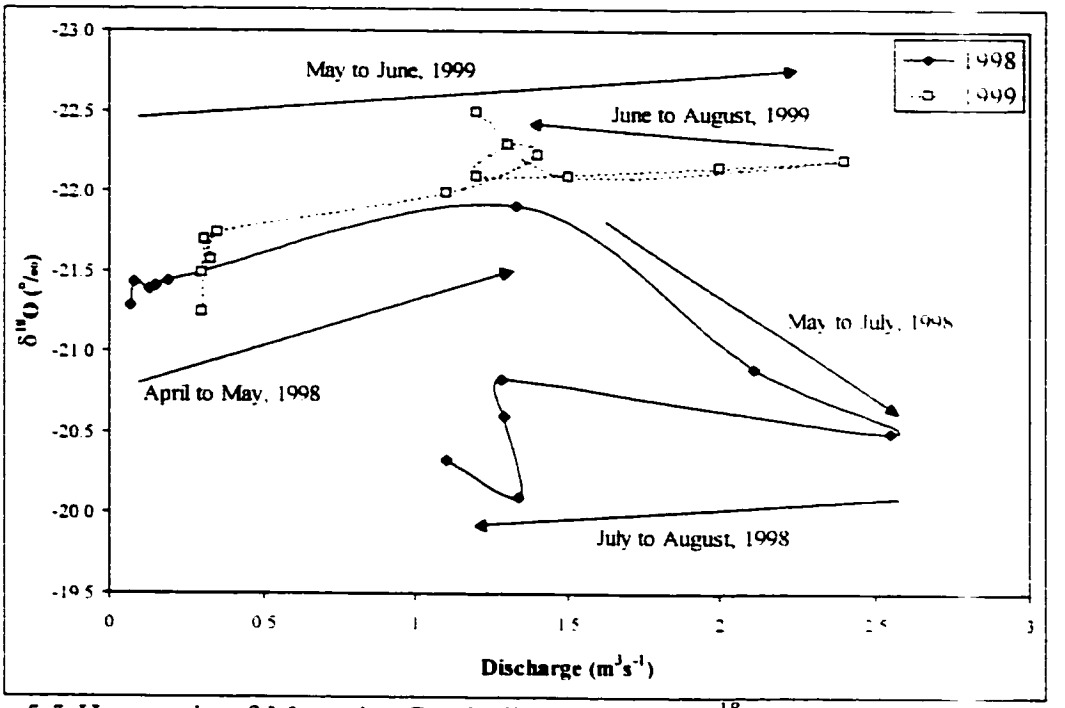

Figure 5.5 Hysteresis of Mosquito Creek discharge with $\delta^{18}O$ for April to August 1998 and 1999.

In Figure 5.5 it is evident that during the melt season of 1998 there was distinct hysteresis in the $\delta^{18}O$ / discharge relationship. Depleted signatures early in the time series were replaced with relatively enriched $\delta^{18}O$ values for commensurate discharges later in the summer. Therefore, this exemplifies the reducing snowmelt contribution through the summer of 1998. A simple two-component mixing model (equation 2.8) using the average 1998 snowpack and rainfall signatures of -21.6 ‰ and -11.3 ‰ (see section 3.6.1), respectively, returns a maximum rainfall contribution for summer 1998 of 15%. However, for 1999 summer $\delta^{18}O$ did not enrich as discharge dropped but actually continued to deplete. Therefore suggesting that snowmelt contributions (probably from high elevations within the basin) were increasing despite a reduction in discharge. This could be possible if the basin-wide summertime groundwater baseflow signature was dominated by spring and summer snowmelt. This corroborates the hypotheses of the last

chapter that snowmelt was the dominant hydrological component in both groundwater and baseflow during 1999, and that the influence of snowmelt on groundwater baseflow was maximised during late summer. However, if snow was indeed such a major component of surface runoff in mid to late summer, then this raises a question as to the fate of rainfall within the basin. This issue will be returned to in section 5.2.6.

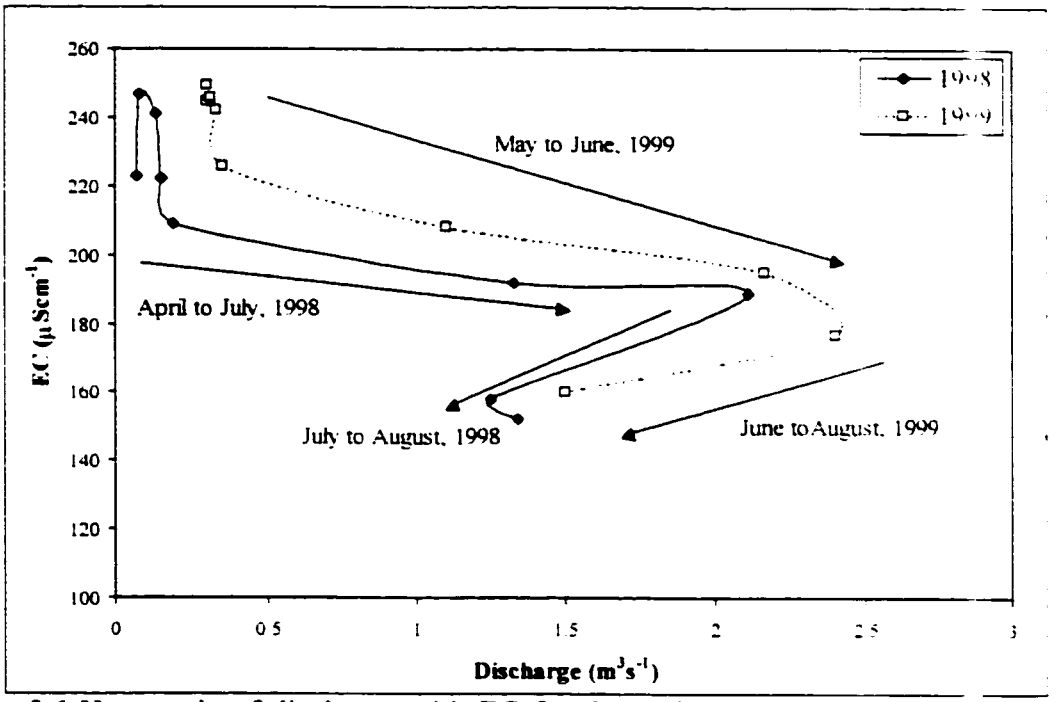

Figure 5.6 Hysteresis of discharge with EC for the melt and late summer periods, 1998 and 1999. (Event data "averaged" for easier interpretation.)

For both years, the EC readings were above 220 μScm^{-1} during winter baseflow before dropping by up to 100 μScm^{-1} during the main melt season (Figure 5.4). The relationship between discharge and EC for corresponding times of the year during 1998 and 1999 appeared to be relatively similar (Figure 5.6). The main difference between the two years was that EC for 1999 tended to be consistently slightly higher. At the onset of melt in 1998, EC increased slightly, perhaps in response to acidic snowmelt and rapid weathering as the melt water traverses flow pathways that had been inactive for months,

or due to shunting out old water from the riparian zone (e.g. Sklash and Farvolden, 1979). The seasonal EC signature for 1998 then appeared to drop in two stages: firstly during May and June in response to volumetric dilution from snowmelt and rainfall input and secondly during July. (A similar pattern may have occurred during 1999 but due to fewer data points and the reduced temporal coverage of the sample data this cannot be investigated.) The second drop in EC occurred during late summer, long after the annual snowmelt peak around May to June and seasonal runoff was already starting to decline. Therefore, this second reduction in EC cannot be associated with simple volumetric dilution due to high discharges.

Of further interest is that the second drop in EC observed in the 1998 data tended to correspond with a distinct enrichment of $\delta^{18}O$ (up to 0.8 $^{o}/_{oo}$) (Figures 5.4, 5.5, 5.6). This suggests that the reduced EC in the river in late summer 1998 was related to recent summertime rainfall (see Figure 1.7). During 1999, however, the summertime reduction in EC corresponded with a depletion of the $\delta^{18}O$ signature (up to 0.4 $^{o}/_{oo}$) indicating that this dilution was probably associated with snowmelt or glacial melt inputs from high elevation within the basin.

The fact that the EC patterns appeared to be relatively similar from year to year suggests that the seasonal variability in flow pathway development may not have been very different. Combined with the slight shift towards systematically higher EC values for corresponding discharges in 1999, these observations indicate that whatever the differences in hydrological processes, there was one change that affected the entire range of basin discharges.

Hydrologically, the most significant difference between the two years was the > 50% increase in snowpack in 1999. However, common sense would dictate that with 50% greater water availability during the spring of 1999, then if all else remained equal, the effect of this excess melt water would be to increase the volume and rate of water flux through the basin. This should act to increase the levels of dilution and therefore reduce the EC levels in runoff. However, despite an increase in snowpack volume, the 1999 EC concentrations were generally higher than 1998, thus demonstrating that EC was not simply related to volumetric dilution from basin water availability. This increase in EC, therefore, suggests a higher antecedent weathering potential within the basin, probably due to longer groundwater residence times and/or a reduction in overland flow and enhanced infiltration during 1999; or, more simply put, an increase in available basin storage. This provides further evidence for the earlier hypothesis that groundwater table levels may indeed have been lower at the beginning of 1999, and there was probably more opportunity for infiltration and groundwater routing during the subsequent summer.

Putting all of the above together then, a plausible explanation for the three stages of EC concentration and different $\delta^{18}O$ patterns observed in the runoff from Mosquito Creek Basin during 1998 and 1999 may be related to the seasonal variation in the dominant lithology and elevation of major runoff contribution areas. This is outlined below:

1) High EC (> 200 μScm^{-1}) – interannual baseflow (low flow originating in the saturated zone with long residence time);
2) Intermediate EC (~170 - 200 μScm^{-1}) – spring melt season (high flow dominated by soil matrix and preferential flow paths of short residence time in low elevation forested areas);

3) Low EC (< 170 μScm^{-1}) – summertime runoff (surface rainfall runoff [mainly 1998] and snow or ice melt contributions [1998 and mainly 1999] at high elevations where soil development is minimal and overland flow potential relatively high in impervious parts of the basin).

1.2.5 Snowmelt Events

The seasonal hydrograph is an amalgamation of several superimposed events. In order to learn more about the hydrological processes controlling hydrograph development, therefore, it is necessary to reduce the temporal scale from the seasonal overview just provided and focus attention on individual events. In this and the following sections, two snowmelt and one rainfall event will be studied to investigate the proportional contributions of old water and event water and associated flow paths.

5.2.5.1 April 1998

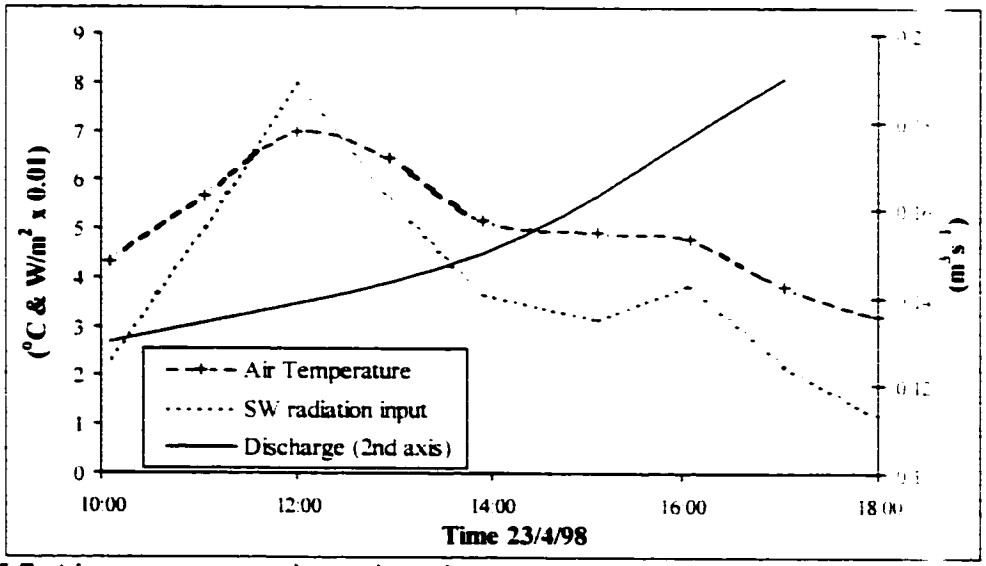

Figure 5.7 Air temperature, incoming short-wave radiation and discharge at Mosquito Creek (below confluence) during early snowmelt event in 1998.

In this section, an early season melt event at Mosquito Creek has been investigated. Figure 5.7 plots local incoming solar radiation, air temperature and discharge from 10:00

to 18:00 hrs on the 23rd of April 1998. During this snowmelt period, observed discharge increased from interannual baseflow levels by 46% (0.13 to 0.19 m^3s^{-1}, measured by manual area-velocity techniques). Compared to discharge measurements later in the year, this was a very minor event but nonetheless important in that it represented the first noticeable diurnal melt cycle of 1998 and it provides a reference for comparison to the event investigated in early 1999 (next section).

The EC and $\delta^{18}O$ signatures for this small melt event are plotted in Figure 5.8. Of note is that despite an increase in flow of ~50%, the change in $\delta^{18}O$ was small (< 0.1 $^{o}/_{oo}$) and within the range of analytical precision (± 0.16 $^{o}/_{oo}$), and there was a reduction in EC of only 13%. No conclusion can be made from the $\delta^{18}O$ results due to the lack of significant change and the fact that baseflow had a $\delta^{18}O$ signature close to average snowpack for 1998 (-21.6 $^{o}/_{oo}$). However, the small reduction of the EC signature despite an increase in discharge of ~50% suggests that a high proportion of the flow was routed through the ground. A straightforward dilution approach, using the average snowpack EC of 10 µS and baseflow EC of 240 µS to represent groundwater, suggests that up to 86% of the peak measured flow could have been ground routed. However, if the EC of snowmelt increased during overland flow, then the estimated ground component would reduce.

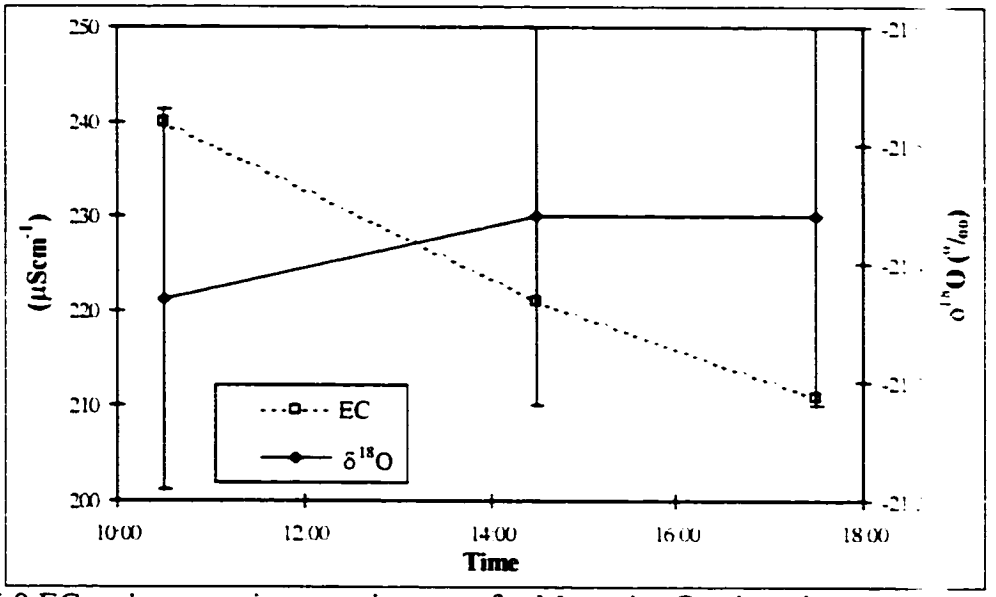

Figure 5.8 EC and oxygen isotope signature for Mosquito Creek melt event, April 1998.

5.2.5.2 May 1999

The snowpack within Bow Basin for 1999 was > 50 % deeper than in 1998 (see section 1.4.2) and therefore the potential for high melt runoff was greater. The first major melt event of the season commenced on May 23rd. Figure 5.9 plots the incoming solar radiation, air temperature and discharge from 09:00 hrs on May 23rd to 09:00 hrs on May 24th 1999. The maximum air temperature was 8 °C higher than for the 1998 event with peak solar irradiance being over 100 Wm^{-2} greater. During this snowmelt period, there were clear skies with no rainfall and the observed discharge increased by 200%. Within this one diurnal cycle, the discharge on Mosquito Creek rose from near interannual baseflow levels up to almost half of the peak measured flow during 1999 (see Figure 5.2).

Discharge on Mosquito Creek did not rise uniformly from one side of the basin to the other. It can be seen on Figure 5.10 that the north tributary began slightly higher but by late afternoon, the south tributary was yielding twice the flow volume of the north basin. Although both sub-basins are physiographically similar, the marked difference between the flow regimes during the first major melt event could be linked to radiation input,

temperature and the general aspects of each sub-basin. During the morning, when temperatures were cold, the north sub-basin received more radiation due to its southeasterly aspect. Around noon, at peak radiation, both basins probably received similar quantities of radiation. However, in the afternoon when temperatures were higher, the north sub-basin would have largely been shaded while the south sub-basin, with its northwesterly aspect, would have been in sunlight. The combined sensible and radiant heat inputs over the south sub-basin during the afternoon were probably higher than over the north basin and could have led to enhanced melt runoff.

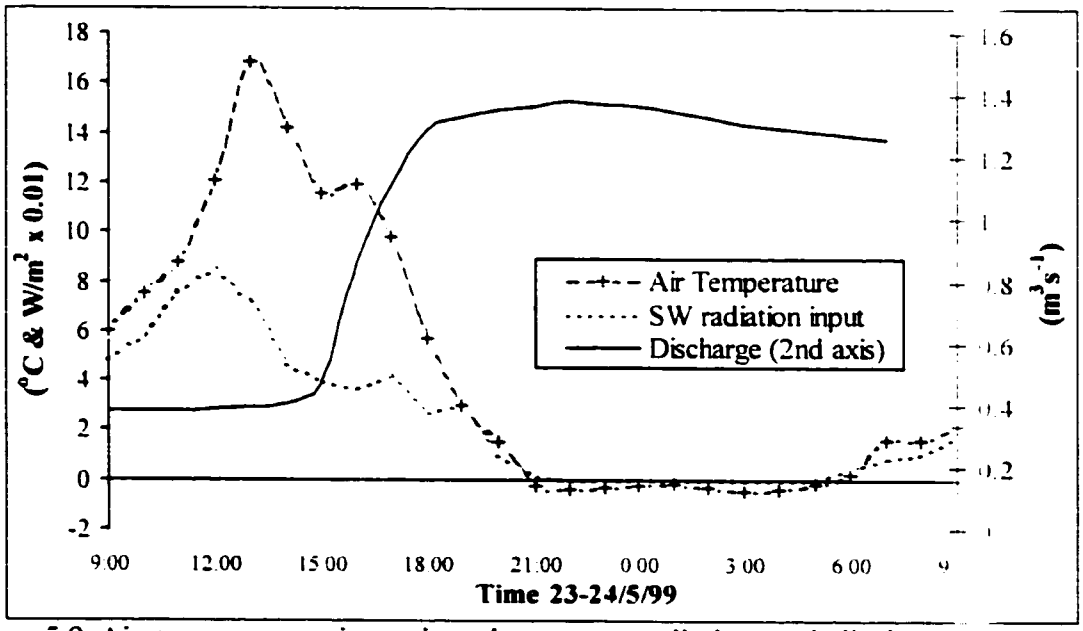

Figure 5.9 Air temperature, incoming short-wave radiation and discharge at Mosquito Creek during the first snowmelt event in 1999.

Another process that could have led to subdued flows from the north sub-basin is linked to the observations in section 4.4.3.3 of apparent flow regulation from areas of karst drainage. Although it is believed that both the north and south sub-basins of Mosquito Creek probably contain regions of karst, the north sub-basin has less surface drainage and more visible sinkhole features, thus suggesting that subsurface karst

drainage may be better developed on this side of Mosquito Creek Basin. If this is the case, then it might be expected that during the first spring melt of the year a high proportion of snowmelt water would rapidly drain into sinkholes and recharge the north sub-basin aquifers. Therefore, the difference in discharges between the north and south tributaries of Mosquito Creek during the early snowmelt could be evidence for karst groundwater recharge in the upper north side of the basin.

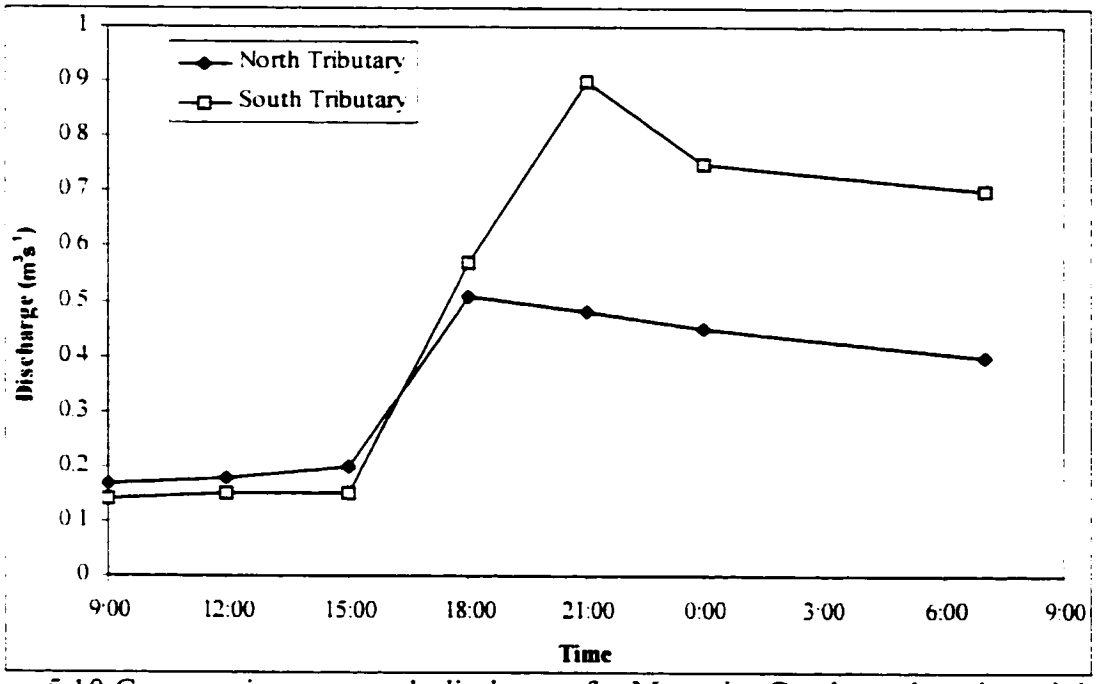

Figure 5.10 Comparative snowmelt discharges for Mosquito Creek north and south basin tributaries during major melt event, May 1999.

EC and $\delta^{18}O$ data were collected from both the north and south tributaries of Mosquito Creek every three hours from 09:00 to 24:00 hrs on May 23rd and then once again at 07:00 hrs on May 24th. The EC and $\delta^{18}O$ data were volume weighted and combined to provide the overall signatures for Mosquito Creek below the confluence (see Figure 5.11). There was a marked response to the snowmelt in the $\delta^{18}O$ signature with a subdued response in the EC. The average basin $\delta^{18}O$ signature appeared to enrich by

greater than 0.1 ‰ between 09:00 and 12:00 (> 0.2 ‰ on the north branch), perhaps in response to early melt shunting out old (possibly enriched vadose zone) water by piston flow. During the same time period, EC changed very little. However, after mid-day, the average $\delta^{18}O$ signature depleted by greater than 0.2 ‰ as snowmelt began to contribute to flow and EC dropped, either in response to dilution from surface and preferential flow pathways, or from reduced groundwater residence times.

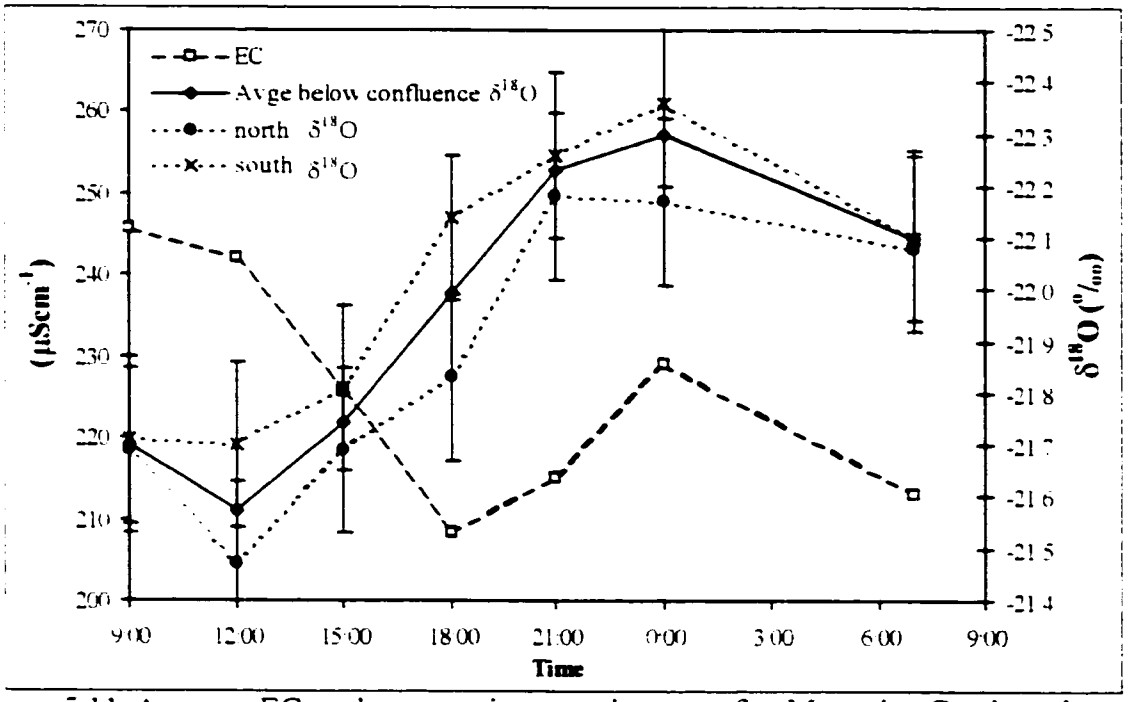

Figure 5.11 Average EC and oxygen isotope signature for Mosquito Creek melt event (including raw isotope data from the north and south tributaries), May 23rd – 24th 1999.

The relationship between average north and south tributary discharge and $\delta^{18}O$ is illustrated in Figure 5.12. After the initial stages of melt, discharge in Mosquito Creek rose rapidly and this was accompanied by a generally linear depletion of $\delta^{18}O$. Following peak runoff, $\delta^{18}O$ appeared to deplete even further before starting to return to baseflow levels, possibly indicating that even on the recessional limb of the hydrograph, the snowmelt contribution continued to rise for some time.

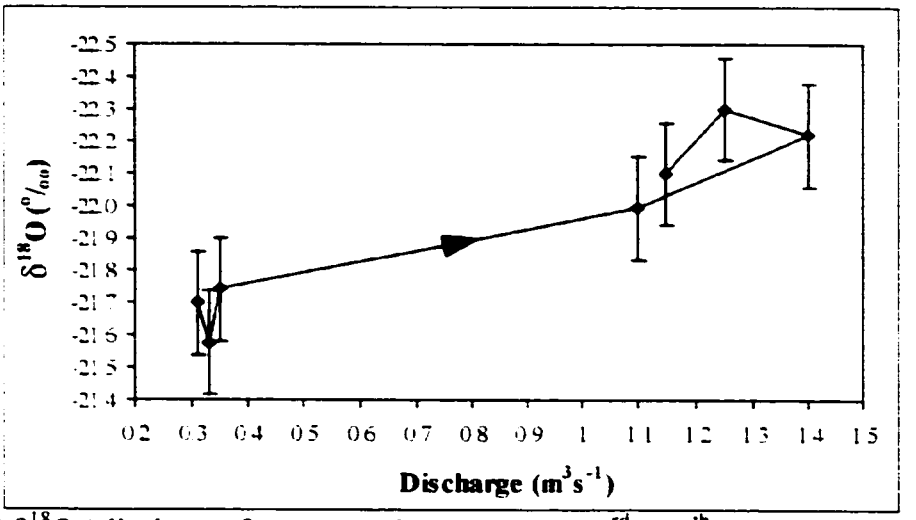

Figure 5.12 $\delta^{18}O$ / discharge for snowmelt event, May 23rd - 24th, 1999

In order to estimate the proportional contribution of new snowmelt to the hydrograph, a two-component hydrograph separation was performed using equation 2.8, and uncertainty at the standard deviation level (70% confidence) was assessed using equation 2.11 (after Genereux, 1998). The old water baseflow $\delta^{18}O$ value was taken to be the average value of four baseflow samples collected during the four days immediately leading up to the event (-21.60 ‰, σ = 0.13 ‰). The uncertainty level in the baseflow or the "old" component (W_{Co}) was estimated by multiplying σ by t (for three degrees of freedom) and was, therefore, set at 0.15 ‰. The "new" snowmelt signature was defined as the average of two bulk snowpack samples collected from 2150 m a.s.l. and 2700 m a.s.l. on the day of the melt event (-22.90 ‰, σ = 0.28 ‰). The uncertainty level in this snowmelt component (W_{Cn}) was estimated by multiplying σ by t (for one degree of freedom) and was, therefore, set at 0.55 ‰. The uncertainty level for the stream water $\delta^{18}O$ signature (W_{Cs}) was estimated from the standard deviation of analytical uncertainty, which was earlier found to be 0.08 ‰ (see section 3.2).

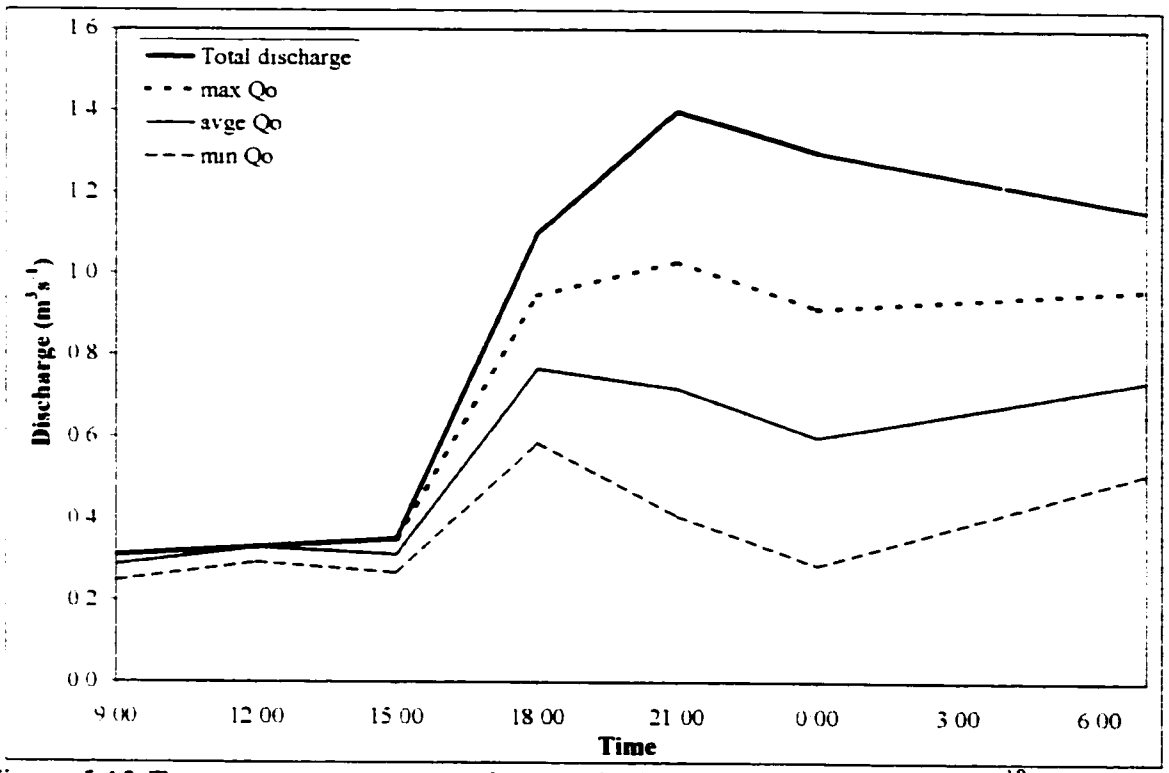

Figure 5.13 Two-component snowmelt event hydrograph separation using $\delta^{18}O$ of "new" snowmelt (Q_n) and "old" pre-melt (Q_o) components. May 23rd - 24th, 1999. Minimum and maximum based on a single standard deviation of uncertainty.

It would appear from Figure 5.13 that shortly after discharge began to rise in Mosquito Creek, the volume of pre-melt or old water also began to rise noticeably. The estimated average old premelt contribution (Q_o) to event runoff from the start to the end of sampling was 71% (±17% for an uncertainty of one standard deviation). The new snowmelt hydrograph component (Q_n) was, therefore, estimated to contribute an average of 29% (±17%), with a peak contribution of 54% (±24%) at around midnight. This is still a relatively large proportion of the hydrograph and suggests that some of the newly melted event water must have reached the stream relatively rapidly by one of the following mechanisms:

1) Hortonian overland flow in areas of impervious ground covers or where soils were too frozen to allow high infiltration rates;

2) Saturation overland flow in riparian zones and zero order channel depressions where the water table was near the ground surface;

3) Preferential or bypass flow through macropores and pipes in the upper soil matrix, and broken regolith deposits typical of mountainous environments.

The observation that the peak new water contribution occurred on the recessional limb of the hydrograph suggests a retardation of the transfer of new water to the stream, which could be linked to either: i) temporary basin storages and return flow; or ii) a change in surface saturation and drainage conditions as water tables approached the ground surface. If there was a retardation of snow melt inputs to the stream through basin storages, such as in soils and karst, it would be expected that this new water may take on an ionic signature close to that of groundwater. However, if the peak new water component in the hydrograph was related to rising water table levels and increasing areas of surface saturation leading to excess overland flow, then this water would be expected to have a reduced ionic concentration closer to that of snowmelt. This can be investigated further by examining the level of dilution of the stream EC signature during the event.

From Figure 5.14, it is apparent that EC (hence dissolved solids) decreased as flow increased during the event. The hysteresis within the EC curve (Figure 5.14) suggests that in general, weathering material contact was reduced and residence times probably shorter on the rising limb of the event. During peak flow and the early recessional period, the EC increased suggesting that groundwater flow pathways became more dominant. Therefore, it is more likely that the occurrence of peak new water contributions on the recessional limb was not due to enhanced saturation overland flow processes but rather temporary basin storages.

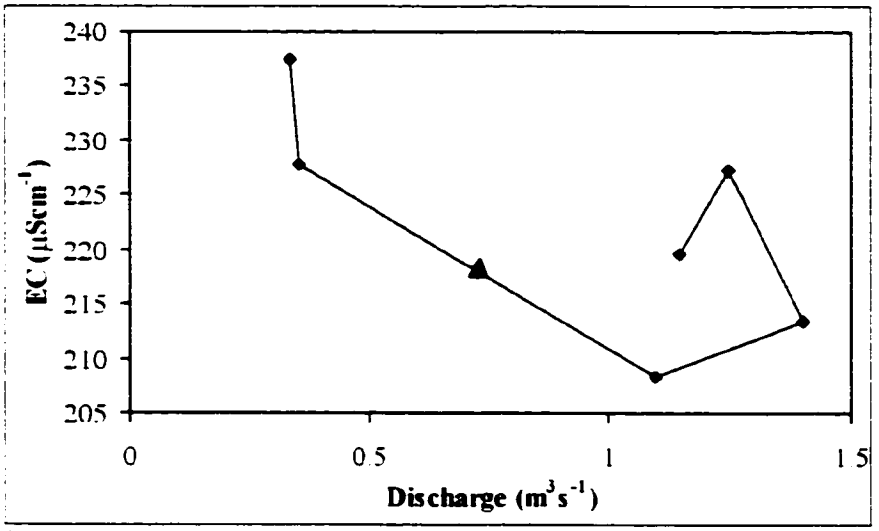

Figure 5.14 Hysteresis in the EC signature during the Mosquito Creek May 23rd - 24th 1999 snowmelt event.

Assuming that most of the reduction observed in the EC signature was due to volumetric dilution, a two-component hydrograph separation was performed to divide the event water into surface (Q_f) and sub-surface (Q_g) components. The surface runoff EC signature was assumed to be the same as that for snowpack EC within the Bow Valley (10 µScm^{-1}, σ = 7.8 µScm^{-1}). The uncertainty level in the surface snowmelt EC signature (W_{Cf}) was estimated by multiplying σ by t (15 degrees of freedom) and was, therefore, set at 8.4 µScm^{-1}. The subsurface EC signature was assumed to be the same as groundwater maintained baseflow, and was taken to be the average value of six stream baseflow samples collected during the week immediately prior to the event (246 µScm^{-1}, σ = 7.3 µScm^{-1}). The uncertainty level in the subsurface EC signature (W_{Cg}) was estimated by multiplying σ by t (5 degrees of freedom) and was, therefore, set at 8.5 µScm^{-1}.

According to this simple hydrograph separation (Figure 5.15), the small dilution of the EC signature for the large increase in volume suggests that between 88% and 94% of the total flow was routed through sub-surface pathways. Of note is that the maximum surface runoff contribution (16% ±3%) occurred at peak discharge and the minimum

surface contribution after initiation of the event occurred at midnight. Therefore, from the two hydrograph separations performed for this event (Figures 5.13 and 5.15) it is suggested that the maximum new snowmelt contribution coincided with the minimum surface runoff. Although there is some uncertainty as to the exact proportional contributions of these components to the hydrograph, it would seem that during hydrograph recession a large volume of flow was subsurface routed snowmelt water.

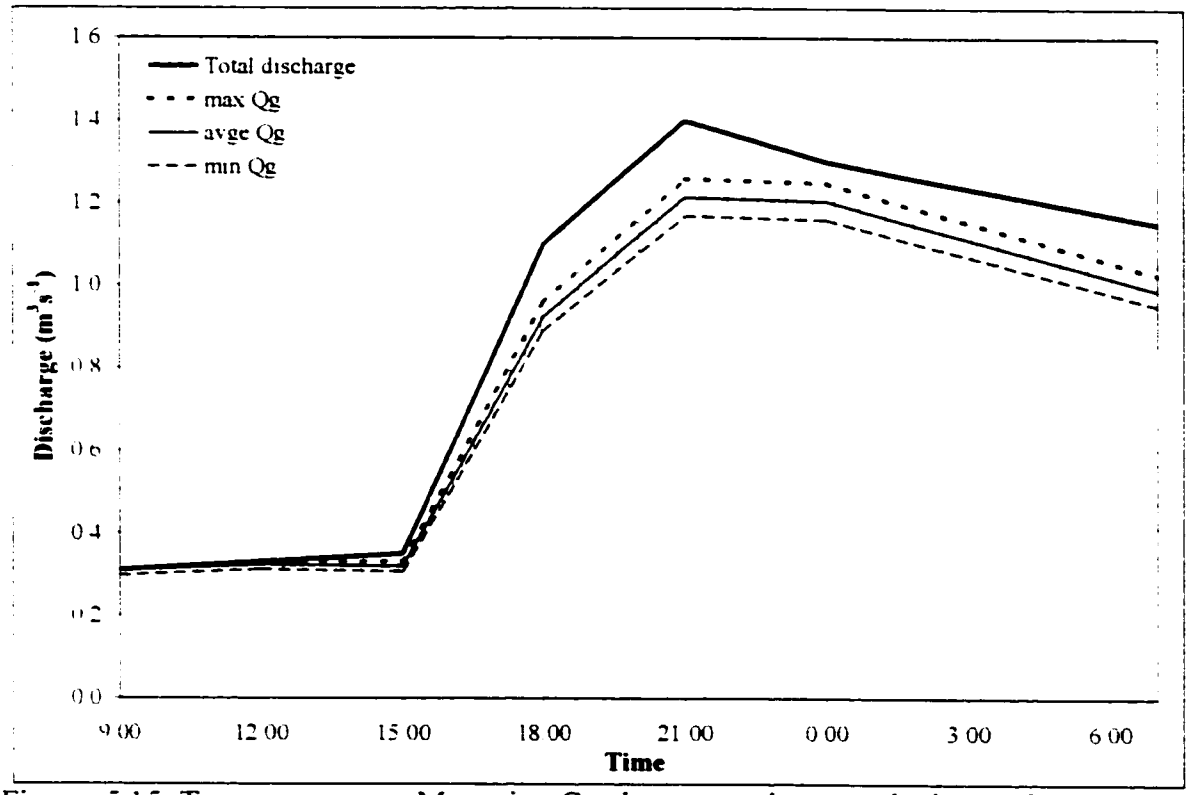

Figure 5.15 Two-component Mosquito Creek snowmelt event hydrograph separation using EC surface (Q_f) and sub-surface (Q_g) flow components. May 23rd - 24th, 1999. Minimum and maximum based on a single standard deviation of uncertainty.

A considerable volume of surface runoff might be expected in a mountainous basin with large areas of impermeable rock and frozen soils but if this did occur, it did not lead to much dilution of the EC signature. This may suggest that the simplistic assumption of two major flow components (surface and subsurface) was invalid, or the characterisation

of these flow components was incorrect. Prior to the event, baseflow was likely maintained by deep groundwater contributions only, as it had been several months since any recharge could have occurred. Water flowing through mineral soil, till and bedrock pathways, therefore, would have dominated premelt baseflow. However, during this first melt event of the year, it is likely that a significant proportion of water would have encountered upper organic soil layers in forested areas (either due to rising water tables or preferential flow paths) before reaching the channel. If the upper organic soil zone in forest areas had a distinct end-member signature then a three-component separation of deep groundwater, soil zone and surface runoff pathways would be more appropriate.

One way to separate out these three components would be to combine the two hydrograph separations already carried out. This would require the assumption that the old or premelt water in the $\delta^{18}O$ based separation was equivalent to the deeper groundwater component of the proposed three-component separation. From earlier observations and discussions of hydrometeorological, baseflow and groundwater conditions within the Bow Basin (Chapters Four and Five), it has been considered likely that water table levels prior to spring melt in 1999 were lower than normal. This being the case, it would also seem likely that in-stream baseflow prior to the melt event was largely maintained by deep groundwater sources from the tills and bedrock beneath the shallow organic soil matrix (rarely exceeding 0.3 m in depth). If this was the case, then the new water component of the prior $\delta^{18}O$ hydrograph separation (Figure 5.13) would be mostly surface and shallow soil routed snowmelt water and the old water component would be mostly deep groundwater.

The proposed separation does have a potential flaw, however, due to the presence of water held under tension in the shallow soil matrix. As meltwater infiltrates this soil zone the tension water and meltwater components would mix and therefore the new water component would not be totally comprised of snowmelt. Unfortunately, the $\delta^{18}O$ signature of this component was unknown and so a standard three-component hydrograph separation cannot be performed. However, it is thought that soil wetness in shallow forest soils that have been covered in deep snow for up to five months would be well below field capacity. In addition, any small volume of old water within the soil may have frozen during the winter (average wintertime daily temperatures between -5° C and -15°C prior to this event) and would not commence melting as early as the overlying snowpack. In either case, it is not thought likely that old soil water could be a major flow component within the hydrograph.

If the above assumptions are acceptable, then the old (premelt) component of the first $\delta^{18}O$ hydrograph separation (Figure 5.13), and the deep groundwater component of the proposed three component separation can be considered equivalent. Therefore, the remaining new snowmelt water can be separated into two pathway components (upper soil water and surface runoff), using a simple EC based two-component separation. A summary of this approach is outlined below:

If: $$Q_R - Q_G = Q_F + Q_S = x \quad (5.3)$$

And: $$Q_R C_R - Q_G C_G = Q_F C_F + Q_S C_S = y \quad (5.4)$$

Then: $$Q_F = \frac{(y - xC_S)}{(C_F - C_S)} \quad (5.5)$$

Where Q and C are the discharge and EC concentration of each flow component, and the subscripts R, G, F and S are river, groundwater, surface routed water and soil routed water, respectively. The deep groundwater component (Q_G) was assumed equal to Q_o in the earlier isotopic hydrograph separation, the total river runoff (Q_R) was known, and so it was simple to solve equation 5.5 for the remaining surface (Q_F) and soil water (Q_S) components.

The same EC signatures and uncertainty levels for Q_G and Q_F were used in this three-component separation as were used for Q_g and Q_f, above (Q_G = 246 μScm^{-1}, W_{Cg} = 8.5 μScm^{-1}; and Q_F = 10 μScm^{-1}, W_{Cf} = 8.4 μScm^{-1}). Unfortunately, there were no observations of EC in upper soil water layers taken during the snowmelt event. However, earlier summertime measurements from a shallow (< 0.3 m) soil water well in Mosquito Creek's forested floodplain area during 1998 indicated an average EC of 309 μScm^{-1} (n = 5, σ = 40 μScm^{-1}). The standard deviation uncertainty level for this component was set at σ multiplied by t for four degrees of freedom (W_{CS} = 47.6 μScm^{-1}). The overall uncertainty for the Q_F/Q_S separation was added to that of the earlier uncertainty level estimated for Q_o in the isotopic hydrograph separation (Figure 5.13) so that a range of hydrograph proportions could be estimated for each of the three components.

Using this approach, the average proportional flow contributions for surface runoff, shallow soil water and deep groundwater were estimated to be 16% (2 – 34%), 13% (0 - 32%) and 71% (±17%), respectively (Figure 5.16). Some of the assumptions used may be open to question and the uncertainty ranges are high, and so the component proportions illustrated in Figure 5.16 must be considered a very rough approximation of the hydrologic behaviour during the onset of melt for non-glacierised headwater basins in the

Bow Valley. The slow decrease in surface runoff contribution late on the recessional limb could be the result of delayed responses from areas of relatively low weathering potential (due to surface runoff and reduced soil cover) at higher elevations. The time for water to flow from below the headwaters to the sample site was observed to take approximately two hours during summertime dye trace experiments at discharges over 2 m^3s^{-1} and so a longer journey at lower flow should take much longer.

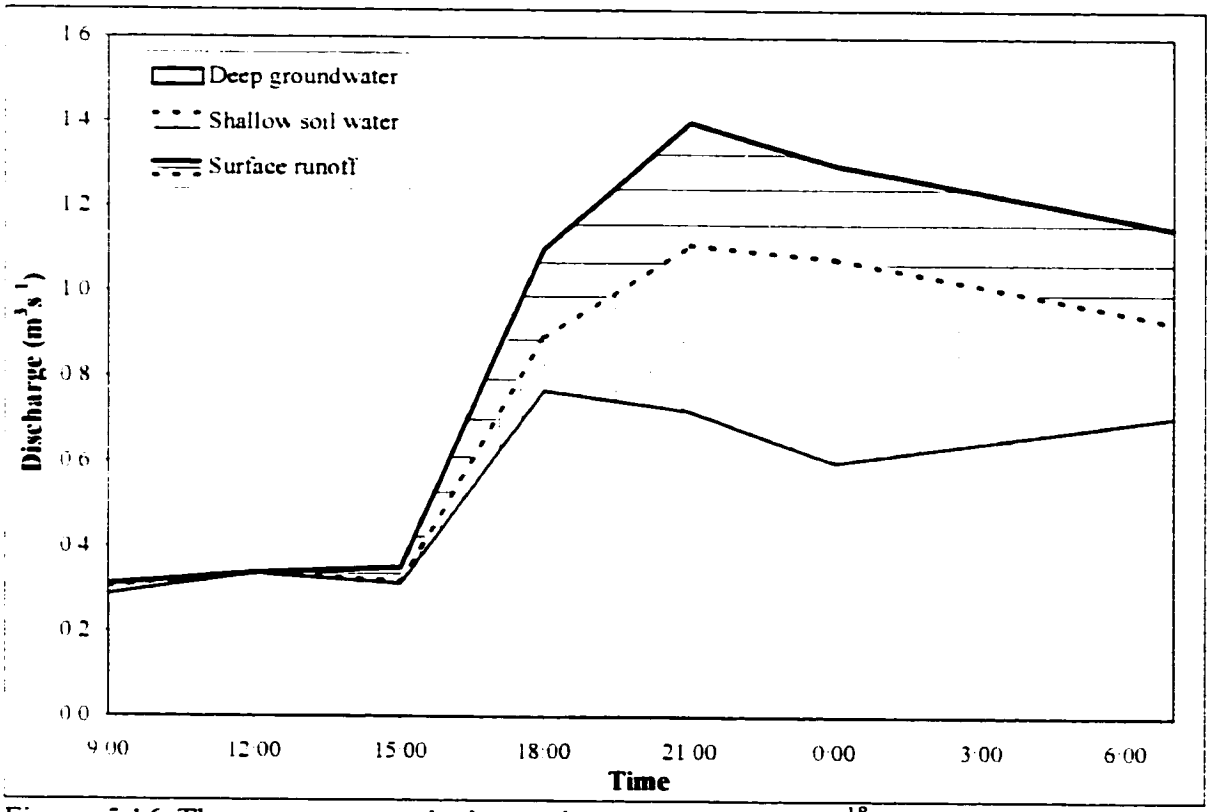

Figure 5.16 Three-component hydrograph separation using $\delta^{18}O$ and EC to divide the hydrograph into surface runoff, soil water and deep groundwater. May 23rd - 24th, 1999.

5.2.6 Rainfall Event – August 1998

During the time in the field, there were several rainfall episodes but there was only one intense rain event that lasted long enough to have a noticeable and prolonged effect on the stream hydrograph. Unfortunately, the event occurred at 01:00 hrs on August 16th 1998, on the night prior to the end of the summer field campaign, and it was not possible

to monitor discharge or EC. However, rainfall was monitored hourly at the Bow Summit weather station, 14 km to the northwest of Mosquito Creek. There is some confidence that the record collected at Bow Summit reflects the rainfall conditions at Mosquito Creek as the station is vertically less than 100 m above the basin endpoint and the recorded duration of the storm coincided exactly with field observations at the sample site. In-stream samples were collected every two to three hours following the start of the storm. Baseflow was sampled four days and two days prior to the storm and again at the beginning of the event. Rainfall was collected at the basin endpoint for the duration of the storm and all baseflow, rainfall and in-stream samples were analysed for pH and $\delta^{18}O$ (see Figure 5.17). (Note: pH in-stream was measured in real time and pH of rainwater was measured immediately following the rainfall event).

Although discharge was not measured at Mosquito Creek, it was automatically recorded at Bow Creek on the other side of the Bow Valley. The two basins are physiographically different with Bow Creek Basin being 10 km^2 smaller than Mosquito Creek and dominated by glacier cover. However, Bow Creek was the only basin nearby of a similar size where discharge data were being monitored and was therefore the only record available that could provide any information regarding the local storm runoff duration and magnitude. Fortunately, the storm occurred during diurnal baseflow conditions on the glacierised Bow Creek and the event showed up clearly in the hydrograph. In an attempt to reconstruct an approximate hydrograph for Mosquito Creek, the hourly areal yields that exceeded baseflow levels during and immediately following the rainfall event were calculated for Bow Creek, then converted to a discharge for Mosquito Creek and superimposed on top of the measured baseflow two days prior to the

event (Figure 5.17). This method of estimating the discharge for rainfall runoff on Mosquito Creek is invalid given the large difference in basin physiographies but should at least provide an indicator of the magnitude and duration of the real event. Due to the smaller basin size and greater area of impervious surfaces in Bow Creek, any errors associated with this reconstruction would lead to an underestimation of storm runoff duration and an overestimation of runoff yield.

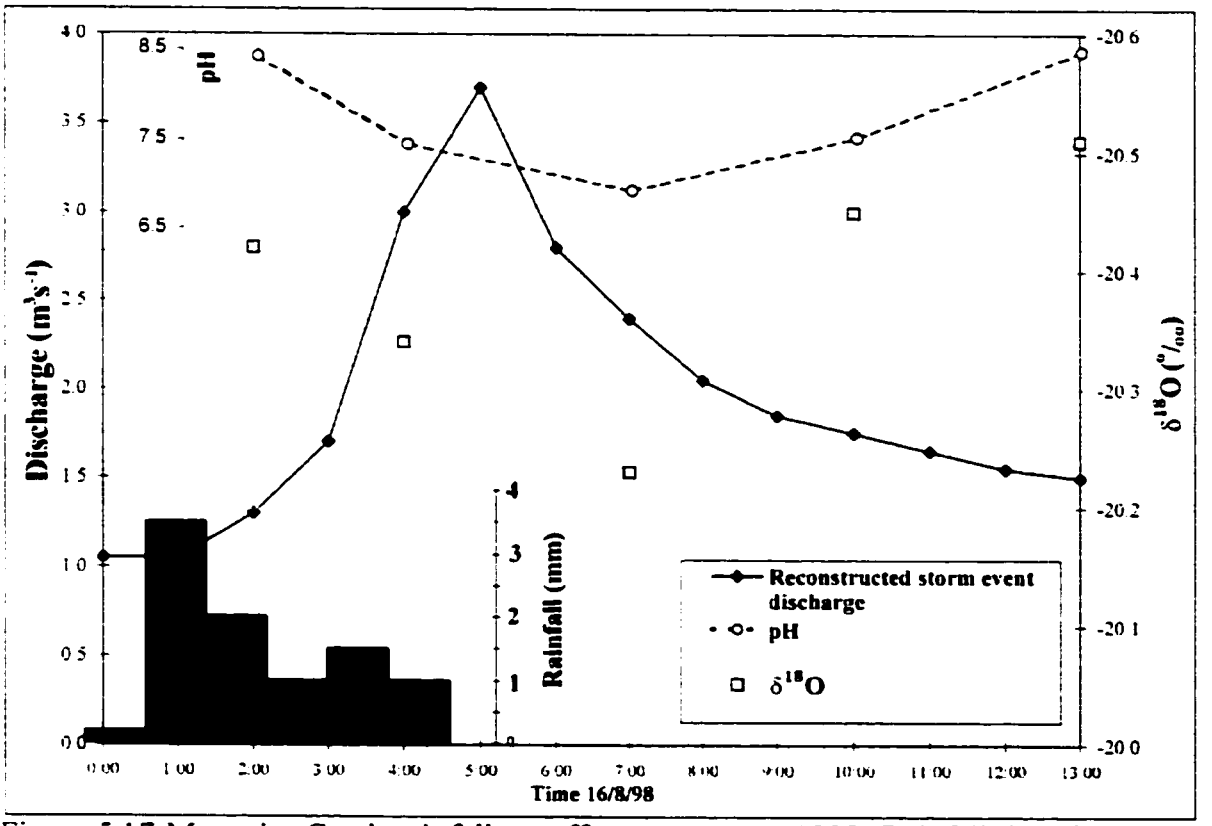

Figure 5.17 Mosquito Creek rainfall runoff event, August 1998. Rainfall data from Bow Summit. $\delta^{18}O$ samples and pH data collected from the creek during the storm event. (Discharge was not measured at the stream and the curve shown here has been reconstructed using Bow Creek records.)

The depth of rainfall recorded at Bow Summit was 9.3 mm and the storm was approximately five hours in duration. The timing of the storm between Mosquito Creek and Bow Summit was coincident suggesting that it was widespread and probably

associated with a synoptic scale frontal system. Therefore, it was assumed that a similar amount of rainfall fell over the Mosquito Creek Basin. The estimated total areal yield for Mosquito Creek (34.9 km^2) during the 13 hours following the start of the event was 2.8 mm over the entire basin, but with the baseflow discharge of 1.1 m^3s^{-1} removed the event areal yield became approximately 1.3 mm. The recessional limb of the storm could not be observed beyond mid-day at Bow Creek due to the influence of melt inputs. However, linearly extending the recessional limb forwards in time until it reached pre-event baseflow levels increased the total and event areal yields to 4.0 mm and 2.5 mm, respectively. Therefore, around 6.8 mm (or 73%) of the total rainfall could not be accounted for and presumably went into temporary storage.

The low estimated yields for the rain event runoff relative to the measured total rainfall raises a question as to the validity of the hydrograph reconstruction. To this end, it would be useful to compare the event duration and areal yield from Mosquito Creek with a nearby basin of similar physiography. Other than Bow Creek the next nearest basin to Mosquito is Pipestone River Basin (as described in Chapter One). Pipestone is an order of magnitude larger than Mosquito but is physiographically almost identical and both basins are adjacent to one another. In addition, hourly discharge is collected at the basin endpoint and can therefore be used for a yield comparison. (It should be noted that the Pipestone record could not have been used for hydrograph reconstruction due to the basin being more than an order of magnitude larger with a commensurate retardation in basin response times.)

The hydrograph on Pipestone River was observed to start climbing 16 hours after the start of the rainfall event and then fell back to the pre-event baseflow discharge of 8.5

m^3s^{-1} after a further 29 hours. The rise of the hydrograph above prior baseflow levels during this 29-hour period peaked at 11.5 m^3s^{-1} and delivered a basin-wide yield of 0.5 mm (the influence of basin area to runoff yield will be explored later in section 6.4). This value is significantly less than that estimated for Mosquito Creek and supports the earlier suggestion that using Bow Creek records to reconstruct the Mosquito Creek hydrograph probably systematically over-estimated flow. To this end, it should be noted that the recreated peak discharge on Mosquito Creek was 1.3 m^3s^{-1} or 50% greater than the highest discharge measured at any time during 1998 and 1999. If the Mosquito Creek rain event yield was over-estimated, then total rainfall unaccounted for in the balance was greater than the 6.8 mm calculated. There is reasonable confidence, therefore, that a high proportion of the rainfall input volume was not transferred (either directly or indirectly) to the channel during the event response in the hydrograph.

The observation that the hydrograph response was volumetrically around four times below the event input indicates a large storage potential within Mosquito Creek Basin. This storage potential has been hinted at previously in two previous observations:

1) Seasonal cycles of snowmelt and rainfall were lagged by several weeks to months in the annual baseflow isotopic record (see Chapter Four);
2) The approximate basin hydrological yields for 1998 and 1999 only differed by 14% despite observed increases of precipitation from 1998 to 1999 of 42% and 177% at two different basin locations (see Table 1.2).

Although some lakes exist in Mosquito Creek Basin, they are small and could not constitute a significant hydrological storage. Therefore, the groundwater zone is the largest potential store for any hydrological inputs. It has already been shown in section

4.4.3 that karst areas within the basin appear to have relatively stable areal yields and may constitute a large proportion of basin storage.

The complex lithological compositions within mountainous areas offer numerous potential storage units: e.g. fractured or porous bedrock, karst, tills and moraines, soils and talus. The interaction (or coupling) between these materials and their topographic situation and proximity to the stream are also important determinants of storage potential (e.g. Forster and Smith, 1988), and therefore influence how event water is transmitted to the stream. For example, a basin-wide groundwater storage that acts like a simple reservoir with inputs at one end and outputs at the other may be expected to respond to a rain event by pushing out of storage a commensurate volume of old water. However, a more complex system with several different storages with varying proximity to the stream may be expected to deliver some proportion of the new event water to the stream quite rapidly. Hydrograph separations of event and pathway contributions during the rainfall event would therefore assist with this interpretation.

Unfortunately, EC could not be measured during this event and so it is not known if there was any dilution of the runoff associated with rapid transfers of event water to the channel. However, pH and $\delta^{18}O$ were sampled and both displayed a pattern indicating some contribution of rainfall to stream flow (Figure 5.17). Rainfall pH was measured to be 5.5 and the drop in stream concentration from 8.5 to 6.9 pH units suggested some direct transfer of rain to the channel. Unfortunately, pH is not a reliable geochemical tracer and so a hydrograph separation of new and old water was performed using the $\delta^{18}O$ signatures only (Figure 5.18).

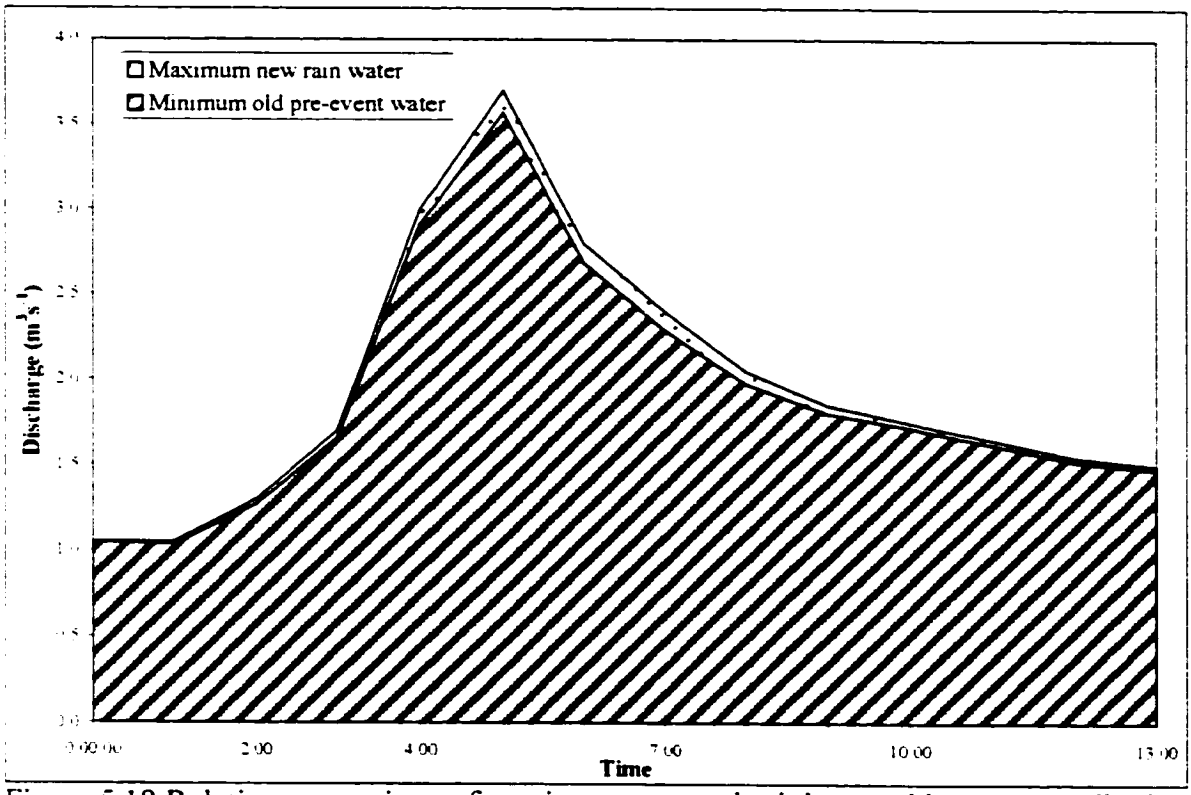

Figure 5.18 Relative proportions of maximum new and minimum old water contributions (at the standard deviation uncertainty level) during the rainfall event at Mosquito Creek.

Rainfall sampled at the basin endpoint had a signature of -12.7 °/₀₀. The uncertainty level of the new rainwater component (W_{Cn}) could not be estimated from the single sample collected, and so the σ value for all rainfall samples collected within the Bow Valley from 1996 to 1999 (σ = 2.2 °/₀₀) was multiplied by t for 15 degrees of freedom (W_{Cn}= 2.4 °/₀₀). The pre-event baseflow five days, one day and immediately preceding the event had an average value of -20.46 °/₀₀ (n = 3, σ = 0.04 °/₀₀). The uncertainty level of this old baseflow component, estimated from σ x t for two degrees of freedom, was below the standard deviation level of analytical error and so W_{Co} was set at 0.08 °/₀₀ (see section 3.2). Uncertainty in stream $\delta^{18}O$ was also set at the standard deviation level of analytical error (W_{Cr} = 0.08 °/₀₀). A simple two-component separation (equation 2.8) was

then performed using the end-member signatures and the $\delta^{18}O$ values collected from the stream during the event (Figure 5.18).

The results of the $\delta^{18}O$ hydrograph separation suggest that the maximum rainfall contribution to the hydrograph at any time was only 5% with a total rainfall contribution to runoff of between 0 and 0.1 mm. These results are similar to findings from studies in other non-mountainous areas (e.g. McDonnell *et al.*, 1991) but disagree with the qualitative interpretation of the pH observations and other studies undertaken in alpine environments (e.g. Laudon and Slaymaker, 1997). Also, given the large volume of rainfall input it would appear, at least intuitively, that this division of the hydrograph is probably incorrect. If the two-component hydrograph separation is in error then one or both of the end-member signatures is wrong or there are more end-members. Considering the size of the basin, the error could lie with any of these options. However, it may be possible to establish the most likely source of error (if there is one) if each potential source is considered individually:

1) Old water end-member – Baseflow was sampled four days and two days prior to the day of the storm and again at the start of the event. The $\delta^{18}O$ values observed were all between -20.4 $^{o}/_{oo}$ and -20.5 $^{o}/_{oo}$ and so there is confidence that the chosen value of -20.5 $^{o}/_{oo}$ is reasonable.
2) Rainwater end-member – Only one sample of rainfall was collected. Temporally, the sample represents the entire storm but spatially there could be a problem with the sample location being at the lowest point in the basin. Although no relationship was found between $\delta^{18}O$ and elevation in this study, it is generally accepted that elevational gradients do occur in precipitation. A range of isotopic depletion between

0.15 ‰ and 0.3 ‰ per 100 m rise in elevation is quoted in other literature (e.g. Schotterer *et al.*, 1996). The sample location was 400 m below the average basin height and so it might be expected that the sample could be up to 1.2 ‰ too enriched relative to average rainfall. However, changing the rainfall signature by this amount makes no difference to the separation.

3) Number of end-members – The assumption that baseflow is representative of all water in the basin prior to the event is, in this case, probably invalid. During summer, the water table was likely higher than interannual baseflow levels due to spring snowmelt and summer rain inputs, and water could potentially have been held in temporary storage in many parts of the basin. During pre-event summer baseflow, it is possible that not all of the potential storages were contributing to flow. During an event, however, these storages could have been triggered to contribute. Two potential storage sources are:

    a) Soil water under tension;

    b) Groundwater lying in karst or talus aquifers with major drainage pathways or conduits located just above the pre-event water table and low hydraulic conductivity pathways below.

Groundwater storage zones with the properties outlined above and displaying isotopic signatures more depleted than pre-event baseflow could, therefore, constitute a third end-member that would mask the rainfall contribution. From Tables 4.2, 4.4 and 4.5 in Chapter Four, it is apparent that the most isotopically depleted baseflow contributions in these areas were often associated with tributaries draining karstic regions of the basin or

in areas of forest springs. Could either or both of these sources be the missing end-member(s) if the rainfall contribution has been under-estimated?

It was already postulated in Chapter Four that water lying in karst aquifers probably has a depleted summertime signature due to the high proportion of snowmelt that rapidly infiltrates to this store during spring. In addition, the geology of Mosquito Creek is dominated by interbedded limestone, dolostone, gritstone and shale, and therefore the potential for geological aquicludes would probably lead to a huge storage potential in the more permeable rocks of the basin. Discharge observations from the nearby Red Spring of the Castleguard karst system indicated a high aquifer storage potential but with relatively rapid response to rainfall events (Smart and Ford, 1986). A karst aquifer with similar properties to Red Spring lying in the headwaters of Mosquito Creek could potentially provide a third relatively depleted end-member. However, the second possibility of an isotopically depleted forest soils end-member cannot be discounted.

Forest springs in Bow and Mosquito Creeks tended to display lighter signatures than other nearby springs from other lithological groups (see section 4.4.2 and Table 4.2) and therefore could be an indicator that forest soils may contribute a high volume of isotopically depleted runoff during events. To meet the conditions in 3a above, isotopically depleted forest soil water under tension would need to be released as event water infiltrated into the soil matrix. However, a problem with this is that although springs issuing from forested slopes may be isotopically depleted relative to stream baseflow, it is likely that during late summer, water in the unsaturated zone of forest soils would be enriched from earlier rainfall infiltration and perhaps evaporation. Thus, it would seem unlikely that forest soils could be the source of the missing end-member. The

observations of depleted forest spring water (Table 4.2) may originate from deeper groundwater in tills or karst that is remnant snowmelt water from earlier in the year, and NOT from tension water in the soil matrix.

In summary, then, a high volume of rainfall fell over Mosquito Creek during the event and it was estimated that the runoff response yielded around 27% of the hydrological rainfall input, therefore, illustrating that this non-glacierised basin has a high storage potential. From the $\delta^{18}O$ hydrograph separation it was found that the direct rainfall contribution to runoff was either very small (never more than 5%) or almost completely masked by other end-member inputs. Measurements of in-stream pH suggested that there probably was a direct rainfall contribution, and that there was likely a dominant third end-member with an isotopically depleted signature. Regions of karst in the basin headwaters were considered to be the most likely missing end-member based on earlier findings that these areas had isotopically depleted signatures with relatively stable baseflow characteristics. The temporal coincidence of rainfall with warmer temperatures and high water tables, combined with the observation that only a small proportion of the rainfall reached the basin outlet suggests that in these areas rainfall is preferentially evaporated out of the basin over other hydrological balance components.

5.3 Bow Creek – Glacierised Basin

5.3.1 Field Sampling and Data Acquisition

Hydrometric studies at Bow Creek (~ 32% glacierised – see section 1.3.2) commenced in May 1996, when a pressure transducer stage gauge was installed on the major tributary known as Bow Waterfall Creek (~ 50% glacierised) with data being logged every hour. The gauge was calibrated for discharge using standard area-velocity

and dye dilution techniques during subsequent site visits from 1996 to 1998. Unfortunately, the record for Bow Waterfall Creek was not available for 1997 due to the gauge being located near a popular tourist route and subsequent vandalism leading to loss of data. A further gauge was installed on the other major basin tributary, Bow Hut Creek (~ 20% glacierised), in early 1998 by the University of Alberta and these data were kindly made available for this study. Stage data for Bow Hut Creek were also calibrated using the same techniques as noted for Bow Waterfall Creek. No automatic data for either gauge were available for 1999 although some manual readings were made on Bow Waterfall Creek during the spring.

Fortunately, 1996 and 1998 were hydrometeorologically very different, displaying deep and shallow winter snowpacks, respectively (see section 1.4 and appendix 1). In addition, the annual mass balance at Peyto Glacier, contiguous with and therefore indicative of conditions over the icefields of Bow Creek Basin, was positive in 1996 and negative in 1998 (Mike Demuth, personal communication). Manual and automatically monitored discharge data for Bow Creek tributaries during 1996 and 1998 are illustrated in Figures 5.19 and 5.20. These years were considered representative of important hydrological end-member conditions and therefore intercomparison of monthly areal yields and dominant temporal periodicities were performed.

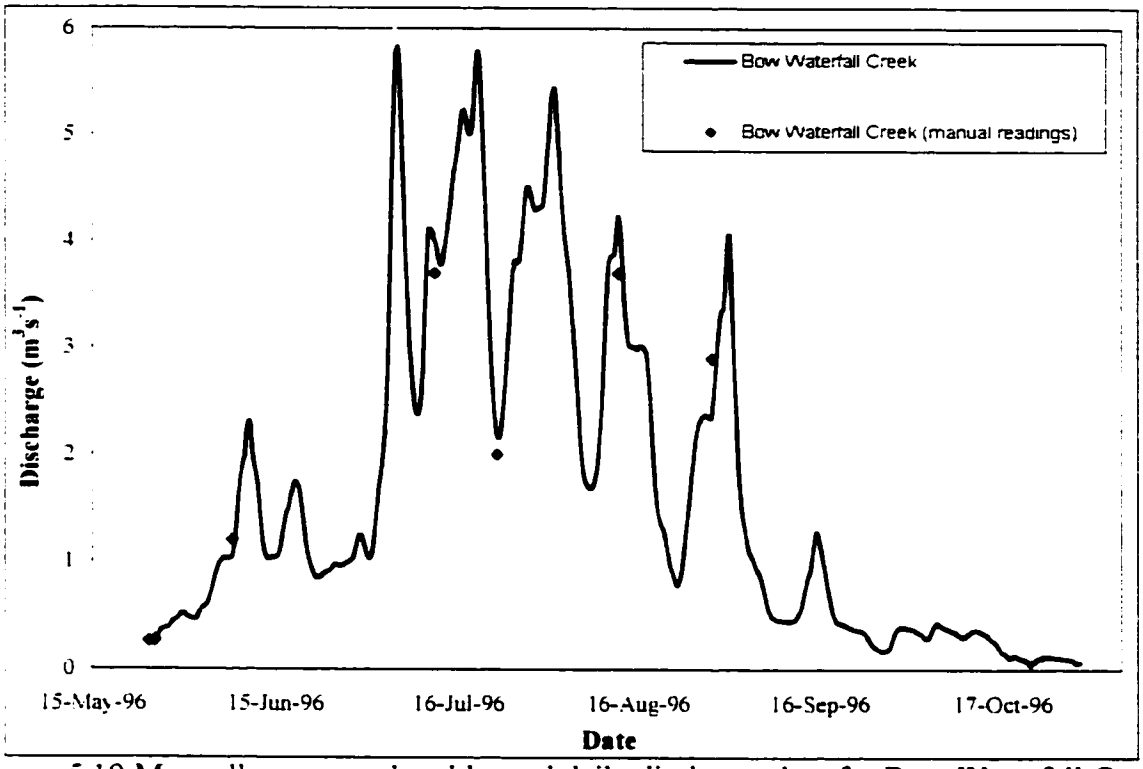

Figure 5.19 Manually measured and logged daily discharge data for Bow Waterfall Creek during 1996.

To investigate changing seasonal geochemical patterns, stream samples were collected from Bow Creek approximately every 5 to 15 days (usually during mid afternoon) during the field visits of 1998 and 1999 (see section 5.2.1.1). EC was measured on site, with $\delta^{18}O$ and enriched tritium samples subsequently analysed at the University of Waterloo Environmental Isotope Laboratory. A diurnal melt event was investigated by measuring EC and collecting water samples for $\delta^{18}O$ analysis simultaneously at both Bow Hut and Waterfall Creeks. The diurnal sample set commenced at 19:00 on the 9th of August 1998 and continued until 17:00 the following day with measurements and samples collected every 3 to 4 hours.

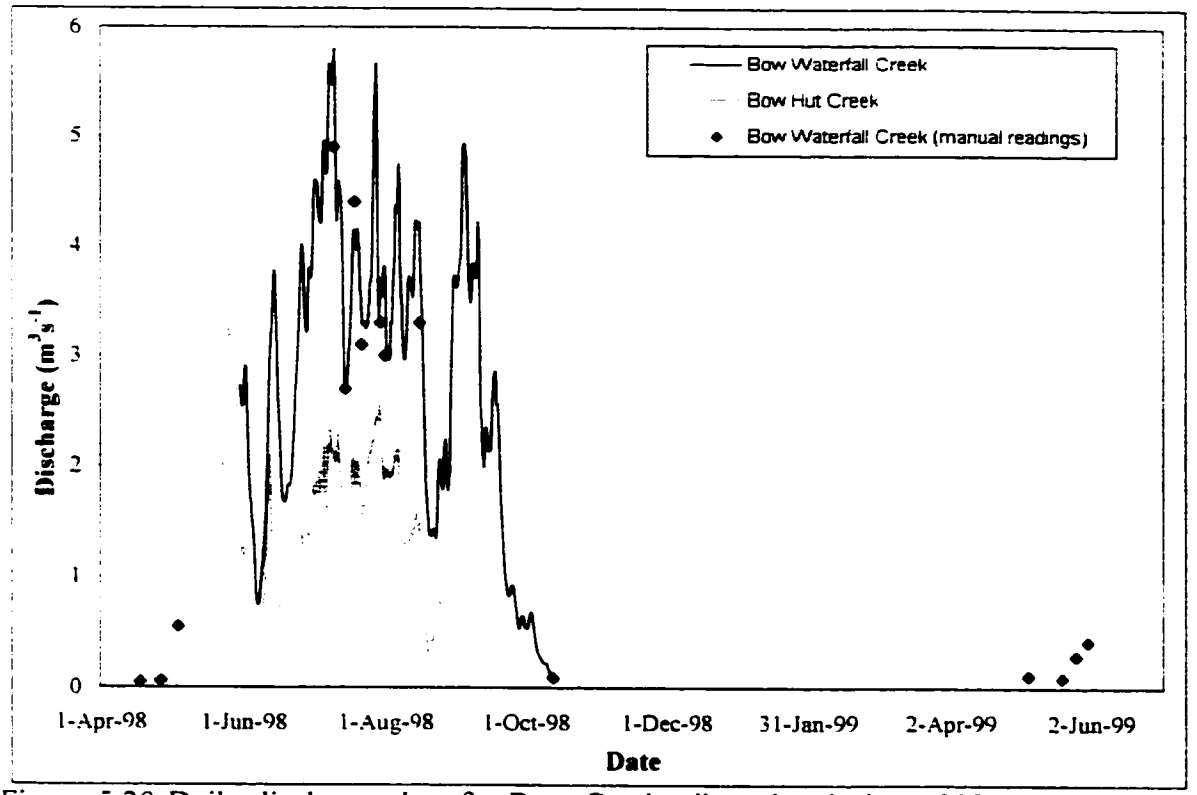

Figure 5.20 Daily discharge data for Bow Creek tributaries during 1998 and early 1999 (Bow Hut Creek stage data courtesy of Melissa Lafreniere, University of Alberta).

5.3.2 Areal Hydrological Yield

From measured discharge records and the assumption that stream flow does not vary during the baseflow period from October to April, it was possible to estimate the areal yields of Bow Waterfall Creek for the 1996 hydrological year, and for both Bow Creek tributaries in 1998. The areal yields for Bow Waterfall Creek during 1996 and 1998 were approximately 2040 mm and 3100 mm, respectively. Therefore, the yield was 50% greater during a year of approximately 50% less snowpack volume (see section 1.4.2). For Bow Hut Creek in 1998, the yield was less than half that of Bow Waterfall Creek at approximately 1220 mm. Of note is that all of these yield estimates are several times larger than local precipitation measurements 6 km away at Bow Summit weather station,

where 850 mm was recorded for 1996 and 300 mm for 1998. Even for Bow Hut Creek, the yield is four times greater than local precipitation measurements.

Given that most of the upper areas of Bow Creek Basin are covered by the Wapta Icefields, the high yields can generally be attributed to the deep winter snowpacks experienced here. Bow Waterfall Creek has a greater glacierised area than Bow Hut Creek (50% compared to 20%), hence the higher relative yield in 1998. However, the increased yield for Bow Waterfall Creek in 1998 relative to 1996 was not due to snowmelt input but rather was a result of reduced snowpack during *El Niño* conditions, leading to increased glacial ice exposure and subsequent ablation.

During 1996, the deep snowpack led to a positive mass balance of approximately 130 mm at Peyto Glacier (Mike Demuth, Pers. Comm.) leading to a net hydrological storage within the basin. Glacier cover within Bow Creek Basin is contiguous with Peyto; both basins have similar aspects and elevation ranges, and would therefore be expected to experience similar mass balance conditions. It is interesting then that even during a year of net storage, the hydrological yield was so high compared to precipitation levels and the hydrological yields of nearby basins during similar deep snowpack conditions (e.g. Mosquito Creek during 1999). It must be concluded, therefore, that glacierised parts of the Bow Basin headwaters are always high yielding, even during years when glaciers hold back snowmelt, and that local precipitation records bear little relationship to the snow and icemelt yields from such areas.

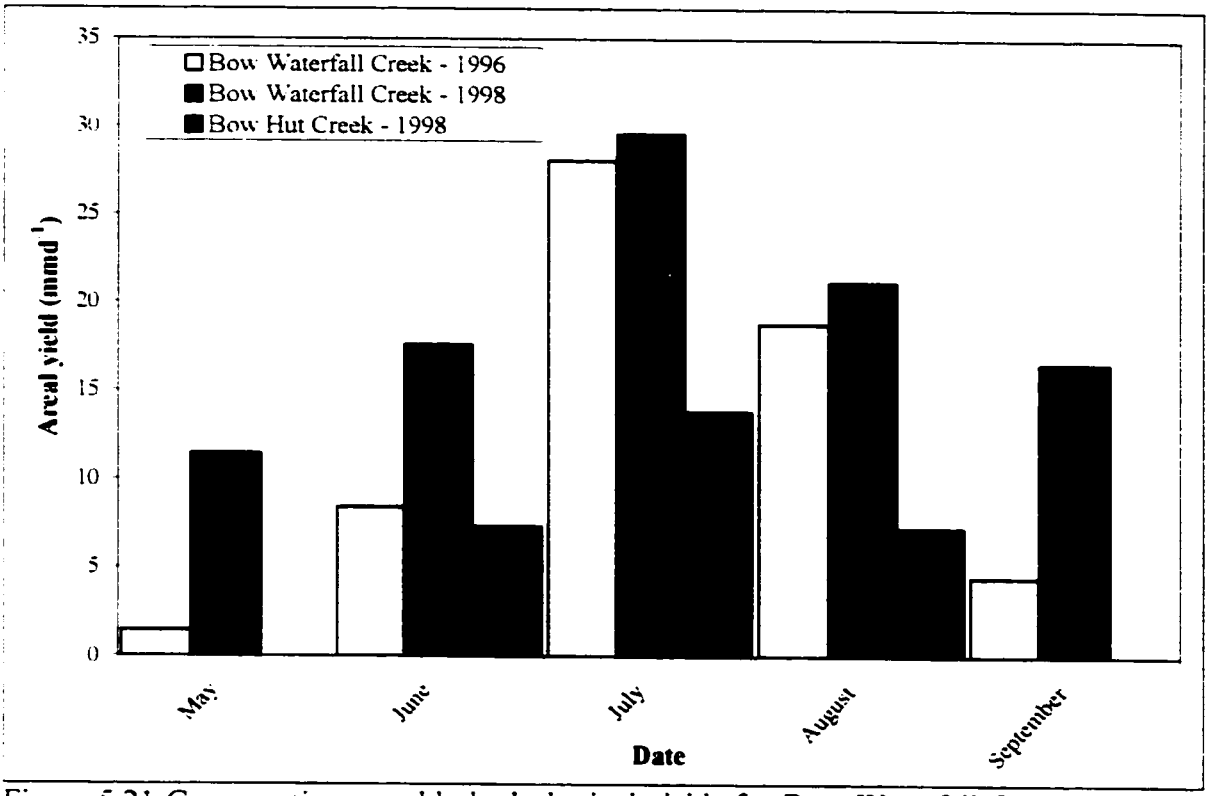

Figure 5.21 Comparative monthly hydrological yields for Bow Waterfall Creek 1996 and 1998, and Bow Hut Creek 1998 only.

The difference between the yields for 1996 and 1998 at Bow Waterfall Creek was largely a function of the longer glacial melt season in 1998 rather than due to higher flows. Although higher discharges were encountered in 1998 than 1996 (peak flows of 7.2 m^3s^{-1} compared to 6.2 m^3s^{-1}, respectively), it can be seen in Figure 5.21 that the largest differences in yield were not during peak flow periods but rather at the start and end of the melt season. This was because in 1996, the deep snowpack acted to insulate glacial ice from melting, whereas in 1998 the shallow snowpack melted out very early (late April compared to late May in 1996 and 1999), rapidly exposing a high proportion of glacial ice. The net effect of upward snowline progression, ice exposure and solar altitude interactions on the seasonal hydrograph is illustrated in Figure 5.21. For the shallow snowpack year, the areal yields for Bow Hut and Waterfall Creeks were

relatively symmetrical around July, largely reflecting seasonal radiation fluxes. However, for 1996, the seasonal distribution of yield for Bow Waterfall Creek was slightly less symmetrical and biased more towards the latter half of the melt season due to the slow upward progression of the transient snowline, leading to enhanced ice exposure and melt later in the season.

From the areal yield data presented above, it was possible to estimate monthly glacial melt contributions to basin-wide runoff at Banff during July, August and September 1998. First, a simple basin water balance was performed to estimate the hydrological yield over glacierised portions of the basin. This was achieved by subtracting non-glacial baseflow, precipitation and evaporation from the observed basin yield, and assuming that the remaining yield was due to melt runoff from the glacierised portion of the basin. After establishing the areal yield for the 5.2 km^2 glacierised area in Bow Waterfall Creek, this yield was then converted to a discharge by applying it to the 51.4 km^2 glacier cover within the Bow Basin above Banff. The estimated monthly glacier melt contributions were then compared with the average monthly discharge at Banff to estimate the relative contribution of flow from glacial melt runoff. The same assessment could not be performed for any of the other three years due to insufficient comparable baseflow and runoff data from both headwater basins.

Non-glacial baseflow was estimated from the average basin baseflow yields of Mosquito Creek (Table 4.6) for July (~ 7 mmd^{-1}) and October (~ 1 mmd^{-1}), and assuming a linear drop in baseflow levels from July to October. The baseflow yields for July were similar to the areal groundwater yields measured on Bow Hut Creek (Table 4.3) in areas of no surface tributaries (~ 8 mmd^{-1}); and also in October when the measured baseflow

yield on Bow Waterfall was also ~ 1 mmd^{-1}. Total precipitation measured each month (Table 1.2) at Bow Summit (2030 m a.s.l.), was linearly extrapolated to the Bow Waterfall Creek average basin elevation of 2600 m a.s.l. using the observed orographic enhancement of 8% per 100 m (see section 1.4.2). Evaporation could not be measured but it was thought to be a minor component of the balance in this unvegetated, glacial basin. From a study of evaporation in a similar environment in the Swiss Alps, it was found that at this time of year values range between 0 and 2 mmd^{-1} depending on landcover (Menzel and Lang, 1998). Therefore, a constant value of 1 mmd^{-1} was assumed from July to September (changing this value by ± 1 mmd^{-1} altered the final result by < 3%). A summary of the yield estimates and basin-wide glacial melt contributions for July to September 1998 is provided in Table 5.1.

Location	Bow Waterfall Creek balance inputs/outputs for entire basin (50% glacierised) (mmd^{-1})				BWF glacier area (5.2 km^2) (mmd^{-1})		Bow River above Banff		
							Glacier area 51 km^2	Basin 2207 km^2	
1998 Month	Basin yield	Baseflow Yield	Precipitation at 2600 m	Evaporation	Basin glacial yield	Areal yield	Discharge (m^3s^{-1})		Glacial %
July	29.6	6.4	0.8	-1	23.4	46.9	27.9	135	21
August	21.2	4.6	2.4	-1	15.2	30.3	18.1	65	28
September	16.6	2.7	1.0	-1	13.9	27.9	16.6	36	47

Table 5.1 Hydrological balance areal yield components for Bow Waterfall Creek illustrating basin-wide glacial melt contributions upstream of Banff during summer 1998.

From Table 5.1 it is apparent that glacial melt from the 2% basin glacier cover upstream of Banff, contributed a high proportion of total basin runoff during the main glacial melt season of 1998. This glacial contribution was around 20% during high radiation inputs and peak glacial melt in July, but the proportional contribution to basin runoff peaked at almost 50% in September (despite a drop in glacial runoff of 40%) due to a reduction in flow from the remainder of the Bow Basin of around 80%.

5.3.3 Temporal Signals in the Hydrograph

5.3.3.1 Introduction

As was demonstrated earlier when investigating the hydrology of Mosquito Creek (section 5.2.3), applying a continuous wavelet filter to the time series discharge data can highlight temporal patterns within the hydrograph. In this section, the same methods and resources were used as for Mosquito Creek; however, entire melt season discharge records for Bow Hut (1998) and Waterfall (1996 and 1998) Creeks were examined. The interactive procedure available on the World Wide Web (Torrence and Compo, 1998) can only handle 2000 data points during one operation and therefore, it was not possible to run the filter across hourly time series for entire seasons. For convenience, the time series data for each location were separated into individual years and then the main melt season of each year was further divided into two time periods: start of individual time series (late May) to July 15th, and July 16th to September 30th or end of each time series. Data during annual baseflow conditions (October 1st to April 30th) were not available. Dividing the data up in this way was useful, in that it facilitated three comparative analyses:

1) Comparison of hydrograph periodicity (recurring temporal signals) between years of deep and shallow snowpack for Bow Waterfall Creek;
2) Comparison of hydrograph periodicity between early and late season melt;
3) Comparison of hydrograph periodicity between two glacierised basins of slightly different landcover characteristics: one with 50% glacier cover and a small lake upstream of the gauge (Bow Waterfall Creek) and one with only 20% glacier cover (Bow Hut Creek).

The variance plots (wavelet scalograms) for each time series analysed are plotted in Figure 5.22.

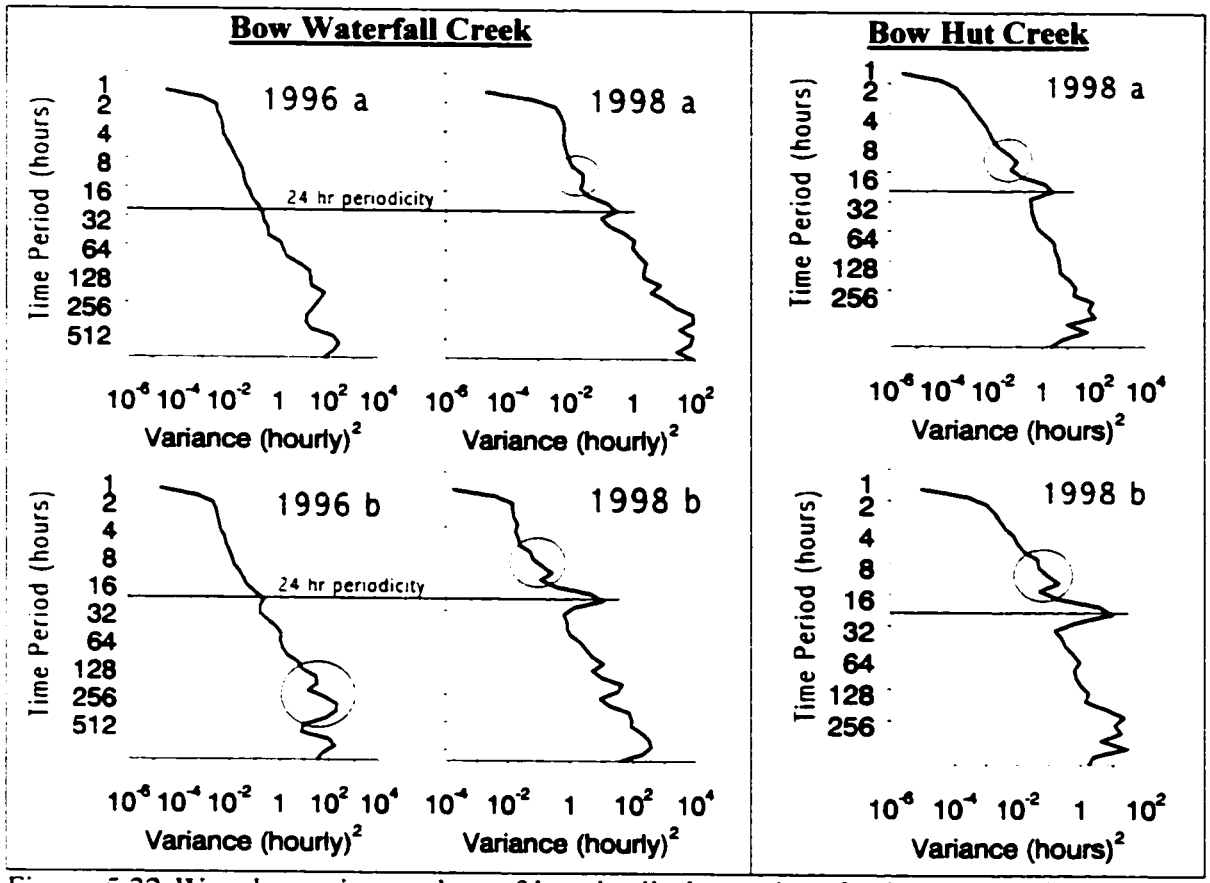

Figure 5.22 Wavelet variance plots of hourly discharge data for Bow Waterfall and Hut Creeks during 1996 and 1998. Plots divided into two time periods: (a) early summer melt (nival) and (b) late summer melt (glacial). (Full wavelet filter outputs in appendix 5).

5.3.3.2 Snowpack Depth and Hydrograph Periodicity

By examining the variance plots in Figure 5.22 for Bow Waterfall Creek it is clear that during the deep snowpack year of 1996, diurnal melt periodicities in the hydrograph were subdued and only became discernable during the latter half of the melt season. A relatively strong signal with a periodicity ranging between 200 and 400 hours or 8 to 16 days was apparent, however, in plot 1996 b for Bow Waterfall Creek (circled at bottom of variance plot). This periodic pattern was also clearly visible in the raw hydrograph (Figure 5.19) and was likely related to synoptic scale influences such as tracking cyclones or switching high and low pressure systems.

By applying a wavelet filter to the daily solar radiation record collected at Peyto Glacier from April to October 1996 (data provided by Dr. Scott Munro) similar dominant periodicities were evident (see Figure 5.23). These observations suggest that during the deep snowpack year of 1996, Bow Waterfall Creek runoff was influenced to a greater extent by synoptic scale radiation load changes over days to weeks rather than the constantly recurring diurnal variation in radiation due to Earth rotation.

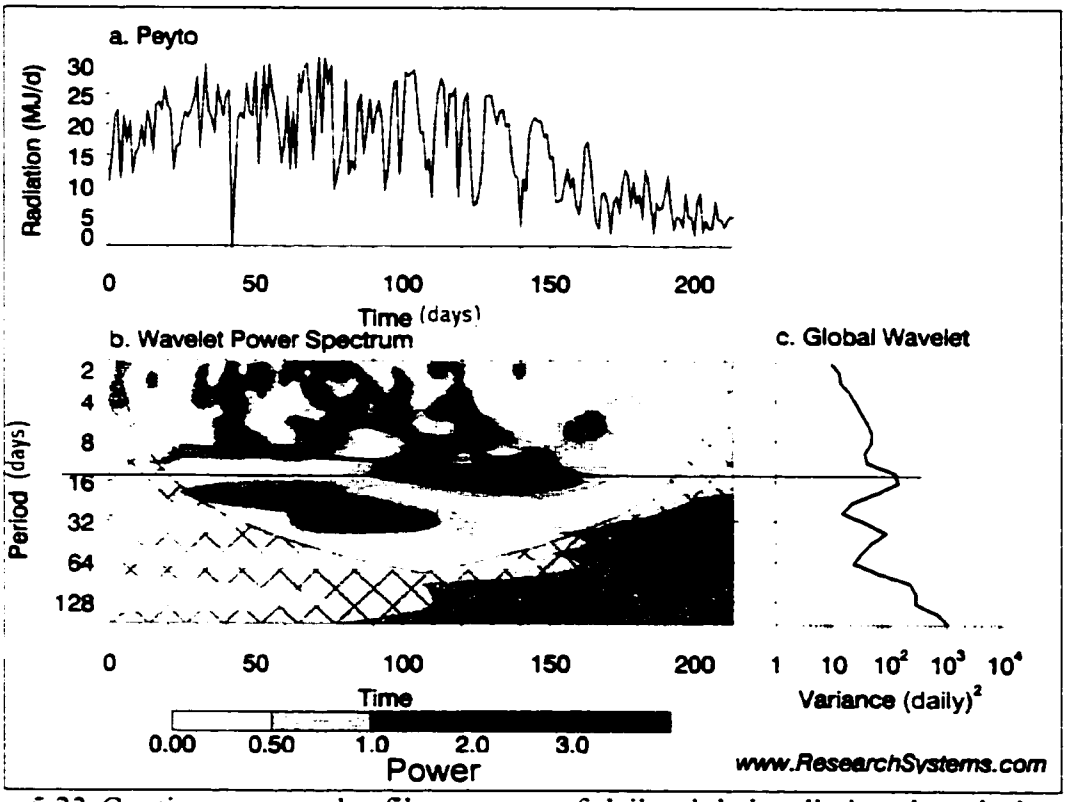

Figure 5.23 Continuous wavelet filter output of daily global radiation data during 1996 (starting May 1st) at Peyto Glacier (data courtesy of Dr. Scott Munro). (Figure generated on World Wide Web courtesy of Research Systems Incorporated (2001))

During the shallow snowpack year of 1998, diurnal periodicities were strongly evident during both halves of the melt season. Longer time period cycles were apparent but the diurnal signal was clearly the most dominant. The apparent recurring periodicities in the range of 8 to 12 hours (circled on both Bow Waterfall and Hut Creek variance plots

for 1998) increases in strength with diurnal periodicity and is thought to be an artifact of the wavelet filtering technique; i.e. if a 24-hr wavelet template fits the hydrograph at any particular time, then multiples of 12-hr, 8-hr, 6-hr, 4-hr and 2-hr templates will also fit the data. Therefore, no meaning (in terms of hydrological processes) can be attributed to these horizontal spikes on the wavelet variance plots.

5.3.3.3 Seasonal Variability in Hydrograph Periodicity

Wavelet filtering of the time series discharge data for each location was divided into two time periods. The earlier time series up to July 15th reflected spring freshet conditions and the early glacial melt period; whereas the second time series up to the end of September would reflect the late season glacial melt period. The main difference between the early and late melt season variance plots with all three of the discharge data sets analysed was that the diurnal signal became stronger during the latter half of the season. In glacierised basins, such strengthening of the diurnal signal later in the melt season reflects increased ice exposure and commensurate increases in the range of diurnal melt water volumes (e.g. Stenborg, 1969).

5.3.3.4 Hydrograph Periodicity at Bow Hut and Waterfall Creeks

There were two noticeable differences between the wavelet variance plots for Bow Waterfall and Bow Hut Creeks in Figure 5.22:

1) The diurnal periodicities evident on all variance plots for 1998 were more prominent on Bow Hut Creek.
2) The upper section of the wavelet variance plots (temporal periodicity range of 1 to 2 hours) illustrated higher variances for Bow Waterfall Creek than Bow Hut Creek;

The slightly reduced prominence of the periodicities associated with diurnal melt on Bow Waterfall Creek was probably due to the presence of Bow Pond below the Icefield and above the gauge. The pond would have acted to "smooth" the hydrograph somewhat and slightly subdue the diurnal discharge signals. The increase in variance at short periodicities for Bow Waterfall Creek was the result of a more "noisy" hydrograph. This could have been due to movement of the pressure transducer set up or, assuming a solidly installed gauge, the result of minor localised inputs to runoff downstream of Bow Pond.

5.3.4 Seasonal River Geochemistry

In general, the seasonally varying patterns of EC and $\delta^{18}O$ (Figure 5.24) for the glacierised Bow Creek Basin were similar to those observed on the non-glacierised Mosquito Creek (Figure 5.4): i.e. spring and summertime dilution of EC, and initial depletion of $\delta^{18}O$ during spring of both years with summertime enrichment in 1998 but general depletion in 1999. This overall similarity in the patterns suggests that the dominant control on these geochemical patterns is related to basin-wide hydrometeorological conditions such as snowpack volume and melt runoff dilution rather than landcover. However, landcover does play a significant and noticeable role in modifying these climatically driven signatures. The highly glacierised Bow Creek differed from Mosquito in that EC had a greater range of values yet was less variable through time; $\delta^{18}O$ tended to be slightly more enriched throughout the year, again with lower temporal variability; and tritium had a more pronounced seasonal variation.

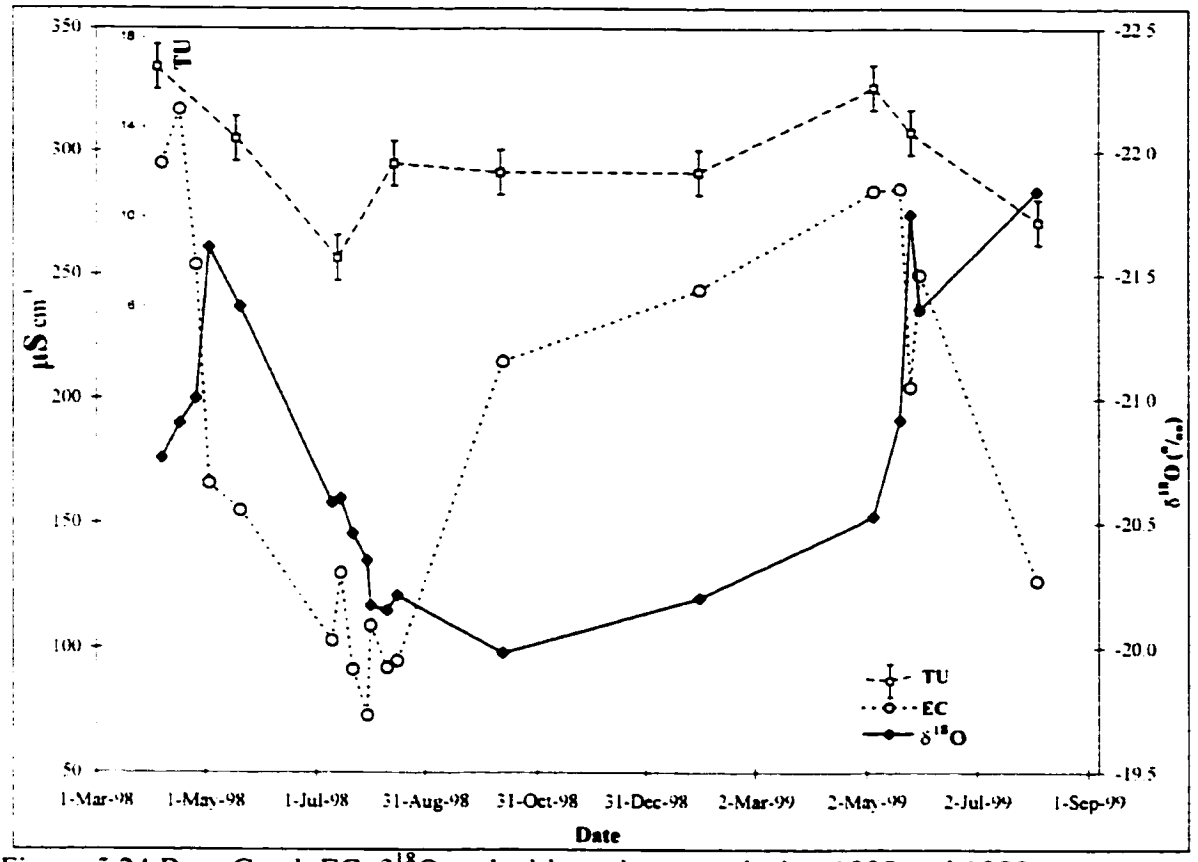

Figure 5.24 Bow Creek EC, $\delta^{18}O$ and tritium signature during 1998 and 1999.

After the spring melt depletion and early summer enrichment of $\delta^{18}O$ on both creeks during 1998, the late summer signatures (August onwards) differed considerably. The $\delta^{18}O$ signature on Bow Creek continued to enrich up until October, whereas that of Mosquito Creek began to deplete (see Figure 5.4), probably due to the lagged snowmelt pulse in groundwater baseflow (discussed in Chapter Four). It is also interesting that despite a greater range in values, the seasonal $\delta^{18}O$ chemograph for Bow Creek during 1998 was "smoother" than that for Mosquito. This reflects the difference in dominant hydrological processes between the basins: i.e. for Bow Creek the largest flux of water is pond routed glacial melt, the volume of which is directly related to the transient snowline and radiation inputs. On Mosquito Creek the dominant hydrological inputs vary more,

both over short periods (individual melt and rainfall events) and seasonally (spring melt and summer rains interspersed with groundwater baseflow inputs).

As noted in Chapter Three, the glacial melt $\delta^{18}O$ signature should be at its most enriched when the snowline is above the equilibrium line altitude, at the end of the season (thus exposing ice and firn originally formed at the lowest possible elevation and possessing a higher rainfall content – see section 3.4.1). This enriched signature on Bow Creek during October, therefore, may have been the result of late season recessional flows from glacier melt, with further enrichment from rainfall runoff. It is likely that rainfall is volumetrically more important in glacierised basins than non-glacierised basins due to the higher proportion of impervious ground cover, temporary storage of rainfall runoff in glacial drainage systems, and potentially reduced evaporation losses due to lower temperatures, reduced soil water storage and minimal vegetation cover. However, even though rainfall may be volumetrically more important from glacierised basins like Bow Creek, its impact on the hydrograph would likely be masked by large fluxes of glacial meltwater. The annual progression from isotopically depleted spring snowmelt inputs to enriched late season ice melt and rain inputs is illustrated in the annual hysteresis plot of $\delta^{18}O$ / discharge for 1998 in Figure 5.25.

During 1999, the baseflow $\delta^{18}O$ signature was relatively enriched (> 0.2 $^{o}/_{oo}$) compared to the prior year (Figure 5.24 and 5.25) and this is thought due to the below normal volume of snowmelt input to the system in 1998. Following the onset of spring melt, however, rapid depletion of the $\delta^{18}O$ signature was evident (Figure 5.24) and summer runoff appeared to remain relatively depleted. This was similar to the

observations at Mosquito Creek and reflected the deep snowpack in the basin and dominance of snowmelt over other hydrological components during 1999.

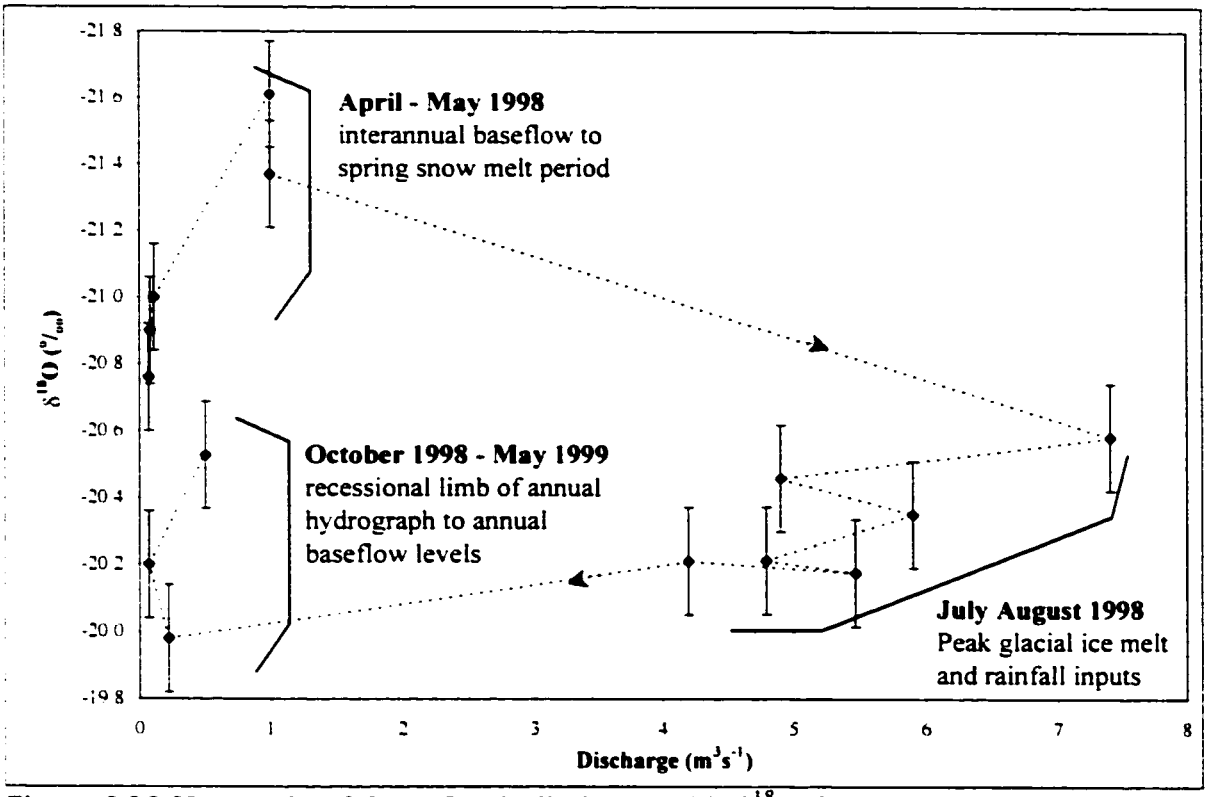

Figure 5.25 Hysteresis of Bow Creek discharge with $\delta^{18}O$ for the April to August melt seasons of 1998 and 1999.

The most noticeable difference between Bow Creek (Figure 5.24) and Mosquito Creek (Figure 5.4) geochemistry was that the EC on Bow Creek was higher during baseflow conditions, lower during peak flow conditions and generally less variable during the summer. Caution must be exercised comparing EC levels for these two basins as hydrological contact with weathering materials is controlled by different processes. In Mosquito Creek Basin, EC (Figure 5.4) is largely controlled by flow through groundwater zones and in-situ weathering. In Bow Creek, however, mechanical weathering at the glacier subsole elevates sediment levels, which are subsequently

transported out of the glacier system, suspended within streamflow. During winter, the levels of suspended sediment are typically low due to reduced mechanical weathering, undeveloped subglacial pathways and settling out. However, relatively long transit times of slowly moving baseflow water within this environment of high carbonate mineral contact lead to elevated concentrations of dissolved solids. During summer months when melt volumes are large, the suspended sediment content can also be high but transit times are commensurately shorter leading to a marked reduction in solute content (e.g. Collins, 1995). Therefore, the changing in-stream transit time from glacier surface to downstream sampling point largely controls EC levels in Bow Creek. For Mosquito Creek, however, groundwater residence time, although important, is perhaps less so than the actual flow pathway taken by parcels of water flowing from the ground surface to the stream (e.g. flow through forest soils, karst drainage conduits or high elevation talus slopes).

During 1999, the increased basin-wide snowpack volume led to reduced melt input over glacierised areas throughout the melt season. This probably reduced the levels of volumetric dilution and increased the transit times in the glaciohydrological system, therefore causing the observed increases in EC levels for spring and summer 1999.

For both 1998 and 1999, the tritium levels (Figure 5.24) prior to the spring freshet were enriched and displayed higher TU values than rainfall (rain average ~ 15 TUs, section 3.5.2), suggesting that water of several years' residence made up a significant component of the annual baseflow. In both years, the tritium level dropped during the melt season, in part reflecting the increased snowmelt contribution. However, 1998 displayed a late summertime peak flow TU value of 8, which was slightly below the average snow level (~ 9 TUs, section 3.3.2) suggesting that another hydrological

component was contributing to flow at this time. Ancient ice melt that predates bomb testing was earlier found to have a zero TU value. Such ice is found lower on the glacier and would definitely be one of the main contributors to melt runoff during late summer. A similar pattern was observed during 1999 but the seasonal TU depletion was retarded due to the higher volume of snowpack and slower progression of the transient snowline.

Of particular interest is that during August of 1998, while the glacier surface was still actively ablating, the TU level on Bow Creek increased, approaching rainfall levels, and stayed that way for several months. The first impression may be that rainfall or old groundwater contributed significantly to overall runoff at this time and therefore enriched the runoff TU signature. However, rainfall would have to contribute significantly more than 50% of the runoff volume to result in such a marked transition in tritium level and groundwater would need a very high TU value to have a noticeable impact on the glacial melt signature.

From the areal yield results provided in section 5.3.2, the combined runoff yield for Bow Waterfall and Hut Creeks during August 1998 (330 mm, Figure 5.21) exceeded the total annual precipitation measured at nearby Bow Summit (310 mm) and therefore, it is impossible that rainfall could have constituted anywhere near 50% of the flow during peak runoff. If groundwater had such a high TU level that it could influence the TU signature of large melt volumes, then this high TU signature would show up in other records where the melt contribution was relatively low. However, using Mosquito Creek as an example (Figure 5.4), 1998 summertime TU values elsewhere in the headwaters did not display a noticeably elevated reading. It would seem more plausible that much of this enrichment of the TU signature from Bow Creek was actually associated with the icemelt

component that dominated runoff and subsequent baseflow. This is in disagreement with the earlier observations of zero icemelt TU levels but it should be noted that the ice samples were largely collected below the equilibrium line, where ancient ice is resurgent.

Glacial ice from above the ELA was not sampled for tritium and therefore its true signature is unknown. However, whilst standing high in the accumulation zone during mid August 1998, it was observed that the snowline was well above the long-term ELA, and the last 13 years of firn could be visually discriminated before it blended with older ice. Therefore, it is apparent that much of the surface ice at this high elevation was relatively young and much of the icemelt from this zone would naturally have an increased tritium concentration relative to current background levels. If this is indeed the source of high TU levels in runoff, then it suggests that during late summer, the melt contribution from above the equilibrium line may have actually approached or exceeded the lower ablation zone contributions where icemelt TU values were zero. Such a situation may have occurred due to the Wapta Icefields being largely snow free at this time, and the glacierised area above the equilibrium line being flatter and thus potentially more susceptible to radiation melt than the lower and steeper northeast facing slopes.

5.3.5 Glacial Melt Event

In order to investigate the variation of streamflow characteristics accompanying diurnal glacial melt events in Bow Creek, water samples were collected every 3 to 6 hours from Bow Hut (20% glacierised) and Bow Waterfall (50% glacierised) Creeks during August 1998. Discharge was monitored automatically at the gauge sites and the samples analysed for $\delta^{18}O$ and EC. The purpose here was to assess the discharge, $\delta^{18}O$ and EC variability of these glacierised creeks to investigate the changes, if any, in

hydrograph flow components and pathways during a diurnal melt event. In addition, although Bow Hut and Waterfall Creeks are both highly glacierised, they have slightly differing landcover characteristics. Most notably, Bow Waterfall Creek has a pond upstream of the gauge, and is comprised entirely of glacier cover, bare rock and tills, whereas Bow Hut Creek has substantial areas of developed soil cover, wetland areas and some (between 5 – 10%) forest cover. A secondary objective here, therefore, was to investigate any pond or landcover induced differences in discharge and geochemical signatures.

Discharge, $\delta^{18}O$ and EC for the diurnal glacial melt event on both creeks are displayed in Figure 5.26. Bow Waterfall Creek has the greater proportional glacial coverage and this is reflected in the higher discharge on this creek (more than double that of Bow Hut Creek). The minimum discharge on both creeks was at approximately 10:00 hrs in the morning but peak flow occurred at different times. For Bow Hut Creek the peak occurred between 17:00 and 19:00 hrs, whereas for Bow Waterfall Creek, the peak was several hours later, around 23:00 hrs. This was probably largely due to the location of the small lake (Bow Pond) lying between the glacial melt inputs and the stream gauge, leading to a subdued and lagged basin response. However, the fact that peak flow occurred on both creeks between 5 and 11 hours following peak solar insolation indicates that the main mass of melt input occurred some distance upstream of the gauges. For Bow Waterfall Creek and Bow Hut Creek, the distances of the gauges to nearest glacier portals are, respectively 1.1 km and 3.0 km. From a dye trace of Bow Hut Creek during similar early morning stream flow conditions 10 days prior to the diurnal sample set illustrated here, it was observed that the 3 km distance from portal to gauge was traveled

in less than 1 hour. This suggests that peak melt inputs occurred a significant distance up glacier from the portal and perhaps corroborates the assertion in the last section, based upon TU observations, that August glacial melt inputs include a high volume of input from above the ELA.

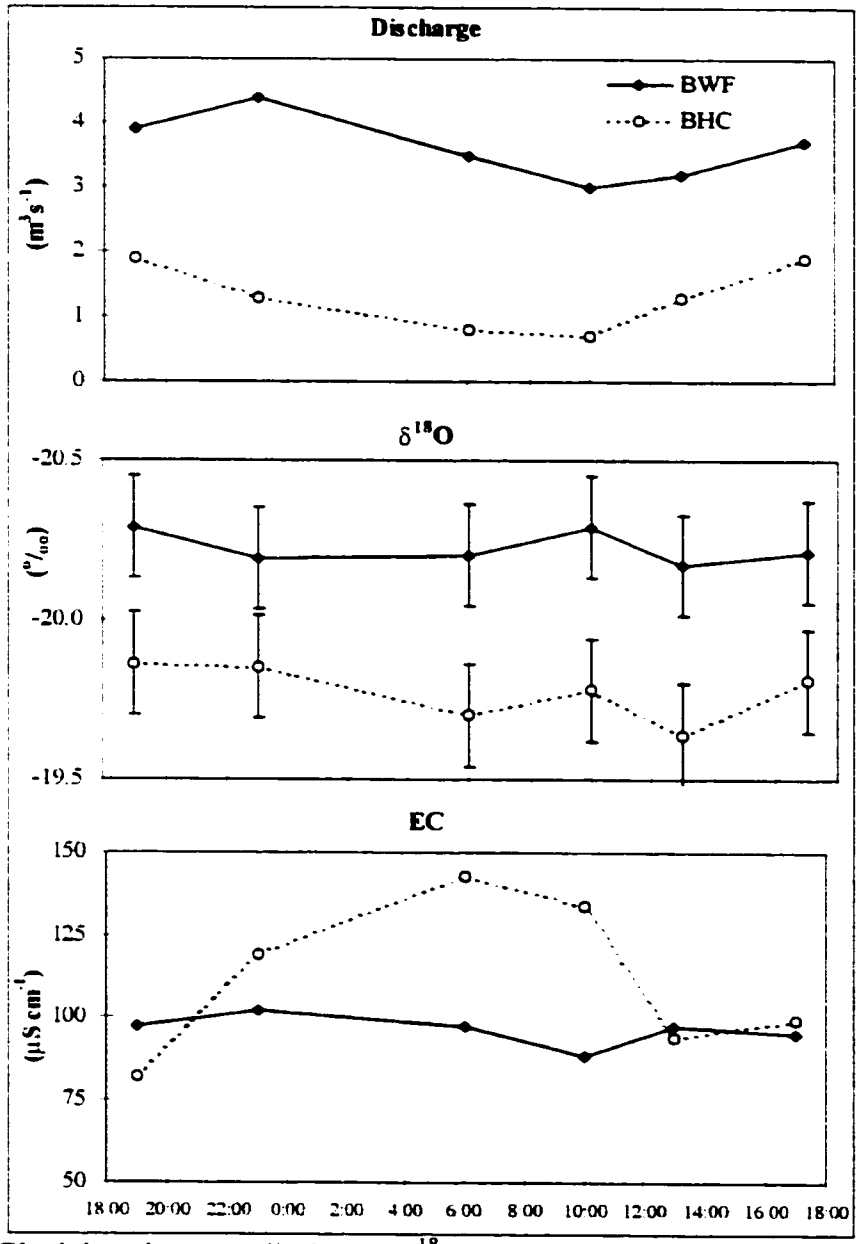

Figure 5.26 Glacial melt event discharge, $\delta^{18}O$ and EC signatures for the Bow Waterfall (BWF) and Bow Hut (BHC) Creeks, August 1998.

During the melt event, Bow Waterfall Creek always displayed a more depleted $\delta^{18}O$ signature than Bow Hut Creek with average values of -20.3 $^{o}/_{oo}$ and -19.8 $^{o}/_{oo}$, respectively (see Figure 5.26). This also probably reflects the greater relative glacial coverage and snowpack content within the basin. Bow Hut Creek has 30% less glacier cover and higher proportions of soil and wetland covers. Therefore, rainfall would likely make up a higher proportion of the hydrological balance and evaporative enrichment of melt and rainfall components within soil and wetland areas should be more prevalent.

Both creeks displayed minimal variation in $\delta^{18}O$ signature throughout the diurnal cycle despite large variations in discharge. This suggests that the composition of creek runoff did not vary significantly from minimum to peak flow. (Incidentally, this observation also suggests that daily timing of sample collection in areas prone to diurnal glacial melt fluctuations is not a critical factor when determining seasonal $\delta^{18}O$ characteristics of a basin). However, both creeks did indicate a possible depletion in $\delta^{18}O$ (> 0.1 $^{o}/_{oo}$, close to the level of analytical error) coincident with minimum flow, suggesting that there might have been a small change in flow composition at this time that was common to both creeks.

Coincident with this slight depletion in isotope signature on both creeks was a small drop in EC of ~ 9 $\mu S\ cm^{-1}$ (analytical precision ~ 2 $\mu S\ cm^{-1}$). This is curious, as at minimum flow basin transit times are longest and an elevated EC signature would be expected. The deviation from this expectation suggests that during minimum daily flow, a different hydrological component or process became more dominant. During this period, it is conceivable that while melt inputs were receding, groundwater could have contributed a relatively high proportion of flow. However, given that this new component

would need both a depleted isotopic and reduced EC (below 100 $\mu S\ cm^{-1}$) signature, groundwater is an unlikely candidate. The slightly depleted $\delta^{18}O$ signature of the missing component suggests that it was probably snow or ice in origin and the low EC indicates that it reached the sample location either very rapidly at the onset of melt or with limited sediment contact.

A scenario that could explain the above observations is that this depleted and dilute signal at the end of the recessional limb was associated with the last high elevation melt inputs of the evening before. The high elevation would explain the isotopically depleted signal and the low EC could be the result of this water remaining for much of the night-time in englacial pools and passageways with no sediment contact. Immediately at the onset of melt, much of this water would be "shunted" out of the glacier system through already well developed and scoured conduits ahead of the main melt wave and before stream discharge really started to increase. If indeed this signal was real and was the result of meltwater shunting in the glacial system, then the fact that this signal was observed downstream of Bow Pond indicates that although the small lake may subdue the geochemical signature of recent hydrological components it does not act to erase them.

The EC patterns for both creeks were markedly different with Bow Hut Creek having a distinct diurnal pattern while little variation was observed on Bow Waterfall Creek. The small lake on Bow Waterfall Creek probably acted to mix old and new water somewhat and thus average out the glacial melt EC signature. The diurnal variation in signature observed on Bow Hut Creek probably reflected the amalgamation and relative transit times of glacial and non-glacial flow components contributing to the stream. For example, during the lower flows of night-time, glacial melt transit times would lengthen,

leading to higher EC, but also as melt runoff receded the relative contribution of high EC groundwater components within the basin would have increased.

5.4 Effect of Bow Lake on Seasonal $\delta^{18}O$ Signature

5.4.1 Introduction

The current chapter has so far investigated seasonal and event hydrology of end-member basin headwaters within the Bow Valley. In the next chapter, a broader scale will be investigated by taking a look at the seasonal hydrology of the Bow River at Banff and two major tributaries: the Bow and Pipestone River Basins at Lake Louise. Naturally, it would be expected that downstream hydrographs would simply display the amalgamation of upstream (hence headwater basin) hydrographs. However, as one of the main tools used to study hydrological processes and components is the tracer $\delta^{18}O$, it needs to be ascertained whether or not any modification of the $\delta^{18}O$ signature through fractionation can occur during transit from the headwaters to basin end points.

From the upper headwaters to Lake Louise is a distance of approximately 50 km for both Pipestone and Bow Rivers and the subsequent distance from Lake Louise to Banff along the Bow River is about another 50 km. These distances would be traversed relatively quickly during summer, and given the high flow volume and generally cool climate, evaporative enrichment of the river signature is not expected to be significant in channel flow. However, within the Bow Valley, particularly on the western slopes above Lake Louise, there are several lakes that can temporarily store water and potentially lose a large amount to evaporation. Bow and Hector Lakes lie in the centre of the main valley and major tributaries of the Bow River pass through both of them. The objective in this

section, therefore, is to assess whether or not evaporative enrichment within large lakes causes a noticeable change to the $\delta^{18}O$ signatures of water transiting through such lakes.

Bow and Hector Lakes are relatively large but they differ slightly in their hydrological relationship with the Bow River. Bow Lake (see Figure 1.4) lies parallel to the main valley and thus the Bow River and the hydrologically more important Bow Creek have to traverse the entire 4000 m of the lake length. Hector Lake, on the other hand, is perpendicular to the main valley and the Bow River inflow is close to its outflow. It is thought, therefore, that if any modification of the main surface input $\delta^{18}O$ signature occurs during lake transit, it would be more evident on Bow Lake.

5.4.2 Data Acquisition and Methods

Discharge was measured at the Bow Lake outflow (lake area = 3.1 km^2 and total basin area = 71 km^2) 11 times using area velocity techniques (with a Marsh McBirney flow meter) from late winter 1998 to late summer 1999. The Bow Creek glacial inflow is the main surface input to the Lake (sub-basin area = 28 km^2 at lake inflow) and the flow was estimated by summing the discharges on the Bow Waterfall and Hut Creeks (described above). The next major surface input to the lake was the Bow River at Num-ti-jah Lodge (basin area = 23 km^2). Unfortunately, this site was not gauged or monitored due to braiding at the lake inflow. However, at this point, the Bow River is a small stream with a catchment of similar size and landcover characteristics to Mosquito Creek's North tributary. It was therefore assumed that flow on the Bow River here could be estimated by extrapolation from the hydrological yield measurements taken at Mosquito Creek North. Although there are other surface inputs to the lake, they are minor compared to Bow Creek and Bow River, and are ephemeral in nature.

The next major potential input to the lake was groundwater, entering the lake from the remaining basin area surrounding the lake of approximately 14 km^2. The low lake level during winter would ensure almost 100% groundwater input at this time. However, total fluxes could not be measured so the net groundwater flux (including ephemeral surface inputs) to the lake during the two years was estimated by performing a simple lake water balance and assuming that it was the difference between the major surface inputs and outputs. Direct rainfall precipitation onto the lake surface during summer months was estimated from the local precipitation records from Bow Summit. The average flux and relative contributing proportions of each of these input components from winter 1998 to summer 1999 were then calculated.

$\delta^{18}O$ was monitored at the Bow Creek and Bow River surface inflows and the lake outflow regularly during the study period. The groundwater $\delta^{18}O$ data collected at the Num-ti-jah well adjacent to the lake was assumed to be representative of the total groundwater to lake input signature. The average rainfall sample $\delta^{18}O$ signatures for 1998 and 1999 (see Table 3.1) were combined and assumed representative of summertime rain inputs to the lake surface. Each of these four lake inputs were then multiplied by their respective proportional volume weighted average $\delta^{18}O$ signature and then summed to compute the average two-year lake input $\delta^{18}O$ signature. This calculated average signature could then be directly compared with the volume weighted output $\delta^{18}O$ to assess if there had been any significant enrichment of the lake outflow signature over the two-year study period.

5.4.3 Results and Discussion

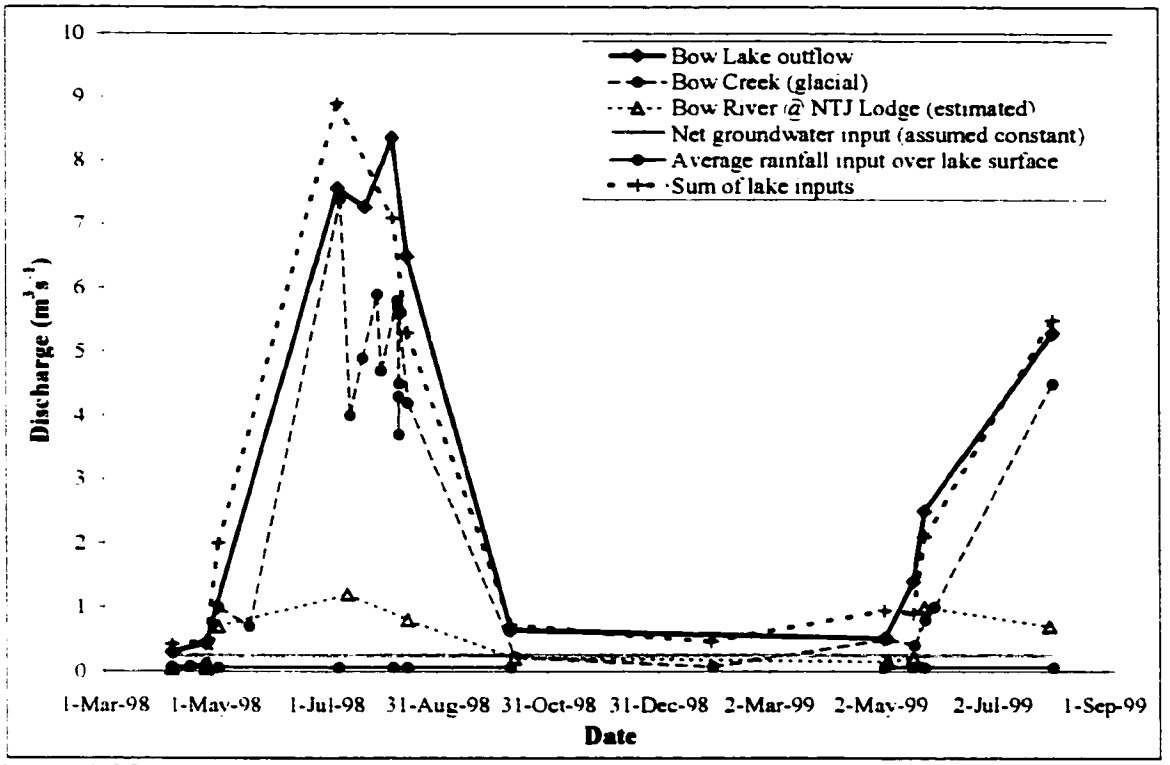

Figure 5.27 Measured and estimated hydrological inputs and surface output for Bow Lake, 1998 to 1999. (Evaporation volume unaccounted for.)

The relative hydrological fluxes of inputs to and the outflow from Bow Lake during 1998 and 1999 are presented in Figure 5.27. It is apparent that the glacial melt inflow from the Bow Creek Basin was the dominant input (78% of lake outflow volume). After summing total rainfall, Bow Creek and estimated Bow River inputs, and subtracting from the total measured outflow, it was found that a net groundwater (and ephemeral surface water) contribution of 0.24 m^3s^{-1} was left over. However, one factor that has been omitted thus far is that the difference between the total lake input and output should also consider the loss from the lake surface due to evaporation. By omitting this component in the water balance a systematic underestimation of the net groundwater contribution may result. This issue will be addressed shortly.

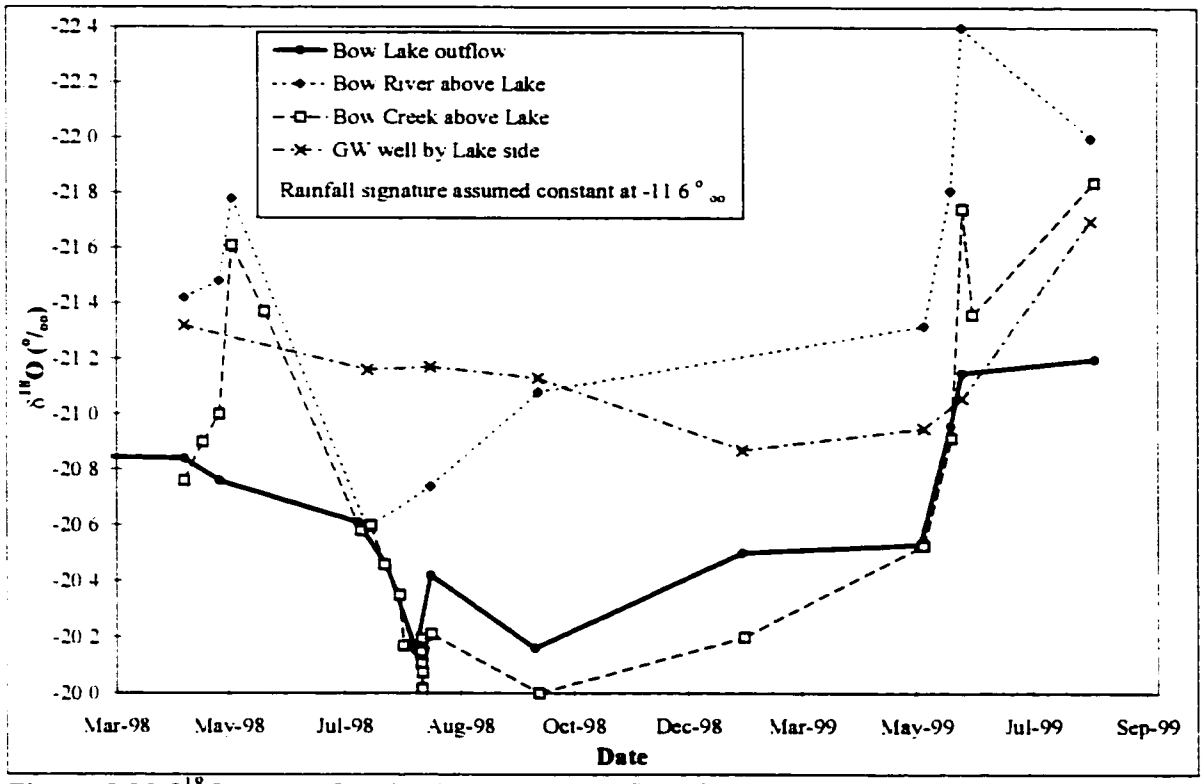

Figure 5.28 $\delta^{18}O$ trace of major inputs and outflow for Bow Lake during 1998 and 1999.

Figure 5.28 illustrates the relative $\delta^{18}O$ signatures for the four major lake input and the lake outflow components. The reduced variability in the outflow signature is to be expected and is the result of lake mixing and a time lag between inflow and outflow. (It should also be borne in mind that samples were collected less frequently at the lake outflow and thus the true variability of this signature may not be represented in Figure 5.28.) This time lag cannot easily be calculated but it is important to note that during late summer of 1998 and spring of 1999, when inflow discharges were high, the outflow $\delta^{18}O$ response to the glacial inflow was very rapid, suggesting a short lag time (perhaps on the order of days).

It is apparent from Figure 5.28 that for the entire study period, both groundwater and the Bow River inputs to the lake were isotopically depleted compared to the lake outflow.

Also, during the early nival period of both years, the inputs from the glacial Bow Creek were also relatively depleted. However, during the late summer of 1998 and interannual baseflow periods, the Bow Creek inputs were isotopically enriched compared to Bow Lake outflow. In general, the lake outflow appeared enriched compared to the main inputs. However, this observation takes no account of the relative volumes of each input component. In Table 5.2 are the volume weighted average $\delta^{18}O$ signatures with measured and estimated average annual yields for each of the lake inputs and output during 1998 and 1999.

Multiplying the average input component $\delta^{18}O$ signatures by their respective input proportions and then summing the results, returns an overall volume weighted average two-year input signature of -20.7 $^{o}/_{oo}$ This is slightly depleted compared to the measured volume weighted average output signature of -20.6 $^{o}/_{oo}$ but is within the range of analytical error. This result suggests, therefore, that during transit the lake $\delta^{18}O$ signature does not enrich significantly from major inflows to outflow.

Flow Component	**Volume weighted average $\delta^{18}O$**	**Average annual lake yield (x 10^6 m^3)**	**Relative proportion**
Direct rainfall on lake surface	-11.6 $^{o}/_{oo}$ (n = 11)	1.9 (approx.)	< 2%
Bow Creek (glacial)	-20.4 $^{o}/_{oo}$ (n = 21)	92.1 (measured)	78%
Bow River (at Num-ti-jah)	-21.4 $^{o}/_{oo}$ (n = 11)	16.4 (estimated)	14%
Groundwater (at Num-ti-jah)	-21.2 $^{o}/_{oo}$ (n = 8)	8.1 (estimated)	7%
Bow Lake outflow	*-20.6 $^{o}/_{oo}$ (n = 11)*	*118 (measured)*	*100%*

Table 5.2 $\delta^{18}O$ signatures and yield proportions for Bow Lake inputs and output during 1998 and 1999.

A difficulty with this lake balance is that the difference between measured surface inputs and outflow does not incorporate volumetric loss due to evaporation. This could potentially lead to a systematic underestimation of the proportional groundwater contribution to the lake if all flow inputs were equally susceptible to evaporation.

Therefore, the net flux of 0.24 m^3s^{-1} attributed to groundwater (and minor ephemeral inputs) should be viewed as a minimum.

A sensitivity analysis was performed to assess the potential impact of underestimating the groundwater component. This was achieved by performing the $\delta^{18}O$ water balance calculation again but with a doubling of the groundwater contribution to 0.48 m^3s^{-1} (~ 14% of all inputs). This resulted in a net volume weighted lake input signature of -20.8 $^{o}/_{oo}$. This difference of 0.2 $^{o}/_{oo}$ from the average outflow signature of -20.6 is slightly more than the level of analytical error. However, it should be highlighted that for the groundwater contribution to increase, then the level of evaporation from the lake surface must also increase to maintain the water balance. For Bow Lake with a surface area of 3.1 km^2, a surplus input of a constant 0.24 m^3s^{-1} would be balanced by an average evaporation rate of over 6.5 mmd^{-1} (or 2.4 ma^{-1}). Such a high rate of evaporation is impossible given that it is over six times greater than the 0.3 ma^{-1} potential evaporation levels quoted for this region in the hydrological atlas (Environment Canada, 1978).

Another way of approaching this problem was to estimate the depth of evaporation for the time period of study (April 4th 1998 to August 8th 1999) and apply this depth of evaporative loss to the lake surface and divide through by the lake area. This would facilitate a direct comparison of the relative importance of lake surface evaporation to all other hydrological inputs. From the estimates of potential evaporation from the Bow Summit weather station (less than 6 km from and 100 m above the lake) using the Turc equation (equation 5.1; Turc, 1961) provided in section 5.2.2, it was estimated that annual P.E. during 1998 to 1999 was between 230 and 260 mm. Applying this to the time period of interest resulted in a maximum loss due to evaporation of 330 mm (maximum because

the lake would be ice covered for some of the time that evaporation could take place). Applying this to the lake area of 3.1 km^2, returned an evaporative loss of approximately 1 x 10^6 m^3 (compared to 118 x 10^6 m^3 for all basin hydrological inputs) or 0.9% of the total lake flux.

It is felt, therefore, that these calculations demonstrate that although Bow Lake may cause a time lag between input and output tracer signatures of days to weeks, depending on time of year, the input $\delta^{18}O$ signatures do not significantly enrich due to evaporation during transit. Combining these findings with the observation that $\delta^{18}O$ signatures beneath Bow Pond on Bow Waterfall Creek were depleted compared to the signature on the adjacent Bow Hut Creek (section 5.3.5) suggests that headwater lakes in the upper Bow Valley tend not to modify the surface water $\delta^{18}O$ trace through evaporative enrichment.

5.5 Concluding Remarks

In this chapter an attempt has been made to compare some of the main controlling influences on hydrological processes within glacierised and non-glacierised headwater basins of the Canadian Rockies during years of different snowpack conditions. To this end, hydrological yields, temporal periodicities, and both seasonal and event geochemical signatures within hydrographs from different end-member basins have been studied. Further, the influence of headwater lakes on the stable oxygen isotope signature of river runoff was examined.

Hydrological yields tended always to be higher (by two to four times) from the glacierised basins (greater than 20% glacier covered), regardless of the precipitation or snowpack conditions for the year. However, years of deep snowpack led to greater yields

on non-glacierised basins and reduced yields in glacierised basins. This is because in the non-glacierised headwaters, snowmelt is by far the dominant water balance component, whereas in highly glacierised basins deeper snowpack tends to reduce the runoff contribution from the dominant icemelt component. Runoff increased on Bow Creek during the shallow snowpack year of 1998, not so much by virtue of elevated ice melt inputs but rather due to the extension of the glacial icemelt season afforded by rapid melt out of the snowpack. By estimating basin-wide glacial melt runoff from the monthly summertime areal yields on Bow Waterfall Creek, it was estimated that glacial melt contributed 47% of the average monthly runoff for the Bow River above Banff during September 1998. These results exemplify the disproportionate importance of the relatively small (~2%) glacier cover to late summertime runoff in the Bow Basin.

The increase in runoff from shallow (1998) to deep (1999) snowpack years on Mosquito Creek was approximately 14% despite there being a large difference of up to 177% in precipitation and snowpack input for the two years. This indicated a level of runoff moderation by groundwater storages with a net loss from storage during shallow snowpack years and a net gain during deep snowpack years. On Bow Creek, however, the reduction in runoff from shallow (1998) to deep (1996) snowpack years was up to 50%, highlighting the enhanced seasonal sensitivity of runoff in glacierised basins to snow cover depth.

By investigating the frequency of different temporal cycles in basin discharge data using wavelet analysis (Figure 5.22), it was found that shallow snowpack conditions in Bow Creek during 1998 led to dominant recurring patterns at the 24-hr periodicity. This illustrates the importance of diurnal melt cycles over the glacier surface to the runoff

hydrograph. During the deep snowpack year of 1996, this diurnal signal was evident but subdued. Although daily melt cycles were still important, the higher albedo and reduced density of snowpack compared to glacial ice led to a reduced frequency of noticeable diurnal melt events and a smaller range in diurnal melt volumes.

The most dominant temporal cycle in the seasonal melt hydrograph for the deep snowpack year appeared to be associated with synoptic scale influences with a recurrence of approximately 8 to 16 days, as observed at Bow Waterfall Creek (Figure 5.22, 1996 b). After examining global radiation records from nearby Peyto Glacier (Figure 5.23), this cycle was thought related to general increases and decreases in radiation inputs associated with synoptic scale frontal or low pressure systems. These observations suggest that temporal runoff patterns from the glacierised Bow Creek Basin are largely a function of snowpack depth; with diurnal radiation fluxes dominating the hydrograph during shallow snowpack years, and synoptic scale variability being more dominant in deep snowpack years.

The spring freshet dominated annual runoff at Mosquito Creek with subsequent summer baseflow $\delta^{18}O$ signatures displaying a lagged snowmelt response indicating that summer baseflow was maintained by snowmelt that infiltrated to ground several weeks to months earlier. This pattern was similar for both deep and shallow snowpack years but with an increased rainfall contribution in 1998 (Figure 5.4 and 5.5). The rapid melt out of the basin snowpack in Mosquito Creek during 1998 led to a step in the seasonal EC signature (Figures 5.4 and 5.6) indicating that there were probably three main categories of flow pathway: high EC (> 200 $\mu S\ cm^{-1}$) during interannual baseflow; intermediate EC levels (170 - 200 $\mu S\ cm^{-1}$) during spring melt and flow through organic forest soils; low

EC levels (< 170 $\mu S\ cm^{-1}$) during late summer when melt contributions and rainfall runoff originated higher in the basin from areas with little soil development leading to rapid runoff, minimal solute uptake and dilution of the baseflow signature. This pattern may also have occurred in 1999 but due to the reduced number of samples collected during this year (Figure 5.4) this is inconclusive. However, it was observed that EC levels in 1999 were generally higher than 1998 (Figure 5.6) despite greater snowpack volumes, suggesting that basin storage capacity at the start of 1999 may have been higher leading to longer groundwater residence times and more water routed through the ground.

The seasonal patterns of $\delta^{18}O$, EC and TU for both glacierised and non-glacierised basins were generally similar (Figures 5.4 and 5.24) indicating that the dominant controls on stream water geochemistry in this area were climatic, and largely related to the winter snowpack volume. However, there were noticeable differences between basin geochemical signatures that were directly related to landcover. The EC on Bow Creek was higher during annual baseflow and lower during glacial melt periods. This greater range in EC reflected enhanced weathering during baseflow conditions due to mechanical inputs of sediment beneath glaciers, and greater dilution in summer due to large inputs of melt water. Tritium was found to have a greater range on Bow Creek with values lower and higher than current background. The dilution during early summer was associated with melt inputs of ancient ice with zero TU concentrations, and later elevated readings were probably associated with more recent ice melt of an age post-dating the H-bomb tests of the 1950s.

The $\delta^{18}O$ signatures of seasonal baseflow and event runoff draining from the non-glacierised Mosquito Basin tended to be more depleted than the glacierised Bow Creek

Basin. This was due to the difference in dominant hydrological components between basins: i.e. glacial ice in Bow Creek and snowmelt in Mosquito (~ 89% snow and 11% rain in annual baseflow). For both basins, the stream $\delta^{18}O$ signature became progressively more depleted and closer to that of snow or ice melt during summer months despite increasing volumes of enriched rain input.

An enriched rainfall component seems to have been largely missing in stream water in both basin types at either seasonal or event time scales. In fact enriched $\delta^{18}O$ signatures in the glacierised basin suggested that rainfall was volumetrically a more important runoff contributor from such areas due to more impervious surfaces, storage in glacial drainage systems and reduced evaporation. After analysing the largest rainfall runoff event during summer 1998 (section 5.2.6), it was found that the volume of rain leaving the Mosquito Basin as runoff was several times lower than the volume entering the catchment as rainfall. In addition, the actual rainfall $\delta^{18}O$ signature during the event was virtually non-existent. However, it was hypothesised that during the event, rainfall in upper parts of the basin may have been flushing out relatively depleted water from large groundwater storage reservoirs; perhaps karst aquifers.

These observations naturally lead to questions surrounding the ultimate fate of rainfall in such basins. If indeed, as the observations suggest, rainfall was a relatively minor contributor to annual and event runoff in these headwater basins despite large inputs, it must be concluded that much of the rain input was lost from the basin via different routes. Rainfall occurs during the warmer months when water tables are relatively high and potential evaporation maximised. Therefore, of the hydrological balance components found in these basins, rainfall is the one most likely affected by loss

to evapotranspiration, leaving behind disproportionate volumes of other components in basin storage and runoff.

During the beginning stages of an early major snowmelt event in 1999 on Mosquito Creek (section 5.2.5.2) it was found that a high proportion of the flow was probably groundwater routed, perhaps resulting from shunting out of old water in the riparian zone. EC did not change much (< 14 %) during the event despite a large increase in discharge (290 %) suggesting that little of the runoff occurred over the ground surface. After performing a three-component separation, it was estimated that approximately 13% (2% - 34%) of the entire flow volume travelled as overland flow with 13% (0% - 32%) routed through upper soil layers and 17% (±17%) originated as deeper groundwater.

In contrast to snowmelt events, it was found that the runoff from a diurnal glacial melt event displayed little variability in $\delta^{18}O$ signature on both Bow Hut and Waterfall Creeks, suggesting that all the components were well mixed (section 5.3.5). This therefore suggested that much mixing of components occurred within the glacial drainage network and that there was a huge storage volume within the glacierised areas of Bow Creek Basin. However, a small but noticeable depletion of the $\delta^{18}O$ signature did occur at the onset of melt coincident with a small reduction in EC (Figure 5.26), which suggested that melt water from the evening before may have been shunted out ahead of the early morning melt wave. This small aberration in the diurnal melt cycle was observed at approximately the same time on both glacierised creeks. One of these creeks has a small lake upstream of the sample point and the other does not. The stream with the lake had no other inputs between the lake and the sample point suggesting that glacial melt signatures may make it across the lake relatively rapidly, although somewhat subdued.

Larger lakes within the headwaters were thought to potentially modify the river $\delta^{18}O$ signature through evaporative enrichment and through lagging the downstream response to upstream inputs. However, by performing a simple water balance calculation using measured and estimated inputs and outputs, and respective component $\delta^{18}O$ signatures it was found that although some enrichment of the inflow signature may occur, it is within the range of analytical error and therefore insignificant. Further, during the early nival period, the lake outflow $\delta^{18}O$ signature response to major inputs could take up to a few weeks. However, during the later high discharge glacial melt dominated period, the response was almost instantaneous and definitely occurred within days. The implications of these observations are important as they suggest that large lakes in the headwaters of the Bow Valley only modify river $\delta^{18}O$ signatures by mixing input components and causing a slight temporal lag between major surface inflows and outflow.

Chapter 6 Seasonal Hydrogeochemistry of the Bow River above Banff

6.1 Introduction

In the previous chapter, the effects of glacier cover on headwater basins of different proportional glacial coverages were shown to be clearly discernible in hydrological yields, temporal hydrograph patterns and geochemical signatures. Greater glacier cover in headwater basins leads to higher yields, a dominant diurnal periodicity in the hydrograph, greater ranges in solute and tritium concentrations, and a smoother seasonal variation in $\delta^{18}O$. In addition, it was shown that the relatively small glacier coverages of the headwaters contribute a high proportion (up to 50%) of late summertime runoff within the entire Bow Basin above Banff during warm and dry years. This chapter focuses on the larger basin scale using paired catchments an order of magnitude greater in size, and attempts to integrate observations at the headwater scale with those at the basin scale.

The objectives of this chapter are similar to the last but here the emphasis is on the effects of basin size and elevation, and not just landcover. Although the larger basin scale study basins (Pipestone and the Bow River at Lake Louise) are different in landcover characteristics (see section 1.3), the watershed of each contains sub-basins of both highly glacierised and completely non-glacierised coverages. In general, however, the Bow at Lake Louise (426 km^2, 2365 m a.s.l. average elevation) is significantly glacierised (10%), with all western slope sub-basins being similar to Bow Creek Basin (32% glacierised). Pipestone (308 km^2, 2425 m a.s.l. average elevation, 3% glacierised) is physiographically similar to Mosquito Creek (1% glacierised). The main difference is that at Lake Louise, the Bow and Pipestone Rivers are approximately an order of magnitude larger in size

than their counterpart headwater end-member basins. The largest basin investigated is the Bow Basin above Banff (2207 km^2, 2280 m a.s.l. average elevation), which is physiographically similar to Mosquito Creek and Pipestone River basins. See Figure 6.1 for basin and sub-basin proximities.

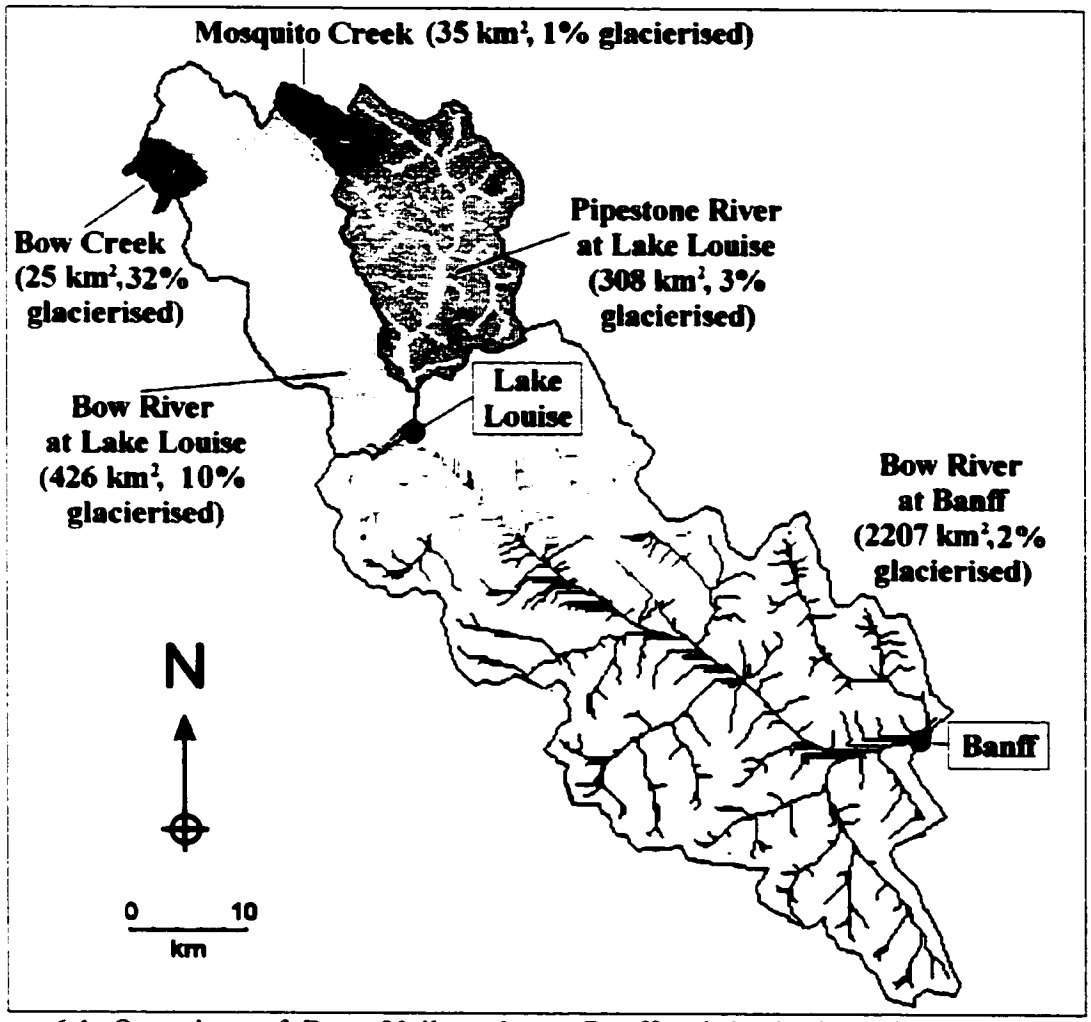

Figure 6.1 Overview of Bow Valley above Banff sub-basin boundaries with stream network and glacierised proportions.

The main temporal focus of this chapter is to investigate seasonal variabilities in runoff volumes and processes. However, the effects of short-term melt and rainfall events on basin-wide hydrographs will also be investigated.

Specific objectives of this chapter are to address the following questions:

1) Are events that are clearly distinguishable in headwater hydrographs also evident much further downstream at larger basin scales?
2) Are the effects of glaciers distinguishable in downstream hydrographs (other than in terms of yield alone – see section 5.3.2) of basins with reduced glacial proportions, an order of magnitude larger than the headwater end-member basin already studied?
3) Do lakes in the main river valley introduce significant lags in overall basin response to headwater events?
4) How do basin drainage and storage properties vary with glacier cover and through time within the Bow Basin?
5) How do the hydrograph properties change from the headwaters to basin endpoint and what are the main controls or changes in source?

Answering these questions will provide the basis for some of the assumptions made in the next chapter when attempting to isotopically evaluate the hydrological balance predicted by the UBC Model over a period of years. The format of this chapter is similar to the last in that many of the same tools and techniques are used. The chapter is broken down into the following sections:

1) Methods (section 6.2);
2) Basin-wide baseflow and event hydrographs are investigated to assess changing hydrograph properties with landcover and scale (section 6.3);
3) Comparison of interannual and seasonal basin yields for the large downstream basins of the Bow and Pipestone Rivers at Lake Louise and Bow at Banff (section 6.4);

4) Seasonal hydrograph periodicities are studied to identify the relative strengths of nival and glacial melt dominance within each of the larger sub-basins (section 6.5);
5) Seasonal geochemistry data for the larger basins are then presented to facilitate a comparison with findings from earlier chapters (section 6.6);
6) Recession analysis is performed on all basin hydrographs to investigate basin-wide variability in storage characteristics (section 6.7);
7) Concluding remarks (section 6.8).

6.2 Methods

Average hourly and daily discharges for the Bow (Water Survey of Canada basin I.D. = 05BA001) and Pipestone (05BA002) Rivers at Lake Louise and Bow River at Banff (05BB001) were obtained from the Water Survey of Canada archives for the time period May 1st 1998 to October 31st 1999. Unfortunately, from November 1998 to April 1999 discharge data were not collected at the Lake Louise Bow River gauge. These baseflow levels were estimated by linking the baseflow records from October 31st 1998 to May 1st 1999 and assuming that the winter recession curve was linear.

The snowmelt, glacial melt and rainfall events studied in the previous chapter have been re-investigated in this chapter. The hourly areal yields of runoff from the Bow Valley sub-basins Mosquito and Bow Creeks, Bow and Pipestone Rivers at Lake Louise and the Bow at Banff were calculated for several days prior to and following each event. The yields were then compared to see which basins yielded the most during individual events and assess the influences of landcover and basin size on event response. No water samples were collected for the more downstream locations during these events due to logistical constrains, and therefore no tracer-based analyses could be carried out.

For the three larger basins above Lake Louise and Banff, the seasonal hydrographs were compared to observe qualitative differences in hydrological regime due to glacier cover. Annual and seasonal areal yields during 1998 and 1999 were calculated to see if the same relative differences and patterns in yield experienced in the headwaters were also evident downstream. Areal yields were also compared with all other sub-basins studied to investigate the effect of landcover, elevation, groundwater and scale on flow volume in the Canadian Rockies. These analyses were carried out in order to ascertain whether or not the headwater regions of the basin control the patterns and sources of runoff in the main river system.

Wavelet analysis was employed to investigate the temporal patterns within each of the seasonal hydrographs, and to assess whether similar patterns to those evident in the headwaters were also apparent downstream. The hydrographs were seasonally divided and analysed using exactly the same methods as described in the last chapter (sections 5.2.3 and 5.3.3). For convenience, the time series data for each location were separated into individual years, and then the melt season of each year was divided into two time periods: May 1st to July 15th and July 16th to September 30th. The data during annual baseflow conditions (October 1st to April 30th) were left out of the analysis, as runoff fluctuated little at this time and the data availability for Lake Louise was limited.

By looking at the relative strengths of diurnal cycles within the time series discharge data, it was possible to discern whether melt cycles were strongest during the nival or glacial periods and whether or not such signals were subdued in the larger basins relative to headwaters. Stronger 24-hr periodicities during the nival rather than glacial period of a particular year indicated that melt inputs to the river system were more prominent whilst

snow cover in the basin was still widespread. If however, 24-hr periodicities were stronger during the later glacial period, this indicated that melt inputs were more prominent when snow cover was much reduced and glacial ice extent maximised. From these observations, it was assumed that the relative importance of spring snowmelt or glacial melt for a particular basin and year could be ascertained.

Discussion of the discharge wavelet filter intercomparison between basins is divided into four areas: 1) The effect of deep snowpack (compare 1998 with 1999); 2) Differences between nival and glacial melt periods; 3) Differences between the basin associated with landcover (compare Pipestone and Bow at Lake Louise); 4) Differences within the basins associated with size (compare Pipestone with Bow at Banff). The raw wavelet filter time-frequency plots are presented in appendix 5.

As with the prior chapter, seasonal variations in $\delta^{18}O$, EC and tritium have been explored to qualitatively investigate flow component contributions and basin flow pathways. The analytical techniques are identical to those outlined in prior chapters but the sampling frequency was slightly reduced.

The final piece of analysis presented in this chapter is the application of a simple linear reservoir function (see section 2.3.3.2 and equation 2.6) to basin-wide hydrograph recession curves to investigate variations in the hydrograph recession index α^{-1}. Seasonal and interannual recession curves for the Bow River at Banff and Lake Louise, Pipestone River and Bow Creek were evaluated for 1998 and 1999. This analysis provides a comparable estimate of the time taken for Q_o (initial discharge) to fall down to Q_o/e, which is a surrogate measure of basin storage. Higher values of α^{-1} indicate longer and shallower hydrograph recession curves. Recession characteristics for each basin will be

assessed to evaluate the spatial influences of basin size and glacier cover, and temporal differences associated with interannual and seasonal hydrometeorological variability.

For ease of comparison between 1998 and 1999, the dominant recession curve for each of three annual periods within each year's hydrograph was extracted. The three periods chosen were:

1) Nival – the major spring melt hydrograph recessions (May – June);

2) Glacial – late summer runoff (August – September);

3) Annual recession – the last discernible recession curve of the year (October).

Recession curves were extracted from each basin's hourly hydrograph during coincident time periods, and had to meet the following criteria: 1) Q_0 was at least one hour following the peak discharge for any of the basin hydrographs; 2) There was at least one full day of continuous hydrograph recession for all basins.

6.3 Short-term Basin-wide Hydrograph Intercomparison

6.3.1 Interannual Baseflow and Snowmelt Events

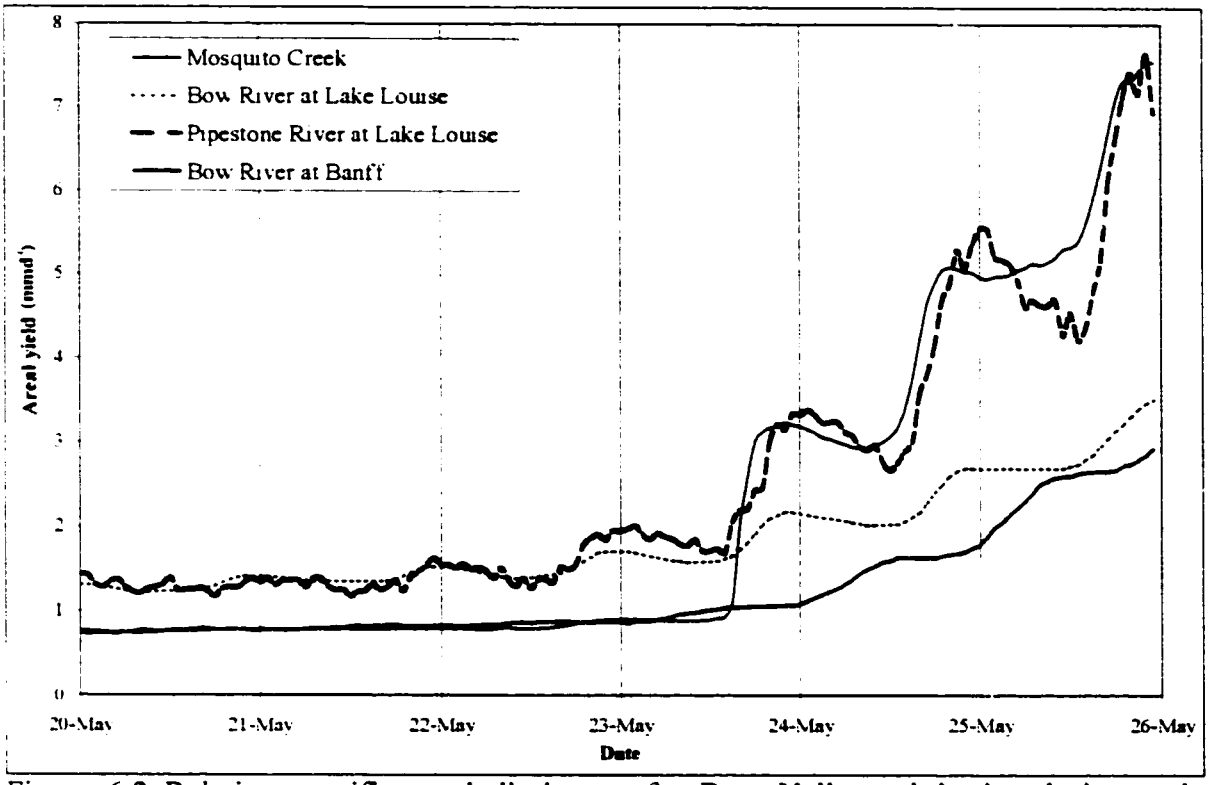

Figure 6.2 Relative specific areal discharges for Bow Valley sub-basins during early snowmelt events in May 1999.

6.3.1.1 Interannual Baseflow

The areal discharges for Mosquito Creek, Bow and Pipestone Rivers at Lake Louise and the Bow River at Banff during the transitional period from late winter baseflow to early spring snowmelt (May 20th to May 26th, 1999) are compared in Figure 6.2. The first interesting observation from this intercomparison is that despite different basin sizes and landcovers, the areal yield prior to melt (May 20th to May 22nd) was almost identical for the two basins at Lake Louise with both the headwater at Mosquito Creek and the basin end-point at Banff displaying lower but equivalent yields. (Even if there is an assumed error of ±10% in discharge values, then Mosquito and Banff still display closer yields to each other than to either of the basins at Lake Louise.) The similar yields for Mosquito

and the Bow at Banff may be due to similar landcover proportions but the higher and similar yields for the two rivers at Lake Louise is interesting as these basins have markedly different landcover proportions (particularly in terms of glacial ice). Therefore, the fact that these basins both display a higher yield at this time suggests that both were influenced by the same yield enhancing process. A likely cause of these patterns in interannual baseflow yield is probably related to the main river valley profile and its interaction with regional water table levels (see Figure 6.3).

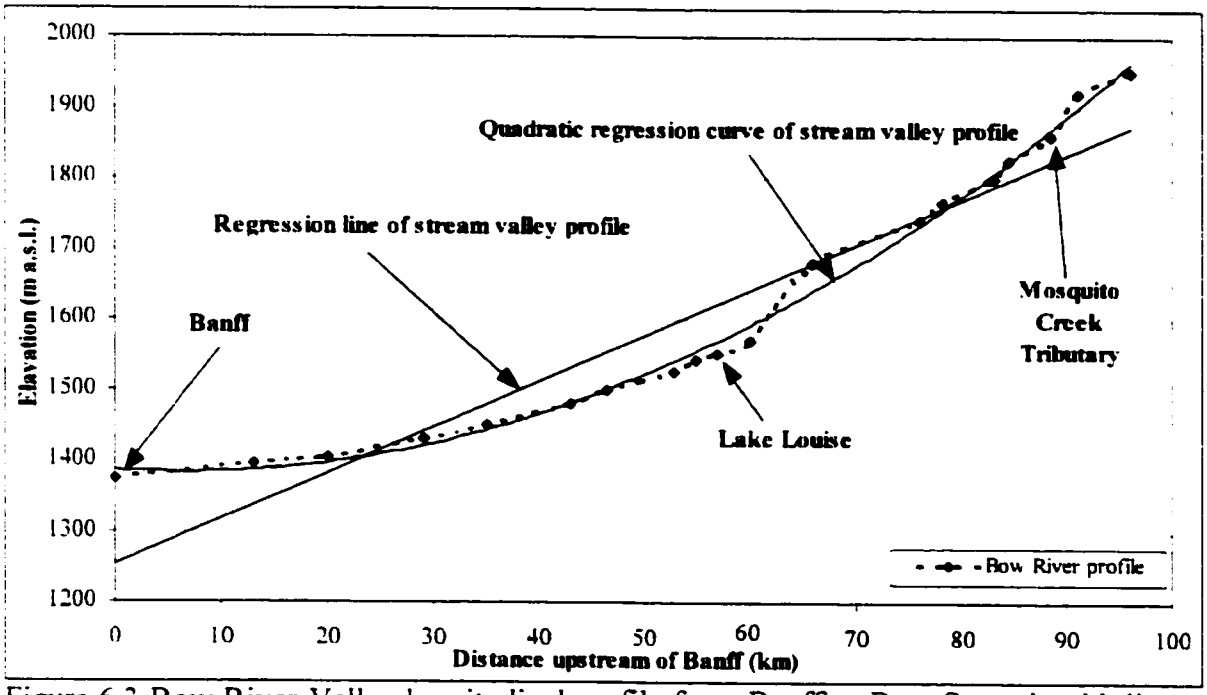

Figure 6.3 Bow River Valley longitudinal profile from Banff to Bow Summit with linear and quadratic regression lines to illustrate high and low points along the profile.

Although regional water table data were not available in this area, it would be logical to assume that the hydraulic gradient would most likely favour gaining water courses in locations where the stream profile dips below the general trend of the overall profile. This assumption stems from the knowledge that regional groundwater stream lines tend to converge where equipotential lines rise above the ground surface in depressions on long

shallow slopes (Toth, 1963). In Figure 6.3, it is apparent that in the vicinity of Lake Louise, there is a noticeable depression in main Bow River Valley profile. At this point, the stream lies below both the linear and quadratic curve trends of the main valley and it would seem likely that regional groundwater gradients from surrounding mountain masses would be higher than elsewhere along the profile. It is thought, therefore, that the observation of approximately 50% higher yields on Bow and Pipestone Rivers during interannual baseflow was probably due to both rivers experiencing gaining (influent) flow at this point due to the "dip" in the main valley profile. The lower yields on the Mosquito Creek tributary and the Bow River at Banff, would probably be due to smaller relative groundwater to stream hydraulic gradients. Both of these locations have a similar proximity to the regression curve of the overall basin profile, and it may be that similarities in interannual baseflow yield are more a function of regional groundwater levels than landcover proportions.

6.3.1.2 Snowmelt event

Of the hydrographs investigated in Figure 6.2, the Bow River at Banff was the first to begin to rise at the onset of the spring freshet but the response was subdued and there was no diurnal signal. Banff is the lowest point in the basin and local small melt inputs probably contributed to this minor rise in discharge. The first diurnal melt signal was observed on Pipestone River on the 21st of May, becoming more pronounced with each day. On the 22nd of May, the Bow River at Lake Louise responded with a weak signal lagging that of Pipestone due to the basin's predominantly easterly aspect and commensurate reduction in early season melt. However, on the 23rd of May, all basin hydrographs responded strongly to diurnal melt with the steepest rise from baseflow on

Mosquito Creek Basin (this was the snowmelt event studied in the last chapter, section 5.2.5.2). The rise in areal yield on Mosquito Creek from annual baseflow levels of less than 1 mmd^{-1} to over 3 mmd^{-1} occurred in just three hours. In subsequent days, the discharge continued to rise on all basins with the non-glacierised eastern slope basins of Mosquito Creek and Pipestone River similarly displaying the most voluminous and rapid responses to melt inputs.

Typically, peak flow from the 23rd to 25th of May occurred around 20:00 hrs for Mosquito Creek, 23:00 to midnight for Bow and Pipestone at Lake Louise, and around mid-day the following day for the Bow at Banff. Assuming peak melt occurred during the early afternoon (around 15:00 for example) for each of these days, then the basin response times from peak melt to peak runoff were around 4, 8 and 20 hours for Mosquito Creek, Bow and Pipestone at Lake Louise, and Bow at Banff, respectively. In terms of areal yield, Mosquito Creek displayed the greatest rise from baseflow levels but was close to Pipestone once melt was underway.

The main difference between Mosquito and Pipestone was that the recessional limb on Pipestone's hydrograph displayed a more rapid return towards baseflow levels. This is an interesting observation as the Bow River at Banff and Lake Louise displayed virtually no daily minima, indicating that for larger basins there was some mechanism acting as a temporary storage. For the Bow at Banff and Lake Louise, large lakes in the river network could account for this storage but lake coverage in Mosquito and Pipestone is relatively small and cannot explain the lack of a recessional limb on the smaller basin hydrograph. However, from observations of sinkholes and karst landscape formations in the headwaters of Mosquito Creek, it was earlier hypothesised that karst aquifers could

provide a hydrological storage mechanism (see Chapter Four and section 5.2.6). These groundwater aquifers probably fill up quickly during snowmelt and then drain more slowly after melting has ceased, providing continued flow augmentation during the night-time. It is felt that this lack of a daily minima in the Mosquito Creek hydrograph, therefore, is further evidence that karst areas play an important regulatory role on the hydrograph in some of the headwater areas of Bow Basin. (Properties of basin-wide storage will be explored further in section 6.7.)

6.3.2 Glacial Melt Events

The areal discharges for Bow Creek, Bow and Pipestone Rivers at Lake Louise and the Bow River at Banff during a major late summer glacial melt period (August 6th to August 11th, 1999) are compared in Figure 6.4. The most responsive hydrograph was that of the highly glacierised Bow Creek and the least responsive was that of the Bow at Banff. However, the fact that a diurnal melt signature was present in all hydrographs indicated that headwater glacial melt signatures were apparent in the hydrograph possibly up to 100 km downstream.

The areal discharge for the Bow River at Banff tended to be close to that of the Pipestone River during this period of summer baseflow. This suggests that during summer periods, basin yield is influenced more by basin landcover properties (proportionally similar between Pipestone and the Bow at Banff) than the regional water table, as was probably the case during the winter baseflow period. However, despite similar yields, the small diurnal cycles visible on both rivers were completely out of phase with each other due to the approximate 12-hour difference in overall basin response times (noted in the previous section). The approximate summertime basin

response time was similar, therefore, to the early nival melt period. This could be because although the basins may have actually responded faster later in the season, the main melt contribution areas were higher in the headwaters and therefore a compensation effect occurred leading to a stabilisation of the overall basin response time.

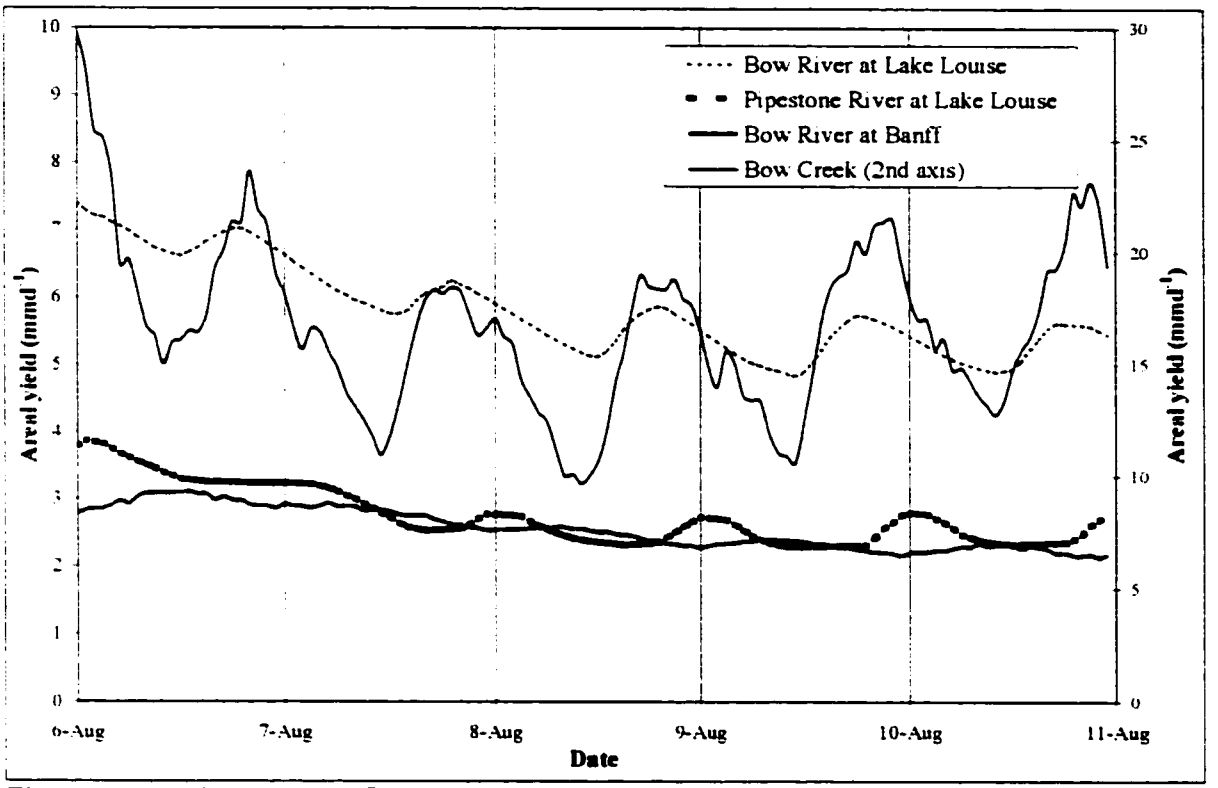

Figure 6.4 Relative specific areal discharges for Bow Valley sub-basins during major glacial melt period in August 1999.

During the period of glacial melt in Figure 6.4, the yield for the Bow at Lake Louise was greater than both Pipestone and the Bow at Banff. This was due to the early melt out of snow on the eastern slopes of the basin and the high proportion of glacier cover on the western slopes of the Bow Valley above Lake Louise. However, the effect of proportional glacier coverage on yield during this time was most pronounced on Bow Creek with instantaneous areal discharges of up to 30 mmd^{-1} or ten times the yield at

Banff. The relationship between proportional glacier cover and areal yield during this period of five days was strong (r^2 of 1.0) and is illustrated in Figure 6.5. This indicates that proportional glacier cover was one of the main determinants of areal yield in these basins during late summer, and that this relationship was approximately linear for the range of glacier proportions observed. Also, from Figure 6.5 it is suggested that for a basin of zero glacier cover, the areal yield would be around 0.7 mmd^{-1}. This is the same as late winter baseflow levels observed at both Banff and Mosquito Creek (see Figure 6.2) and suggests that without any glacier cover, early August runoff in these basins would approach interannual baseflow levels.

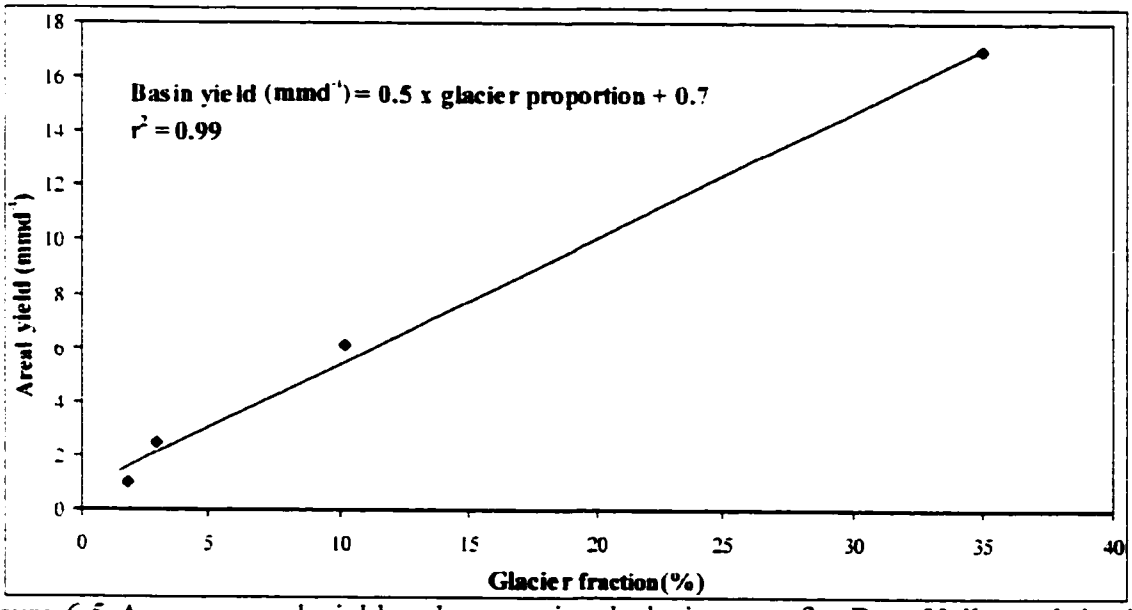

Figure 6.5 Average areal yield and proportional glacier area for Bow Valley sub-basins during major glacial melt period in August 1999.

The relatively small glacier coverage in the high and distal locations within the Pipestone Basin led to small ranges in diurnal melt (Figure 6.4), which lagged behind the signature on the Bow River at Lake Louise. The observation that the Bow River peak preceded that of Pipestone's is interesting as there are several more lakes within the Bow

Basin above Lake Louise. This suggests, therefore, that these lakes responded quite rapidly to late season melt inputs and corroborates similar findings in the last chapter (section 5.4). The slow response to melt inputs in the Bow at Lake Louise during the early nival period (Figure 6.2) was probably due to lakes taking large quantities of snowmelt to fill up, while late summer lake levels would already be expected to be high and therefore more responsive.

6.3.3 Rainfall Event

The data presented in Figure 6.6 provide a comparison of the runoff yields for the main sub-basins of the Bow Valley prior to and following two major rainfall events in the Bow Valley. The rainfall events were both heavy and sustained (~10 and 21 mm in the headwaters, respectively), resulting from a low-pressure system overhead. Rainfall covered a wide area of the Bow Valley with rain gauges detecting the event at either end of the basin. The rainfall and temperature data presented in Figure 6.6 were collected from Bow Summit at 2030 m a.s.l. in the basin headwaters. Unfortunately, actual runoff data for Mosquito Creek were not available during this period (as discussed in the last chapter, section 5.2.6). However, Bow Creek and the larger basin hydrographs were available for scrutiny.

The first large rainfall episode was very much in evidence on the Bow Creek hydrograph, with peak flow occurring only three hours following peak rainfall. The response to this event was not so marked at other locations but the Bow River at Lake Louise did show some rise in flow simultaneous with that on Bow Creek. The only response to the event on Pipestone was a slight lengthening of the prior day's diurnal melt signal. For the Bow at Banff, there was no evidence of this event in the hydrograph.

This is surprising given that the event was known to be widespread across much of the basin and suggests that at the larger basin scale the rainfall event was either: 1) not a significant contributor to runoff; or 2) the rainfall hydrograph was totally subdued. These observations corroborate earlier suggestions put forwards in Chapters Four and Five that glacierised basins tend to deliver more rainfall to the stream than non-glacierised basins.

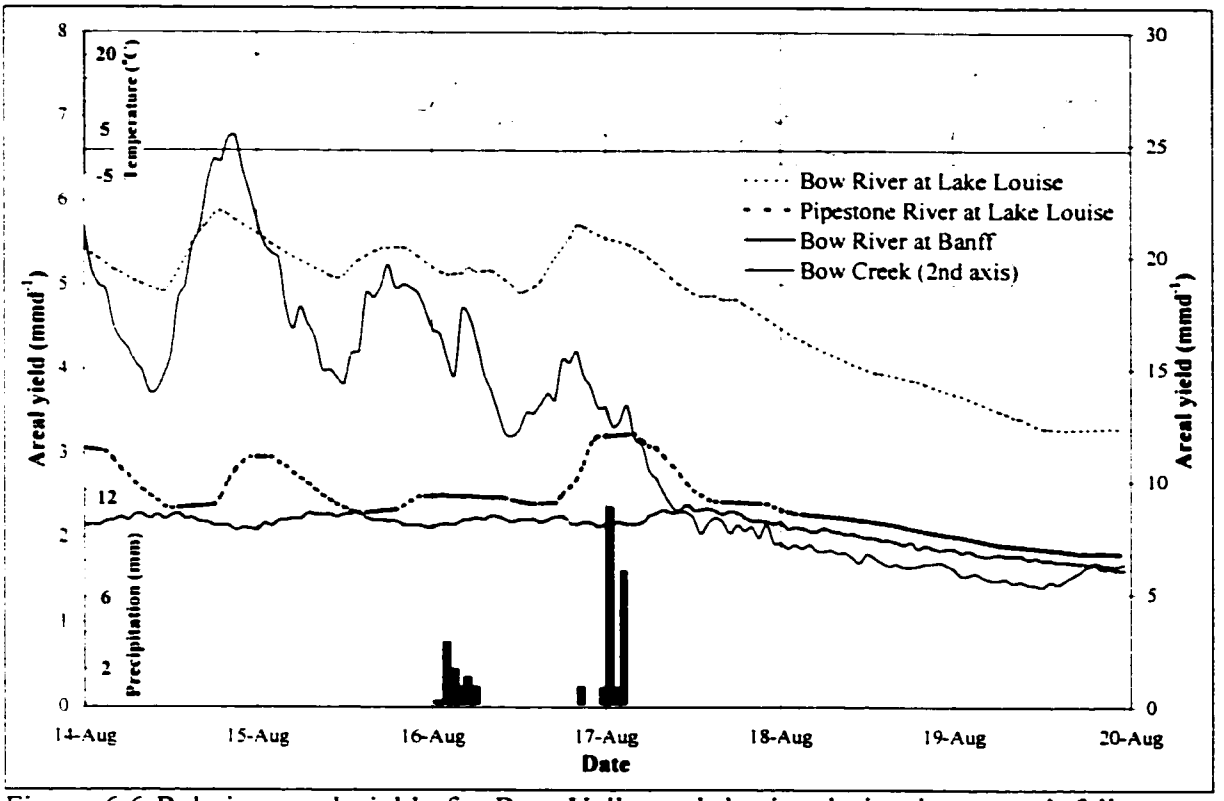

Figure 6.6 Relative areal yields for Bow Valley sub-basins during largest rainfall events of 1999 during August. Rainfall and temperature data from Bow Summit weather station (2030 m a.s.l.).

The second rainfall event observed at Bow Summit on the following day was approximately two times larger than the first and the hydrograph response was visible at all basin end-points. The hydrograph response was clearly visible at Bow Creek but the magnitude was subdued compared to the first event. This was thought due to the reduced temperatures during this event and the likelihood that much of the high elevation

precipitation fell as snowfall. This is evidenced by the observation that after this event, all basins displayed recessional flow with no diurnal melt signals, suggesting that fresh snow had fallen and was reflecting incoming radiation away from the ground surface. However, event responses in the larger basins appeared greater in volume and slightly more rapid than the first. This may have been related to enhanced antecedent basin moisture conditions from the prior event but was probably also somewhat linked to the event being super-imposed onto the previous day's melt runoff.

6.4 Basin-wide Areal Yield Intercomparison

6.4.1 Annual Areal Yields

Presented in Table 6.1 is a comparison of the calculated annual areal yields for each of the sub-basins studied within the Bow Valley (the 1999 yield for Bow Creek was assumed to be similar to that of 1996 due to snow cover having the dominant control on runoff and the observation that basin-wide snow course data for 1996 and 1999 had mean SWE values within 5% of each other - see appendix 1). From these yield data, simple inferences regarding basin size and proportional glacier cover could be made. Firstly, it is apparent that the two upper western slope basins with large areas of glacier cover both experienced a decline in yield during the year of deeper snowpack. A statistically significant relationship between snow depth, glacier cover and yield could not be calculated for the entire basin, as there were insufficient data. However, it is clear that larger glacier covers lead to a greater inverse relationship between snowpack depth and basin hydrological yield.

Parameter / Basin	Size (km^2)	Glacier Cover	1998 yield (mm)	1999 yield (mm)	Change from 1998 – 1999
Mosquito Creek	35	~ 1 %	640	730	+ 14% (+ 90 mm)
Bow Creek	25	~ 32 %	3100	*2040 (est.)*	- 34 % (- 1060 mm)
Pipestone River	309	~ 3 %	610	730	+ 19 % (+ 120 mm)
Bow at Louise	426	~ 10%	740	720	- 2 % (- 20 mm)
Bow at Banff	2207	~ 2 %	490	600	+22 % (+ 110 mm)

Table 6.1 Annual areal yields for Bow Valley sub-basins during years of shallow (1998) and deep (1999) snowpack.

Although a drop in the Bow River at Lake Louise yield was observed from 1998 to 1999, this drop was the smallest change in yield for any of the basins. This may suggest that the variability of runoff yield due to snowpack conditions in the Bow Valley may be minimised for the Bow River at Lake Louise. Long-term data for all of these basins were not available to test this hypothesis; however, data collected over 32 years (1910 – 1920 and 1965 – 1986 by the Water Survey of Canada) for both the Bow River at Banff and Lake Louise did indicate that annual yields had a 44% lower standard deviation (expressed as a proportion of mean annual flow) at Lake Louise. Perhaps, then, sub-basins in the Bow Valley with glacier coverages of around 10% are the most prone to glacier induced flow regulation. More highly glacierised basins are obviously sensitive to snow conditions, as deeper and more widespread snowpack reduces glacier melt and overall basin yield. Conversely, basins with reduced areas of glacierisation cannot offer a significant level of flow regulation and are therefore controlled by more short-term hydro-climatic conditions. (Further discussion of glacial flow regulation in this basin and others is provided in Hopkinson and Young (1998) and Fountain and Tangborn (1995).)

In addition to the question of glacier cover influences on the hydrograph is the issue of basin size and average elevation. To assess these influences on areal yield it was essential that basins of similar landcover proportions were compared. Mosquito Creek, Pipestone River and the Bow River at Banff were therefore chosen for this purpose as

they each contain very little high elevation glacier cover (≤ 3%), and have large areas of forest cover (between 20 and 40%) in the main valley areas (see section 1.3).

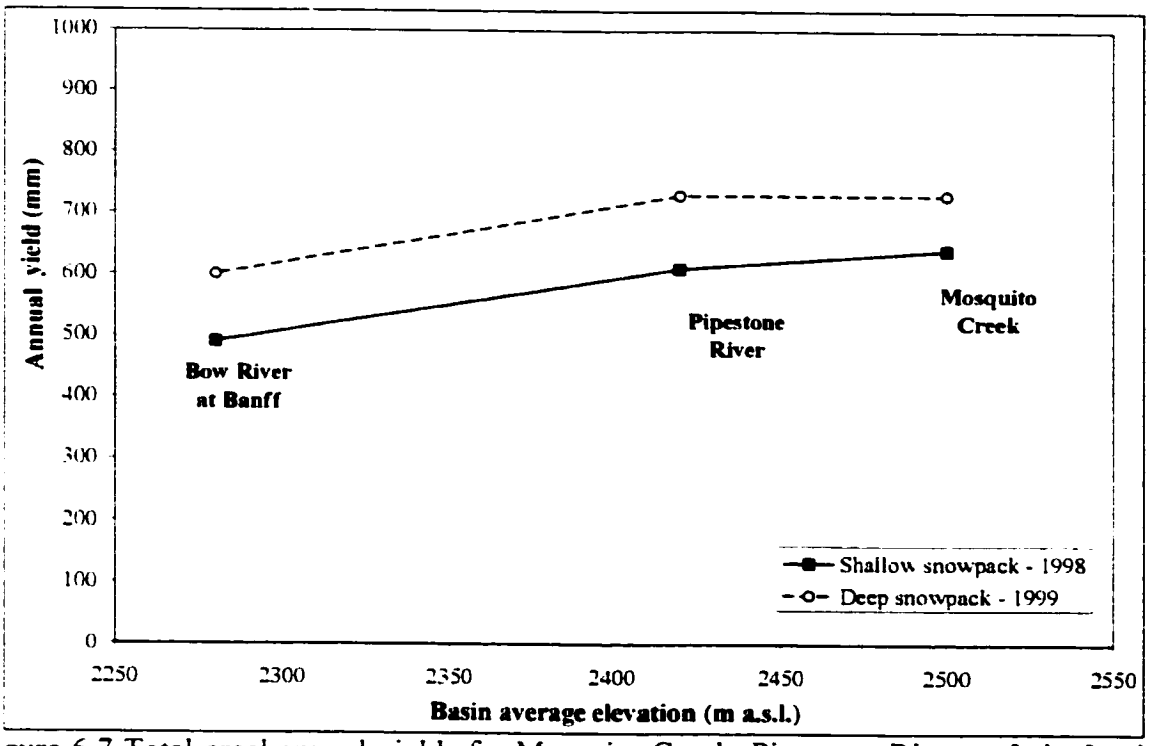

Figure 6.7 Total areal annual yields for Mosquito Creek, Pipestone River at Lake Louise and Bow River at Banff (raw data courtesy of Water Survey of Canada)

In Figure 6.7 it is apparent that the 1999 annual yield for each of these low glacier cover basins was approximately 90 – 120 mm greater than 1998 levels due to the deeper snowpack conditions of that year. Of interest, however, was the relationship between basin elevation and yield. From Table 6.1 and Figure 6.7 it is apparent that the largest and lowest basin, the Bow at Banff, displayed the smallest overall areal yield. The greatest yield was found in the highest and smallest basin of Mosquito Creek. These observations reflect the increasing input of precipitation (and possibly reduced evaporation) per unit area at the higher basin elevations and illustrate the importance of headwater contributions to downstream runoff. It is also interesting that for these three basins the yield/elevation relationship is close to being linear with a small reduction in yield

observed for Mosquito Creek during the deep snowpack year. This slight deviation from the apparent basin elevation/yield trend may be due to groundwater storage based flow regulation in Mosquito Creek (see Chapters Four and Five). However, no firm conclusions can be drawn from this observation as the yield estimates for Mosquito Creek were generated from a limited data set (see section 5.2.2).

6.4.2 Seasonal Areal Yields

By comparing the yields of Pipestone and the Bow at Lake Louise, the influence of basin size, elevation and enhanced deep groundwater contributions could be largely ignored. Therefore, any differences in yield could be attributed to landcover and hydrometeorological differences. The general seasonal patterns of runoff yield for both basins were similar (Figure 6.8). As would be expected, however, the difference between the two basins was greatest during 1998 when the basin-wide shallow snowpack led to enhanced late summer glacial melt. However, even during 1999 when the snowpack was deep and glacial contributions minimised, late summer yield was higher on the Bow River. In fact, despite the extreme difference in basin snowpack conditions, the inter-relationship between the Bow and Pipestone River yields for these two years was markedly similar. Part of this interannual similarity was due to snowmelt always occurring earlier in the season on Pipestone due to the basin's more southwesterly aspect.

During the early nival period of both years, the yield on Pipestone was always well above that of the Bow at Lake Louise. However, during the later glacial melt dominated period the Bow consistently showed higher yields. In fact, the transitions between these two periods, those of nival and glacial melt domination, were so clear in both years that the time at which the Pipestone yield dropped below that of the Bow could be used to

define this transition point. For 1998, this occurred at the end of June and for 1999 at the end of July, around one month later. Therefore, it could be surmised that the reduced snowpack associated with *El Niño* led to a shortening of the nival and extension of the glacial melt period by up to one month.

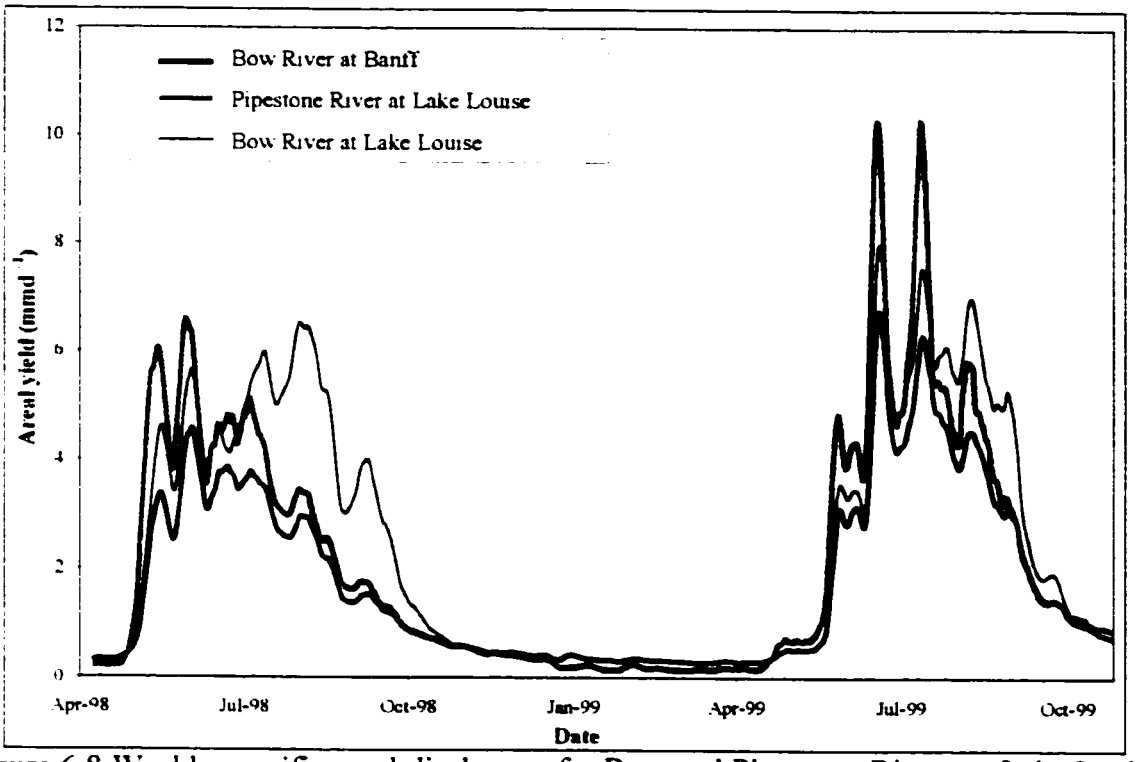

Figure 6.8 Weekly specific areal discharges for Bow and Pipestone Rivers at Lake Louise and Bow River at Banff (data courtesy of Water Survey of Canada).

6.5 Lower Basin Seasonal Hydrograph Periodicities

In Figure 6.9 recurring temporal periodicities during nival and glacial melt periods for the Bow and Pipestone Rivers from May to October of 1998 and 1999 are illustrated in the respective wavelet variance plots (scalograms). As with the observations from the headwater time frequency analyses, diurnal periodicities within the larger basins were strongest during the shallow snowpack year of 1998. This was true for all locations and it can, therefore, be inferred that deeper snowpack conditions tend to subdue the diurnal melt cycle regardless of time of year, basin size or landcover dominance.

Deeper snowpack leads to enhanced temporary storage of melt water within the pack, longer basin-wide snow cover with a commensurate increase in the overall reflection of incoming radiation, and so the above observation may appear to be somewhat trivial. However, if the seasonal differences in diurnal melt cycle strength are examined for each basin, it becomes apparent that for 1999 the diurnal signal tended to be strongest during the earlier nival period and almost absent during the latter glacial half of the melt season. This is interesting, as it is known from observations in the field that a large amount of snow persisted in the basins in the late summer of 1999 yet none of the basins demonstrated a significant diurnal signal. This lack of a late season melt signal may have been due to the snowpack being high in the basin in a region of cooler temperatures with melt discharges being more difficult to discern within the hydrographs. It also indicates that glacial melt inputs were small during 1999.

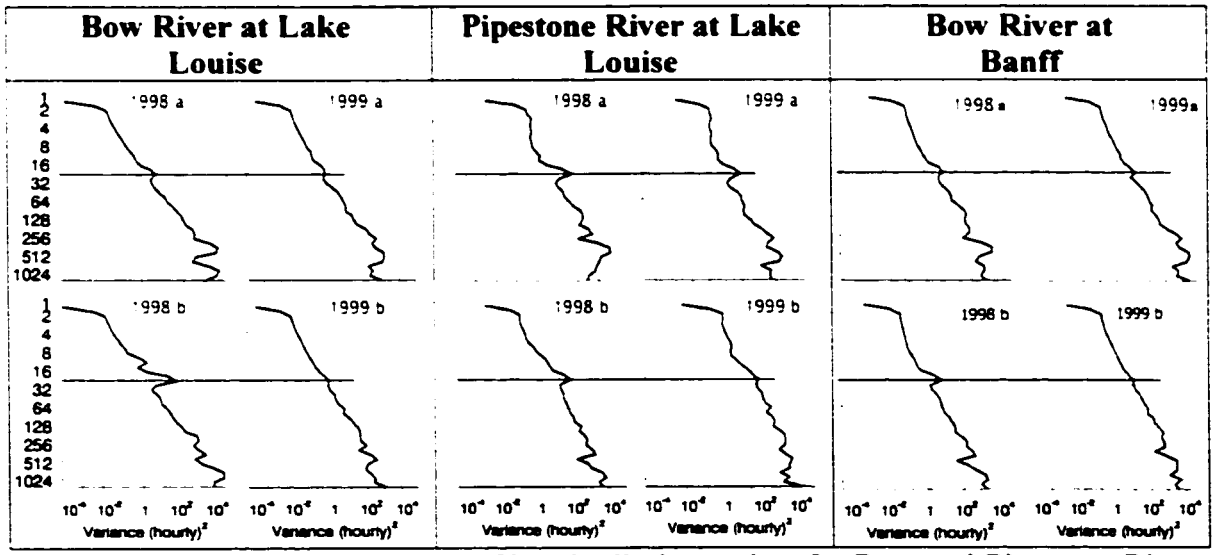

Figure 6.9 Wavelet variance plots of hourly discharge data for Bow and Pipestone Rivers at Lake Louise, and Bow at Banff during 1998 and 1999. Plots divided into two time periods: (a) early summer melt (nival) and (b) late summer melt (glacial). (Horizontal line = 24 hour time periodicity).

For Pipestone and the Bow at Banff it is interesting that the late 1999 diurnal signal was so weak, since in late 1998 it was strong. This suggests that in 1998 the strong signal was associated with glacial melt inputs. This is despite the small proportional glacier cover within these basins. In addition, it was earlier hypothesized in Chapter Four that groundwater levels at the beginning of 1999 would have been lower than 1998 due to the shallow snowpack of 1998. Therefore, it is possible that late summer snowmelt inputs for 1999 may have been slightly subdued in all basins from losses to groundwater recharge.

In general, then, it would appear that snowpack depth and elevation, and possibly antecedent groundwater conditions control much of the diurnal melt signal response downstream of the headwaters within the Bow Valley over interannual and seasonal time periods. The relative glacier coverage in headwater basins tends to control the diurnal melt regime but during years of shallow snowpack conditions small differences in glacier cover become important for the larger basins also. For example, even though the Bow Basin above Lake Louise only has around 10% glacier cover, it displayed a strong diurnal melt signal in late 1998.

Another possible effect of landcover and or stream network distribution is the steep upper curve of the Pipestone River variance plot during early 1998 and 1999 (Figure 6.9). This was associated with a greater frequency of short temporal periodicities of between 1 and 4 hours, and may have been due to rapid but variable responses to rainfall and melt event pulses from different locations within the basin. The same patterns were likely not evident in the other basins due to the higher lake coverage on the Bow River, thus masking out smaller events, and also due to the Bow at Banff being a further 50 km downstream leading to elongation and mixing of event hydrographs.

6.6 Lower Basin Seasonal Geochemistry

6.6.1 Interannual $\delta^{18}O$ Signature

6.6.1.1 Interannual Average $\delta^{18}O$ Signature

Parameter / Basin	Glacier cover	Average elevation (m a.s.l.)	Average $\delta^{18}O$ (‰)	End of winter baseflow $\delta^{18}O$ (‰)
Mosquito Creek	~ 1 %	2500	-21.5 (n = 24)	-21.2 (n = 2)
Bow Creek	~ 32 %	2600	-20.6 (n = 18)	-20.5 (n = 1)
Pipestone River	~ 3 %	2425	-21.2 (n = 15)	-21.0 (n = 1)
Bow at Louise	~ 10 %	2365	-20.6 (n = 15)	-20.8 (n = 2)
Bow at Banff	~ 2 %	2280	-20.6 (n = 17)	-20.6 (n = 2)

Table 6.2 Average spring 1998 – fall 1999 discharge weighted and winter baseflow $\delta^{18}O$ signatures with respective basin glacier cover proportions and overall average elevations.

From the average basin $\delta^{18}O$ signatures presented in Table 6.2 it is apparent that the three basins of minor glacier coverage (Mosquito, Pipestone and Bow at Banff) demonstrated a trend of $\delta^{18}O$ depletion with average basin height of approximately -0.4 ‰ per 100 m. This reflects the increasing snow to rain proportions in the headwater regions of the Bow Basin. A simple two-component mixing model using the combined average $\delta^{18}O$ values for 1998 and 1999 (see Chapter Three) for snow and rain of -22.1 ‰ and -11.8 ‰, returns approximate rain contributions of 6%, 9% and 15% for Mosquito Creek, Pipestone and the Bow at Banff, respectively. The same calculation using the average end of winter baseflow $\delta^{18}O$ values with the snow and rain signatures for 1998 of -21.6 ‰ and -11.3 ‰ give results of 4%, 6% and 10%, respectively.

Whether using average or winter baseflow $\delta^{18}O$ values, the isotope water balance separation suggests that rainfall contributions to runoff were small in all of the basins during 1998 and 1999. This corroborates the earlier findings that rainfall did not appear to contribute much to basin groundwater (Chapter Four) or surface runoff during large rainfall events (section 5.2.6) despite long-term average annual rainfall proportions of 54

% and 45 % at Banff and Lake Louise, respectively (see section 4.2.1). It should be cautioned, however, that rainfall proportions measured in the valley bottom are not indicative of basin-wide rainfall proportions due to the increase in snow proportion with height (see section 1.4 and 4.2.1). Despite this cautionary note, a basin-wide rainfall contribution to interannual runoff of between 10 and 15% does appear to be low and perhaps corroborates the earlier assertion that of all of the hydrological end-members in this basin, rainfall is the most susceptible to loss by evaporation (section 5.26).

Three of the five 1998 - 1999 volume weighted average $\delta^{18}O$ signatures for each of the basins were slightly depleted relative to end of winter baseflow, with the basin endpoint signature at Banff displaying no difference. This generally reflects the higher proportion of snowmelt in summer runoff and suggests that there is a time lag between snowmelt and rainfall infiltration to ground and its subsequent release to baseflow later in the year, as was earlier hypothesised (section 4.3.1 and 4.5.2). However, the comparative $\delta^{18}O$ signatures for the Bow River at Lake Louise deviated from this generalisation in that they displayed a more enriched total annual runoff signature relative to annual baseflow. There are three possible explanations for this deviation:

1) Analytical or sampling error;

2) Evaporative enrichment of the annual river signature;

3) Rainfall enrichment of the river signature.

The difference between average and baseflow $\delta^{18}O$ was greater than the analytical error (0.16 $^{o}/_{oo}$) and the two baseflow samples both had the same value of -20.8 $^{o}/_{oo}$, so analytical error is possible but unlikely. There were only 15 samples collected in 1998 and 1999 at Lake Louise and so biased samples could introduce error into the average

discharge weighted $\delta^{18}O$ signature. However, efforts were made to ensure that all samples from the rivers at Lake Louise and Banff were collected at similar times (usually the same day) and so the relative bias should be minimised. Although it is possible that the annual river signature for the Bow at Lake Louise was preferentially influenced by evaporation from lake surfaces this is not thought likely as the earlier test in section 5.4 indicated that lake evaporation did not lead to significant enrichment. However, it has already been suggested that rainfall runs off from glacierised basins more efficiently than from non-glacierised basins and thus it would be expected that the enriched rainfall signature would be shifted more toward the summer than winter baseflow. This could explain why the Bow at Lake Louise displayed a more enriched average annual signature than end of winter baseflow.

This logic would also suggest that the same pattern should have been observed on the highly glacierised Bow Creek. However, it should be borne in mind that the interannual average $\delta^{18}O$ values were calculated from only 18 samples over two melt seasons and therefore the sample frequency was probably inadequate to represent randomly occurring rainfall events within the headwaters. It was shown in the last chapter that rainfall events do have more noticeable hydrograph responses in glacierised basins and there is likely a high proportion of rapid rainfall runoff. This being the case, it might be difficult to "catch" this rainfall runoff if samples are not collected during or immediately following such events. Further downstream at Lake Louise and Banff, temporary storages within the channel and lakes would lead to elongation and mixing of event hydrographs downstream (e.g. Figures 6.2, 6.4 and 6.6), such that the timing of sampling (although still important) should be less critical. It may be that the earlier observation in Chapter

Five (section 5.3.4) that the Bow Creek $\delta^{18}O$ signature was "smooth" relative to other basins was due to the fact that rainfall episodes were missed. If this was the case then, the actual average annual runoff $\delta^{18}O$ signature for Bow Creek should have been more enriched than the -20.6 $^{o}/_{oo}$ calculated.

6.6.1.2 Seasonal $\delta^{18}O$ Signature

Illustrated in Figure 6.10 are the $\delta^{18}O$ signatures for the three larger Bow Valley sub-basins for the years 1998 and 1999. In general, the seasonal patterns displayed by each basin were similar to each other and the headwater basins (compare with Figures 5.4 and 5.24). Therefore, the dominant control on the temporal distribution of $\delta^{18}O$ signatures within the Bow Valley during 1998 and 1999 was related to snowpack conditions rather than landcover. However, landcover and average basin elevation did have a noticeable effect on the general isotopic weight of $\delta^{18}O$ in basin runoff and this is illustrated in Table 6.2. Landcover differences affected slight modifications to each of the basin $\delta^{18}O$ signatures and these relative effects will be discussed with respect to the time period of occurrence: i.e. during baseflow, nival or glacial melt periods.

End of winter $\delta^{18}O$ signatures during 1998 suggest that Pipestone River Basin baseflow had the highest snow to rain ratio with smaller ratios on the Bow River at Lake Louise and Banff. During the interannual baseflow period from 1998 to 1999 the Pipestone and Bow at Banff signatures depleted slightly towards the end of winter reaching values similar to the year before. This apparent gradual change during the course of the winter may have been indicative of gradual changes in composition of the baseflow as local water tables dropped.

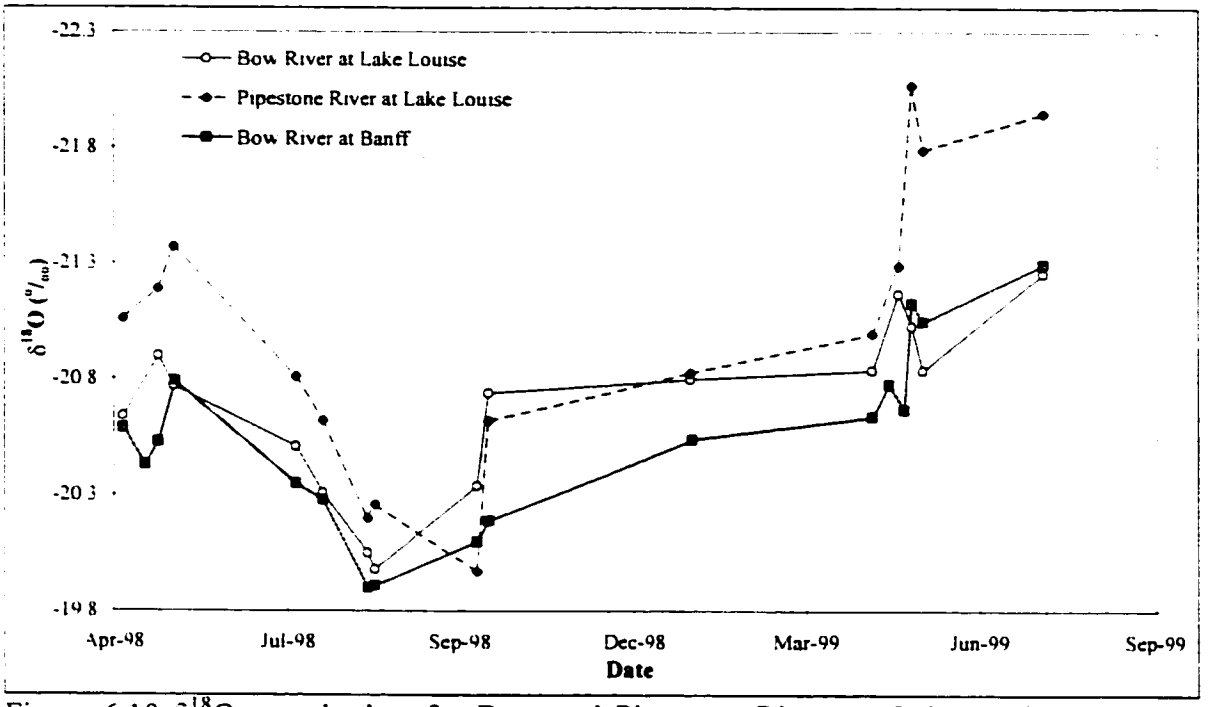

Figure 6.10 $\delta^{18}O$ sample data for Bow and Pipestone Rivers at Lake Louise and Bow River at Banff during 1998 – 1999.

The nival periods of 1998 and 1999 displayed similar patterns on all three basins but were quite different from year to year. In 1998, there was a slight depletion of around 0.3 ‰ in the $\delta^{18}O$ signature of all basins in May. The melt signal was slightly lagged lower down in the basin at Banff with an apparent initial enrichment of the signal, possibly related to shunting out of old water at the onset of melt. During the nival period of 1999, the deeper snowpack took much longer to melt out in all basins and the associated depletion of the $\delta^{18}O$ signature was much more pronounced. For all three rivers, the initial depletion of the $\delta^{18}O$ signature at the onset of snowmelt was followed by a noticeable enrichment even before peak snowmelt occurred. This was probably related to rainfall events occurring after the initiation of melt.

Unfortunately, not enough data were collected during late summer of 1999 to look in detail at the $\delta^{18}O$ signatures of the basins during the glacial period. However, from the

one sample collected from all basins in August of this year, it is apparent that runoff in summer 1999 was significantly more depleted than in 1998. This observation concurs with those of the headwaters presented in the last chapter. Of interest is that Pipestone displayed both the most enriched and depleted signatures during late summer to fall of both 1998 and 1999, respectively. This reflects the enhanced sensitivity of non-glacierised headwater basins to differences in antecedent snowpack conditions. The Bow River at both Lake Louise and Banff is somewhat protected from such extreme $\delta^{18}O$ signals due to the moderating influences of glacier melt and in-transit mixing in channel and lakes.

6.6.2 Seasonal Electrical Conductivity Signature

6.6.2.1 Interannual Average EC Signature

From the average basin EC signatures presented in Table 6.3 it is apparent that the three basins of minimal glacier coverage demonstrated a strong linear increase in both volume weighted average and baseflow EC with basin size and average basin elevation (see Figure 6.11). A relationship between river EC (or dissolved solids content) and basin would be expected, due to increased residence times and contact with weathering material as catchment area increases. Basin elevation may also exert a strong influence on river EC due to: 1) basin morphological influences such as hydraulic gradients, which tend to be greater at higher elevations potentially leading to reduced infiltration and shorter residence times; 2) elevationally dependant hydroclimatic processes such as snowpack depth, which influences melt volumes and dissolution dilution, or average temperature, which affects length of melt season and weathering reaction rates; or 3) land

surface permeability, which may decrease with elevation due to increasing exposures of bare rock.

Parameter / Basin	Basin Elevation (m a.s.l.)	Basin size (km^2)	Glacier cover	Average EC ($\mu S\ cm^{-1}$)	End winter 98 –99 baseflow EC ($\mu S\ cm^{-1}$)	Difference and Ratio ($\mu S\ cm^{-1}$)
Mosquito Creek	2500	35	~ 1 %	196 (n = 21)	249 (n = 3)	53 (27%)
Bow Creek	2600	25	~ 32 %	113 (n = 23)	284 (n = 2)	171 (151%)
Pipestone River	2425	309	~ 3 %	213 (n = 15)	273 (n = 1)	60 (28%)
Bow at Louise	2365	426	~ 10 %	183 (n = 15)	222 (n = 1)	39 (21%)
Bow at Banff	2280	2207	~ 2 %	257 (n = 16)	324 (n = 3)	67 (26%)

Table 6.3 Average discharge weighted and winter baseflow EC signatures with respective basin glacier cover proportions and overall average basin elevations.

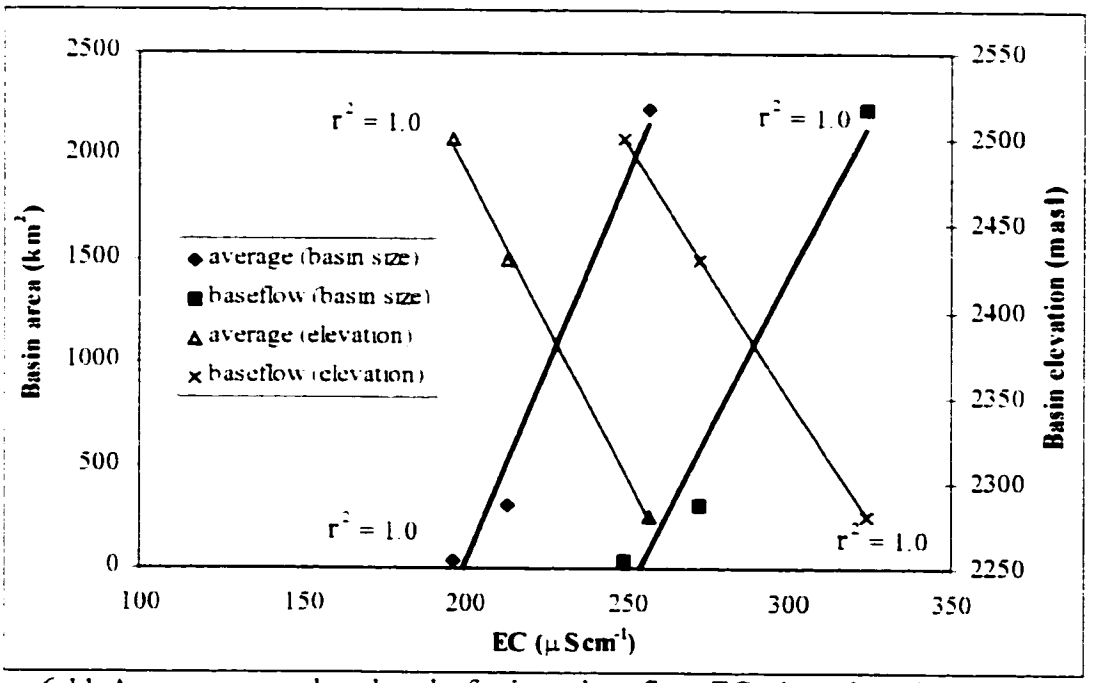

Figure 6.11 Average annual and end of winter baseflow EC plotted against both average basin elevation and basin area.

Deviating from the strong relationship between elevation and in-stream EC observed in Figure 6.11 were both basins containing relatively large glacier covers. In both cases average interannual EC levels were lower than all other basins due to the large volume of glacial melt occurring in the summer and the associated reduced basin transit times and increased volumetric dilution of the dissolved solids content.

Further to the diluted average EC signature in these more highly glacierised basins, the differences between average annual and winter baseflow EC values deviated from the constant ratio of around 27% observed in low glacier cover basins (Table 6.3). For the highly glacierised Bow Creek Basin, the massive increase of 151% from average annual to winter baseflow EC levels testifies to the huge difference in flow composition between summer and winter. The average interannual EC signature is heavily biased toward the diluted summertime EC levels due to the high discharges during this time (particularly in 1998). Some of the winter baseflow, however, may originate as melt water at the glacier subsole with long basin transit times and high levels of contact with mechanically weathered material leading to the high levels of dissolution (high ECs) observed.

Given that Bow Creek displayed high ECs in winter baseflow compared to average annual levels, it is slightly surprising to find that the baseflow EC for the Bow at Lake Louise is only 21% greater than the average annual and apparently more dilute than baseflow levels in all other basins (Table 6.3). This reduction in baseflow EC cannot be directly related to glacier cover, as from the observations on Bow Creek, elevated EC readings would be expected at Lake Louise also. The major difference between the Bow at Lake Louise Basin and other basins is the lake coverage upstream. It has already been shown that during summer months, the lakes do not impede the transfer of headwater runoff to downstream locations by more than a few weeks. However, commensurate lag times during winter are unknown but can be assumed to be longer due to reduced fluxes transiting through the lakes. Evidence that upstream inputs may take longer to transit through lakes during baseflow conditions is that Bow Creek EC values (Figure 5.24) continually increased during winter 1998 to 1999 yet this pattern was not in evidence at

the lake outflow (Figure 6.12). The EC pattern evident at Bow Lake outflow showed a decline after mid winter, much like most other basins (e.g. Figure 5.4 and Figure 6.13). It would appear likely, therefore, that the high EC observed during baseflow on Bow Creek did not make it downstream to lake Louise, as it was mixed with lake water during basin transit. The relatively dilute EC levels observed in the Bow River at Lake Louise during baseflow conditions may have been related, therefore, to older more dilute summertime melt water draining out of the Bow and Hector Lakes.

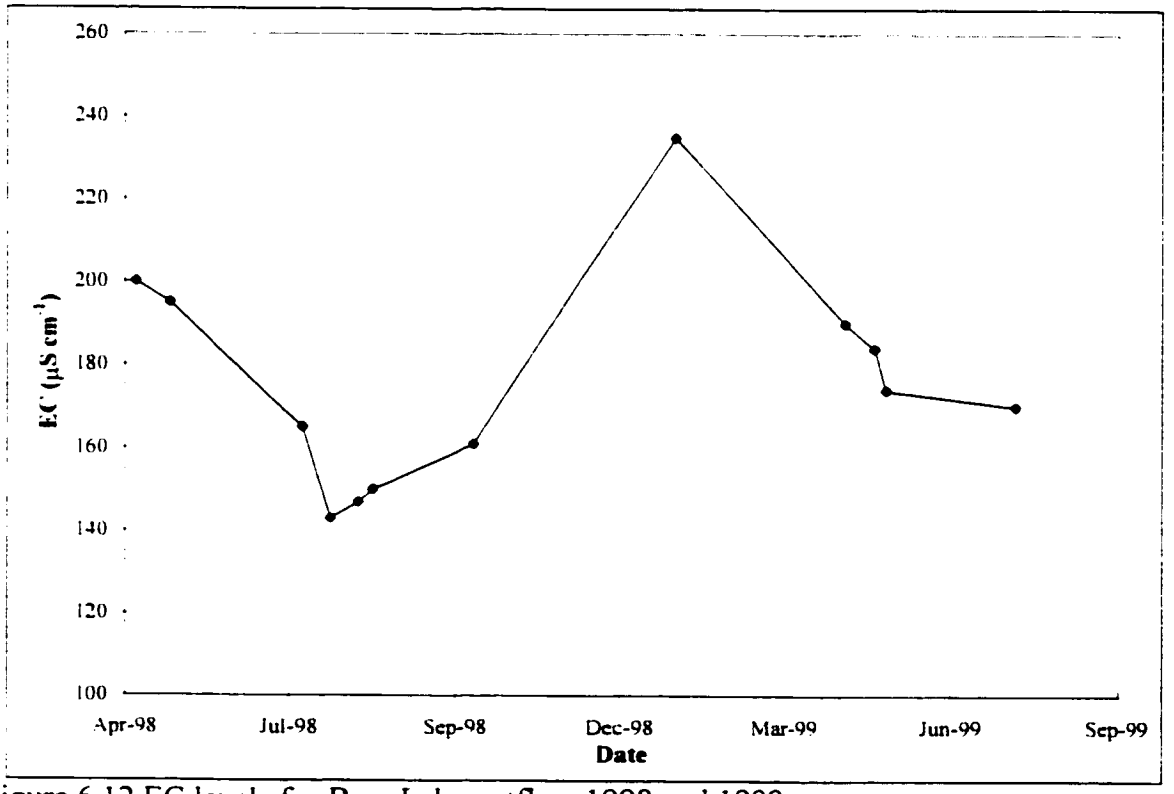

Figure 6.12 EC levels for Bow Lake outflow 1998 and 1999.

6.6.2.2 Seasonal EC Signature

Illustrated in Figure 6.13 are the EC signatures for the three larger Bow Valley sub-basins for the years 1998 and 1999. In general, the seasonal patterns displayed by each basin were similar to each other and the headwater basins (compare with Figures 5.4 and 5.24), with generally more consistent low EC levels at higher basin elevations and greater

glacier coverage. Therefore, the dominant controls on the temporal distribution of EC signatures within the Bow Valley during 1998 and 1999 were related to basin residence times and melt induced volumetric dilution. However, landcover and average basin elevation and size did have a noticeable effect on the general EC levels in basin runoff and this is illustrated in Table 6.3.

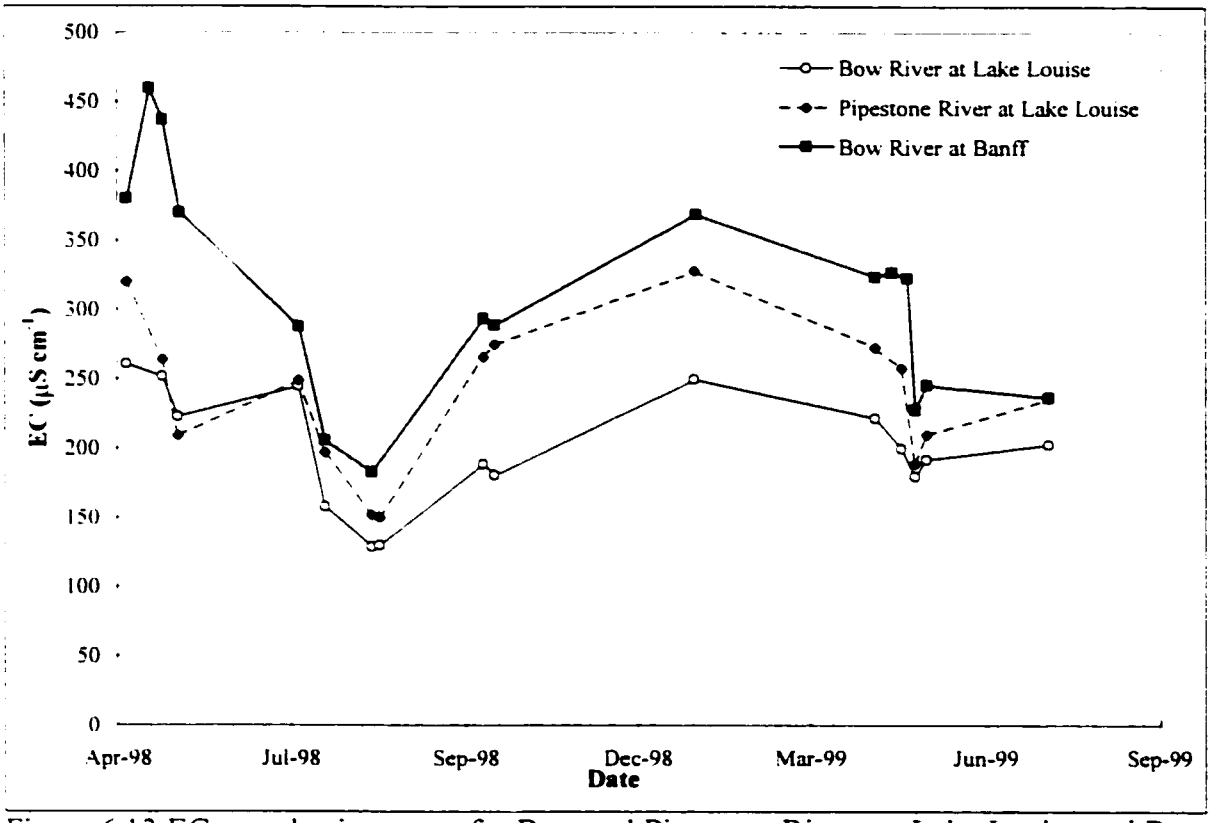

Figure 6.13 EC sample signatures for Bow and Pipestone Rivers at Lake Louise and Bow River at Banff during 1998 – 1999.

During the nival melt period of both years, EC levels on the Bow and Pipestone Rivers at Lake Louise appeared to converge. This was at the time of dominant snowmelt runoff from lower elevations within the basins and also at a time when the effects of different glacier coverage was minimised. During late summer, dilution occurred in glacierised basins from high volumes of ice melt entering the stream, and during

baseflow conditions dilution of the EC signal was still present at Lake Louise due to lake induced lag effects (see above). Therefore during this early melt period, snowmelt pathways and runoff processes in both the Bow and Pipestone Basins above Lake Louise were probably quite similar.

The apparent dilution step in the EC profiles of Bow and Pipestone at Lake Louise during early July 1998 (Figure 6.13) was also visible on Mosquito Creek (Figure 5.4) and discussed in section 5.2.4 of the last chapter. It was thought to mark the transition time from a period dominated by low elevation snowmelt runoff routed through organic forest soil layers to a period dominated by snow, icemelt and rainfall runoff draining the upper reaches of the basins where reduced weathering potential would lead to lower EC levels. As long as there is a significant coverage of forest soils in the lower elevation bands of a basin, this stepped EC pattern might be expected for both moderately glacierised and non-glacierised basins. This step was probably not observed on Bow Creek, therefore, due to a high proportion of glacial melt in runoff (thus masking other signatures) and a lack of forest soil in the lower elevation bands. Also, the step probably was not as pronounced at Banff due to either insufficient sampling or dynamic mixing of flow components in the channel network and upstream lakes.

The approximate treeline elevation in the Bow Valley lies between 2000 and 2250 m a.s.l. and the lower limits of glacier termini lie between 2100 and 2500 m a.s.l. Therefore, although there would be some temporal overlap between the start of the glacial melt period and the end of snowmelt in forested areas, the basin-wide transient snowline elevation would likely play an important role in controlling flow pathway dominance. Strengthening this argument, perhaps, is the observation that the apparent EC dilution

step (Figure 6.13) approximately coincided with the transition from dominant nival yield on Pipestone to dominant glacial yield on Bow (Figure 6.8).

6.6.3 Seasonal Tritium Signature

Illustrated in Figure 6.14 are the tritium signatures for the three larger Bow Valley sub-basins for the years 1998 and 1999. The basin TU signatures generally varied between characteristic rainfall and snowmelt, apart from the interannual baseflow value for Banff, and appeared to have a distinct seasonality. However, few samples were collected and analysed from these basins and so the full range and pattern of fluctuation probably has not been represented.

From the limited samples collected, it is clear that the Bow at Lake Louise was almost always the most depleted in tritium of the larger basins. This probably reflects the higher proportions of old ice melt water draining from the basin with a zero TU value. Pipestone and Bow at Lake Louise did converge briefly at the beginning of the 1999 melt season and apparently both depleted rapidly and by similar amounts as the deep snowpack melted out. The Bow at Banff generally displayed the highest TU values and this was likely associated with higher rainfall levels and old enriched groundwater (particularly during winter baseflow).

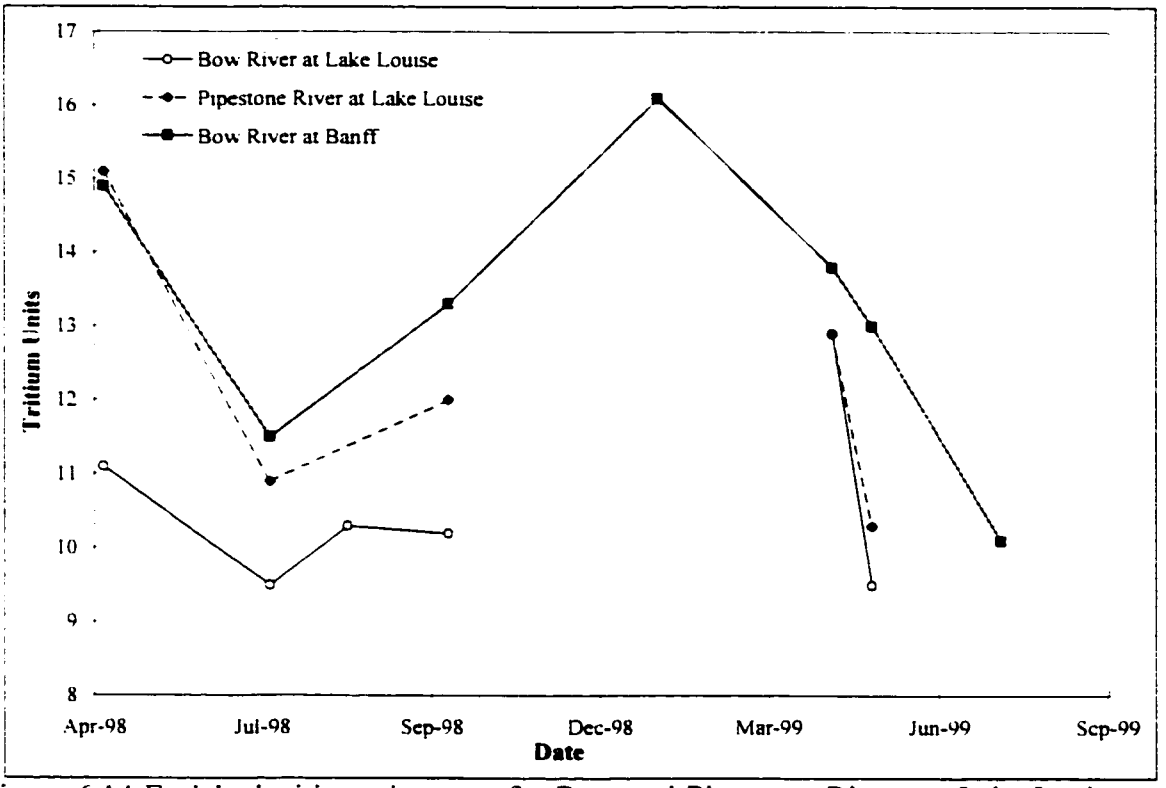

Figure 6.14 Enriched tritium signature for Bow and Pipestone Rivers at Lake Louise and Bow River at Banff during 1998 – 1999.

The seasonal variation in TU signatures for all basins was interesting, as the TU values tended to be highest during winter baseflow months and most depleted during summer. The seasonal atmospheric TU signature is generally the inverse of this, with winter snow having lower and summer rain higher TU values (Schotterer *et al.*, 1996). This observation suggests that winter baseflow tended to be dominated either by late summer rainfall or groundwater of several years in age.

6.7 Basin-wide Hydrograph Recession Intercomparison

The temporal locations of the hydrograph recession curves extracted for the recession analysis are illustrated on the logarithmic discharge plot in Figure 6.15. A summary of the recession parameter statistics generated for each sub-basin is provided in Table 6.4. From the recession analysis statistics presented in Table 6.4, the main observations can

be divided into categories of: 1) influences of basin size; 2) influences of glacier cover; 3) seasonal variation; 4) interannual variation.

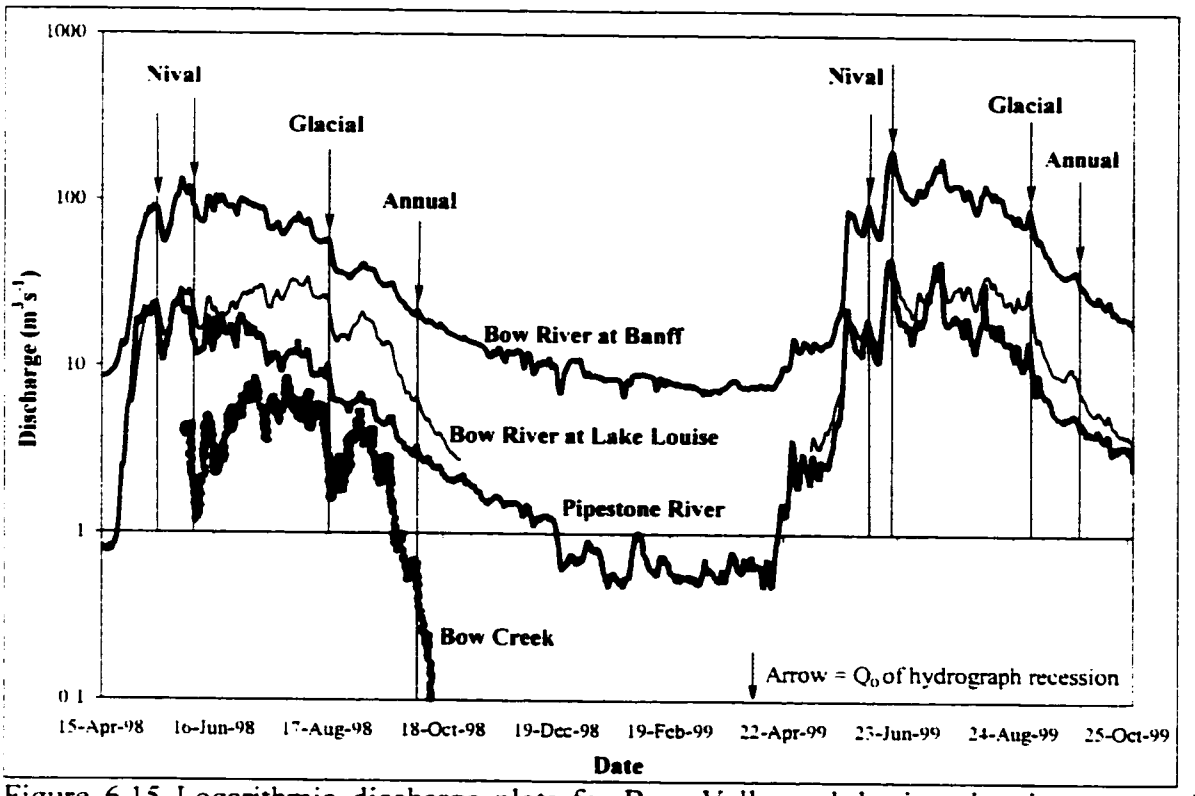

Figure 6.15 Logarithmic discharge plots for Bow Valley sub-basins showing temporal location of hydrograph curves used for recession analysis during 1998 and 1999.

Location		Bow River at Banff			Bow River at Lake Louise			Pipestone River at Lake Louise			Bow Creek (headwaters)		
Basin area, Glacier cover		2207 km^2, 2%			426 km^2, 10%			309 km^2, 3%			25 km^2, 32%		
Recession parameter		Q_o (m^3s^{-1})	α^{-1} (days)	r^2	Q_o (m^3s^{-1})	α^{-1} (days)	r^2	Q_o (m^3s^{-1})	α^{-1} (days)	r^2	Q_o (m^3s^{-1})	α^{-1} (days)	r^2
Period	Date	1998											
Nival	May 15th	88	6.5	0.99	23	7.0	1.00	17	6.1	0.90			
	Jun 4th	93	9.3	0.96	21	8.0	1.00	14	8.5	0.97	2.0	2.7	0.99
Glacial	Aug 17th	58	6.5	0.96	23	4.7	0.98	8.7	7.2	0.98	2.3	4.3	0.89
Annual	Oct 3rd	22	29	0.93	6.2	17	0.99	3.0	32	0.60	0.5	5.4	0.95
		1999											
Nival	Jun 7th	93	9.3	0.99	19	10	1.00	16	10	0.80			
	Jun 22nd	152	10	0.99	34	9.2	1.00	23	11	0.60			
Glacial	Sep 2nd	77	11	0.98	22	7.3	0.99	9.9	7.8	0.89			
Annual	Oct 1st	28	22	0.84	5.6	23	0.99	4.2	23	0.59			

Table 6.4 Hydrograph recession analysis statistics for all basins with hourly data during 1998 and 1999. Analytical precision for $\alpha^{-1} = \pm 0.13$ days.

From Table 6.4, there is insufficient data to draw any conclusions regarding the influence of basin size on recession characteristics. There does not appear to be any systematic difference between α^{-1} values for the basin at Banff and at Lake Louise. This suggests that basins of ~400 km^2 and 2000 km^2 in this area are not significantly different in terms of hydrograph recession characteristics. The smallest basin studied, Bow Creek, does display consistently the smallest α^{-1} index, however, and this does indicate that smaller headwater basins do drain relatively rapidly compared to basins one to two orders of magnitude larger.

Another factor that may be partly responsible for the low α^{-1} index on Bow Creek is the large glacier coverage in this basin (32%). Supporting evidence that glacier cover leads to lower α^{-1} values (more rapid drainage) is that the α^{-1} index for the Bow River at Lake Louise (10% glacierised) during the late nival and glacial periods of both years was consistently lower than (by 0.5 to 3.7 days) the values for the Bow at Banff and the Pipestone River (average = 8.9 days). This consistent drop in α^{-1} was despite there being several large lakes directly upstream of the Bow River at Lake Louise, which might be expected to elongate the recession curve due to their "reservoir" like nature. These observations, therefore, indicate that high glacier proportions within these basins lead to more rapid drainage of hydrological inputs. This is thought due to higher permeabilities within glacier drainage networks, than would be found in non-glacierised basins, where much of the hydrological flux probably drains through groundwater flow pathways.

The data presented in Table 6.4 do not illustrate any seasonal pattern in α^{-1} or any consistent relationship with discharge (Q_0). However, for all basins it is apparent that during the hydrograph recession to interannual baseflow levels in October, α^{-1} is

consistently two to four times larger than at any other time of the year. This probably reflects the low discharges at this time and associated slow drainage as basin storage approaches its annual minimum.

Evidence for differences in annual storage levels at the start of both years was found by comparing the averages of α^{-1} values during the nival periods for the larger three basins. The average α^{-1} for the 1998 nival period of 7.6 days ($n = 6$, $\sigma = 1.2$) was found to be significantly shorter ($P = 0.006$) than the 9.8 days calculated for 1999 ($n = 6$, $\sigma = 0.6$). This suggests that during the 1998 spring melt period, drainage out of the Banff and Lake Louise sub-basins was more rapid than during 1999. A potential cause for the "slow down" during the 1999 nival period may be related to earlier suggestions that basin-wide water tables and associated storage (see Chapter Four) was lower at the beginning of 1999 due to the below normal snowpack and precipitation inputs during 1998 (see section 1.4.2). If this was the case, then at the start of spring melt in 1999 there would be a higher basin-wide storage capacity than in 1998, and a higher proportion of water would be delayed on its way to the stream.

6.8 Concluding Remarks

In order to summarise the pertinent findings of this chapter, each of the questions posed during the introduction of this chapter will be discussed.

6.8.1 *Are events that are clearly distinguishable in headwater hydrographs also evident much further downstream when the contributing basin area increases?*

From investigation of individual events and by wavelet filtering hourly discharge signals, it is apparent that diurnal fluctuations in discharge were visible in runoff from all

basins during both the nival and glacially dominated time periods. The strength of these signals was strongest in the headwaters, in basins of significant glacier cover and during the year of reduced snowpack conditions.

From examining the runoff response to two large rainfall events, it was found that rainfall responses at the larger basin scale were subdued if there had been no other recent rain events but were enhanced if antecedent basin conditions were wet. For the second rainfall episode, during moist antecedent conditions, there was a hydrograph response at all basin endpoints. However, it should be noted that despite these events being widespread throughout the basin and the largest rainfalls of the year, the hydrograph responses were small compared to diurnal melt inputs. The glacierised headwater basin displayed the clearest hydrograph responses to both events but of note is that the second event was relatively subdued, despite the higher rainfall volume and greater response at downstream locations. The reduced response on the glacierised creek for the second event was thought due to most of the precipitation falling as snow at high elevations.

It has already been established that snowmelt is the dominant runoff contributor in the Bow Basin but it is perhaps surprising that large rainfall events appeared to contribute relatively little to runoff. It is thought that the response tended to be relatively high from glacierised areas due to the impervious nature of much of the landcover. In non-glacierised basins, rainfall is more prone to infiltration and probable losses due to subsequent evapotranspiration.

6.8.2 *Are the effects of glacier cover distinguishable in the downstream hydrographs of basins with reduced glacial proportions and sizes an order of magnitude larger than the headwater end-member basin already studied?*

As noted above, diurnal melt from glacierised basins was discernible for all basin sizes. In addition, the areal yields, temporal hydrograph properties and geochemical signatures for the Bow and Pipestone Rivers at Lake Louise displayed different characteristics, which were clearly the result of different glacier proportions. For example, during both 1998 and 1999 the areal yield for Pipestone started off higher than for the Bow during the nival period. During mid summer, the areal yield for the Bow at Lake Louise rose above that of Pipestone and this point in time marked the transition from nival to glacial melt dominance for these basins. In 1999, this transition occurred one month later due to deeper snowpack conditions but indicates that even during deep snowpack years, glacial melt is still evident in the hydrograph for basins with only 10% glacier cover. Further, average EC levels on the Bow River at Lake Louise were generally more dilute than on the Pipestone River or Bow at Banff due to glacial melt inputs.

Another effect of glacier cover on the hydrograph is the moderating influence of excess glacier melt during shallow snowpack years and the enhanced storage capability of glaciers during deep snowpack years. In the headwaters, it was found that large glacier coverages lead to increased yields regardless of snow cover. At Banff, the small glacier coverage proportion does facilitate some form of flow regulation (Hopkinson and Young, 1998) but this level of regulation is difficult to assess by looking at the hydrograph alone. It is therefore interesting that for two hydroclimatically different years (1998 and 1999) the overall yield variability for the Bow at Lake Louise was minimal. This might suggest that in the Bow Valley, the 10% glacier coverage of the Bow Basin above Lake Louise offers the most efficient level of glacier induced interannual flow regulation.

6.8.3 *Do lakes in the main river valley introduce significant lags in overall basin response to headwater events?*

By looking at the wavelet filtered hydrographs, it was clear that short-term diurnal melt signals were present in the river downstream of the large lakes in the Bow Valley and so it is likely that at least the *response* to hydrological inputs makes it downstream quite rapidly. In general, the $\delta^{18}O$ and EC patterns at Lake Louise were similar to the headwaters but slightly more subdued. The relatively enriched average interannual $\delta^{18}O$ signal relative to interannual baseflow indicated that rainfall made a noticeable contribution to runoff at Lake Louise during the summertime when snow and ice melt dominated. This subsequently indicated that much of this rainfall water made it to Lake Louise after traversing one or more lakes. However, during the winter, reduced EC levels at Lake Louise despite high levels in the headwaters, suggest that mixing in the lakes during fall potentially leads to long transit times during interannual baseflow conditions. In summary then, lakes slightly modify downstream geochemical signatures by lagging the transfer of water to downstream. During the summer this time lag is probably days to weeks but during winter baseflow it may take several weeks to months due to changes in lake stratification and mixing.

6.8.4 How do basin drainage and storage properties vary with glacier cover and through time within the Bow Basin?

Although this study could not discern whether or not basin size systematically alters basin drainage rates, the most rapid drainage rates were observed in the small, highly glacierised Bow Creek Basin. This was thought more a function of relative glacier cover,

however, due to observations that the Bow River at Lake Louise displayed more rapid drainage than Pipestone River, despite the Bow Basin containing more lake cover and both basins being similar in size. Increased glacier cover is thought to "speed" up a basin's overall drainage characteristics due to relatively high permeability flow pathways within the glacial drainage system.

No seasonal patterns in basin drainage or storage characteristics were identified in this study but a significant difference in basin storage characteristics was found between the spring runoff periods of 1998 and 1999. From hydrograph recession analysis, it was found that the α^{-1} index for 1999 was over two days slower than for 1998. This reduction in basin-wide drainage rates in early 1999 may have been related to the earlier suggestion that below normal precipitation depths in 1998 probably resulted in comparatively low water tables and reduced overall basin storage volumes at the start of 1999.

6.8.5 *How do the hydrograph properties change from the headwaters to basin endpoint and what are the main controls or changes in source?*

One of the major changes to the hydrograph from the headwaters down to Banff was associated with basin size and response time. It was estimated that during nival and glacial melt, the time from peak melt input to peak runoff was approximately 4, 8 and 20 hours for the headwaters, the Pipestone and Bow Rivers at Lake Louise and the Bow at Banff, respectively. As would be expected, the hydrographs also became more subdued further downstream. The hydrograph was generally always more subdued in event response at Banff due to longer channel distances and residence times, and it being the focus of many sub-basin inputs all with temporally varying peaks.

Average basin elevation plays an important role in controlling hydrological yields, length of melt season and average geochemical signatures. In general, the higher elevation basins display increased areal yields and this is related to increases in precipitation (particularly snowfall) with elevation. This relationship, however, broke down during interannual baseflow conditions for the basins above Lake Louise, however, when it was observed that areal yield was maximised at intermediate elevations. This was thought due to Lake Louise occupying a pronounced dip in the main valley profile, likely causing local river reaches to experience strongly influent conditions from regional groundwater discharge.

During the early spring melt period of both 1998 and 1999, it was observed that Pipestone River responded to melt ahead of and more intensely than the Bow River. This subdued response on the Bow above Lake Louise could be in part related to temporary melt runoff storage in lakes with initially low levels but is thought equally likely related to the relative basin aspects. As with Mosquito and Bow Creek, the Pipestone and Bow above Lake Louise drain different sides of the Bow Valley and as such have generally opposing aspects. That of Pipestone and Mosquito is southwesterly and that of Bow Creek and Bow at Lake Louise is more easterly. The southwesterly facing basins are exposed to sunlight earlier in the season and for longer time periods and this probably explains why Pipestone responds faster to spring melt than the Bow.

Pipestone and Bow at Lake Louise are similar in size, hypsometry and elevation but differ mainly in terms of their relative glacial coverages with about 3% and 10%, respectively. This difference in glacier cover manifests itself in the hydrograph in many ways. The most obvious is the temporal shift in peak runoff yield, which is much later on

in the Bow due to late summer icemelt following melt out of high elevation snowpack. Also, $\delta^{18}O$, EC and tritium signatures in seasonal runoff vary between the two due to their difference in glacier melt contributions. Overall, $\delta^{18}O$ is more enriched for the Bow at Lake Louise due to higher icemelt over snowmelt inputs, and also due to enhanced rainfall runoff over more impervious bare rock and glacier surfaces. Tritium levels tend to be reduced for the Bow River relative to Pipestone due to the greater proportion of ice melt in this basin and ancient (low elevation) ice having a zero TU level. During spring melt, the two basins display similar EC levels but as soon as glacial melt commences, the EC levels on the Bow drop due to volumetric dilution.

In summary, hydroclimatic inputs control the general seasonal patterns of runoff yield and geochemical patterns at all scales, and the responses from all basins can be linked to one another. However, the effects of basin size, elevation, aspect and landcover explain the subtle differences between basins. In the following chapter, a hydrological model will be optimised and run for the Bow River above Banff and evaluated using $\delta^{18}O$ tracers. The modelled hydrological breakdown of the constituent hydrograph components will be investigated to assess whether or not the model calibration adequately represents some of these important basin properties.

Chapter 7 Using Oxygen Isotope Tracers to Evaluate Flow Components Generated by the UBC Watershed Model

7.1 Introduction

This chapter investigates the use of conservative stable oxygen isotope tracers to assess the accuracy of water balance predictions within a hydrological model used in mountainous basins. The UBC Watershed Model (UBCWM) was chosen for this study as it was designed for and is operationally used in basins similar in climatic regime, size, relief and ground cover to the Bow Valley and can handle the limited data available in this study area. It is important to note that the aim of this chapter is not to draw conclusions about the UBCWM but rather investigate areas in which the calibrations of the model may be in error, despite obtaining reasonable statistical efficiencies. See section 2.5.5 for a brief introduction to the model and its main components.

Hydrological models can be calibrated to recreate past hydrographs with high statistical efficiency. Even in large, hydrometeorologically complex mountainous basins, Nash-Sutcliffe efficiencies (indicating volumetric and temporal model hydrograph accuracy) greater than 90% can be obtained over inter-annual periods (e.g. Kite and Kouwen, 1992). These high efficiencies tend to imply that the hydrological balance predicted by such model calibrations is reasonably accurate. Even if a low efficiency is obtained with the available input data, it may be very difficult to decide which hydrological balance components have been over- or under-estimated. These are important considerations if the model is used for predictions of future water yields, particularly in environments where the hydrological breakdown of components is not well understood.

Zawadzki (1997) used the UBC Watershed Model to assess changes to the future river flow regime in the Canadian Rockies given a 2 x CO_2 scenario and reduced glacial extents. Despite reasonable initial model calibrations (r^2 > 93% for the calibration year), the results raised a question as to the accuracy of the modelled glacial melt contribution, a key component of the study. For large increases in temperature, the commensurate increases in glacial ice melt were very low during late summer (Zawadzki, 1997). Therefore, regardless of the overall efficiency of any model calibration, the temporal and volumetric accuracy of the hydrological balance prediction always remains in question.

In this chapter, a technique is tested which attempts to address the question of simulated hydrograph accuracy by assessing the modelled break down of hydrological water balance components rather than simply calculating the fit between observed and modeled hydrographs. The specific objectives are:

1) To develop and test a technique of model evaluation using observations of oxygen isotopic signatures for main hydrological balance components;
2) To assess whether or not incorporating the temporal oxygen isotope signature variation in hydrological end-member components improves the evaluation procedure.
3) To isotopically evaluate and optimise a modelled water balance over a period of years with highly variable hydrometeorological conditions (1996 to 1999).

7.2 Methods

7.2.1 Overview

Monthly water balances for hydrological years 1996 to 1997 and 1996 to 1999 were generated from two separate runs of the UBCWM (version 4) for the Bow River at Banff.

The first run was performed to test the utility of using stable isotope tracers for model evaluation on two independently calibrated years of high efficiency. In the second model run a continuous inter-annual time series of diverse hydrological years was statistically optimised. The conceptual model of $\delta^{18}O$ signatures for each of the hydrological balance components provided in Chapter Three was plugged into the model to generate a $\delta^{18}O$ chemograph. The validity of UBCWM predicted hydrological balances were investigated, and improvements to the optimised parameter sets explored by comparing the modelled and observed isotope chemographs.

7.2.2 Modelling River Discharge

7.2.2.1 Two Independently Calibrated Years – 1996 and 1997

A watershed calibration description file was generated containing landcover and user specified parametric data (see appendix 6). Basin landcover and hypsometric information were gathered from digital topographic maps and classified Landsat TM imagery (see appendix 2). Discharge data for the Bow River at Banff, precipitation and temperature data from Castle Mountain (approximately in the centre of the basin at an altitude of 1500 m a.s.l.) and Bow Summit (at the northern end of the basin at 2030 m a.s.l.) were then formatted for use within the model. The model extrapolated basin-wide precipitation from Castle Mountain Village and Bow Summit weather stations. An orographic enhancement factor of 4.5% per 100 m was used to calculate precipitation for all elevations. These values were based on the observed interannual increase in precipitation from Castle Mountain at 1500 m a.s.l. up to Bow Summit at 2030 m a.s.l (see section 1.4.2). The deeper snow depths observed over glacierised areas (Chapter One, Figure 1.8) could not be accounted for in the model and early runs suggested that runoff from these

areas was under-estimated. In an attempt to compensate for this, the orientation of all glacierised areas was set to south facing (as in Zawadzki, 1997) to increase melt runoff from these areas. The environmental temperature lapse rate above the upper weather station was set at 0.6 °C to be consistent with earlier findings in section 1.4.3. All other meteorological parameter values were set using the default values (Quick and Pipes, 1996), which were also adopted in an earlier study using the UBCWM in this basin and were found to provide reasonable results (Zawadzki, 1997).

Groundwater percolation rates and residence time data were not available and had to be estimated or optimised. The impervious fraction of the basin from which "fast runoff" occurs was defined as all areas of bare rock. The default maximum daily groundwater percolation rate to "slow runoff" of 20 mm per day over the remainder of the basin made the hydrological response rather sluggish. However, using the value used in the earlier study by Zawadzki (1997) of 5 mm per day provided improved results as it better represented the basin's relatively fast response to hydrological inputs. Any hydrological input exceeding this value was shifted to interflow or "medium runoff" (see section 2.5 and Figure 2.2 for an overview of these model components). The proportions of the slow runoff component that went to either the upper or deeper groundwater zones were calculated in the optimisation routine of the model. Following model optimisation, 55% was arbitrarily sent to the deep groundwater zone share and 45% to the upper zone. For the deep groundwater zone time constant (assumed to approximate the groundwater component maintaining interannual baseflow) it was assumed that the time taken for the geochemical snowmelt wave to reach its peak, observed in the groundwater $\delta^{18}O$ signature as approximately 4 months (section 4.5.2), would provide a reasonable

surrogate. Therefore, a discharge constant of 130 days was assigned to the deep groundwater share and after optimisation, a shorter discharge constant of 80 days was set for the upper groundwater zone. All other parameter settings used the default values suggested in Quick and Pipes (1996).

The calibration for 1996 was reasonable, with an overall Nash Sutcliffe efficiency (e') of 93%. When this calibration was applied to the 1997 data, e' dropped to below 85% due to spring melt being volumetrically overestimated. Model output improved if basin-wide precipitation volume occurring when the temperature was below 0 °C (i.e. snowfall) was reduced by 8% in the precipitation modelling routine. This increased e' to 89% for the entire year. Using two different calibrations to account for the slight differences in hydrological character for each year was thought to give the model the "best chance" of generating accurate predictions of the hydrological balance. The output of the UBCWM was broken down into three "fast" runoff and "interflow" components: snowmelt, glacial icemelt, rainfall and a fourth component of groundwater baseflow. The observed and modelled hydrographs at Banff, along with these four flow components, are illustrated in Figure 7.1.

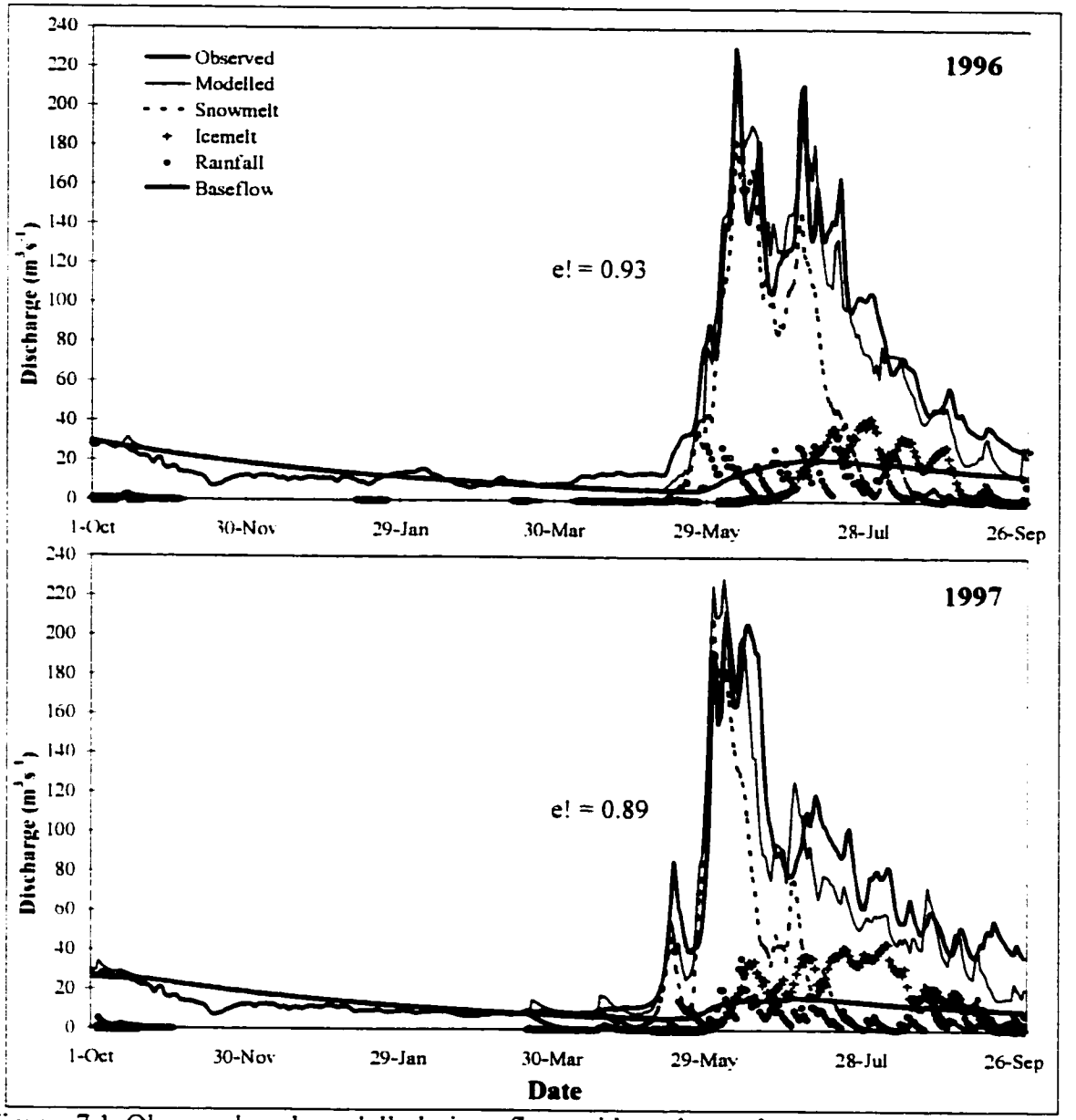

Figure 7.1 Observed and modelled river flow with end-member components at Banff, 1996-97 hydrological years (years calibrated individually).

7.2.2.2 Continuous Model Calibration for 1996 to 1999.

A completely optimised run of the model was performed over the four hydrological years from 1996 to 1999 as one continuous time series (see Quick and Pipes (1996) for optimisation procedure). This time series is of significant interest because it spans years of diverse hydrological characteristics. The model optimisation procedure was applied to all major parameters but the starting parameters used were taken from the earlier 1996

run. The years 1996, 1997 and 1999 all experienced deep snowpack conditions (see section 1.4.2 and appendix 1). However, 1998 was an *El Niño* year and as such was one of the driest on record in this region (between 23% and 62% less precipitation than the other three years studied – see Table 1.2). Calibrating a model over such a range of hydrological conditions is a challenge but these are the conditions a model has to deal with if it is to be used in long-term studies to assess climate and landcover changes. This model run provided an interesting test of the isotopic model evaluation process.

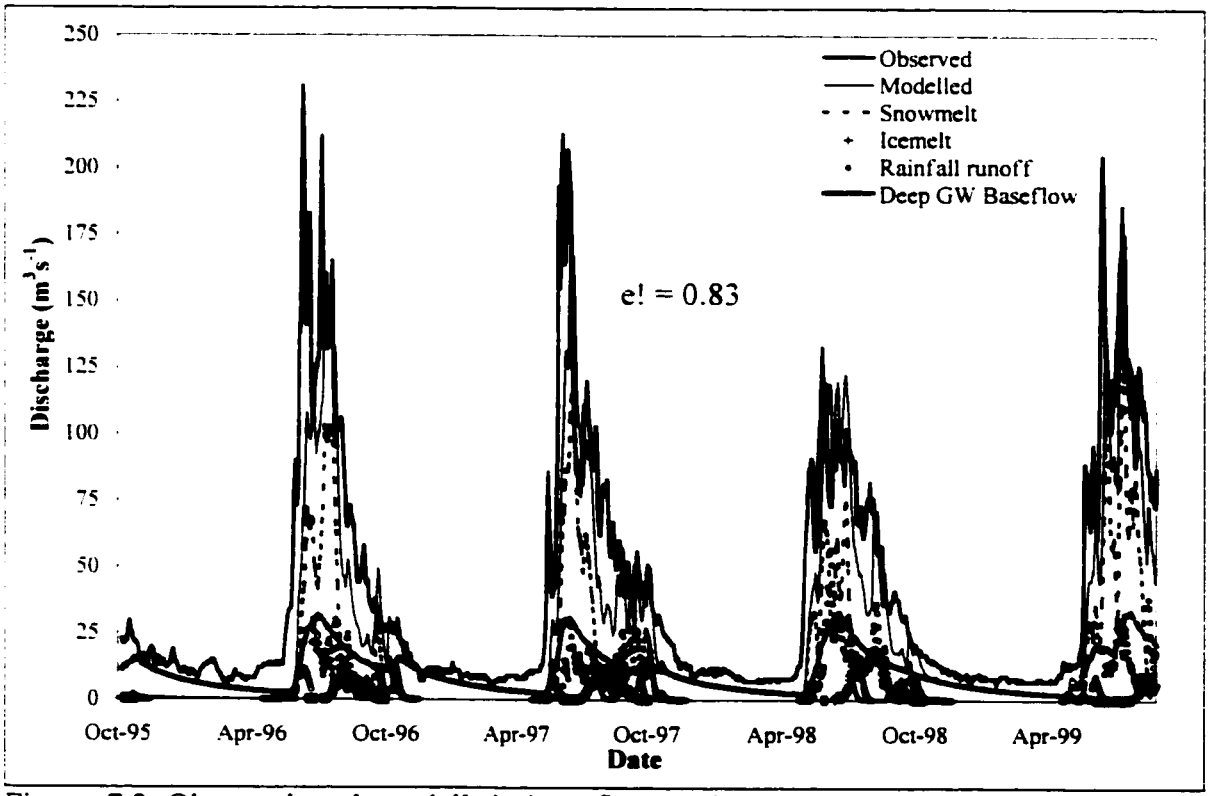

Figure 7.2 Observed and modelled river flow and components at Banff, 1996-1999 hydrological years.

There were some occasional gaps of a few days each in the records of the two meteorological stations (less than two months in total) and these were filled by regressing the remainder of the time series with each other and extrapolating from one to the other.

After performing the optimisation procedure, the major changes in the parameter values were an increase in the groundwater percolation rate from 5 mm to 20 mm (the default value); an increase in the deep groundwater zone share of the slow runoff component; a slight increase in the timing of the deep groundwater discharge constant and a significant reduction in the timing of the upper groundwater discharge constant (see Appendix 6 for model calibration values used in all model runs). These changes led to a slight under-estimation of interannual baseflow levels but improved the overall fit of the summertime hydrographs for the 4 years. A coefficient of efficiency (*e!*) of 83% was obtained and the modelled hydrograph is illustrated in Figure 7.2. This model calibration was thought to be more typical of what might occur during operational model runs for forecasting purposes or during climatic change impact studies.

7.2.3 Modelling the River $\delta^{18}O$ Chemograph

The sampling methodology and end-member $\delta^{18}O$ characteristics of hydrological flow components within the Bow Valley above Banff were summarised in Chapter Three. Two approaches have been used to assign appropriate isotope signatures to each flow component of the UBCWM simulated hydrological balance. The first was to assume average or "static" $\delta^{18}O$ values from the sample data (Table 7.1) for each of the four end-members. This provided a simple first round model to assess whether or not this technique had potential and also provided a reference for subsequent improvements. The second approach incorporated the temporally changing or "dynamic" hydrological balance signatures (Table 7.1) over the course of each melt season. These two signature sets were first applied to the two independently modelled years, 1996 and 1997. Then the dynamic end-member signatures were applied to the continuously modelled time series

from 1996 to 1999. Finally, the dynamic isotope signatures were applied to the four-year time series a second time following the interpretation of potential errors in the UBCWM calculated balance from the previous model run.

River samples were collected every week during the summers of 1996 and 1997 and approximately every 10 to 20 days during 1998 and 1999. The samples were analysed for $\delta^{18}O$ (as described in Chapter Three), then volume weighted according to river discharge on the day of sample collection at Banff, and aggregated to a monthly time step. Each of the modelled flow components was also aggregated to the same time step and its proportion of the hydrograph multiplied by its respective $\delta^{18}O$ signature. These values were then summed and a modelled chemograph generated. In Figure 7.3, the observed isotope chemograph is plotted (both raw data and volume weighted) along with the first modelled chemograph using static isotope signatures for the independently calibrated years of 1996 and 1997.

Static isotope signatures (‰)		**Dynamic isotope signatures (‰)**	
Snow	Avg = -22.2 σ = 1.4 n = 20	Hydrological years: 1996 =	-22.3 (σ = 1.5, n = 6)
		1997 =	-22.3 (estimated from 1996)
		1998 =	-21.6 (σ = 1.6, n = 7)
		1999 =	-22.6 (σ = 1.0, n = 6)
Ice	Avg = -20.9 σ = 0.7 n = 23	All years: May =	-21.5
		June =	-21.3
		July =	-21.0
		August =	-20.8
		September =	-20.5
Rain	Avg = -13.2 σ = 2.2 n = 16	Hydrological years: 1996 =	-14.3 (σ = 1.4, n = 3)
		1997 =	-14.9 (σ = 0.3, n = 2)
		1998 =	-11.3 (σ = 2.0, n = 7)
		1999 =	-12.3 (σ = 1.8, n = 4)
Baseflow	Avg = -20.5 σ = 0.17 n = 15 (winter samples only)	December to April of each year = -20.5 Baseflow shifts linearly to a peak during August each year of:	
		1996 =	-21.0
		1997 =	-21.0
		1998 =	-19.6
		1999 =	-21.5

Table 7.1 Static and temporal summary of hydrological end-member $\delta^{18}O$ signatures within the Bow Valley above Banff from observations discussed in Chapters 3 and 4.

A sensitivity analysis of the end-member $\delta^{18}O$ signature influence on the modelled chemograph was performed by using the standard deviation of error either way in the end-member signatures. In the case of summertime baseflow, a standard deviation was not available so a broad value of ± 0.5 $^{o}/_{oo}$ was used, despite the small variability ($\sigma < 0.2$ $^{o}/_{oo}$) observed during winter months, to account for unknown changes during the summer.

7.3 Results

7.3.1 Static Isotope Signatures for UBC Model Run 1

For the chemograph modelled with static $\delta^{18}O$ signatures (Figure 7.3), the modelled isotope chemograph was consistently more enriched than observed in the river. The volume weighted average isotope signatures for the entire study period differed by over 0.3 $^{o}/_{oo}$ and, during September 1997, the observed chemograph was lighter than predicted by the model even when each of the components was isotopically depleted by 1 standard deviation. However, the overall shape of the chemograph was at least approximately correct and, for the most part, did lie within the standard deviation range. It was simply exaggerated in one direction, i.e. it was generally too heavy or isotopically enriched. There are several reasons why this may have occurred but before discussing these reasons, observations of the dynamic chemograph model for the same time period will be outlined.

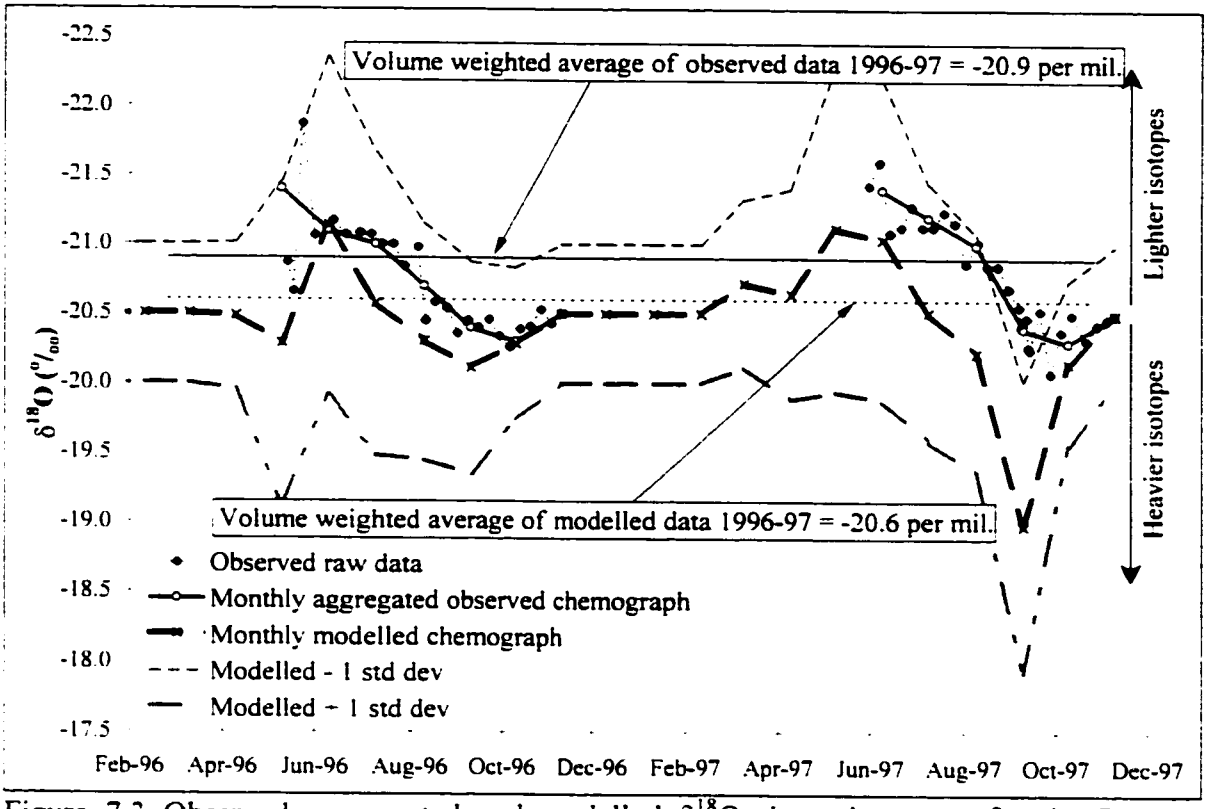

Figure 7.3 Observed, aggregated and modelled $\delta^{18}O$ river signatures for the Bow at Banff, 1996 – 1997 (static flow component signatures).

7.3.2 Dynamic Isotope Signatures for UBC Model Run 1

As with the first chemograph using static $\delta^{18}O$ signatures, the modelled values using dynamic signatures were generally too enriched (Figure 7.4). The difference between observed and modelled river isotope signatures for the study period was reduced, however, to 0.2 °/oo (approaching the range of analytical error). This was a visible improvement but the fact that it was only slightly better than the static signature graph suggests that the effort taken to characterise inter-annual and seasonal variations in isotope signatures may only provide minimal returns. This, in turn, suggests that if this technique of isotopic model evaluation is found to be useful, then the static signature method could be a robust first round approach.

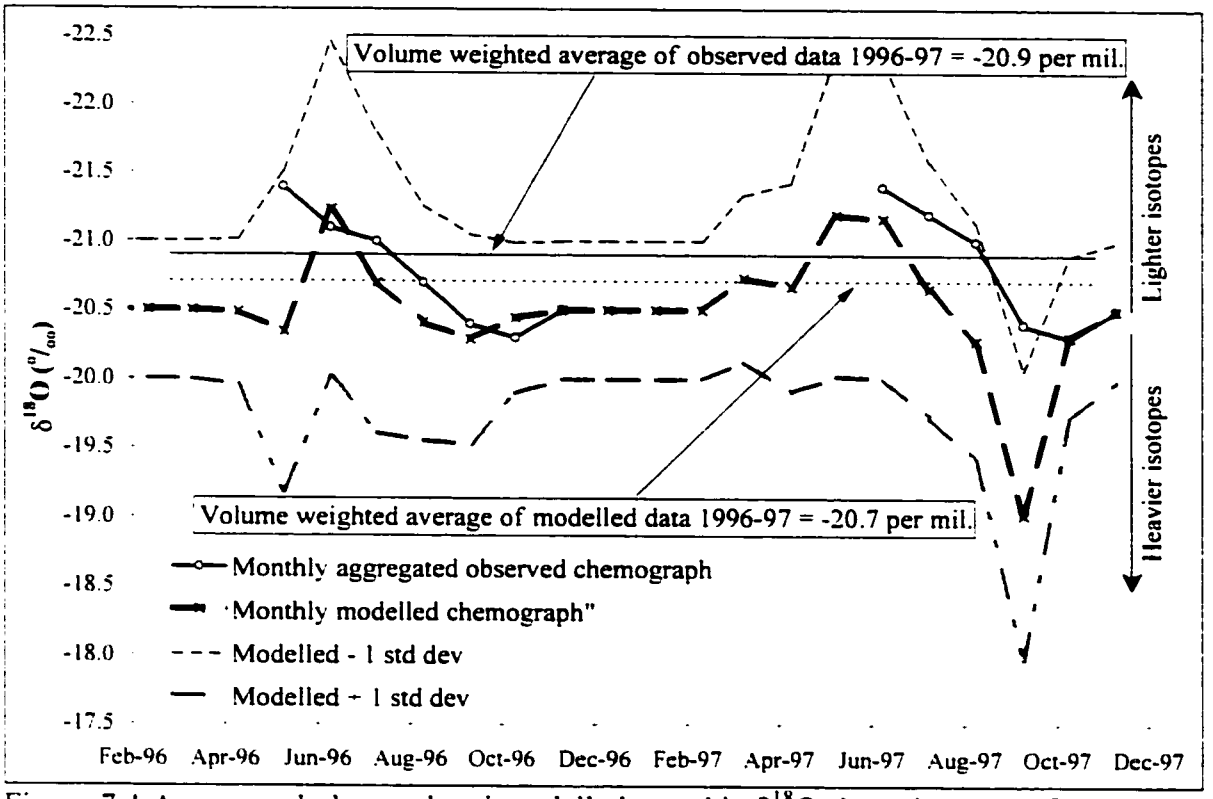

Figure 7.4 Aggregated observed and modelled monthly $\delta^{18}O$ river signatures for the Bow at Banff. 1996 – 1997 (dynamic flow component signatures).

Four potential reasons for the difference between the modelled and observed chemographs are considered below:

1) The $\delta^{18}O$ values attributed to the four modelled flow components were in error.

In the case of snow, the signature may change due to preferential initial melting of lighter isotopes early on (Maule and Stein, 1990) and this could be partly responsible for the difference between observed and modelled chemographs during spring, but over the year the bulk snowpack signature should even out. The static signature applied to glacial ice in this area was corroborated in unpublished data by West (1972). The majority of rain samples were taken from valley locations, which could potentially bias rain with a heavy signature. However, those rainfall samples taken from high elevations did not indicate isotopic depletion with elevation (see section 3.5.1). It is possible that the

sampling strategies were inadequate to characterise the components but considering the relatively low standard deviations this is not thought to be the main reason for the observed discrepancy.

2) The $\delta^{18}O$ signature changed during transit along the course of the river.

One likely change to the river isotope signature during and following mixture of the flow components would be fractionation due to evaporation leading to a more enriched signature than predicted. However, this is the opposite of what was observed, i.e. the real river chemograph was in fact lighter than predicted. Another potential source of change to the chemograph during transit could result from channel losses to groundwater in areas of stream effluence. This could potentially alter the hydrological balance characteristics of runoff. However, although some stream effluence was observed in the high headwaters, this is not thought to be possible at the larger basin scale due to the massive groundwater storage potential of surrounding slopes and a tendency for hydraulic gradients to be directed towards the valley bottom. Therefore, it is not felt that a changing $\delta^{18}O$ signature during channel transit was responsible for the observed chemograph discrepancy.

3) Lakes induced a lag effect.

The fit between the modelled and observed chemographs would improve if the modelled chemograph were retarded by approximately one month. In section 5.4 it was shown that lakes in the headwaters of the Bow Valley introduce noticeable lags between upstream and downstream river geochemical signatures. The UBC model cannot account for lake induced lag effects and this may be partly responsible for the lack temporal coincidence in the modelled and observed chemographs.

4) The simulated balance was in error.

It is felt that much of the observed discrepancy is due to the predicted balance being biased toward an overestimation of isotopically heavy rainfall input that was volumetrically balanced by an underestimation of lighter snow and ice components. There are various lines of evidence to support this hypothesis.

For the first run of the UBC model, basin-wide snowpack was modelled as having completely disappeared at the end of both years and not supplying any melt water directly to river flow. This is highly unlikely, as both of these years had a relatively deep snow pack (section 1.4.2) and it is known (from personal field observations) that a large proportion of the snowpack remained at the end of each year. If snowmelt contributions were underestimated in late summer runoff then which balance component (glacial icemelt, rainwater or groundwater baseflow) compensated this loss with an over-estimated volume?

During late summer, earlier observations of groundwater and river baseflow in the headwaters (see Chapter Four) indicated that this component of the balance was generally isotopically depleted due to snowmelt infiltration during spring. As such, the isotopic signature assigned this component during August of both years was -21.0 $^{o}/_{oo}$, only 1.3 $^{o}/_{oo}$ below snowmelt. Similarly, glacial melt was also only slightly enriched compared to snowmelt at this time (1.5 $^{o}/_{oo}$). For either of these components to be responsible for the 0.2 $^{o}/_{oo}$ level of enrichment in the interannual signature would take a large error in the simulated balance. Rainfall, however, was generally significantly enriched compared to snow (approximately 8 $^{o}/_{oo}$) and it would only take a relatively small error in the modelled rainfall volume to introduce significant error into the chemograph.

In Figure 7.1, it is apparent that the observed hydrograph was generally higher than the model's during summer and it was only during rain events that the two sometimes converged. This suggests that the model was routing rain to the channel too quickly (hence the increase in the maximum groundwater percolation rate in subsequent model runs). This could also partly explain why the most isotopically enriched point in the modelled chemograph was one month ahead of that observed in the river for both years (Figures 7.3 and 7.4). Furthermore, the precipitation records from Castle Mountain indicated that the summer months (June to September) of 1997 experienced 18 – 25% more rainfall than that of 1996 (Table 1.3) and this was the only period where the observed chemograph lies outside one modelled standard deviation. If the model were indeed routing rain to the channel too quickly then there would be less opportunity for loss of this component due to evaporation, thus explaining why there could be too much rainwater in the balance.

Alternatively, there could be a slight overestimation of the total rainfall entering the basin and this could be the result of using only two precipitation gauges plus a simple orographic enhancement factor to characterise rainfall for the entire basin. Evidence to support this argument is that although interannual precipitation indicate an average basin-wide orographic enhancement of approximately 4.5%, this is not the case during the summer months. From the data in Table 1.3, it is apparent that summertime orographic enhancement between Castle Mountain Village at 1500 m a.s.l. and Bow Summit at 2030 m a.s.l. is approximately 1.6% per 100 m rise in elevation. Therefore, the model's inability to account for seasonally changing orographic patterns is probably another major cause of rainfall over-estimations and snowmelt under-estimations in the balance.

It should be noted, however, that the differences between the observed and modelled river chemograph are quite minor compared to the differences between end-member component signatures. This suggests that these calibrations of the UBC model for 1996 and 1997 may actually provide a reasonable breakdown of the hydrograph components with slight errors in routing parameter selection and the orographic enhancement function.

7.3.3 Isotopic Model Optimisation, UBC Model Run 2

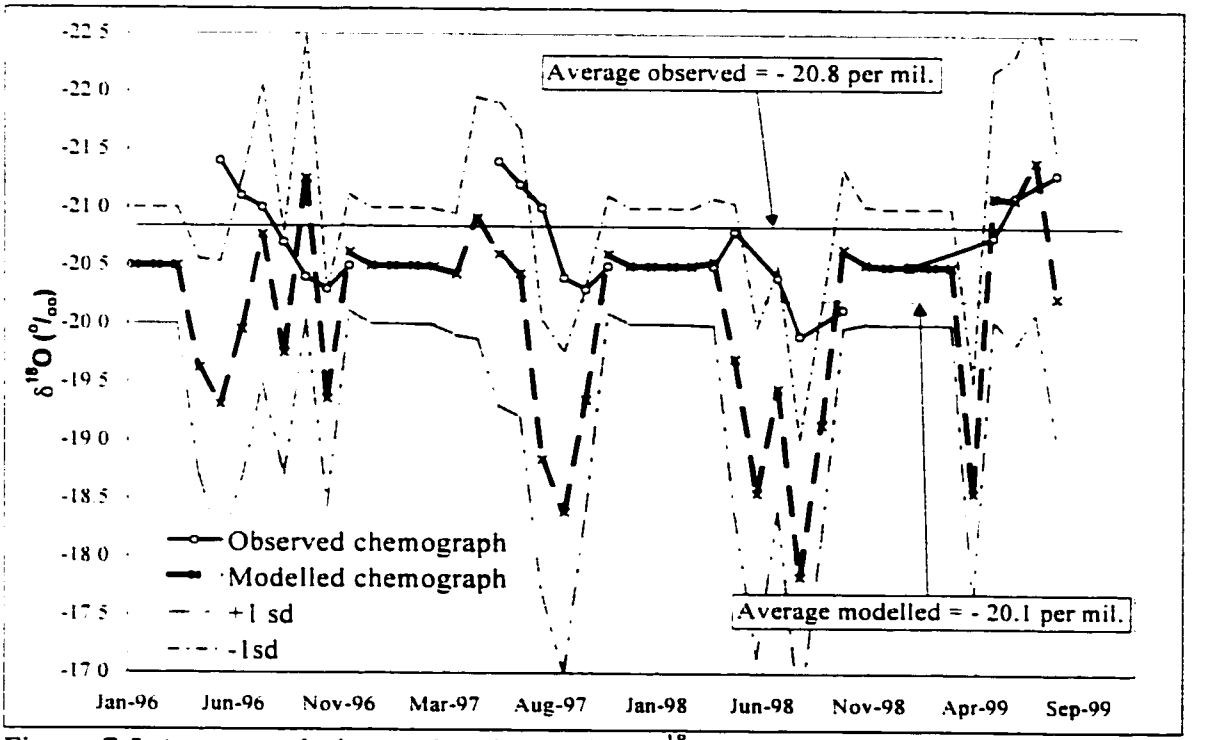

Figure 7.5 Aggregated observed and modelled $\delta^{18}O$ river signature (showing 1 standard deviation of error) for the Bow at Banff, 1996 – 1999 (continuous time series with dynamic end-member signatures).

Combining the dynamic isotope signatures with the first completely optimised continuous UBCWM run from 1996 to 1999 did not provide favourable results (Figure 7.5) despite a reasonable *e!* of 0.83. This exemplifies the difficulty of calibrating a model accurately over a time series for years of very differing hydrological character. The

chemograph of Figure 7.5 was on average 0.7 ‰ too heavy, fluctuated markedly and was frequently outside the standard deviation range. These observations suggest that there was too much rain in the balance and that the modelled response was too rapid.

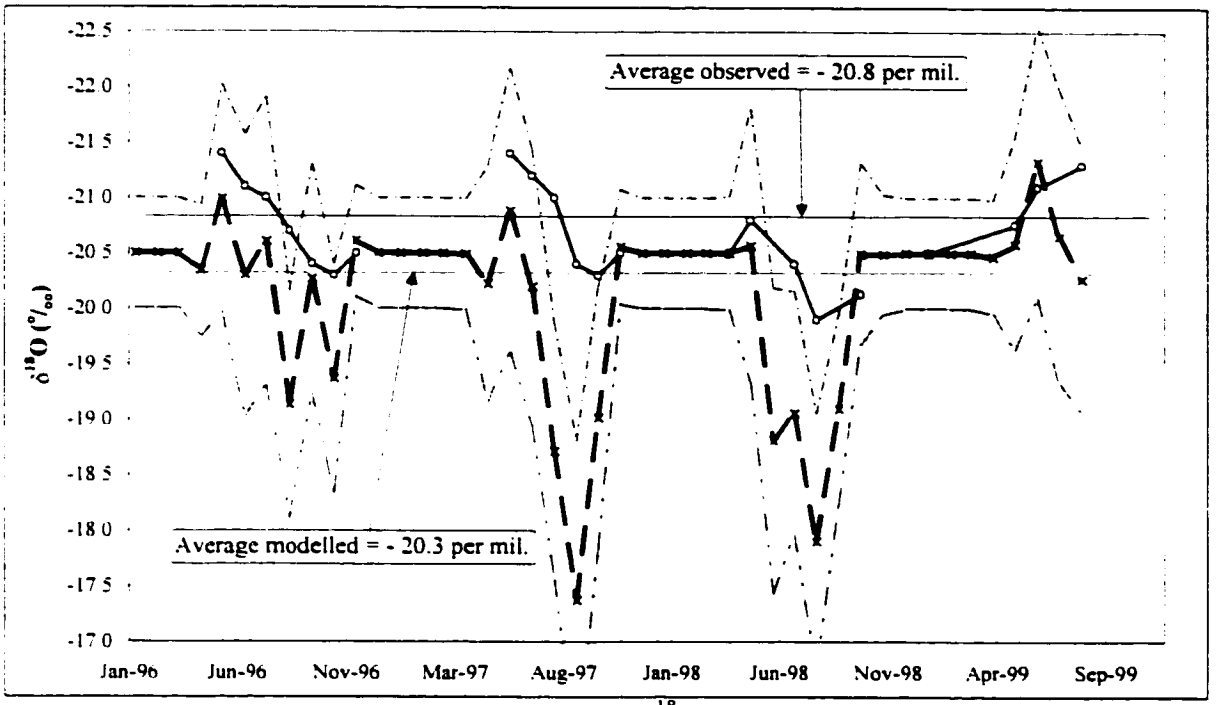

Figure 7.6 Aggregated observed and modelled $\delta^{18}O$ river signature for the Bow at Banff, 1996 – 1999 (following recalibration).

To increase the snowmelt proportion in the balance some of the snowmelt function parameters were altered manually; i.e. the sun exposure factor, albedo decay constant, initial albedo decay, snowfall required to change albedo and water retention in snowpack values were all raised to increase snowmelt runoff. In addition, the precipitation interception fraction value was increased to enhance evaporative loss and reduce the amount of rainfall reaching the ground (see appendix 6.2 for a list of the parameter values and Quick and Pipes (1996) for a discussion of their meaning). The model was then re-optimised, run again and tested in the same way as above. The coefficient of efficiency increased from 0.83 to 0.88 and the chemograph improved slightly (Figure 7.6). The

difference between modelled and observed chemographs dropped to below 0.5 $^{o}/_{oo}$ but the modelled chemograph was still too heavy and variable. A problem with the routing and storage parameters of the model was thought to be the cause of the flashy behaviour but after further optimisation and model simulations, no more improvements in both *e!* and isotope chemograph were achieved. It may have been possible to improve the coefficient of efficiency with further manipulation (particularly of the groundwater storage components) but it is thought that this would have reduced the accuracy of the hydrological balance and therefore the modelled isotope chemograph.

7.4 Concluding Remarks

This chapter has provided valuable insights in two areas:

1) A methodology for hydrological model evaluation and optimisation using oxygen isotope tracers has been demonstrated;
2) Some of the potential problems modelling hydrological processes in mountainous environments over interannual time series containing years of very different hydrological character have been illustrated.

From the first run of the UBC model from 1996 to 1997, it was shown that despite a reasonable statistical fit between observed and modelled data, the predicted hydrological balance was probably in error. The main cause of this error was thought likely to be a volumetric over-estimation of rainfall due to either:

a) an incorrect flow routing parameter and a commensurate underestimation of the loss of the rainfall component due to evapotranspiration or

b) an inability of the model to account for the seasonally varying nature of orographic enhancement patterns in mountainous basins leading to an over-estimation of rainfall at high elevations in the basin during the summer months.

In the cases demonstrated here, it is also believed that too much rainfall was allowed into the balance during optimisation because the total basin snowpack was under-estimated and therefore melted out too quickly.

In this chapter, therefore, it has been demonstrated that hydrological models can be evaluated and parameter optimisation assisted using oxygen isotope data taken from end-member hydrological components and the river being modelled. This kind of evaluation can provide a greater insight into potential errors with model routing and parameter value selection than a simple statistical test of the overall fit between observed and modelled hydrographs. Even a simple approach such as using long-term averages of conservative stable isotope signatures of key flow components can be robust and produce useful results. A more accurate approach is to consider the spatio-temporal variations in these signatures but this may provide only a minimal improvement in the modelled chemograph for the considerable effort involved.

Although the method of this test has been manually intensive and costly, it may sometimes be useful to pursue similar forms of model validation in cases of long-term water resource forecasting to assess the effects of climate and land cover changes. In such studies, it is essential to start off with an accurate estimation of the hydrological balance for current or previous conditions. If the modelled balance were in error during calibration, then it would likely become worse the further into the future the prediction.

Chapter 8 Concluding Summary

8.1 Overview

The two broad questions posed in this thesis were:

1) How do interannual hydrological balance and pathway components vary in complex temperate high mountain environments at various spatio-temporal scales?
2) Is it possible, using dedicated hydrological models, for there to be large errors in the predicted balance for a high mountain basin despite obtaining good recreations of past hydrographs? And, if so, what kinds of errors are encountered, and how are they compensated?

The first question has been investigated in some detail (although not completely) while concentrating on a meso-scale basin and headwater sub-basins within the Canadian Rocky Mountains. Various hydrometric, geochemical and mathematical tools were used in order to discern spatio-temporal dominances of water balance and pathway components. The analysis for this thesis commenced by studying basin water balance input end-members and associated hydrological processes. Properties and variation of basin baseflow characteristics were investigated next. With the dominant controls on, and characteristic properties of, hydrological end-members and baseflow noted, it was then possible to investigate both headwater and basin-wide responses to short-term events and interannual variations in hydrometeorological conditions.

Finally, the second question was addressed in the previous chapter by calibrating the dedicated UBC mountain hydrological model for years of diverse hydrological character and assessing the hydrograph break down. Basin characteristics established in earlier

sections were combined with end-member geochemical properties to test the hydrological divisions within a model calibration using a technique that did not simply assess model output using a statistical approach.

The main findings associated with the above questions are outlined in the chapter summaries below.

8.2 End-members and Basin Baseflow

In Chapters Three and Four, the atmospheric and physiographic controls on geochemical properties for the hydrological end-members of snow, ice, rain and basin baseflow were explored. A summary of the conceptual model describing basin-wide end-member $\delta^{18}O$ patterns is provided in Table 7.1.

Contrary to the body of literature on this subject, elevation was not found to exert a strong controlling influence on $\delta^{18}O$ in either snowpack or rainfall. Limited sampling procedures may be responsible for the lack of strong elevational gradients in these end-members but it is thought likely that turbulent mixing of air masses and redistribution of snowpack within the basin homogenises the basin snow and rain $\delta^{18}O$ patterns. In addition, winter inversion conditions at high elevations within the Bow Basin may act to reduce the "normal" pattern of isotopic depletion with increasing elevation.

Glacial ice tended to have a low variability in overall $\delta^{18}O$ signature across the several locations sampled and when all data were plotted together, there was no strong elevation effect. However, from an earlier study on Peyto Glacier (West, 1972) and more localised sampling in the same area, it was clear that local reverse isotope elevation relationships do occur over glacier surfaces. This reverse elevation effect is a function of

glacial ice dynamics and manifests itself in glacial melt waters by becoming gradually more enriched as the transient snow line approaches the equilibrium line altitude.

Elevational $\delta^{18}O$ depletion was observed, however, in basin-wide baseflow samples from major tributaries during both summer and winter. Much of the literature on this subject implies that such depletion in baseflow is related to the temperature gradients of these environments and, more importantly, reflects the changing isotopic signature evident in precipitation. However, if precipitation does not, in itself, display this elevational depletion then there must be another cause for the pattern observed in baseflow. The observed $\delta^{18}O$ signatures for rain and snow were markedly different and baseflow always displayed a value between these two extremes. Therefore, the elevational $\delta^{18}O$ gradient in baseflow is thought not directly related to a similar gradient in precipitation but rather the changing mixing ratio of rain to snow as basin elevation increases.

This changing ratio of snow to rain (or older, more enriched groundwater) is also reflected in the temporal variability in groundwater baseflow $\delta^{18}O$ patterns. During winter, when basin temperatures are coldest, groundwater baseflow tends to display its most enriched annual signature (at least during "average" hydrometeorological years with deep snowpack conditions). During August, when temperatures are near maximum, groundwater baseflow tends to display its most depleted $\delta^{18}O$ signature and reflects earlier snowmelt inputs. This suggests that there is generally a time lag from both spring melt and late summer rainfall infiltration to subsequent groundwater baseflow of approximately four months. This could be thought of as the "average" basin baseflow response time.

Of particular interest is that at all elevations and during the entire year, baseflow and groundwater $\delta^{18}O$ signatures were much closer to snow melt than rain, with average mixing ratios exceeding 85% snow (90% in the headwaters). Snow is known to be the dominant hydrological component in the Bow Valley but if local hydrometric data and precipitation gradients alone were used to estimate the relative contributions to annual baseflow, the rainfall proportion would be estimated to be higher (~25 % in the headwaters). From these observations, it may be concluded that rainfall either runs off rapidly and does not percolate to basin-wide groundwater, or some time after such events much of the volume is lost to evapotranspiration.

Other potential sinks of event water were found in the headwaters but these sinks could not keep rainfall out of the balance indefinitely. Karst areas in the headwaters of Mosquito Creek were found to have relatively high areal yields year round and were thought to provide a large potential storage medium.

8.3 Headwater Hydrological Processes

In Chapter Five an attempt was made to compare some of the main controlling influences on hydrological processes within glacierised and non-glacierised headwater basins of the Canadian Rockies during two years of different snowpack conditions. The influence of headwater lakes on the downstream $\delta^{18}O$ signature in the river was also examined.

Areal yield varied dramatically between glacierised and non-glacierised basins in the Bow Valley. The glacierised Bow Creek Basin yielded several times more water volume than the neighbouring Mosquito Creek during both deep and shallow snowpack years. However, the inter-relationships between snowpack and basin yield were opposed for

both basins; deeper snowpack led to increased yield on Mosquito Creek but the reverse on Bow Creek. This was largely due to the lengthening of the ice melt period facilitated by early melt out of the shallow snowpack. The change in yield experienced on Mosquito Creek was low considering the large difference in precipitation for these two years and suggests that some form of flow regulation was in effect. It is speculated that if flow regulation occurred, it may have been related to either: a) headwater karst areas acting as groundwater storage reservoirs; b) temporary losses of water from upper basin streams resulting from convexities in valley profiles, low water tables, hyporheic flows, or large-scale bypass flow through fault lines; or c) melt runoff augmentation from small glacier areas in the headwaters during warm and dry years.

Annual and diurnal cycles naturally dominate the hydrographs in snow covered mountainous basins. Diurnal cycles are strongest in the headwaters for glacierised basins during shallow snowpack years. However, of particular interest is that during a year of relatively deep snowpack, when melt processes were still the dominant hydrological input in the headwaters, the diurnal signal strength in the hydrograph was surpassed by recurrent cycles associated with synoptic scale events. Thus, in glacierised basins it would appear that temporal variability within the hydrograph is largely a function of basin snowpack depth.

Landcover and snow depth influences on interannual hydrological balance and pathways were investigated by comparing the geochemical signatures for the two basins over the years of deep and shallow snowpack. In general, the geochemical signals of EC, TU and $\delta^{18}O$ displayed similar seasonal patterns on both basins, indicating that

hydroclimatic conditions are the dominant control on mountain basin geochemistry. However, there were noticeable differences that could be attributed to glacier coverage.

Compared to the non-glacierised Mosquito Creek Basin, the highly glacierised Bow Creek differed in that: i) $\delta^{18}O$ was more enriched due to increased icemelt and rainfall contributions; and ii) $\delta^{18}O$ appeared to have a smoother seasonal trace due to the more gradual rise in transient snow line elevation and the related increase in ice exposure. This lack of short-term variability in the glacierised basin's seasonal $\delta^{18}O$ pattern was also reflected in a late summer diurnal glacier melt event, thus indicating that even though there is a rapid response to melt inputs in these basins, the actual event water is likely well mixed due to temporary glacial storage. In addition, EC and tritium values had larger seasonal ranges in the glacierised basin due to extreme fluctuations in baseflow dilution from ice melt that varied from ancient (zero TU) to relatively recent (elevated TU) origin.

At a finer temporal resolution, the changing dominance of hydrological flow components within the headwater basins was studied during major melt and rainfall events. During both rainfall and snowmelt events, a significant proportion of event runoff was found to be old baseflow water routed through the ground. The two types of event differed enormously, however, in terms of the amount of new event water actually present in runoff. For an early snowmelt event in May 1999, new snowmelt was readily apparent in the event hydrograph but for a large rainfall event in August 1998, there was little evidence of new water in the hydrograph. However, it is thought that the actual presence of rainfall in the hydrograph could have been masked by: a) old water being shunted out from high elevation storage zones such as may be found in karst terrain; and b) temporary losses to groundwater storage due to dry antecedent basin conditions.

By studying the Bow Lake input and output geochemistry over the two-year time period, the modifying influence of lakes on headwater events was investigated. It was found that relatively large lakes in the centre of the main valley induce a temporal lag of several days in the summer and up to several weeks to months in the winter. There is, however, no significant change in the $\delta^{18}O$ signature but a modified level of dissolved solids does occur probably due to lengthened residence times and within lake dissolution of highly sediment laden glacial runoff.

8.4 Landcover and Elevation Influences on Basin Hydrology

At the larger basin scale of the Bow River above Banff and Lake Louise, the differences between basins are less obvious, events are superimposed and become indistinguishable, and it is difficult to discern the influences of landcover and elevation on the hydrograph. In Chapter Six these issues were explored at three scales: the headwaters (< 40 km^2); the intermediate basin scale at Lake Louise (< 500 km^2); and at Banff (> 2000 km^2). For the two smaller basin scales, paired catchments of differing glacier coverages were investigated.

The interannual baseflow areal yields were compared at all three scales and it was found that the yield was approximately 50% greater at Lake Louise basin end-points than either the headwaters or at Banff. After examining the longitudinal Bow River Valley profile it was found that Lake Louise occupies a dip in the slope and it is thought that yields could be enhanced in this approximate location during annual baseflow due to increased regional groundwater discharge.

By assessing the relative yields for each of the basins during deep and shallow snowpack years, it was found that the influence of interannual snowpack conditions was

minimised when basin glacial coverage was approximately 10%. For basins with less glacial coverage, there was a positive correlation between snowpack depth and runoff yield but for basins with greater glacier coverage there was an inverse relationship. In addition, for basins with similar glacier coverage proportions, the yield tended to increase linearly with both average basin elevation and diminishing size.

Moving from headwaters to the basin outlet at Banff, there was naturally a tendency for events to become more subdued as contributing area increased. However, diurnal cycles associated with snow and glacier melt were evident at all basin outlets. Interestingly, these diurnal cycles were also strongly evident downstream of large lakes within the basins and exemplify the rapid basin-wide response to such events. In addition, the isotope chemograph for all basins tended to be close to snow and icemelt year round.

Rainfall, on the other hand, was not strongly evident either in geochemical or event responses within basin runoff at any of the scales studied. As would be expected, rainfall responses at larger basin scales were subdued following dry antecedent conditions but were enhanced if other events had occurred recently. Compared to diurnal melt events, the general response to widespread rainfall in the basin was small (although certainly discernible at all scales) and suggests that rainfall probably stays within basin storage for some time, rather than rapidly running off into stream channels, as may be expected in high mountainous environments. Such storages of rainfall could be snowpack, vegetation canopies and groundwater. It is felt that temporary storage of rainfall in groundwater and vegetated areas during the summer leads to the preferential loss of this hydrological balance component to evapotranspiration. Conversely, the reduced opportunity for such storage in glacierised basins leads to an enhanced runoff response to rainfall events and

probably an overall increase in the amount of rainfall draining glacierised basins. (Drainage from the glacierised headwaters and for the Bow River at Lake Louise was found to be more rapid than other basins with less glacier cover, where more of the runoff would be expected to be groundwater routed.)

8.5 Hydrological Model Evaluation

Using the findings of earlier sections of the thesis, the UBC Watershed Model was calibrated and run for 1996 and 1997 independently and then run again for a continuous four year time period (1996 to 1999). Using the conservative $\delta^{18}O$ tracer to characterise each of the model end-members of snow, rain, ice and deep groundwater baseflow, isotope chemographs were generated which could be compared to actual river isotope signatures for the Bow River at Banff. The technique was found to be a useful method of assessing the calibration accuracy of a hydrological model by testing the modelled hydrological flow components rather than simply the overall statistical fit between modelled and observed hydrographs.

For all model calibrations it was found that the snowmelt component of the hydrological balance was underestimated and this was compensated for by an overestimation of rain inputs. Manually increasing these snowmelt inputs reduced the overall coefficient of efficiency. Considering the earlier findings that rainfall appears to be a generally minor component of annual runoff despite hydrometric observations that might indicate otherwise, it is felt that there may be a conceptual misunderstanding of the importance of rainfall contributions to runoff in mountainous basins. Rainfall occurs during summer months and is the most susceptible of all hydrological components to evapotranspiration losses. However, rain, snow and ice are not separated from one

another in many modelled evaporation routines and this may be part of the cause for systematic overestimations of rainfall in the balance. In addition, there is without doubt a gross simplification of seasonal orographic enhancement, glacial melt volumes, storage and runoff processes within this model and many others, and so any underestimation of particular components will systematically be compensated for during model optimisation.

8.6 Summary

Variations in climate and ground cover have a marked impact on river flow in high mountain regions. Water resource managers in these areas are aware that continued climate warming and glacial recession have a marked and often detrimental impact on river flow. In order to investigate the potential magnitudes and timing of hydrological variations due to climatic and land cover changes, it is becoming standard practice to perform some kind of impact assessment. This procedure typically involves calibrating a hydrological model "off the shelf" for today's conditions and running it into the future with possible future climatic and landcover scenarios. This study has illustrated that this can be problematic in mountainous regions where it is difficult to accurately simulate changing hydrological conditions even for today. Using tracer studies, it has been found that although models can simulate past and present river flow to a reasonable level of accuracy, the breakdown of the river flow into its contributing hydrological components (such as snow melt, rainfall and glacial melt) may be in error. These errors would inevitably be magnified if such model calibrations were then used in simulations of future conditions for impact assessment purposes. Complimentary hydrometric and tracer studies to assist modelling efforts, therefore, offer a means to minimise these errors in the initial model development and calibration stage of such impact assessments.

References

Alberta Environmental Protection, 2000. *Snow Survey Report for the Bow River Basin, Alberta, Canada.* Provided by Dick Allison of Alberta Environmental Protection.

Anderson, M.G., Burt, T.P. Subsurface runoff in: Anderson, M.G., Burt, T.P. (eds.), 1990. *Process Studies in Hillslope Hydrology.* John Wiley and Sons Ltd. Chichester. 365-400

Appelo, C., Becht, R., Van De Griend, A., Spierings, T., 1983. Build of discharge along the course of a mountain stream deduced from water quality routings. *J. Hydrol.* **66,** 305-318.

Aston, A.R., 1979. Rainfall interception by eight small trees. *J. Hydrol.* **42**, 383-396.

Atlas of Alberta, 1969. University of Alberta Press, Edmonton Alberta, 158 pages.

Bailey, W. G., Saunders, I.R., Bowers, J.D., 1990. Atmosphere and surface control on evaporation from alpine tundra in the Canadian Cordillera. *IAHS Publ.* **193,** 45-52.

Ball,J., Trudgill,S., 1997. Potentials and limitations in using geochemical tracers. *IAHS Publ.* **244**. 185-194.

Barnes, C.J., Allison, G.B., Hughes, M.W., 1989. Temperature gradient effects on stable isotope and chloride profiles in dry soils. *J. Hydrol.* **112,** 69-87.

Barrie, L.A., Hales, J.M., 1984. The spatial distribution of precipitation acidity and major ion wet deposition in North America during 1980. *Tellus,* **36 B,** 333-355.

Barry, R., 1979. High altitude Climates. In: Webber, P.J., (ed.) *High Altitude Geoecology.* AAAS selected symposium 12. Westview Press, Inc. 55-74.

Barry, R.G. 1992. *Mountain Weather and Climate.* (2nd edn), Routledge, London, 402 pp

Becker, A., McDonnell, J.J. 1998. Topographical and ecological controls of runoff generation and lateral flows in mountain catchments. *IAHS Publ.* **248**. 199-206.

Behrens, H., Bergman, H., Moser, H., Rauert, W., Stichler, W., Ambach, W., Eisner, H., Pessel, H., 1975. Study of the discharge of alpine glaciers by means of environmental isotopes and dye tracers. *IAHS Publ.* **104**, 219-224.

Billelo, M.A. 1967. *Water Temperatures in a Shallow Lake During Ice Formation, Growth and Decay.* Cold Regions Research and Engineering Laboratory report No. 213. Hanover, New Hampshire, 22pp

Braun, L.N., Aellen, M. 1990. Modelling discharge of glacierised basins assisted by direct measurements of glacier mass balance. In: *Hydrology in Mountainous Basins. IAHS Publ.* **193**. 99-106

Brimblecombe, P., Tranter, M., Abrahams, P.W., Blackwood, I., Davies, T.D., Vincent, C., 1985. Relocation and preferential elution of acidic solute through the snowpack of a small, remote high altitude Scottish catchment. *Ann. Glaciol.* **7**, 141-147.

Brown, G.H., Tranter, M., 1990. Hydrograph and chemograph separation of bulk meltwaters draining the upper Arolla Glacier, Valais, Switzerland. *IAHS Publ.* **193,** 429-437.

Burn, C.R., 1991. Snowmelt infiltration into frozen soil at sites in the discontinuous permafrost zone near Mayo, Yukon Territory. In: Prowse, T.D., Ommanney, C.S.L., (eds.) 1991. *Northern Hydrology. Selected Perspectives.* NHRI symposium no. 6. Environment Canada, Saskatchewan. 446-457.

Burrus, C. S., Gopinath, R. A., Guo, H., *Introduction to Wavelets and Wavelet Transforms: A Primer*. Prentice Hall: New Jersey, 1998. 268 pp.

Caine, N., 1989. Hydrograph separation in a small alpine basin based on inorganic solute concentrations. *J. Hydrol.* **112,** 89-101.

Chapman, P., Reynolds, B., Wheater, H., 1993. Hydrochemical changes along storm pathways in a small moorland headwater catchment in Mid-Wales, UK. *J. Hydrol.* **151**, 241-265.

Christophersen, N. Neal, C. Hooper, R.P. Vogt, R.D. Andersen, S. 1990. Modelling streamwater chemistry as a mixture of soil water end-members - A step towards second-generation acidification models. *J. Hydrol.*, **116**, 307-320.

Clark, I., Fritz, P., 1997, *Environmental Isotopes in Hydrogeology*. Lewis Publishers, New York.

Cline, D. 1995. Snow surface energy exchanges and snowmelt at a continental alpine site. *IAHS Publ.* **228**. 157-166.

Clow, D.W., Mast, A. 1995. Composition of precipitation, bulk deposition and runoff at a granitic bedrock catchment in the Loch Vale Watershed, Colorado. *IAHS Publ.* **228**. 235-242.

Collier, E.P. 1958. Glacier variation and trends in runoff in the Canadian Cordillera. IAHS Publ. No. **46**, 344-357.

Collins, D.N., 1982. Water storage in an alpine glacier. *IAHS publ.* **138,** 113-122.

Collins, D.N., 1995. Daily patterns of discharge, solute content and solute flux in meltwaters draining from two alpine glaciers. *IAHS Publ.* **228**. 371-378.

Collins, D.N., Young, G.J. 1979. Hydrochemical separation of components of discharge in alpine catchments. In: *Proceedings of the Western Snow Conference, Reno, Nevada, 18-20 April, 1979*. pages 1-9.

Dansgaard, W., 1964. Stable isotopes in precipitation. *Tellus*. **16**, 436-68.

Davies, R.E., Petersen, C.E., Bales, R.C., 1995. Ion flux through a shallow snowpack: effects of initial conditions and melt sequences. *IAHS Publ.* **228**. 115-127.

Davies, T.D., Vincent, C., Brimblecombe, P., 1982. Preferential elution of strong acids from a Norwegian ice cap. *Nature*. **300**, 161-163.

Demuth, M.N., Pietroniro, A. 1999. Inferring glacier mass balance using Radarsat: Results from Peyto Glacier, Canada. *Geografiska Annaler*, **81 A**, 521-540.

Djorovic, M., Kadovic, R., Macan, G., Letic, L., 1997. Precipitation and inorganic chemicals in beech stand at the mountain GOC, Serbia. In: Molnar, L., Miklanek, P., Meszaros, (eds.). *Developments in Mountain Hydrology* Proc. Stara Lesna Conference, 12-16 Sept. 1994, IHP, Paris.

Ellins, K.K., Roman-Mas, A., Lee, R., 1990. Using ^{222}Rn to examine groundwater surface discharge interaction in the Rio Grande de Manati, Puerto Rico. *J. Hydrol.* **115**, 319-341.

Elliston, G.R. 1973. Water Movement Through Gornergletscher. *Symposium on the Hydrology of Glaciers. IAHS Publ.* **95,** 79-84.

Environment Canada, 1978, *Hydrological Atlas of Canada*. Surveys and Mapping Branch, Department of Energy, Mines and Resources. 34 Map sheets.

Environment Canada, 1990, *Historical Streamflow Summary, Alberta*. Inland Waters Directorate, Water Resources Branch, Water Survey of Canada, Ottawa, Canada, 629pp.

Fernald, A.G., Wigington, P.J., Landers, D.H., 2001, Transient storage and hyporheic flow along the Willamette River, Oregon: field measurements and model estimates. *Water Resour. Res.* **37**, 1681-1694.

Ford, D.C. 1971, Characteristics of limestone solution in the Southern Rocky Mountains and Selkirk Mountains, Alberta and British Columbia. *Can. J. Earth Sci.* **8**, 585-609.

Forster, C., Smith, L., 1988, Groundwater flow systems in mountainous terrain 2. Controlling factors. *Water Resour. Res.* **24**, 1011-1023.

Fountain, A., Tangborn, W. 1985a, The Effects of Glaciers on Streamflow Variations. *Water Resour. Res.*, **21**, 579-586.

Fountain, A., Tangborn, W. 1985, Overview of contemporary techniques. In: G.J. Young (ed.) *Techniques for the Prediction of Runoff from Glacierised Areas. IAHS publ.* **149**, 27-41.

Fountain, A.G., 1996, Effect of snow and firn hydrology on the physical and chemical characteristics of glacial runoff. *Hydrol. Proc.* **10**, 509-521.

Fritz, P., 1981. River waters. In: Gat, J.R, Gonfiantini, R., (eds), *Stable Isotope Hydrology: D and ^{18}O in the water cycle.* IAEA, Vienna, Tech. Rep. Ser., No. 210, (177-199), 302pp

Furrer, G., Fitze, P., 1970, Treatise on the Permafrost problem in the Alps. *Viertljahrsschrift der Naturforscenden Gesellschaft in Zurich*, **115**, 353-368. (Translated by D.A. Sinclair, National Library, Ottawa.)

Gabert, G.M., 1986, *Alberta Groundwater Observation Well Network.* Alberta Research Council, Edmonton.

Gadd, B. 1995, *Handbook of the Canadian Rockies* (2nd ed.) Corax Press, Alberta, 831pp.

Gamage, N., W. Blumen, 1993. Comparative analysis of low-level cold fronts: Wavelet, Fourier, and empirical orthogonal function decompositions. *Monthly Weather Review.* **21**, 2867-2878.

Gaspar, E., 1987, *Modern Trends in Tracer Hydrology vol. 1.* CRC Press, Boca Raton, Florida.

Gat, J.R. 1981. Lakes. In: Gat, J.R., Gonfiantini, R., (eds), *Stable Isotope Hydrology, Deuterium and Oxygen in the Water Cycle.* IAEA, Vienna, Tech. Rep. Ser., No. 210, (203-221) 302pp.

Gehrels, J.C., Peeters, J.E.M., De Vries, J.J., Dekkers, M., 1998, The mechanism of soil water movement as inferred from ^{18}O stable isotope studies. *Hydro Sci. Jnl.* **43**, 579-594.

Gibson, J.J., Reid, R., Spence, C. 1998, A six year isotope record of lake evaporation a mine site in the Canadian Sub-arctic: results and validation. *Hydrol. Proc.* **12**, 1779-1792.

Glen, J.W. 1955, The creep of polycrystalline ice. *Proc. R. Soc.* **A 228**, 519-538.

Grasby, S.E. 1997, *Controls on the Chemistry of the Bow River, Southern Alberta, Canada.* Unpubl. Ph.D. thesis, University of Calgary, Alberta. 140 pp.

Grasby, S.E., Hutcheon, I., McFarland, L., 1999, Surface-water-groundwater interaction and the influence of ion exchange reactions on river chemistry. *Geology*, **27**, 223-226.

Gray, D.M., 1970, *Principles of Hydrology.* National Research Council of Canada, Ottawa.

Gray, D.M. and Male, D.H. 1981, *Handbook of Snow.* Pergamon Press, Toronto. 776pp.

Grunow, J., Tollner, H., 1969. Nebelniederschlag im hochgebirge, *Arch. Met. Geophys. Biokl.* **B, 17,** 201-28.

Gubler, H., Rychetnik, J., 1991, Effects of forests near the timberline on avalanche formation. *IAHS Publ.* **205.** 19-37.

Gurnell, A.M., 1993, How many reservoirs? An analysis of flow recessions from a glacier basin. *Jnl Glaciol.* **39,** (132).

Hall, F.R., 1968, Baseflow recessions – a review, *Wat. Res. Rsrch.* **4,** 973-983

Hannah, D. M., Smith, P. B. G., Gurnell, A. M., McGregor, G. R., 2000, An approach to hydrograph classification, *Hydrol. Proc.* **14,** 317-338.

Harrison, R.M., de Mora, S.J., Rapsomanikis, S., Johnston, W.R., 1993, *Introductory Chemistry for the Environmental Sciences.* Cambridge University Press. 354 pp.

Harvey, J.D., Bencala, K.E., 1993, The effect of stream bed topography on surface-subsurface water exchange in mountain catchments. *Water Resour. Res.* **29,** 89-98.

Henoch, W.E.S. 1971, Estimate of glaciers' secular change (1948-1966) volumetric change and its contribution to the discharge in the upper North Saskatchewan River Basin. *J. Hydrol.* **12,** 145-160.

Hewitt, K. 1989, The altitudinal organisation of Karakoram geomorphic and depositional environments, *Z. Geomorph.* **76,** 9-32.

Hewlett, J.D. 1961, *Watershed management,* Report for 1961, South Eastern Forest Experimental Station, US Forest Service, Asheville, North Carolina.

Hillel, D., 1982, *Introduction to soil physics,* Academic Press, New York. 364pp

Hinton, M.J., Schiff, S.L., English, M.C., 1993, Physical properties governing groundwater flow in a glacial till catchment. *J. Hydrol.* **142,** 229-249.

Holko, L., 1997. Variations of deuterium and O-18 in precipitation and snow cover in the Jalovecy Creek catchment. In: Molnar, L., Miklanek, P. and Meszaros, (eds.). *Developments in Mountain Hydrology* Proc. Stara Lesna Conference, 12-16 Sept. 1994, IHP, Paris

Hooper, R.P., Aulenbach, B.T., Burns, D.A., McDonnell, J.J., Freer, J., Kendall, C., Beven, K. 1998, Riparian control of stream water chemistry: Implications for hydrochemical basin models. *IAHS Publ.* **248**. 451-458.

Hooper, R.P., Christopherson, N., Peters, N.E., 1990, Modelling of stream water chemistry as a mixture of soilwater end members - An application to the Panola mountain catchment, Georgia, USA. *J. Hydrol.* **116**, 321-343.

Hopkinson, C., Young, G.J. 1998, The effect of glacier wastage on the flow of the Bow River. *Hydrol. Proc.*, **12**, 1745-1763.

Hudson, R.O., Golding, D.L., 1997, Controls on groundwater chemistry in subalpine catchments in the southern interior of British Columbia. *J. Hydrol.* **201,** 1-20.

Hudson, R.O., Golding, D.L., 1998, Snowpack chemistry during snow accumulation and melt in mature subalpine forest and regenerating clear cut in the southern interior of BC. *Nordic Hydrol.* **29,** 221-244.

Hudson R.O., Quick, A. 1997, A component based water chemistry simulator for small subalpine watershed. *Canadian Water Res. Jnl.* **22**, 299-324

Hutchinson, G.E. 1957. *A Treatise on Limnology.* (Vol. 1), John Wiley and Sons, New York, 1015pp.

Hayakawa, M., N. 1998, *Snow and Ice Science in Hydrology.* IHP Training Course on Snow Hydrology, UNESCO.

Iken, A. 1977. Variations of surface velocities on some Alpine glaciers at intervals of a few hours. Comparison with Arctic glaciers. *Zeit. Gletch. Glaziol* **13.** 23-25

Intergovernmental Panel on Climate Change, 2001, *Climate Change 2001: The Scientific Basis Contribution of Working Group I to the Third Assessment Report of the Intergovernmental Panel on Climate Change*, J. T. Houghton, Y. Ding, D.J. Griggs, M. Noguer, P. J. van der Linden, D. Xiaosu (eds.), Cambridge University Press, UK. 944pp

Johannessen, M., Henriksen, A., 1978, Chemistry of snowmelt water: changes in concentration during melting. *Water Resour. Res.* **14,** 615-619.

Kendall, C., McDonnell, J.J., 1993, Effect of intrastorm isotopic heterogeneities of rainfall, soil water and groundwater on runoff modelling. *IAHS publ.* **215**. 41 - 48.

Kirnbauer, R., Haas, P. 1998, Observations on runoff generation mechanisms in small Alpine catchments. *IAHS Publ.* **248**. 239-248.

Kite, G., Kouwen, N. 1992, "Watershed modelling using land classifications". *Wat. Resour. Res.* **28**, 3193-3200.

Kite, G.W.1999, *Manual for the SLURP Hydrological Model*, National Hydrological Research Institute, Saskatoon.

Klemeš, V. 2000, *Common Sense and Other Heresies – Selected Papers on Hydrology and Water Resources Engineering*. Edited by David Sellars, Canadian Water Resources Association, 378pp.

Kuhn, M., 1993, Methods of assessing the effects of climate change on snow and glacier hydrology. In *Snow and Glacier Hydrology, IAHS Publ.* **218.**

Laudon, H., Slaymaker, O., 1997, Hydrograph separation using stable isotopes, silica and electrical conductivity: an alpine example. *J. Hydrol.* **201**, 82-101.

Leith, R.M.M., Whitfield, P.H., 1998. Evidence of climate change effects on the hydrology of streams in South Central BC. *Can. Water. Resour. Jnl.* **23**, 219-230.

Linacre, E., 1992, *Climate Data and Resources*. Routledge, London. 366pp

Maloszewski, P., Rauert, W., Stichler, W., Herrman, A., 1983, Application of flow models in an alpine catchment area using tritium and deuterium data. *J. Hydrol.*, **66**, 319-30.

Maloszewski, P., Rauert, W., Trimborn, P., Herrman, A., Rau, R., 1992, Isotope hydrological study of mean transit times in an alpine basin (Wimbachtal Germany). *J. Hydrol.* **140**, 343-360.

Marchetto, A., Barbieri, A., Mosello, R., Tartari, G.A., 1994, Acidification and weathering processes in high mountain lakes in Southern Alps. *Hydrobiologia*, **274,** 75-81.

Mast, A., Kendall, C., Campbell, D.H., Clow, D.W., Back, J. 1995, Determination of hydrologic pathways in an alpine-subalpine basin using isotopic and chemical tracers, Loch Vale watershed, Colorado, USA. *IAHS Publ.* **228**. 263-270.

Maule, C.P., Stein, J., 1990, Hydrologic flow path definition and partitioning of spring meltwater. *Water Resour. Res.* **26**, 2959-2970.

McDonnell, J. J., Stewart, M.K., Owens, I.F., 1991, Effect of catchment scale subsurface mixing on stream isotopic response. *Water Resour. Res.* **27,** 3065-3073.

Meek, V. 1948, Glacier observations in the Canadian Cordillera. *IASH Publ.* **30**, 264-275.

Meier, M. 1973. Hydraulics and hydrology of glaciers. In: *The Role of Snow and Ice in Hydrology*. IAHS publication **107**, 353-370.

Meier, M.F. 1969. Glaciers and water supply. In: *J. Amer. Water Works Assoc.*, **61**, 8-13.

Menzel, L., Lang, H. 1998. Spatial variation in evapotranspiration in Swiss Alpine regions. . *IAHS Publ.* **248**. 115-121

Meyboom, P., 1961. Estimating groundwater recharge from stream hydrographs. *J. Geophys. Res.* **66**, 1203-1214.

Meyers, S. D., B. G. Kelly, J. J. O'Brien, 1993. An introduction to wavelet analysis in oceanography and meteorology: With application to the dispersion of Yanai waves. *Monthly Weather Review.* **121,** 2858-2866.

Miller, E.K., Carson, C.D., Friedland, A.J., Blum, J.D., 1995. Chemical and isotopic tracers of snowmelt flowpaths in a subalpine watershed. *IAHS Publ.* **228,** 349-353.

Misiti, M., Y. Misiti, G. Oppenheim, J. M. Poggi: Wavelet Toolbox: For Use With MATLAB. Massachusetts : The Mathworks Inc. 1997.

Moeri, T., Leibundgut, C. 1986. Winter dye tracer experiments on the Findelengletscher. *Zeit. Gletch. Glaziol.* **22.** 33-41.

Moore, R.D., 1993. Application of a conceptual streamflow model in a glacierised drainage basin. *J. Hydrol.* **150**, 151-168

Moore, R.D., 1997. Storage-outflow modelling of streamflow recessions, with application to a shallow-soil forested catchment, *J. Hydrol.* **198,** 260-270.

Moser, H., Stichler, W., 1974. Deuterium and oxygen-18 contents as an index of the properties of snow covers. *IAHS Publ.* **114,** 122-135.

Newson, M. 1994. *Hydrology and the River Environment.* Oxford University Press, 221pp

Nye, J.F. 1957. The distribution of stress and velocity in glaciers and ice sheets. *Proc. R. Soc.* A **239,** 113-133.

Obled, Ch. 1990. Hydrological modelling in regions of rugged relief. *IAHS Publ.* **193,** 599-613.

Oke, T. 1995. *Boundary Layer Climates.* (2nd edn), Routledge, London, 435pp.

Østrem, G. 1959. Ice melting under a thin layer of moraine, and the existence of ice cores in moraine ridges. *Geogr. Ann.* **41**, 228-230.

Østrem, G. 1966. The height of the glaciation limit in Southern British Columbia and Alberta. *Geografiska Annaler.* **48A.** 126-138.

Ozeray, G.F., Barnes, R., 1978. *Hydrogeology of the Calgary Golden Area.* Alberta Research Council, Edmonton.

Pearce, A.J., Stewart, M.K., Sklash, M.G., 1986, Storm runoff generation in humid headwater catchments, I: Where does the water come from? *Water Resour. Res* **22,** 1263-72.

Peschke, G., Miegel, K., Etzenberg, C., Hebentanz, H., 1990, On the spatial variability of hydrologic processes in a small mountainous basin. *IAHS Publ.* **193,** 61-69.

Peters, N. E., Ratcliffe, E.B., 1997. Tracing hydrologic pathways at the Panola Research Watershed, Georgia, USA. *IAHS Publ.* **244,** 275-289.

Pinder, G.F., Jones, J.F. 1969. Determination of the groundwater component of peak discharge from the chemistry of total runoff. *Water Resour. Res.* **5**, 438-445.

Polikar, R. 1996. *The engineer's ultimate guide to wavelet analysis.* Available online from the World Wide Web http://www.public.iastate.edu/~rpolikar/WAVELETS/waveletindex.html (last accessed December 9th, 2001).

Pomeroy, J.W., Gray, D.M. 1995, *Snowcover: accumulation, relocation and management.* NHRI science report no. 7. Environment Canada, Saskatoon. 134pp.
Quick, M.C., Pipes, A. 1977, U.B.C. Watershed Model, *Hydrol. Sci.* **22**, 153-161.
Quick, M.C., Pipes, A. 1996, *Manual of the U.B.C. Watershed Model*, version 4.
Raben, P., Theakstone, W.H. 1995, Changes of ionic and oxygen isotopic composition of the snowpack at the glacier Austre Okstindbreen, Norway, 1998. *Nordic Hydrol.* **29,** 1-20
Reid, H.F. 1896, The Mechanics of Glaciers. *J. Glaciol.* **4**. 912
Research Systems Inc. 2001, *Interactive Wavelets.* http://ion.researchsystems.com/cgi-bin/ion-p?page=wavelet.ion (accessed June 13th, 2001).
Rodhe, A., 1981, Spring flood: meltwater or groundwater? *Nord. Hydrol.*, **12,** 21-30.
Saunders, I.R., Bailey, W. G., 1990, Evaluation of evaporation models for alpine tundra, British Columbia, Canada. *IAHS Publ.* **193,** 71-78
Schotterer, U., Oldfield, F., Frohlich, K., 1996, *Global Network for Isotopes in Precipitation.* IAEA, Bern, Switzerland. 47pp
Shanley, J.B., Kendall, C., Albert, M.A., Hardy, J.P., 1995, Chemical and isotopic evolution of a layered eastern US snowpack and its relation to stream water composition. *IAHS Publ.* **228**. 329-338.
Sirin, A., Kohler, S., Bishop, K. 1998 Resolving flow pathways and geochemistry in a headwater forested wetland with multiple tracers. *IAHS Publ.* **248**. 336-342.
Sklash, M.G., Farvolden, R.N., 1979, The role of groundwater in storm runoff. *J. Hydrol.* **43,** 45-65.
Sklash, M.G., Farvolden, R.N., 1982, The use of environmental isotopes in the study of high runoff episodes in streams. In Perry, E.C., Montgomery, C.W., (eds.) *Isotope Studies of Hydrological Processes,* Northern Illinois University Press, Dekalb, Illinois, 65-74.
Smart, C.C., Ford, D.C., 1986, Structure and function of a conduit aquifer. *Can. J. Earth Sci.* **23**, 919-929.
Smart, C.C., 1988, Quantitative tracing of the Maligne Karst System, Alberta, Canada. *J. Hydrol.* **98,** 185-204.
Smart, C., Owens, I. F., Lawson, W., Morris, A. L., 2000, Exceptional ablation arising from rainfall-induced slushflows: Brewster Glacier, New Zealand. *Hydrol Proc.* **14,** 1045-1052.
Smith, L.C., Turcotte, D.L., Isacks, B.C., 1998 Stream flow characterisation and feature detection using a discrete wavelet transform. *Hydrol. Processes.* **12,** 233-249.
Smith, N.D. 1981. The effect of changing sediment supply on sedimentation in a glacier-fed lake. *Arctic and Alpine Res.* **13**, 75-82.
Smith, N.D., Vendl, M.A., Kennedy, S.K., 1982. Comparison of sedimentation regimes in four glacier-fed lakes of western Alberta. In - *Research in Glacial, Glacio-fluvial and Glacio-lacustrine systems*, Proceedings of 6th Guelph Symposium on Geomorphology, 9-10 May 1980, R. Davidson-Arnott, W. Nickling, B.D. Fahey, (eds.), Geographical Publication No.6, Department of Geography, University of Guelph, Geo Books Norwich, Geo Abstracts, Norwich, 203-238
Sommerfield, R.A., Clark, J., Friedman, I., 1991. Isotopic changes during the formation of depth hoar in experimental snowpacks. In: Taylor, H.P., O'Neil, J.R., Kaplan, I.R.,

Stable Isotope Geochemistry: A Tribute to Samuel Epstein. The Geochemical Society, Calgary.

Souchez, R.A., Lemmens, M.M., 1987, Solutes. In: *Glacio-Fluvial Sediment Transfer, An Alpine Perspective.* A. Gurnell, M.J. Clark (eds.). John Wiley and Sons Ltd. Chichester.

Stenborg, T., 1969, Studies of the internal drainage of glaciers. *Geogr. Ann.* **51A,** 13-41.

Stone, W.J., 1999, *Hydrogeology in practice,* Prentice Hall, New Jersey, 248 pp.

Stringfield, V.T., Rapp, J.R., Anders, R.B., 1979, Effects of karst and geologic structure on the circulation of water and permeability in carbonate aquifers. *J. Hydrol.* **43,** 313-332.

Sueker, J., 1995 Chemical hydrograph separation during snowmelt for three headwater basins in Rocky Mountain National Park, Colorado. *IAHS Publ.* **228**. 271-282.

Sugden, D.E., John, B.S. 1993, *Glaciers and Landscape* (5th ed.). Edward Arnold, London.

Suzuki, K. 1995, Hydrochemical study of snow meltwater and snow cover. *IAHS Publ.* **228**. 107-114.

Tallaksen, L. M., 1995, A review of baseflow recession analysis, *Jnl Hydrol.*, **165**, 349-370

Tolgyessy, J. (ed.) 1993, *Chemistry and Biology of Water, Air and Soil. Environmental Aspects*. Elsevier, London.

Torrence, C. and Compo, G.P., 1998, A practical guide to wavelet analysis. *Bull. Amer. Meteor. Soc.* **79.** 61-78.

Toth, 1963, *Jnl. Geophys. Res.*, **68**, 4795-4981

Tranter, H., Sharp, M., Brown, G., Willis, I., Hubbard, B., Nielsen, M., Smart, C., Gordon, S., Tulley, M., Lamb, H., 1997 (a), Variability in the chemical composition of in situ subglacial meltwaters. *Hydrol. Proc.* **11**, 59-77.

Tranter, M., Lamb, H., Bottrell, S., Raiswell, R., Sharp, M., Brown, G., 1997 (b), Tracing bedrock weathering and hydrologic flowpaths beneath an Alpine glacier using $\delta^{34}S$ and $^{87}Sr / ^{86}Sr$. *IAHS Publ.* **244.** 317-324.

Tsujimura, M., Tadashi, T., Onda, Y. 1998, Effect of subsurface flow on the isotopic composition of soil water in headwater basins. *IAHS Publ.* **248**. 343-352.

Turc, L. 1961, Evaluation des besoins en eau d'irrigation evapotranspiration potentielle. *Ann. Agron.* **12** (13)

Ullman, W.J., 1985, Evaporation rate from a saltpan: Estimates from chemical profiles in near surface groundwaters. *J. Hydrol.* **79,** 365-373.

Walmsley, J.L., Schemenauer, R.S., Bridgman, H.A., 1996. A method for estimating the hydrologic input from mountainous terrain. *J. Applied Met.* **35**, 2237-2247.

Weertman, J., 1957, On the sliding of glaciers. *J. Glaciol.* **3**, 33-8.

Weiler, M., Naef, F., Leibundgut, C., 1998, Study of runoff generation on hillslopes using tracer experiments and a physically based numerical model. *IAHS Publ.* **248**. 353-362.

West, K.E. 1972, *H_2O^{18} / H_2O^{16} variations in ice and snow of mountainous regions of Canada.* Unpubl. Ph.D. thesis, University of Alberta, Edmonton. 123 pp.

Williams, M., Kattelmann, R., Melack, J., 1990, Groundwater contributions to the hydrochemistry of an alpine lake. *IAHS Publ.* **193,** 741-748.

Woo, M.K, 2001. ENSO (El Nino-Southern Oscillation) and Annual Floods in Western Canada. *27th Annual Scientific Meeting of the Canadian Geophysical Union – Program and Abstracts*, Ottawa, 14-17 May, 2001.

Yang, D., Goodison, B., Metcalfe, J.R., Golubev, V.S., Elomaa, E., Gunther, T., Bates, R., Pangburn, T., Hanson, C.L., Emerson, D., Copaciu, V., Milkovic, J. 1995, Accuracy of Tretyakov precipitation gauge: Result of WHO intercomparison. *Hydrol. Proc.* **9**, 877-989.

Yonge, C.J, Goldberg, L., Krouse, H.R., 1989, An isotope study of water bodies along a traverse of southwestern Canada. *J. Hydrol.*, **106**, 245-255.

Young, G.J. 1982, Hydrological relationships in a glacierised mountain basin. In: *Hydrological Aspects of Alpine and High Mountain Areas, IAHS Publ.* **138,** 51-59.

Young, G.J. 1991, Hydrological interactions in the Mistaya Basin, Alberta, Canada. *IAHS Publ.* **205,** 237-244.

Yurtsever, Y., Araguas, L.A. 1993, Environmental isotope applications in hydrology: an overview of the IAEA's activities, experiences and prospects, *IAHS publ.* **215**. 3-20.

Yunnian, Y. 1990, The hydrological effects of forests. *IAHS Publ.* **197,** 413-423.

Zawadzki, A. 1997, *A sensitivity analysis of the hydrology of the Bow Valley above Banff, Alberta using the UBC Watershed Model*. Unpublished MES thesis, Wilfrid Laurier University.

Appendices

Appendix 1 Bow Valley Snow Course and Peyto Glacier Mass Balance Data

Snow course data within the Bow Valley from 1996 to 1999, collected by Alberta Environmental Protection.

STATION BOW RIVER (Lake Louise) — **ID CODE** 05BA801
BASIN BOW — **DATA SOURCE** ALBERTA ENVIRONMENT
LATITUDE 51D 25M — **LONGITUDE** 116D 11M — **ELEVATION** 1580 METRES
REMARKS

YEAR	FEB 1			MAR 1			APR 1			MAY 1			JUN 1		
	DATE	DEPTH CM	W.E. MM	DATE	DEPTH CM	W.E. MM	DATE	DEPTH CM	W.E. MM	DATE	DEPTH CM	W.E. MM	DATE	DEPTH CM	W.E. MM
1996	Jan-30	94	236	Feb-28	103	279	Mar-26	99	307						
1997	Jan-27	99	224	Feb-25	98	274	Apr-03	97	297						
1998	Jan-29	55	117	Feb-25	58	147	Mar-30	59	163						
1999	Jan-27	78	196	Feb-24	91	246	Mar-29	92	259						

STATION BOW SUMMIT — **ID CODE** 05BA813
BASIN BOW — **DATA SOURCE** ALBERTA ENVIRONMENT
LATITUDE 51D 42M — **LONGITUDE** 116D 28M — **ELEVATION** 2080 METRES
REMARKS

YEAR	FEB 1			MAR 1			APR 1			MAY 1			JUN 1		
	DATE	DEPTH CM	W.E. MM	DATE	DEPTH CM	W.E. MM	DATE	DEPTH CM	W.E. MM	DATE	DEPTH CM	W.E. MM	DATE	DEPTH CM	W.E. MM
1996	Jan-30	142	411	Feb-29	156	485	Mar-27	153	527	Apr-25	137	503			
1997	Jan-27	115	336	Feb-24	112	320	Mar-27	153	462	Apr-30	123	455	May-28	63	254
1998				Feb-25	87	239	Mar-30	100	257	Apr-29	71	254	May-27	1	3
1999	Jan-27	117	345	Feb-24	140	447	Mar-30	138	460	May-04	117	490	May-28	69	325

STATION CHATEAU LANN — **ID CODE** 05BA808
BASIN BOW — **DATA SOURCE** ALBERTA ENVIRONMENT
LATITUDE 51D 25M — **LONGITUDE** 116D 13M — **ELEVATION** 1740 METRES
REMARKS

YEAR	FEB 1			MAR 1			APR 1			MAY 1			JUN 1		
	DATE	DEPTH CM	W.E. MM	DATE	DEPTH CM	W.E. MM	DATE	DEPTH CM	W.E. MM	DATE	DEPTH CM	W.E. MM	DATE	DEPTH CM	W.E. MM
1996	Jan-30	111	282	Feb-28	124	368	Mar-26	115	373						
1997	Jan-27	115	282	Feb-25	107	292	Apr-03	115	361						
1998	Jan-29	67	175	Feb-25	74	206	Mar-30	84	236						
1999	Jan-29	91	254	Feb-24	104	329	Mar-29	102	325						

STATION KATHERINE LAKE — **ID CODE** 05BA814
BASIN BOW — **DATA SOURCE** ALBERTA ENVIRONMENT
LATITUDE 51D 41M — **LONGITUDE** 116D 23M — **ELEVATION** 2380 METRES
REMARKS

YEAR	FEB 1			MAR 1			APR 1			MAY 1			JUN 1		
	DATE	DEPTH CM	W.E. MM	DATE	DEPTH CM	W.E. MM	DATE	DEPTH CM	W.E. MM	DATE	DEPTH CM	W.E. MM	DATE	DEPTH CM	W.E. MM
1996				Feb-29	166	541	Mar-27	165	565				Jun-03	174	775
1997				Feb-24	124	325				Apr-30	158	556	May-28	116	531
1998				Feb-26	91	269	Mar-30	116	328	Apr-29	124	343	Jun-05	0	0
1999				Mar-01	158	523	Mar-30	163	544	May-03	160	612	May-27	128	561

STATION LARCH VALLEY — **ID CODE** 05BA812
BASIN BOW — **DATA SOURCE** ALBERTA ENVIRONMENT
LATITUDE 51D 19M — **LONGITUDE** 116D 13M — **ELEVATION** 2230 METRES
REMARKS

YEAR	FEB 1			MAR 1			APR 1			MAY 1			JUN 1		
	DATE	DEPTH CM	W.E. MM	DATE	DEPTH CM	W.E. MM	DATE	DEPTH CM	W.E. MM	DATE	DEPTH CM	W.E. MM	DATE	DEPTH CM	W.E. MM
1996				Feb-29	164	495	Mar-27	165	544	Apr-25	173	594	Jun-03	128	541
1997				Feb-24	150	465	Mar-27	173	564	Apr-30	159	531	May-28	127	559
1998				Feb-26	96	284	Mar-30	126	345	Apr-29	101	368	Jun-05	11	20
1999				Mar-01	164	529	Mar-30	167	561	May-03	135	536	May-27	113	536

STATION MIRROR LAKE — **ID CODE** 05BA806
BASIN BOW — **DATA SOURCE** ALBERTA ENVIRONMENT
LATITUDE 51D 25M — **LONGITUDE** 116D 14M — **ELEVATION** 2030 METRES
REMARKS

YEAR	FEB 1			MAR 1			APR 1			MAY 1			JUN 1		
	DATE	DEPTH CM	W.E. MM	DATE	DEPTH CM	W.E. MM	DATE	DEPTH CM	W.E. MM	DATE	DEPTH CM	W.E. MM	DATE	DEPTH CM	W.E. MM
1996	Jan-30	106	284	Feb-29	124	358	Mar-27	125	389						

1997	Jan-27	105	244	Feb-24	114	318	Mar-27	142	432										
1998	Jan-28	68	160	Feb-25	74	201	Mar-30	91	246										
1999	Jan-28	93	272	Feb-24	102	312	Mar-30	130	404										

STATION **PIPESTONE UPPER** ID CODE 05BA802
BASIN BOW DATA SOURCE ALBERTA ENVIRONMENT
LATITUDE 51D 26M LONGITUDE 116D 10M ELEVATION 1615 METRES
REMARKS

YEAR	FEB 1			MAR 1			APR 1			MAY 1			JUN 1		
	DATE	DEPTH CM	W.E. MM	DATE	DEPTH CM	W.E. MM	DATE	DEPTH CM	W.E. MM	DATE	DEPTH CM	W.E. MM	DATE	DEPTH CM	W.E. MM
1996	Jan-30	102	249	Feb-28	110	302	Mar-27	104	305						
1997	Jan-27	108	244	Feb-24	105	274	Mar-27	111	320						
1998	Jan-28	62	124	Feb-25	66	165	Mar-30	71	185						
1999	Jan-27	84	213	Feb-24	99	262	Mar-30	99	330						

STATION **PTARMIGAN HUT** ID CODE 05BA810
BASIN BOW DATA SOURCE ALBERTA ENVIRONMENT
LATITUDE 51D 28M LONGITUDE 116D 06M ELEVATION 2190 METRES
REMARKS

YEAR	FEB 1			MAR 1			APR 1			MAY 1			JUN 1		
	DATE	DEPTH CM	W.E. MM	DATE	DEPTH CM	W.E. MM	DATE	DEPTH CM	W.E. MM	DATE	DEPTH CM	W.E. MM	DATE	DEPTH CM	W.E. MM
1996				Feb-29	147	437	Mar-27	150	465	Apr-25	142	541	Jun-03	95	381
1997				Feb-24	127	351	Mar-27	145	439	Apr-30	140	483	May-28	77	330
1998				Feb-26	93	264	Mar-30	104	292	Apr-29	73	272	Jun-05	0	0
1999				Mar-01	135	404	Mar-30	141	467	May-03	123	465	May-27	70	340

STATION **SKOKI MOUNTAIN** ID CODE 05CA805
BASIN RED DEER DATA SOURCE ALBERTA ENVIRONMENT
LATITUDE 51D 32M LONGITUDE 116D 03M ELEVATION 2060 METRES
REMARKS SNOW COURSE SITE

YEAR	FEB 1			MAR 1			APR 1			MAY 1			JUN 1		
	DATE	DEPTH CM	W.E. MM	DATE	DEPTH CM	W.E. MM	DATE	DEPTH CM	W.E. MM	DATE	DEPTH CM	W.E. MM	DATE	DEPTH CM	W.E. MM
1996				Feb-29	140	424	Mar-27	135	432	Apr-25	133	467	Jun-03	97	368
1997				Feb-24	119	312	Mar-27	140	386	Apr-30	127	432	May-28	79	325
1998				Feb-26	86	224	Mar-30	100	274	Apr-29	78	262	Jun-05	0	0
1999				Mar-01	127	396	Mar-30	141	429	May-03	126	475	May-27	97	427

STATION **SKOKI MT. PILLOW** ID CODE 16X15S
BASIN RED DEER DATA SOURCE ALBERTA ENVIRONMENT
LATITUDE 51D 32M LONGITUDE 116D 03M ELEVATION 2060 METRES
REMARKS SNOW PILLOW SITE

YEAR	FEB 1			MAR 1			APR 1			MAY 1			JUN 1		
	DATE	DEPTH CM	W.E. MM	DATE	DEPTH CM	W.E. MM	DATE	DEPTH CM	W.E. MM	DATE	DEPTH CM	W.E. MM	DATE	DEPTH CM	W.E. MM
1996	Feb-01		284	Mar-01		319							Jun-01		239
1997	Feb-01		247	Mar-01		279	Apr-01		356	May-01		358	Jun-01		55
1998	Feb- 1		101	Mar-01			Apr-01								
1999	Feb- 1		281				Apr-01		335	May-01		356	Jun-01		113

STATION **SUNSHINE VI. PILLOW** ID CODE 15X03S
BASIN BOW DATA SOURCE ALBERTA ENVIRONMENT
LATITUDE 51D 05M LONGITUDE 115D 47M ELEVATION 2230 METRES
REMARKS SNOW PILLOW SITE

YEAR	FEB 1			MAR 1			APR 1			MAY 1			JUN 1		
	DATE	DEPTH CM	W.E. MM	DATE	DEPTH CM	W.E. MM	DATE	DEPTH CM	W.E. MM	DATE	DEPTH CM	W.E. MM	DATE	DEPTH CM	W.E. MM
1996	Feb-01		537	Mar-01		627	Apr-01		684	May-01		763	Jun-01		737
1997	Feb-01		459	Mar-01		519	Apr-01		668	May-01		711	Jun-01		561
1998	Feb-01		315	Mar-01		339	Apr-01		438				Jun-01		31
1999				Mar-01		620	Apr-01		698	May-01		735	Jun-01		664

STATION **SUNSHINE VILLAGE** ID CODE 05BB803
BASIN BOW DATA SOURCE ALBERTA ENVIRONMENT
LATITUDE 51D 05M LONGITUDE 115D 47M ELEVATION 2230 METRES
REMARKS SNOW COURSE SITE

YEAR	FEB 1			MAR 1			APR 1			MAY 1			JUN 1		
	DATE	DEPTH CM	W.E. MM	DATE	DEPTH CM	W.E. MM	DATE	DEPTH CM	W.E. MM	DATE	DEPTH CM	W.E. MM	DATE	DEPTH CM	W.E. MM
1996	Jan-30	142	559	Feb-28	204	678	Mar-26	203	744	May-02	219	766	May-28	193	798
1997	Jan-27	136	386	Feb-25	171	488	Apr-03	199	693	May-01	192	716	May-29	139	612
1998	Jan-29	119	298	Feb-25	122	345	Mar-31	140	419	Apr-29	112	391	May-27	26	107
1999	Jan-28	184	536	Feb-24	196	696	Mar-29	212	719	May-04	189	796	May-28	149	706

Appendix 2 Basin Physiography

2.1 DEM Preparation and Analysis

Digital elevation data were acquired from Geomatics Canada, Centre for Topographic Information, Sherbrooke, Quebec. Digitised contour lines from 1:50,000 NTS maps of the study area were acquired in *ArcInfo* ASCII ungenerate format (sheets 82 - J13, N01, N08, N09, N10, N15, N16, O04, O05). This format was used as it could be input directly into *Surfer* for gridding. The only editing of this format necessary was to ensure that all height data were in metres. Prior to carrying out the grid procedures, it was necessary to merge all of the contour line vector XYZ data for all 9 map sheets. This was carried out in *Surfer's* worksheet environment as it could handle very large quantities of data (each sheet had approximately 4-5,000,000 data points).

The next step was to generate a raster DEM from the raw XYZ data using one of *Surfer's* Grid procedures. "Kriging" and "Triangulation with Linear Interpolation" were attempted. It was found that with the dataset used, "kriging" was not appropriate for two reasons. Firstly, the data set is very large and running the procedure for a grid of appropriate spatial resolution takes several hours to days, (using a PIII 450MHz with 256Mb RAM). Also, if a "search" option that is too large is specified, the procedure takes even longer or too much smoothing of the data occurs. On the other hand, if a "search" radius that is too small is specified then large areas of blank nodes are created in areas of low relief. For these reasons, the somewhat angular but robust "triangulation" procedure was adopted for its speed and ability to maintain data integrity without blank areas. The preliminary DEM generated was for the Orthorectification of Landsat TM imagery by *RadarSat International* and therefore a cell size of 30m was specified.

A further DEM of the Bow Basin was generated at a spatial resolution appropriate for input to the *Topaz* topographic analysis software that comes with the *SLURP* hydrological model. *Topaz* has the capability to analyse up to a 500 by 500 grid. A larger array could be input but the FORTRAN code of the software would need altering and without a compiler this is problematic. Therefore, the Bow Basin was assigned a grid cell size of200 m. Given the sizes of the basin this resolution was considered to provide sufficient topographic detail. After generating the "resampled" DEM in *Surfer* it was then converted to ASCII XYZ format and edited in a worksheet to conform to the "single variable sequential" format necessary for input to the topographic analysis package *Topaz* (Kite, 1999).

2.2 Landcover Classification and Distribution

In order to determine landcover types of differing hydrological characteristics, a Landsat TM image of the study area, collected on 7th September 1998, was purchased from *Radarsat International (RSI)*. The image (track 43, row 24) was free of cloud and was acquired at a time of long-term minimal snowpack and thus was ideal for landcover classification. Prior to receiving the image and commencing classifications, it was orthorectified by *RSI* using the 30m DEM generated earlier. The orthorectification procedure was necessary in order that the satellite and topographic data exactly coincided during subsequent GIS operations. The Orthorectified Landsat TM images were delivered to Wilfrid Laurier in *PCI* database format as a ".pix" file.

The actual Land Classification was carried out "in house" using *PCI* and its maximum likelihood classification routine within *Imageworks*. Training areas were carefully selected all over the satellite image but mainly within the area of interest. The land classes defined were:

- Water (including lakes and rivers)
- Snow (including firn)
- Glacial ice
- Forest
- Grass and shrubland
- Bare ground (including urban areas and bare rock)
- Shadows
- Off image

The last two categories were necessary as there was significant shadow cover in the high mountain areas and no image data had been collected at the corners of the scene. Shadow areas were manually edited within Imageworks to the correct land cover. It was quite simple to discern the land cover type beneath shadows based upon surrounding land cover and spectral properties but this could not be automated within the maximum likelihood classification procedure due to the overall similarity of all shadow areas. Once the classification was completed it was exported from PCI as a GEO TIF file so that it could be viewed in other applications and maintain its georeferencing information.

2.3 Landcover Hypsometry

The topographic data generated in *Topaz* and converted to *ArcInfo* coverage data were imported into *ArcView* using the "ASCII 3D Raster" import option. The raster elevation band file *elevcla.arc* was converted to an *ArcView Shapefile* to give it elevation attributes and then the watershed boundary was "clipped" using the *bound.arc* file as a template. The resultant theme in the ArcView projects for each basin was a raster DEM of 100m elevation bands that extended only to the boundary of each watershed. The Landcover classification image was then imported to ArcView as an image file. Prior to overlaying the classification and DEM data it was necessary to convert the land cover image from a TIF file to a grid conforming to the grid cell dimensions of each respective DEM. Then this new grid was further converted to an ArcView Shapefile to facilitate grid layer comparisons within the GIS. An "intersect" overlay procedure was then performed between the landcover and elevation grid files to calculate the area of each landcover in each elevation band.

Appendix 3 Raw End-member Sample Geochemistry

Snowpack											
Date	id	Elev	$\delta^{18}O$	*Tr*	*EC (uS cm^{-1})*	*pH*	*Alk (mg l)*	*Na (mg l)*	*K (mg l)*	*Mg (mg l)*	*Ca (mg l)*
5/17/96	ch96_s1	2650	-21.3								
5/17/96	ch96_s2	2200	-23.4								
5/24/96	ch96_s3	2120	-23.6								
6/20/96	ch96_s4	2200	-23.8								
7/25/96	ch96_s5	2600	-20.5								
7/28/96	ch96_s6	2690	-20.9								
5/4/97	ch97_s9	1500	-21.3								
4/7/98	ch98_s17	1880	-23.1	10.7							
4/7/98	ch98_s21	2000	-21.9	10.1							
4/11/98	ch98_s29	2200	-20.1								
4/20/98	ch98_s36	2325	-22.7								
4/20/98	ch98_s37	2800	-23.2								
4/20/98	ch98_s38	2600	-21.0								
5/6/99	ch99_s52	2000	-21.4					1.5	0.84	0.45	1.65
5/6/99	ch99_s53	2480	-21.47					2.7	1.21	0.45	4.2
5/6/99	ch99_s54	2700	-22.52					2.4	0.24	0.15	
5/15/99	ch99_s57a	2700	-23.1	9.4	19	5.7	2.9	3.7	1.4	0.19	
5/15/99	ch99_s61a	2150	-22.7	8	7	6	2.2	2.2	0.4	0.17	
5/20/99	ch99_s79a	1880	-24.1	6.1	6	6.4		2.85			
Ice											
5/28/96	2215	ch96_i1	-20.5								
6/20/96	2300	ch96_i2	-20.6								
7/28/96	2240	ch96_i3	-20.7								
8/14/96	2200	ch96_i4	-20.9								
8/25/96	2220	ch96_i5	-20.9								
8/2/97	2220	ch97_i11	-21.8								
8/20/97	2220	ch97_i12	-21.3								
8/21/97	2220	ch97_i13	-20.1								
7/17/98	2220	ch98_i112	-20.9	0	8.6	7.85	7				
7/17/98	2220	ch98_i113	-20.8								
7/18/98	2300	ch98_i114	-20.2								
7/18/98	2350	ch98_i115	-20.3		31.6	7.81	14				
7/18/98	2300	ch98_i116	-20.6								
7/25/98	2480	ch98_i133	-21.4								
7/25/98	2700	ch98_i134	-19.7								
7/25/98	2700	ch98_i135	-20.1								
10/14/98	2290	ch98_i250	-22.6		43	8.01	5				
8/5/99	2150	ch99_i158	-22.7	0							
8/5/99	2150	ch99_i159	-21.5								
8/5/99	2300	ch99_i160	-21.5								
8/5/99	2275	ch99_i161	-20.5								
8/5/99	2500	ch99_i162	-20.7	0							
8/5/99	2500	ch99_i163	-20.3								
Rain											
5/29/96	1400	ch96_r1	-14.9								
5/29/96	1400	ch96_r2	-15.3								
7/18/96	1400	ch96_r3	-12.7								
8/23/97	2250	ch97_r9	-14.7								
8/23/97	2250	ch97_r10	-15.1								
7/5/98	1600	ch98_r76	-13.6								
7/8/98	1900	ch98_r86	-9.9		30		22				
7/11/98	1900	ch98_r89	-8.8	13.8							
7/16/98	1900	ch98_r108	-11.7								
7/30/98	1900	ch98_r148	-13.2								
8/14/98	1900	ch98_r182	-9.0								
8/16/98	1900	ch98_r206	-12.7			5.6					
8/4/99	2150	ch99_r156	-11.3	14.1							
8/6/99	1900	ch99_r169	-12.8								
8/6/99	1400	ch99_r179	-10.5	16.8							

Appendix 4 Raw Baseflow and Groundwater Data

4.1 Raw Groundwater Sample Geochemistry

Date	id	$d^{18}O$ (‰)	TU	EC (uS cm^{-1})	pH	Alk (mg/l)	SiO_2 (mg/l)	Cl (mg/l)	Na (mg/l)	K (mg/l)	Mg (mg/l)	Ca (mg/l)
Num ti Jah Lodge GW Well												
5/4/97	ch97_gn17	-21.1										
8/4/97	ch97_gn17a	-21.6										
8/25/97	ch97_gn17b	-21.8										
4/7/98	ch98_gn25	-21.3	13	359	7.1		3.9	0.5	0.79	0.4	14.2	36.2
7/13/98	ch98_gn102	-21.2	10	316	7.9	136	2.9					
8/15/98	ch98_gn194	-21.2		303	8.0	144	3.2					
10/12/98	ch98_gn237	-21.1		302	8.0	141						
1/29/99	ch99_gn1	-20.9		301	7.4	130			4.35	0.6	12.9	33.3
5/6/99	ch99_gn49	-21.0		307	8.2	130						
5/26/99	ch99_gn113	-21.1		316	7.9	131			0.75	0.56	14.7	37.2
8/2/99	ch99_gn130	-21.7		368		140			0.75	0.66	13.95	35.7
Hostel GW Well (55')												
8/4/97	ch97_gh21	-21.2										
8/25/97	ch97_gh21a	-21.5										
5/4/98	ch98_gh59	-21.7		275			2.77	1.1	0.72	0.3	10.6	25.1
7/9/98	ch98_gh59a			210	8.0	98		0.8	<1	0.3	10.0	22.0
8/15/98	ch98_gh200	-20.3		156	8.5	88	2.13					
10/10/98	ch98_gh225	-20.6		240	7.8	95						
1/29/99	ch99_gh9	-21.0		250	7.9	101	2.36					
5/6/99	ch99_gh45	-21.1		266	8.2	106	5.21					
5/25/99	ch99_gh108	-21.7		245	8.1	107	2.75					
8/7/99	ch99_gh178	-22.2		179		82						
Campground Well (30')												
5/4/97	ch97_gg20	-21.2										
8/4/97	ch97_gg20a	-21.9										
8/25/97	ch97_gg20b	-21.4										
4/6/98	ch98_gg9	-21.1	12	180	8.6		1.87		0.39	0.2	10.2	22.1
7/6/98	ch98_gg77	-21.0	10	250		99	2.07					
10/10/98	ch98_gg223	-20.3	12	248	8.0	96						
1/29/99	ch99_gg11	-20.8	14	185	8.7	68	1.17					
5/6/99	ch99_gg47	-21.1	15	227	9.0	89	3.94					
5/25/99	ch99_gg106	-21.3	17	244	8.8	100	1.74					
8/7/99	ch99_gg176	-22.6	10	191		90						
Miscellaneous:												
Soil Water (surface water table)												
7/7/58	ch98_gc81	-20.1	8	333		155	4.30					
7/12/98	ch98_gc93	-19.9		335	8.0	154	4.46					
7/16/98	ch98_gc109	-19.4		343	7.9	156	4.44					
8/14/98	ch98_gc185	-20.4		281	7.8	165	4.95					
10/11/98	ch98_gc229	-19.6		251	8.2	141						
Spring @ Peyto (pos. karst)												
5/25/96	ch96_gp1	-20.6	24 (+/- 8)									28.4
6/8/96	ch96_gp2	-20.8										25.1
6/29/96	ch96_gp3	-21.4										22.3
8/12/96	ch96_gp5	-21.5	1 (+/- 8)									19.2
4/11/99	ch98_gp28	-20.6		275	7.9		2.2		0.28	0.3	13.3	31.6
8/18/99	ch99_gp166	-22.6		170		79			0.15	0.22	10.2	32.7
Spring @ Hector Lake Catchment												
7/20/96	ch96_g4	-20.4	11									
Spring @ hwy 93 seep (Louise - Mosquito)												
4/6/98	ch98_g7	-21.5										
Spring @ Protection Campground												
4/8/98	ch98_g27	-20.9										
Spring @ BWF N. side moraine routed (347 228)												
7/13/98	ch98_g97	-19.4		176	7.8	69	1.2					
Spring nr Bow Lake G. inflow @ foot of forested slope (357 245)												
7/13/98	ch98_g99	-20.6		175	8.2	73	1.1					
Till water in floodplain btw WF & HC (350 227)												
7/14/98	ch98_g105	-19.1		224	8.0	135	2.4					

4.2 Water table levels at Marmot Creek Basin

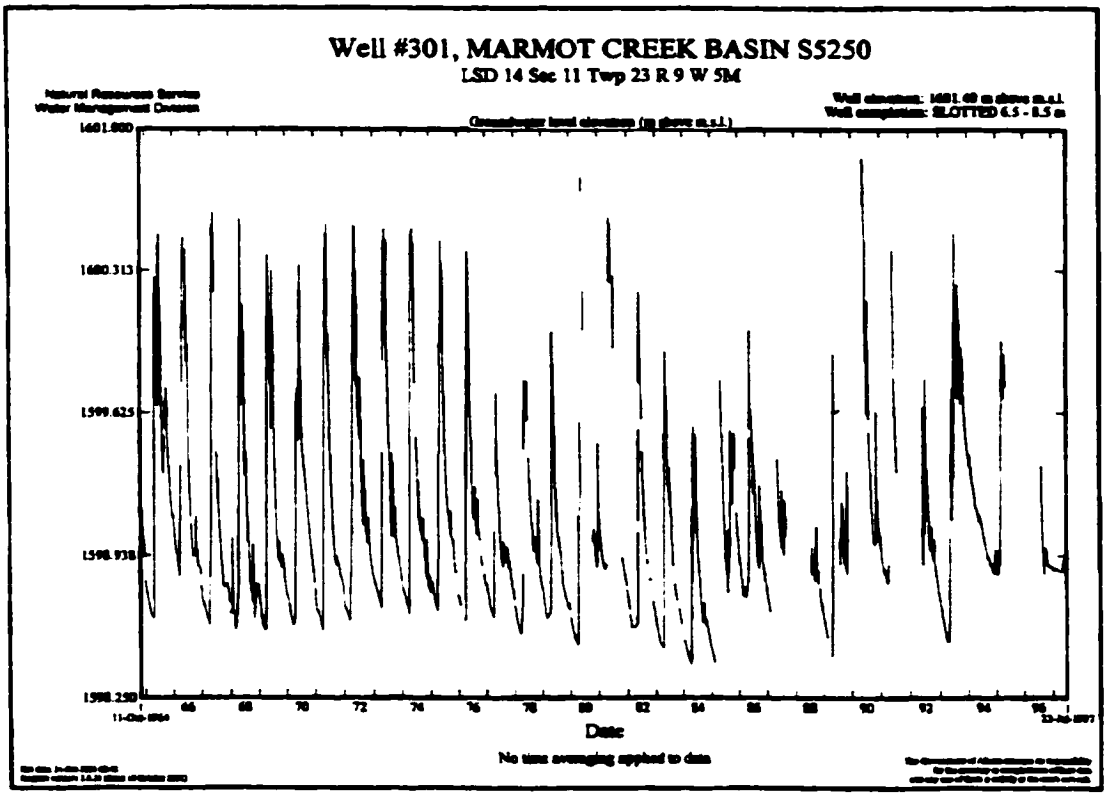

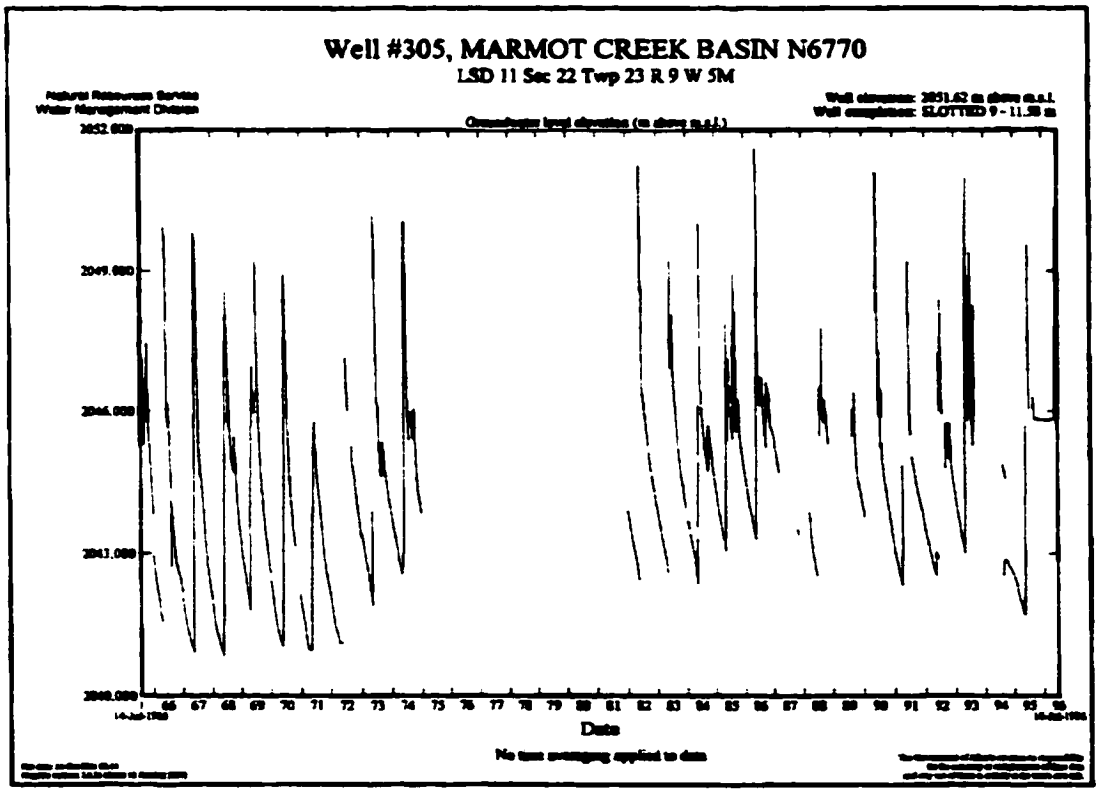

Appendix 5 Raw Web Based Hourly Hydrograph Wavelet Analysis Output

The charts presented in this appendix were generated from raw hourly discharge data for each of the sub-basins studied during 1996 and 1999: Mosquito Creek, Bow Waterfall Creek, Pipestone River at Lake Louise, Bow River at Lake Louise and Bow River at Banff. Unfortunately, not all basins had continuous records for this time period and so only those time periods of continuous hourly data have been studied. A continuous "Morlet 8" wavelet filter was applied to each of the data sets using an automated procedure available on the World Wide Web (http://www.ResearchSystems.com/Cgi-bin/ion-p) to illustrate recurring temporal periodicities within each of the discharge time series. The procedures and in depth description of the filtering technique is provided in Torrence and Compo (1998). The interactive procedure available on the web can only handle 2000 data points during one operation, and therefore it was not possible to run the filter across most of the complete time series. For convenience, the time series data for each location were separated into individual years and then further, the active season of each year was divided into two time periods: May 1st to July 15th and July 16th to September 30th. The data during annual baseflow conditions (October 1st to April 30th) were left out of the analysis. Dividing the data up in this way proved useful, in that temporal dominances of individual years could be compared and the early active nival period of each year could be compared with the later glacial period.

In each of the following sub-sections are the graphical outputs direct from the web page (http://www.ResearchSystems.com/Cgi-bin/ion-p). The first figure for each section is for the early part of the year in question with the latter part of the active season being represented in the second figure. Each figure is divided into four sections. Top left is a graph of the raw hourly discharge data in m^3s^{-1}. Top right is a representation of the wavelet filter used. Bottom left is a time frequency plot of the filtered data. On the left hand axis of this graph is the time periodicity (in hours) of recurring patterns. Along the bottom axis is the time length (in hours) following the start point in the data. On this plot, time periods of recurring temporal periodicity will be illustrated. Darker tones indicate stronger patterns. The hatched area around the edge of the plot is the "cone of influence". Any patterns in the centre of the plot within the hatched region are significant at the 95% level. The line graph in the bottom right is a frequency distribution which illustrates (with data spikes) the dominant periodicities over the entire time series analysed.

5.1 Mosquito Creek 1999

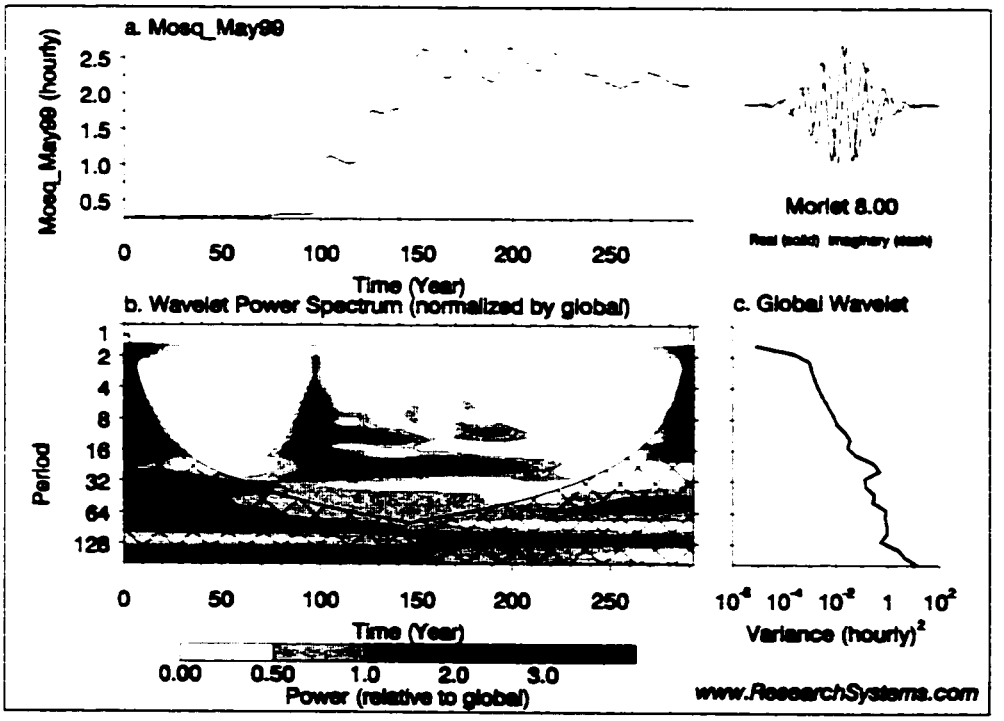

5.2 Bow Waterfall Creek 1996

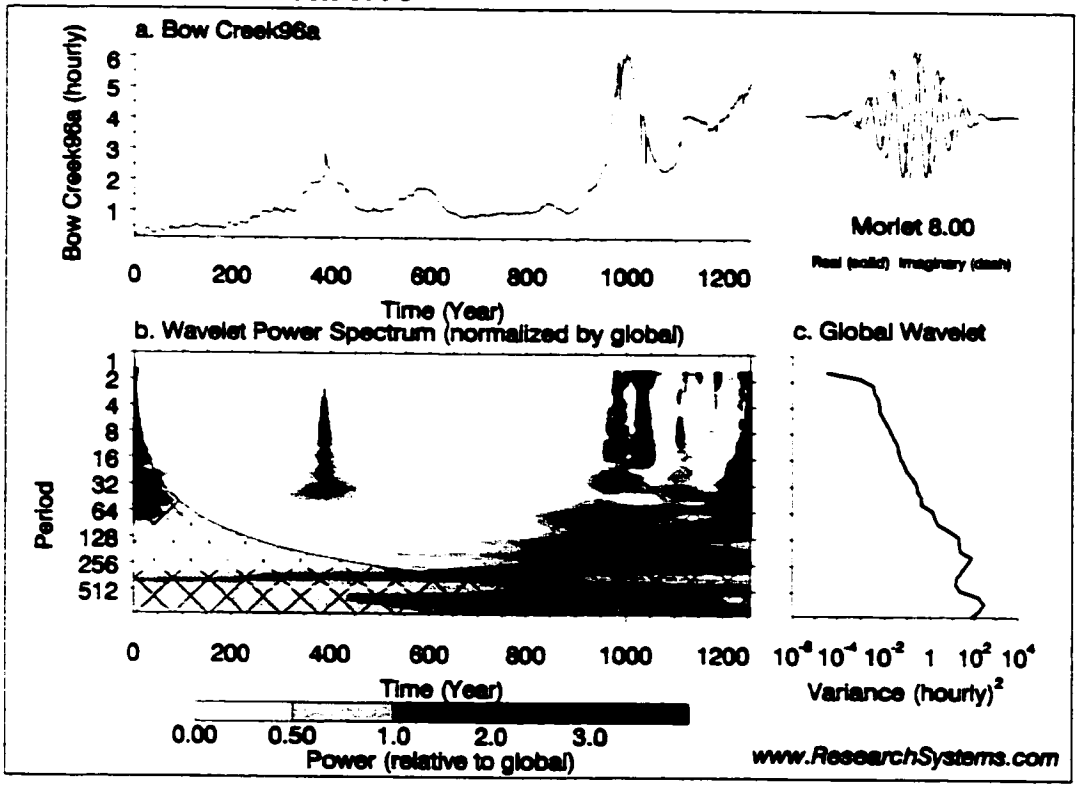

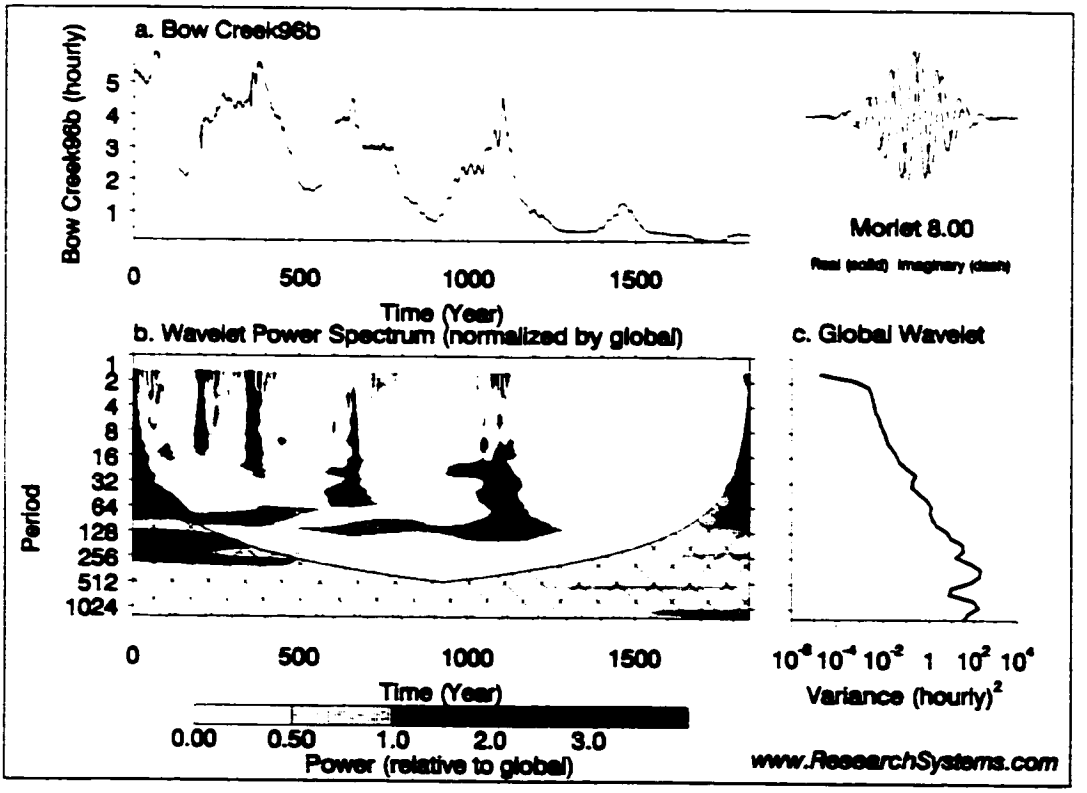

5.3 Bow Waterfall Creek 1998

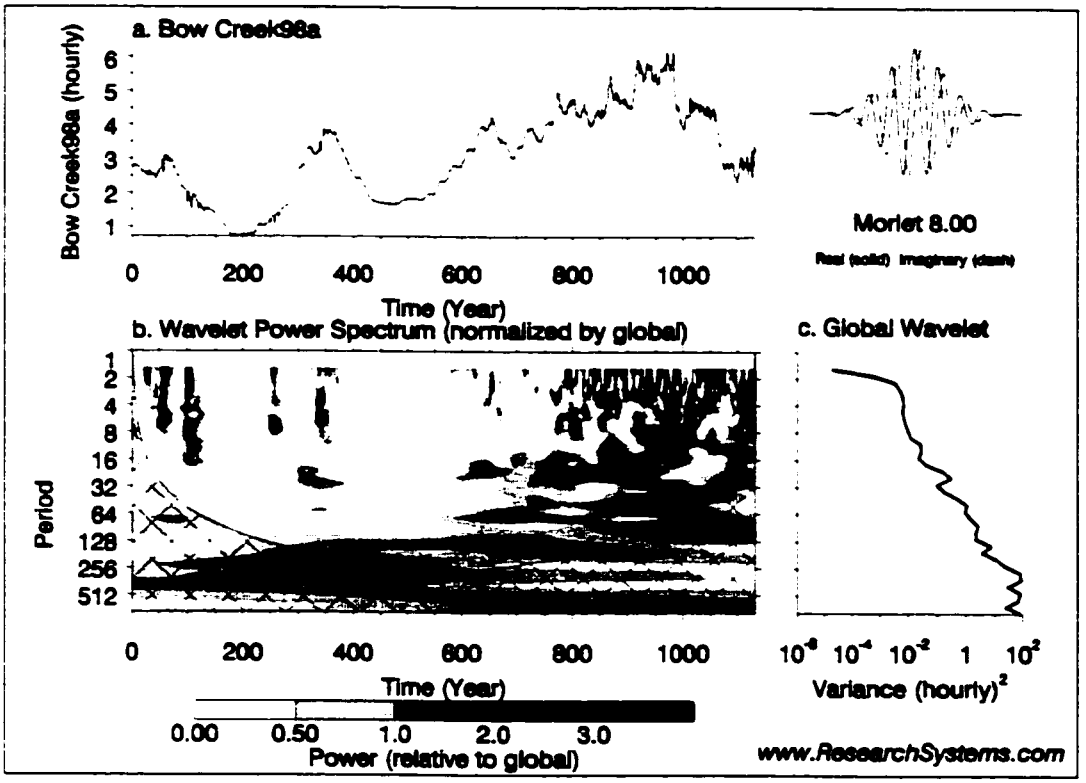

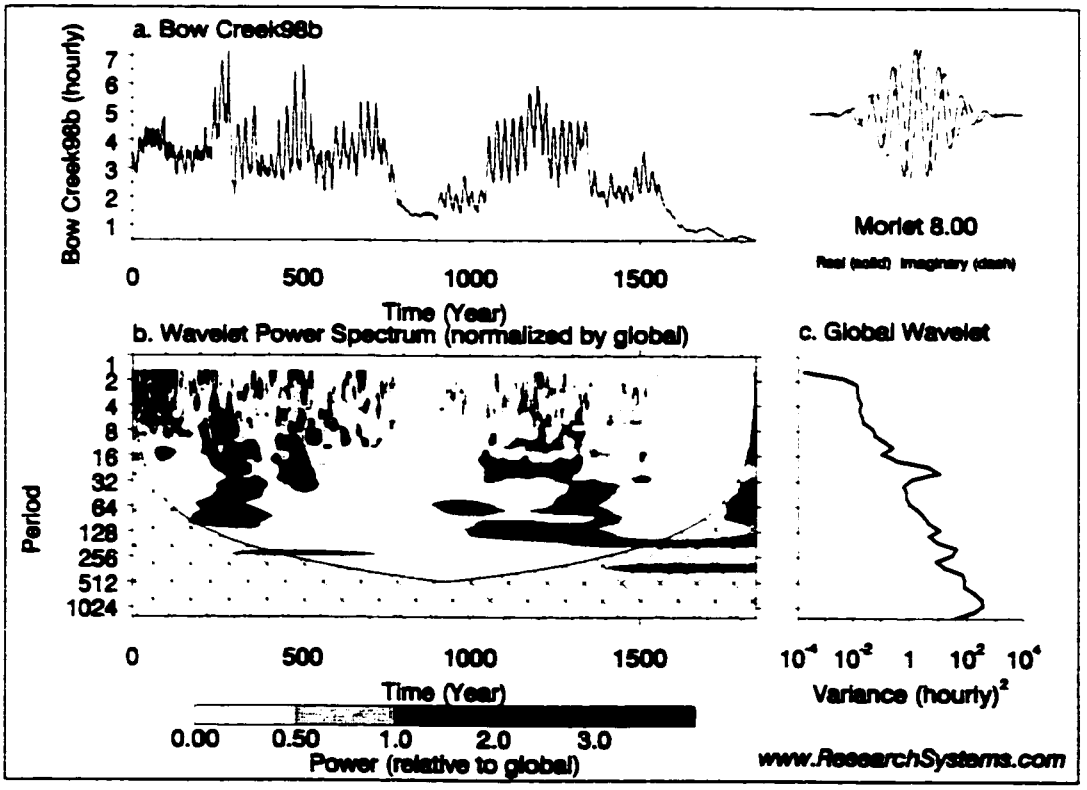

5.4 Pipestone River 1997

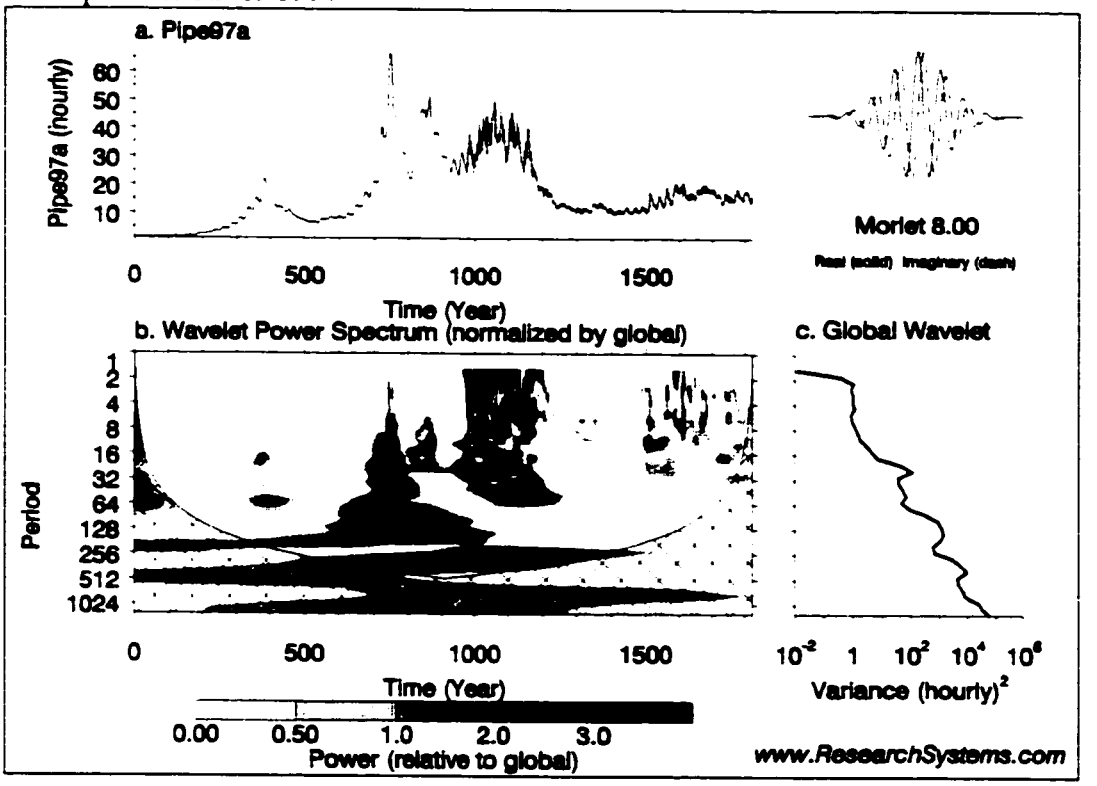

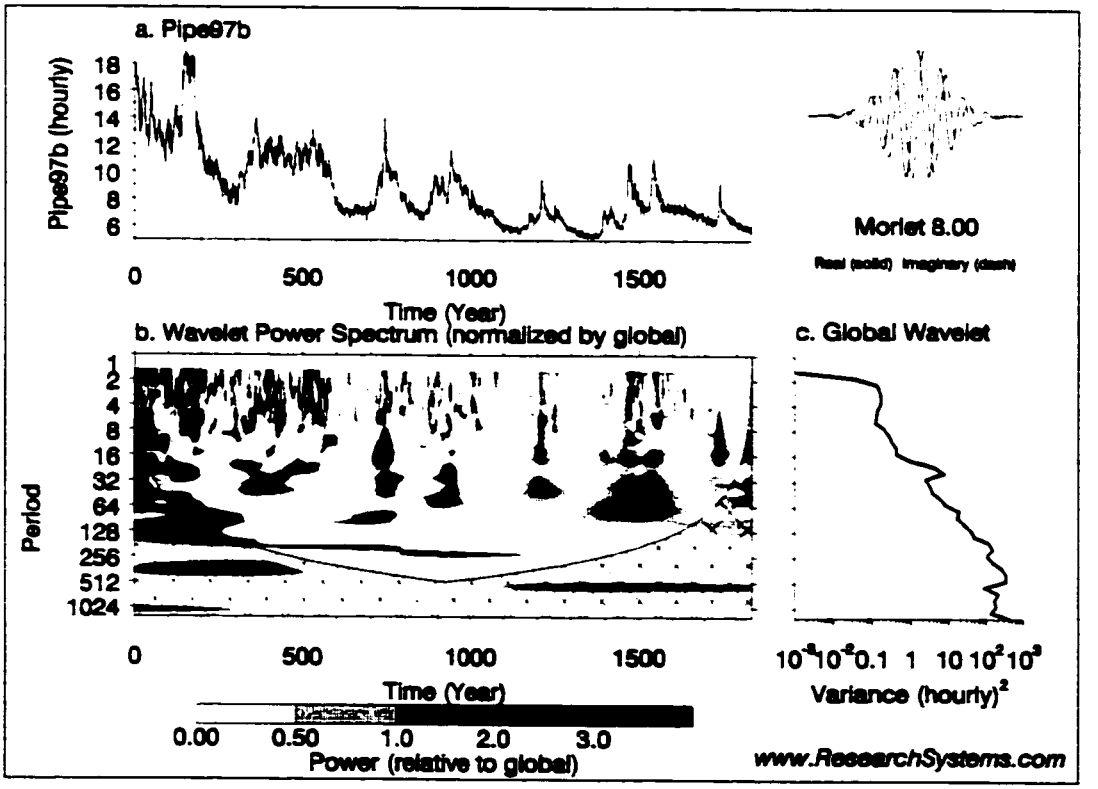

5.5 Pipestone River 1998

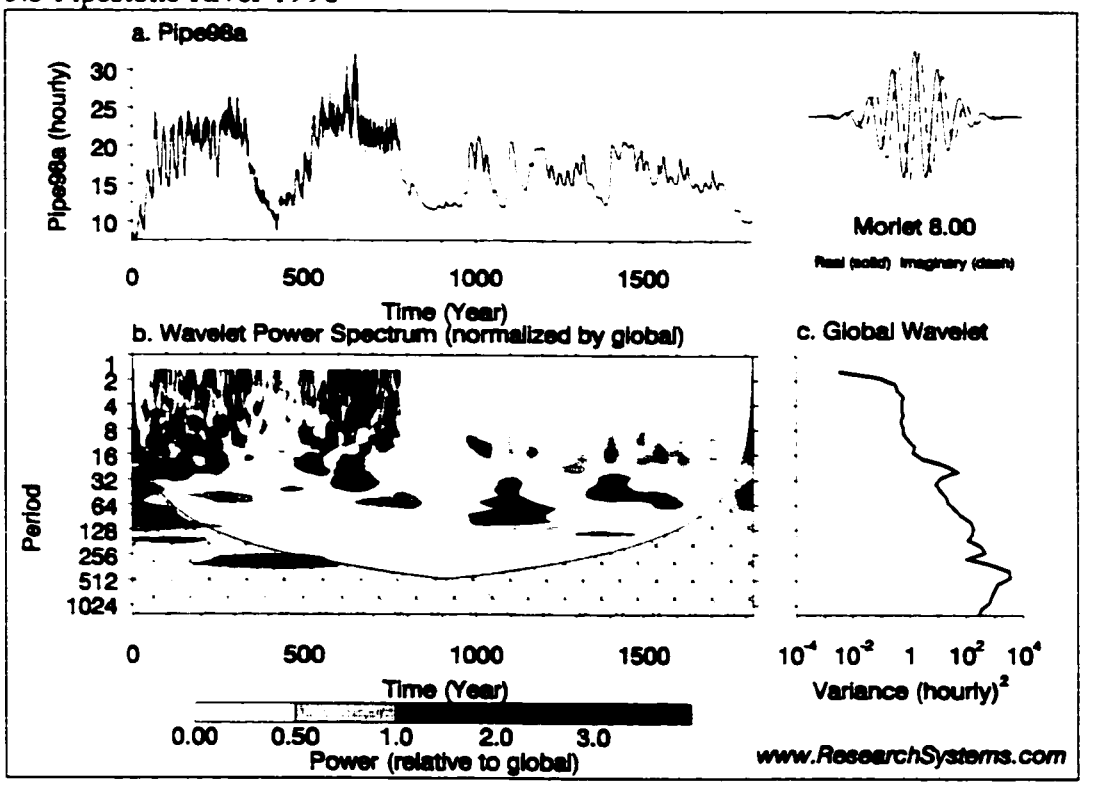

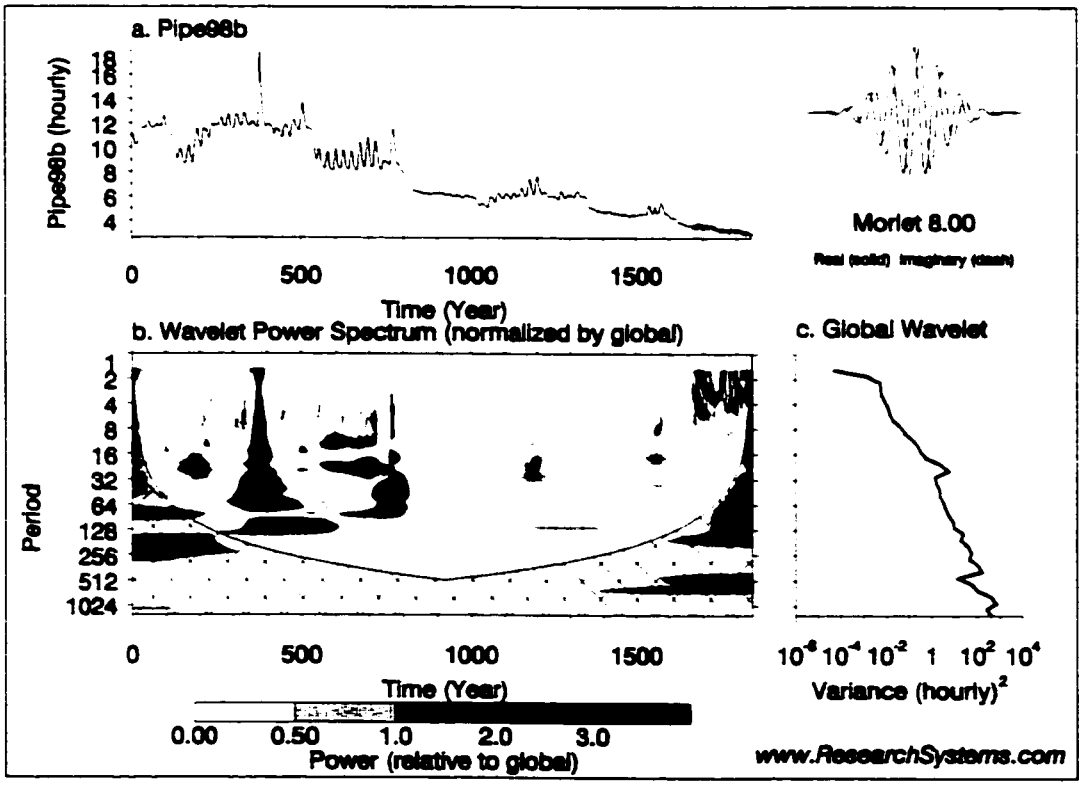

5.6 Pipestone River 1999

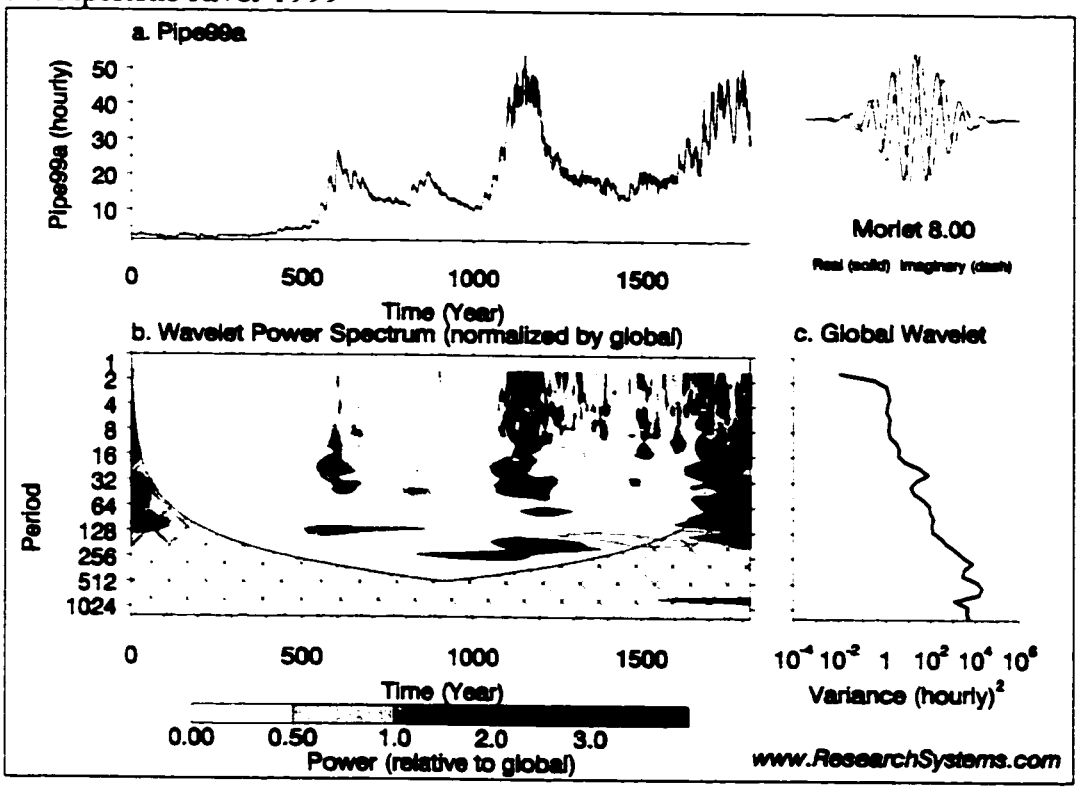

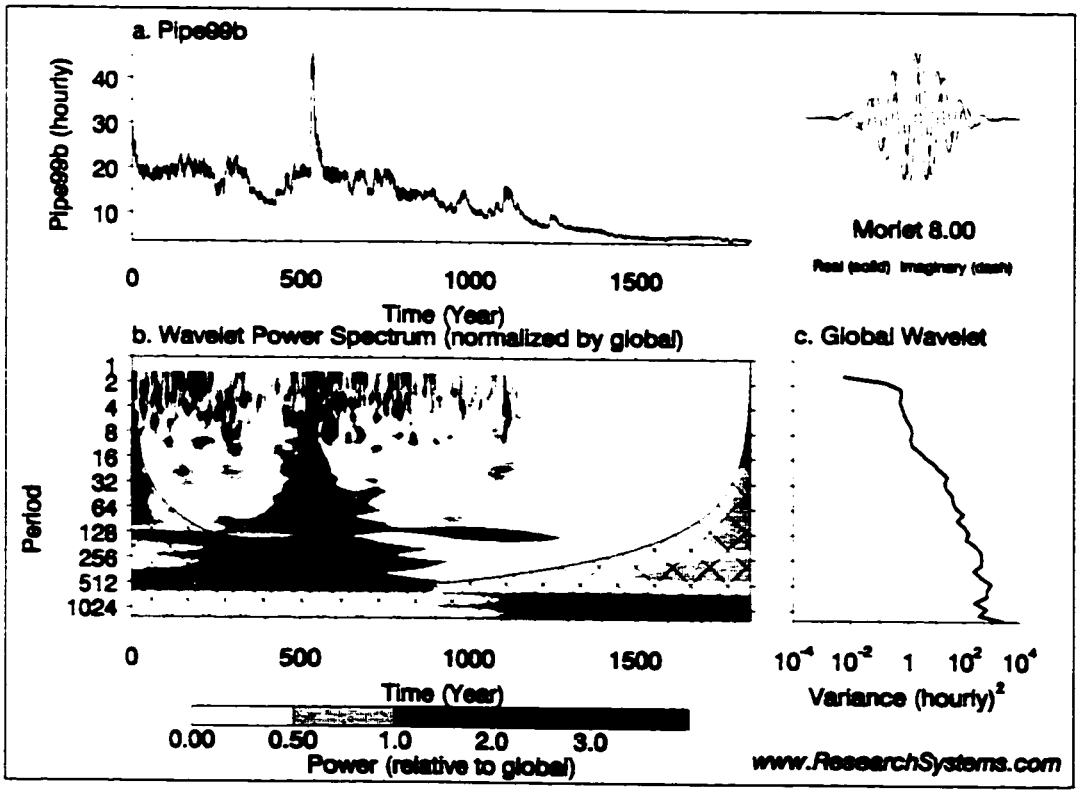

5.7 Bow River at Lake Louise 1997

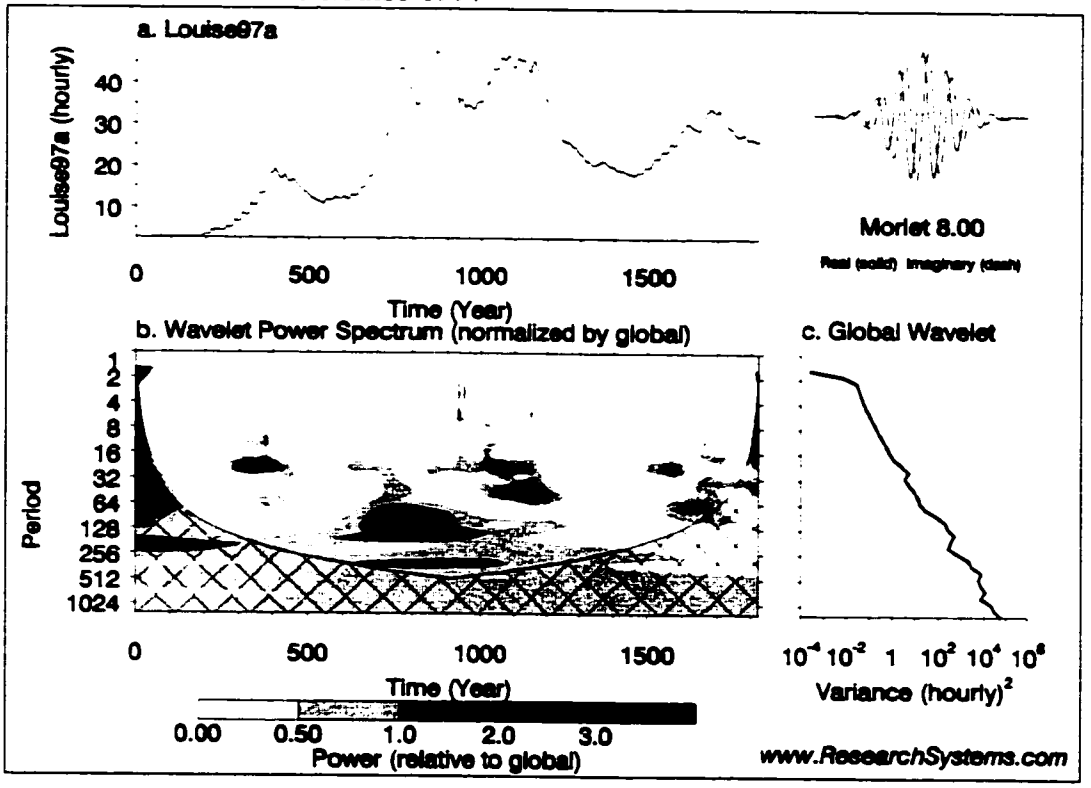

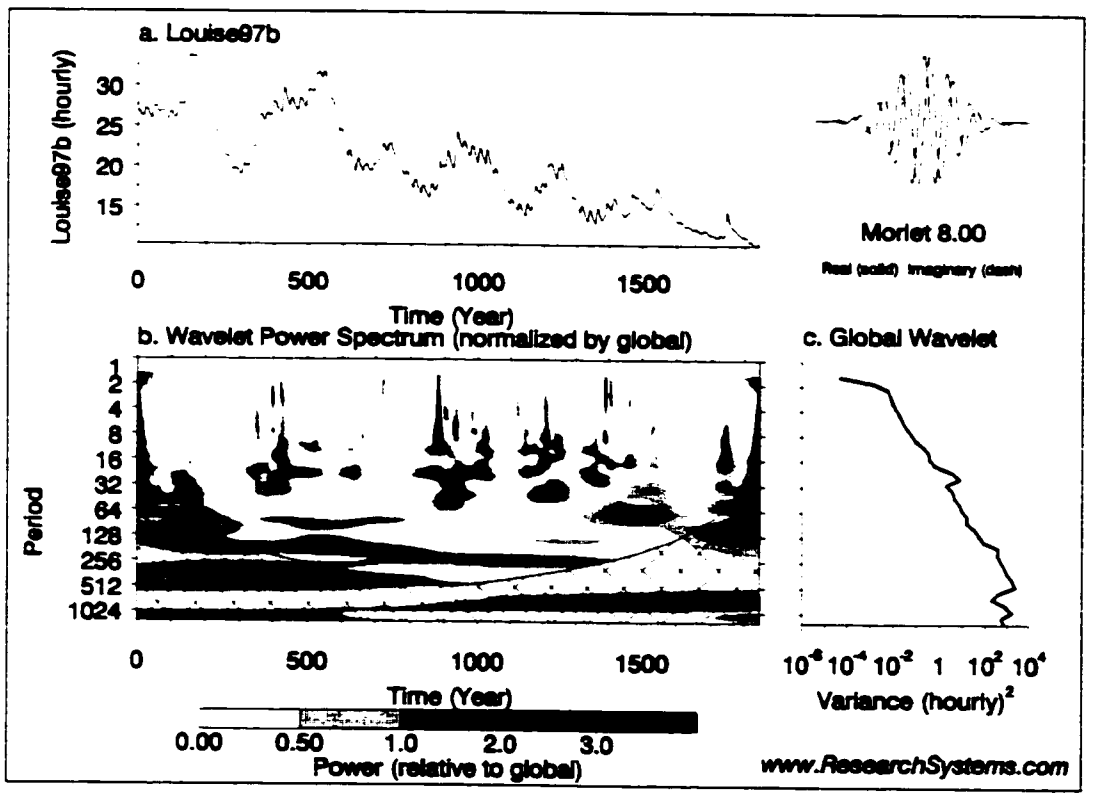

5.8 Bow River at Lake Louise 1998

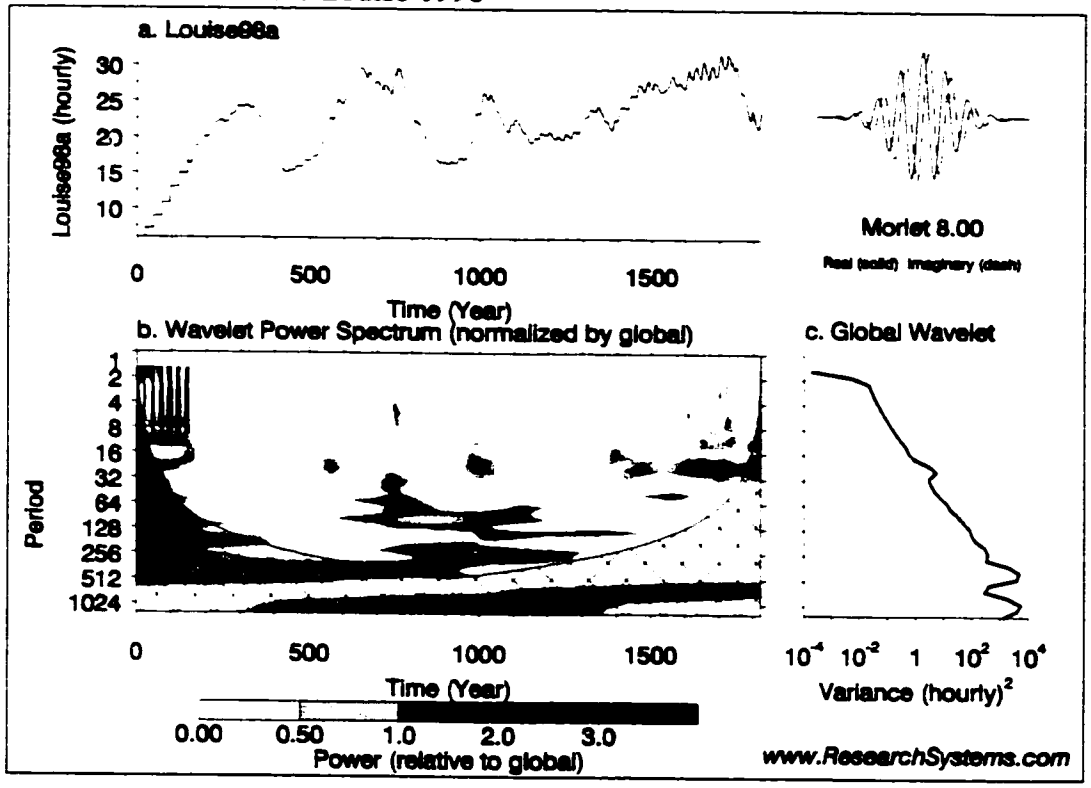

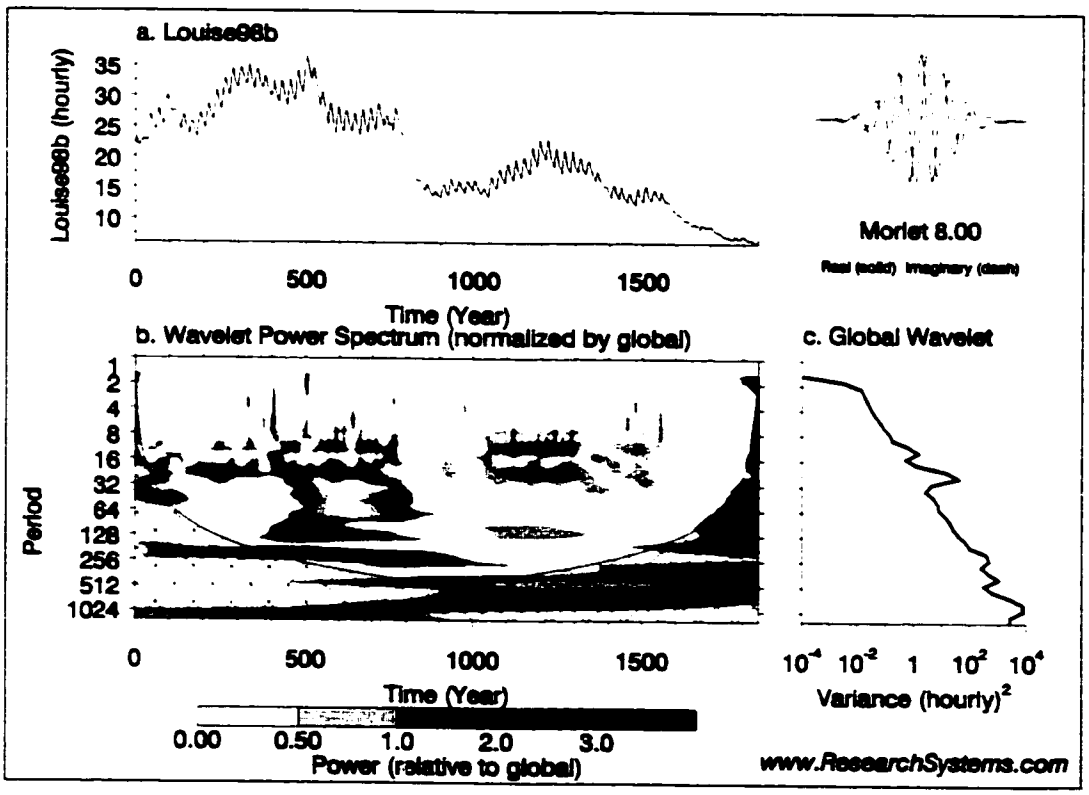

5.9 Bow River at Lake Louise 1999

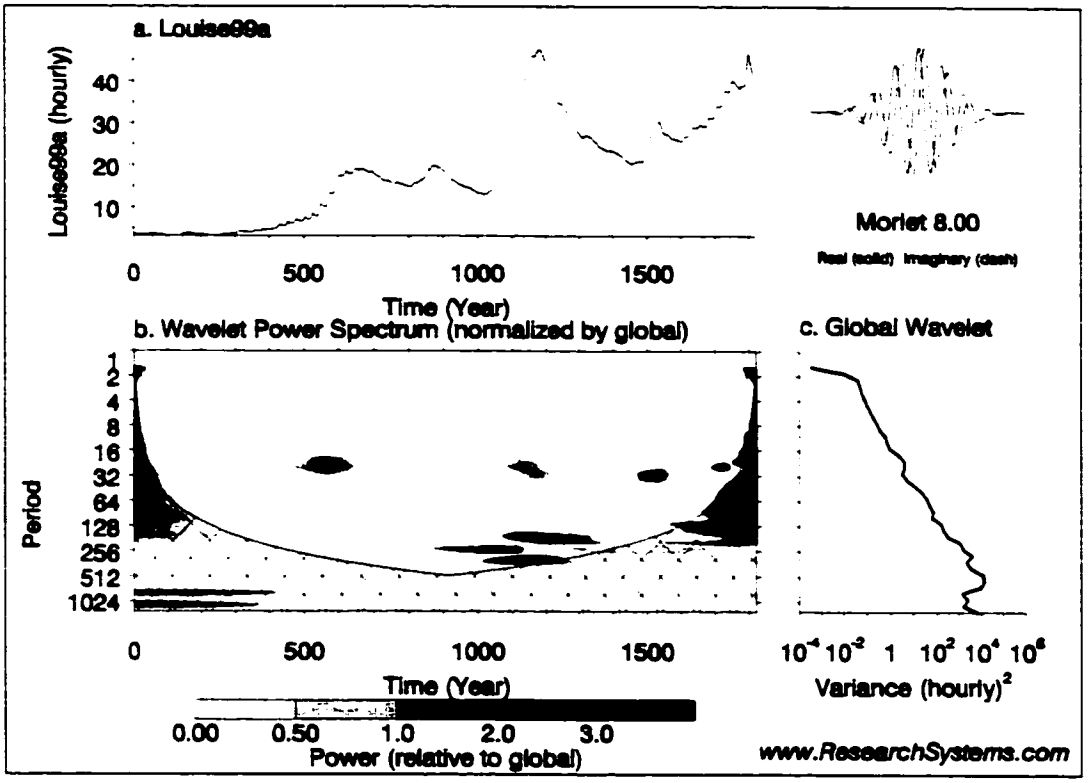

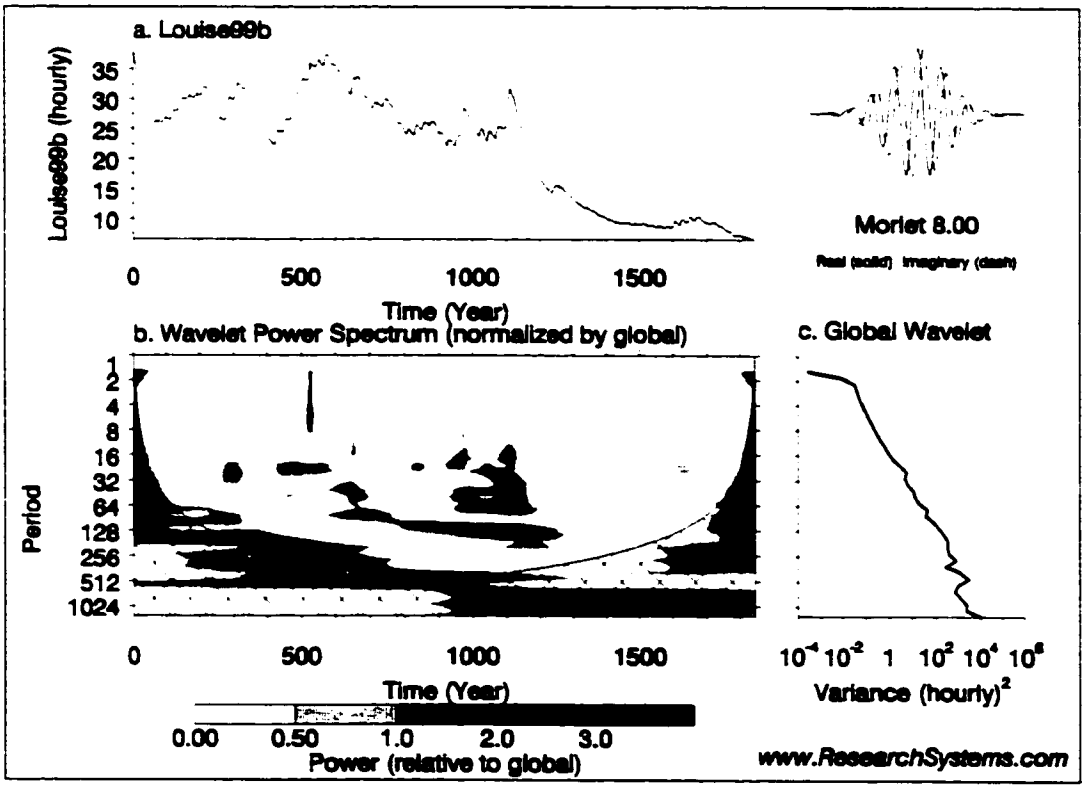

5.10 Bow River at Banff 1996

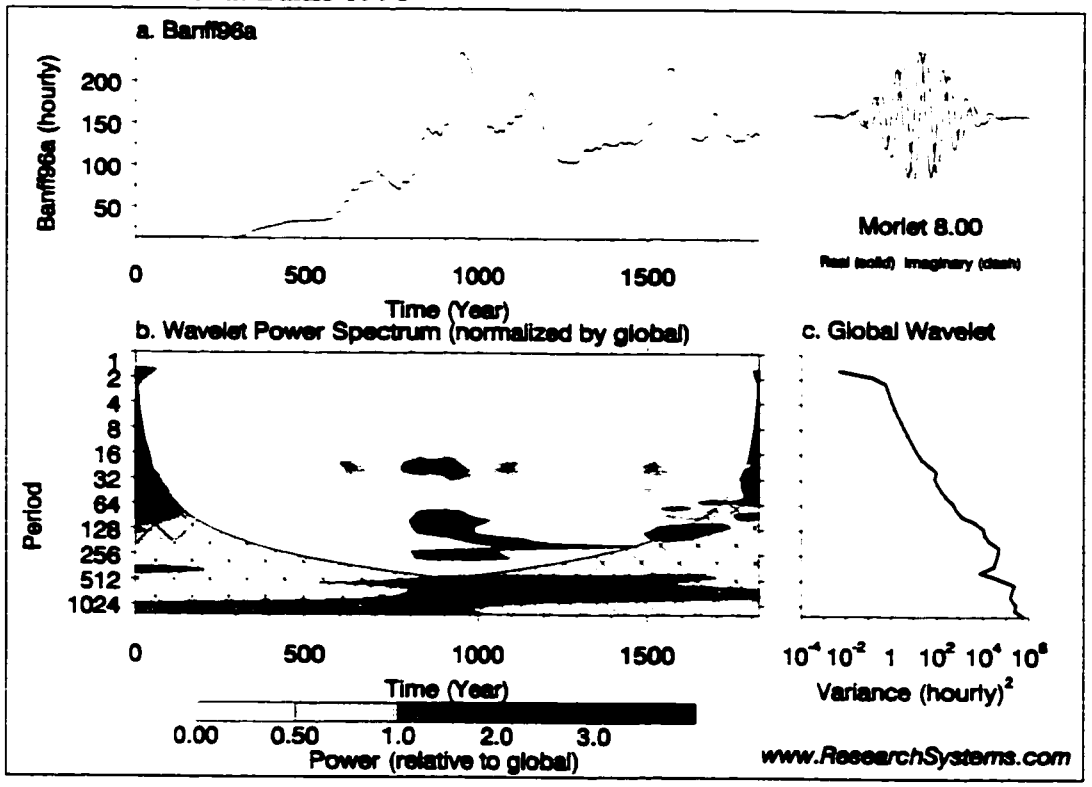

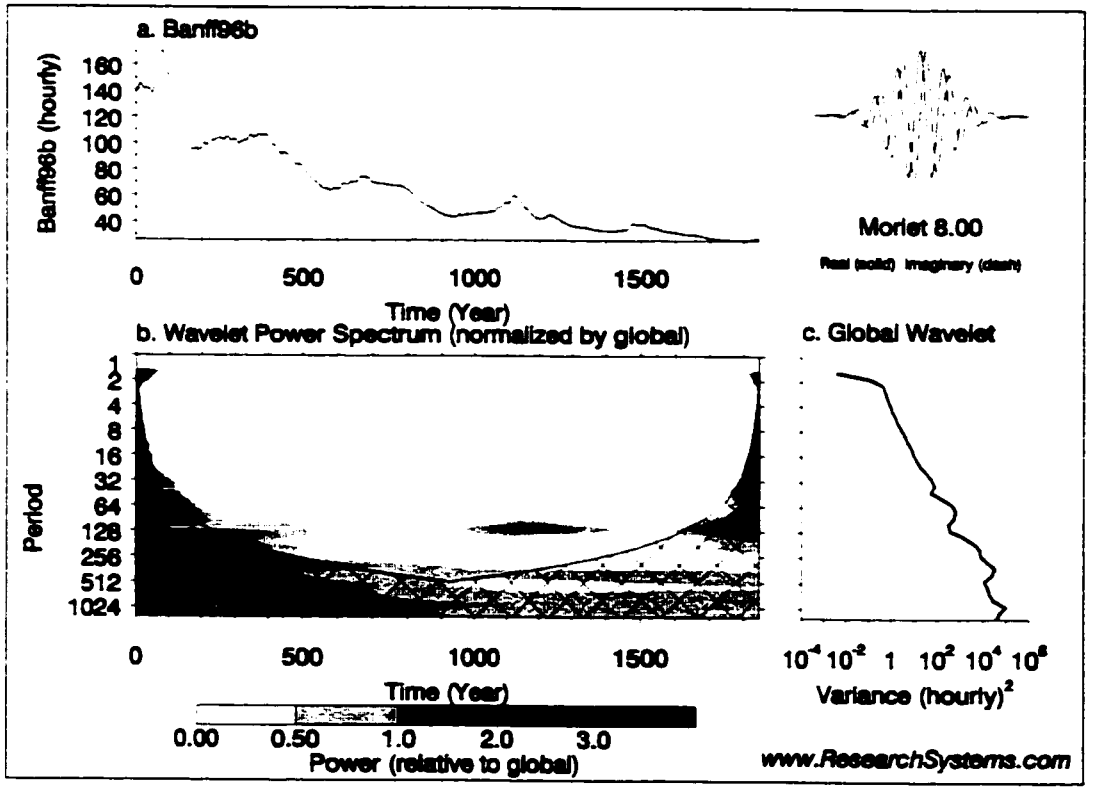

5.11 Bow River at Banff 1997

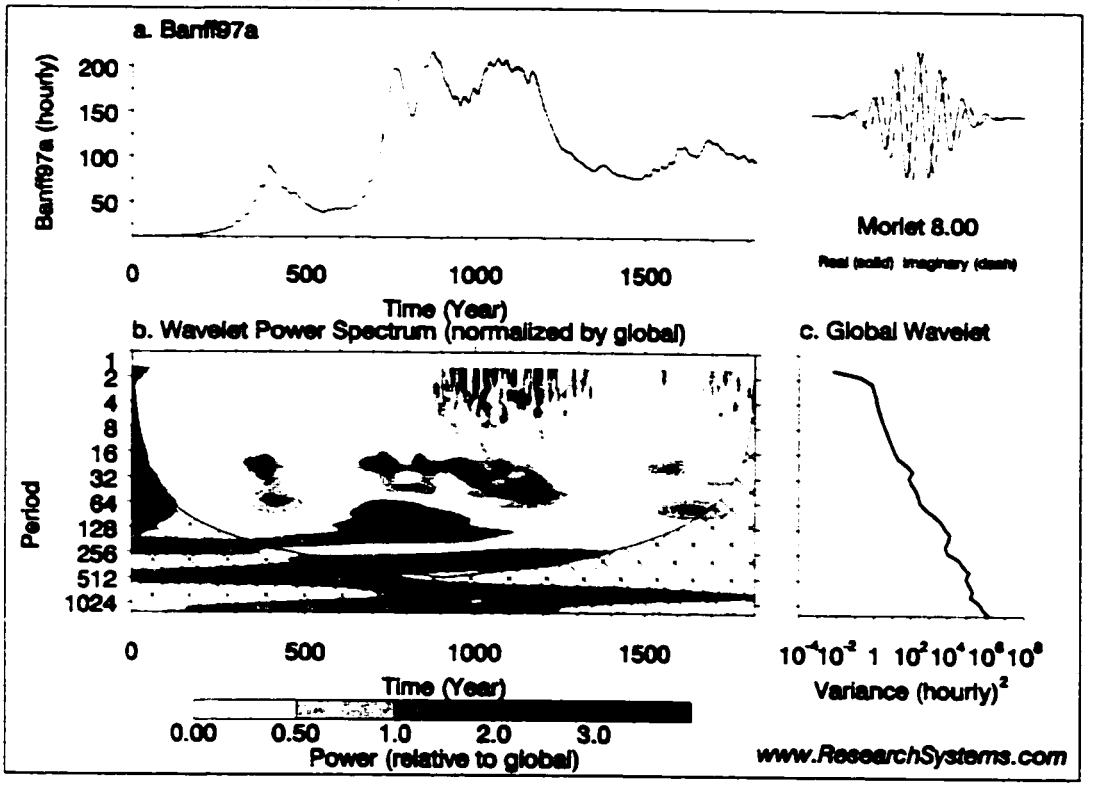

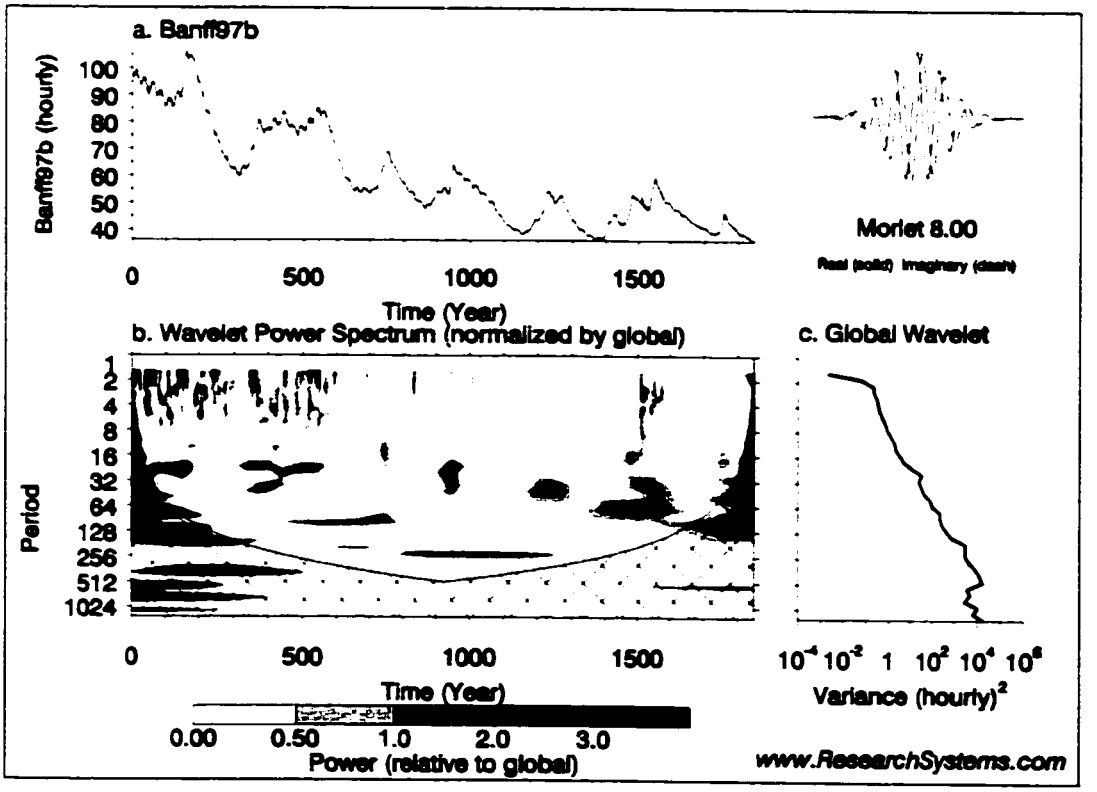

5.12 Bow River at Banff 1998

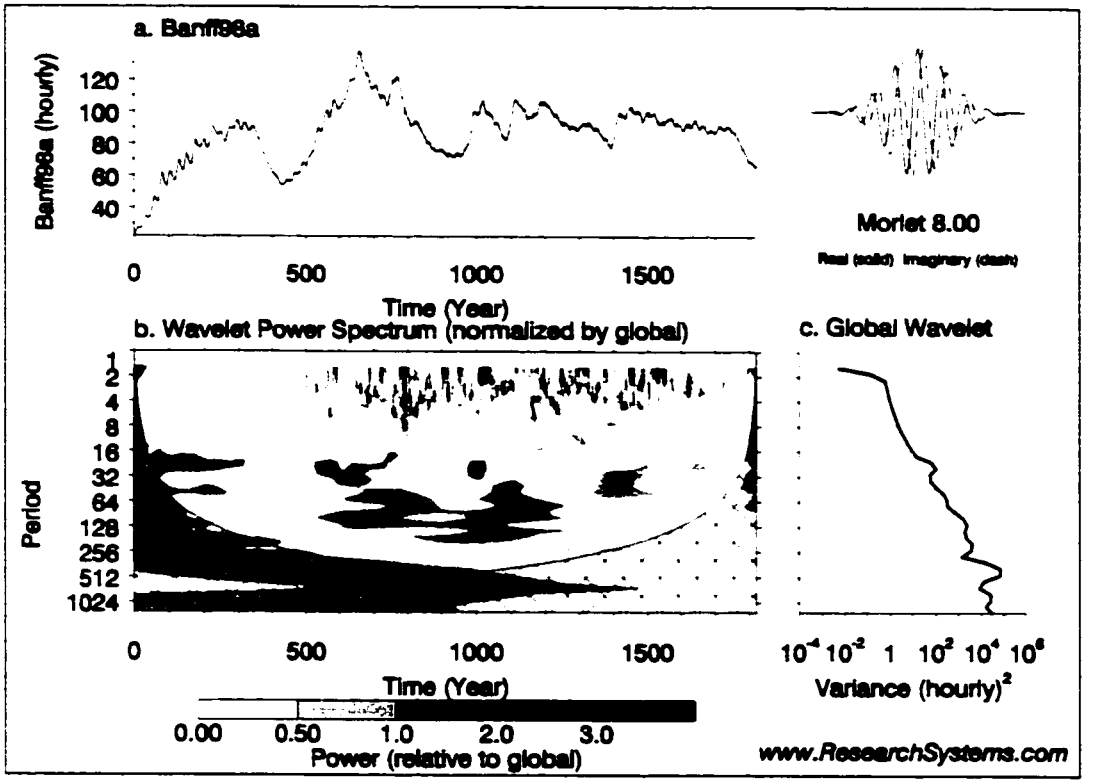

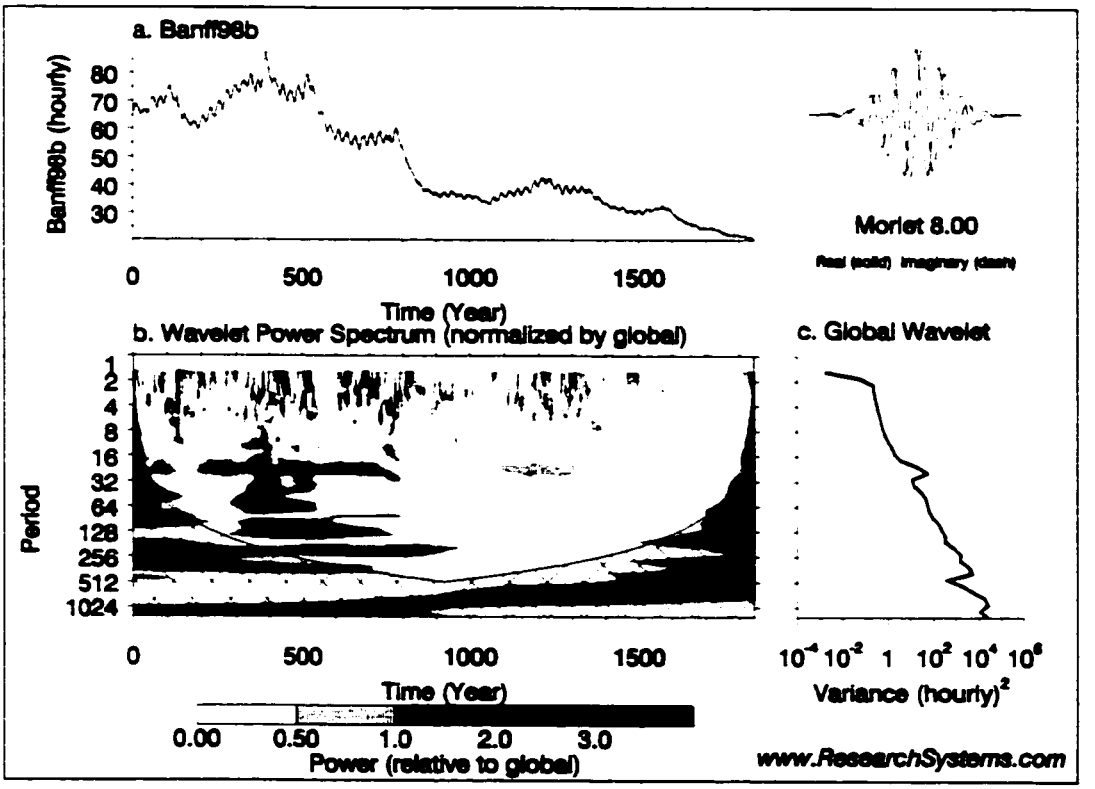

5.13 Bow River at Banff 1999

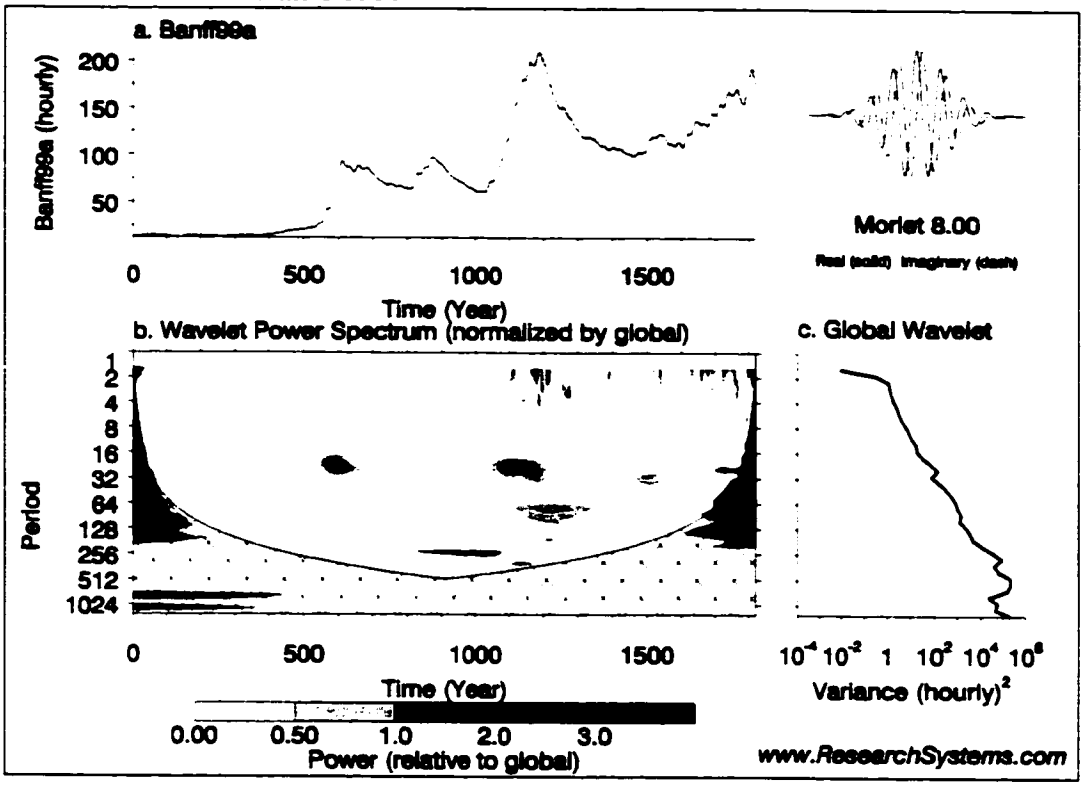

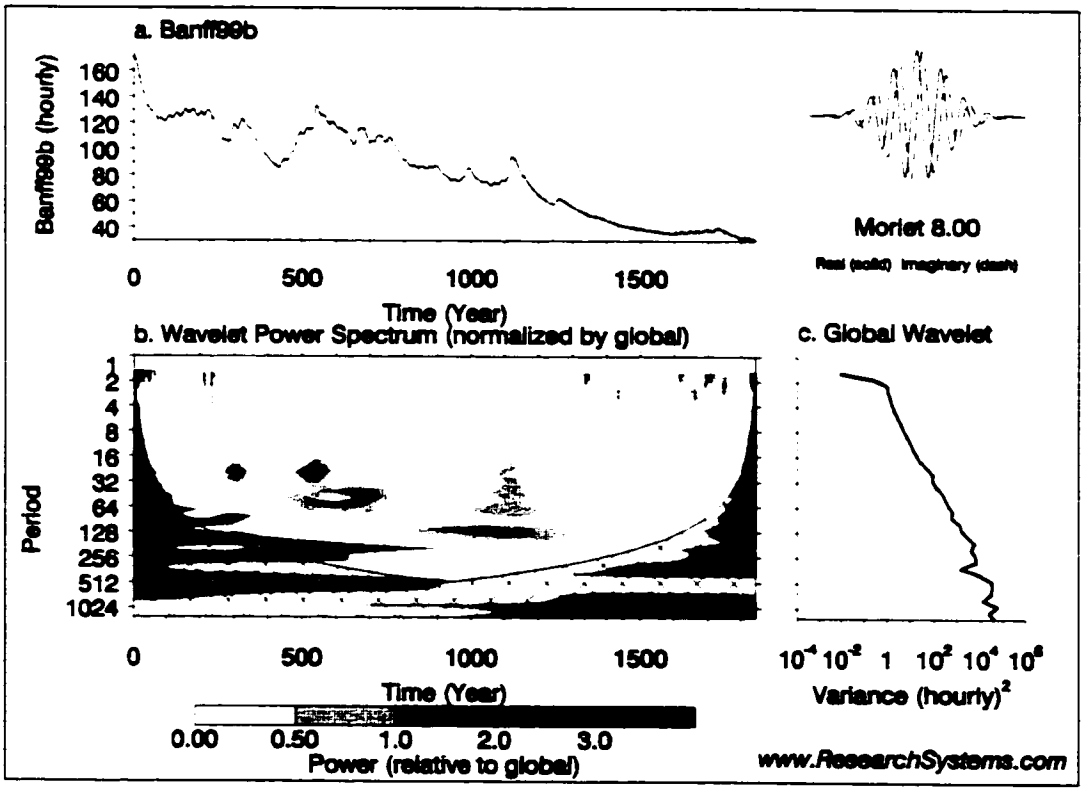

Appendix 6 Parameter Values used in UBC Model Runs

6.1 UBC Watershed Parameter File for Model Run Number 1

All parameter data for first run of UBC model using Castle Mountain and Bow Summit weather station data from for the independently calibrated years of 1996 and 1997 are presented below. Both years had same parameter values throughout apart from three of the groundwater storage coefficients and the weather station snowfall volume adjustment parameter ***(illustrated in bold)***.

```
Bow Valley above Banff 2227 km {identifier},09-25-1998
POLATS  Latitude of watershed (degrees) =. 57
JOTIMA! Start date of run (YYMMDD) =. 951001
JOTIMZ! End date of run (YYMMDD) =. 970930
JORLTA! Start date for detailed BAND output (- for * CAL) =. 0
JORLTZ! End date for detailed BAND output (- for * CAL) =. 0
JOPARR! Generation date of FORECAST.WAT file (YYMMDD) =. 0
TSTEP   Time step in hrs =. 24

                    * METEOROLOGICAL AND FLOW DATA *

NOAESS  Number of AES stations =. 2
AESNAME$ NAMES OF AES FILES USED  =.castle.AES. summit.AES
WSCNAME$ NAME OF WSC FILE USED (TYPE VOID FOR NO DATA)  =.Bow2.WSC
TICAES  Time increment of AES data (daily=24) (hourly=1)  =. 24
TICWSC  Time increment of WSC data (daily=24) (hourly=1)  =. 24
LAPSER  Index for Temp. lapse rate (=1 for algorithm)(=2 AES stations)  =. 1
IGRADP  Index for PP gradient (=1 for algorithm)(=2 for interpolation)  =. 1
TSNCAP  Temperature below which snow capping at upper stat. may occur (C)  =. 2

          ELEVATIONS AND PARAMETERS OF AES STATIONS

**********************************************************************
* Parameter *  ST #1,2 * Description of the parameter          *
**********************************************************************
*  COELPT  . 1500, 2030   . Elevation of the AES stations (m)
*---------------------------------------------------------------------*
*  POSREP  . 0.0    . Adjustment to precipitation when average temperature <0 (snowfall) (-0.08 for 1997)
*---------------------------------------------------------------------*
*  PORREP  . 00     . Adjustment to precipitation when average temperature >A0FORM (rain)
*---------------------------------------------------------------------*
*  A0TERM  . 20 0   . Maximum temperature range
*---------------------------------------------------------------------*
*  A0FOGY  . 6.0    . Temperature range below which the sky is fully covered with clouds
*---------------------------------------------------------------------*
*  A0SUNY  . 18.0   . Temperature range above which the sky is clear of clouds
*---------------------------------------------------------------------*
*  A0EDDF  . 0.35   . Potential evapotranspiration factor in mm/day
**********************************************************************

                    * DESCRIPTION OF THE WATERSHED *

NOBANS (Number of bands) =. 9

**********************************************************************************
*PARAMETER* #1  * #2  * #3  * #4  * #5  * #6  * #7  * #8  * #9  * Description of the parameter
**********************************************************************************
* COELEM . 1371  .1676  . 1905  . 2133  . 2362  . 2590  . 2895 . 3200 . 3505 . Mid-elevation (m) of the band
*---------------------------------------------------------------------------------*
* COALEM . 137.14,433.35. 246.32. 631.85. 389.54. 363.45. 74.57. 6.92 . .51  . Mean area (sq. km.) of the band
*---------------------------------------------------------------------------------*
* COTREE . .9856 ..9579 . .8752 . .581  . .1021 . .0078 . 0.00 . 0   . 0   . Forested fraction of area in the band
*---------------------------------------------------------------------------------*
* COCANY . .800  ..80   . .800  . .700  . .600  . .5   . 0.00 . 0   . 0   . Density of the forest canopy
*---------------------------------------------------------------------------------*
```

```
* C0RIEN . 0.2  .0.2  . 0.5  . 0.5  . .5  . .5  . .7  . .7  . .7  . Orientation index (0=North and 1=South)
*-------------------------------------------------------------------------------*
* C0AGLA . 0.0  .01  . .83  . 7.05  . 11.32 . 38.05 . 14.08. 1.29 . 1  . Glaciated area (sq. km.) in the band
*-------------------------------------------------------------------------------*
* C0AGOR . 0.0  .0.0  . 1  . 1  . 1  . 1  . 1  . 1  . 1  . Fraction of glaciated area with south-orientation
*-------------------------------------------------------------------------------*
* C0IMPA . 2  .2  . 0.2  . 0.25 . .3  . .5  . .5  . 0 535. 0.643. Fraction of impermeable area in the band
*-------------------------------------------------------------------------------*
* I0TSTA . 1  .1  . 1  . 1  . 1  . 1  . 1  . 1  . 1  . AES selection index for temperature
*-------------------------------------------------------------------------------*
* I0PSTA . 1  .1  . 1  . 1  . 1  . 1  . 1  . 1  . 1  . AES selection index for precipitation
*-------------------------------------------------------------------------------*
* P0PADJ . 0 0  .000  . 0000 . 000  . 0.0  . 0.0  . 0.0 . 0  . 0  . Precipitation adjustment factor default=0
*-------------------------------------------------------------------------------*
* I0ESTA . 1  .1  . 1  . 1  . 1  . 1  . 1  . 1  . 1  . AES selection index for evapotranspiration
*********************************************************************************
```

* DISTRIBUTION OF METEOROLOGICAL VARIABLES *

1) Temperature distribution (lapse rates):

A0TLZZ Moist adiabatic temperature lapse rate (C/1000m) =.6.4
A0TLZP Temperature lapse rate (C/1000m) when precipitation > A0PPTP =.6
A0PPTP Threshold precipitation for temperature lapse rate (mm) =.5.0
A0TLXM Lapse rate of Tmax when elev. of aes. < 2000 m =.10
A0TLNM Lapse rate of Tmin when elev. of aes. < 2000 m =.0.5
A0TLXH Lapse rate of Tmax when elev. of aes. > 2000 m =.6.4
A0TLNH Lapse rate of Tmin when elev. of aes. > 2000 m =.2.0
P0TEDL Lapse rate of maximum temperature range (C/1000m) for elevations < 2000 m =.6.0
P0TEDU Lapse rate of maximum temperature range (C/1000m) for elevations > 2000 m =.0

2) Precipitation distribution:

P0GRADL Precipitation gradient factor (%) for elevations below E0LMID =.4.5
P0GRADM Precipitation gradient factor (%) for elevations below E0LHI =.4.5
P0GRADU Precipitation gradient factor (%) for elevations above E0LHI =.10
E0LMID Elevation at which P0GRADM is effective (m) =.2200
E0LHI Elevation above which P0GRADU is effective (m) =.6000
A0STAB Precipitation gradient modification factor =.0.01

3) Interception:

P0PINT Fraction of precipitation intercepted in forest =..25
P0PINX Maximum value of interception in mm/day =.15

4) Form of precipitation:

P0TASR Added to the temperature before determining the form of precipitation =.0.00
A0FORM Temperature above which all precipitation is rain =.2.0

5) Evapotranspiration:

A0PELA Lapse rate (C/1000 m) for the evapotranspiration rate A0EDDF =.0.90
A0PEFO Multiplier for evapotranspiration in forested area =.1
R0SNET If nonzero: snow-covered areas do not contribute any evapotranspiration =.0.0
P0EGEN Determines actual evapotranspiration from potential value =.100.0

* SNOWMELT FUNCTION *

1) Energy method (Activated when R0ERGY is nonzero)

i) Solar incident radiation (shortwave heat input to the snowpack):

F0ERGY Sun exposure factor of forested areas =.0.01
P0CAST Fraction of solar radiation penetrating cloud cover =.0.25

P0BAHT Topographical horizon =.20
P0CLAR Atmospheric turbidity (2 for clear ** 4 to 5 for smog) =.2

ii) Reflectivity (Albedo) of the snowpack:

P0ALBREC Recessional constant for albedo decay of new snow =.0.90
P0ALBSNW Snowfall required to bring albedo to that of new snow (mm) =.15
P0ALBMAX Albedo of fresh snow =..95
P0ALBMIN Albedo of very deep and aged snowpack and of glacier =.0.30
P0ALBMLX Constant of the order of total snowmelt in one year (mm) =.4000
P0ALBASE The albedo initial decay value =.0.65

iii) Wind speed:

F0WIND Ratio of wind in forest to wind in open area =.0.70
P0VBMX Maximum wind speed (kmh) =.8.0

iv) Longwave, advective and condective heat transfer to the snowpack and rain melt:

P0BLUE Longwave multiplier for forested area =..40
P0LWVF Longwave melt multiplier for forested area =.1.900
P0CONV Convection melt multiplier =.0.113
P0COND Condensation melt multiplier =.0.44

3) Other parameters of the snowmelt function:

i) Glacier

R0GLAC Glacier indicator (1=Glacier 0=No glacier) =.1

ii) Cold content of the snowpack:

P0CTKO Cold content decay factor for snowpack in open areas =.1.00
P0CTKF Cold content decay factor for snowpack in forested areas =.1.00
P0CTKG Cold content decay factor for glacial areas =.1.00

iii) Snowpack distribution across the band:

S0PATS Height of snowpack at which patching occurs in open areas (mm) =.200.0
S0FATS Height of snowpack at which patching occurs in forested areas (mm) =.200.0

iv) Rainfall trapped in the snowpack:

A0WEHO Water holding capacity of snow in open areas =.0.05
A0WEHF Water holding capacity of snow in forested areas =.0.05

• WATER DISTRIBUTION •

1) Water budget allocations:

P0AGEN Impermeable area modification factor (function of soil moisture) =.100
V0FLAX Maximum flash factor (mm) =.1600
V0FLAS Flash flood threshold (mm) =.39
P0PERC Groundwater percolation in mm/day =.5
P0DZSH Deep zone share =.0.555

2) Number of routing storages:

N0FASR Number of fast reservoirs for rainfall runoff =.1
N0FASS Number of fast reservoirs for snowmelt runoff =.1
N0GLAC Number of fast reservoirs for glacial runoff =.1

3) Routing (time) constants:

P0FRTK Fast runoff time constant for rain (days) =.2
P0FSTK Fast runoff time constant for snowmelt (days) =.3
P0GLTK Fast runoff time constant for glacial runoff (days) =.2

P0IRTK Interflow time constant for rain (days) =.2
P0ISTK Interflow time constant for snowmelt (days) =.4.8
P0UGTK Time constant for upper groundwater runoff (days) =.80
P0DZTK Time constant for deep groundwater runoff (days) =.130

4) Lags:

LAGS Lag in the snowmelt distribution (0 or 1 time steps) =.0
LAGR Lag in the rainfall distribution (0 or 1 time steps) =.0

* INITIAL CONDITIONS *

PARAMETER	BAND # 1	2	3	4	5	6	7	Description of the parameter
S0SWEF	.0.0	.0.0	.0.0	.0.0	.0.0	.0.0	.0.0	S.W.E. storage in forested area (initial values)
S0CLDF	.0.0	.0.0	.0.0	.0.0	.0.0	.0.0	.0.0	Snowpack cold content storage in forested area (initial values)
S0SWEOS	.0.0	.0.0	.0.0	.0.0	.0.0	.0.0	.0.0	S.W.E. storage in south open area (initial values)
S0SWEON	.0.0	.0.0	.0.0	.0.0	.0.0	.0.0	.0.0	S.W.E. storage in north open area
S0CLDOS	.0.0	.0.0	.0.0	.0.0	.0.0	.0.0	.0.0	Snowpack cold content storage in south open area (initial values)
S0CLDON	.0.0	.0.0	.0.0	.0.0	.0.0	.0.0	.0.0	Snowpack cold content storage in north open area (initial values)
S0CLDGL	.0.0	.0.0	.0.0	.0.0	.0.0	.0.0	.0.0	Glacial cold content storage
S0SOIL	.0.0	.0.0	.0.0	.0.0	.0.0	.0.0	.0.0	Soil moisture storage deficit (initial values)
S0WEDF	.0.0	.0.0	.0.0	.0.0	.0.0	.0.0	.0.0	Snowpack holding storage deficit in forested area (initial values)
S0WEDOS	.0.0	.0.0	.0.0	.0.0	.0.0	.0.0	.0.0	Snowpack holding storage deficit in south open area (initial values)
S0WEDON	.0.0	.0.0	.0.0	.0.0	.0.0	.0.0	.0.0	Snowpack holding storage deficit in north open area (initial values)
ALBFOR	.0.5	.0.5	.0.5	.0.5	.0.5	.0.5	.0.5	Albedo in forest (initial values)
S0MEFS	.0.0	.0.0	.0.0	.0.0	.0.0	.0.0	.0.0	Cumulative snowmelt in forested areas (initial values)
ALBOPNS	.0.5	.0.50	.0.5	.0.5	.0.5	.0.5	.0.5	Albedo in south open areas (initial values)
ALBOPNN	.0.5	.0.50	.0.5	.0.5	.0.5	.0.5	.0.5	Albedo in north open areas (initial values)
S0MEOSS	.0.0	.0.0	.0.0	.0.0	.0.0	.0.0	.0.0	Cumulative snowmelt in south open areas (initial values)
S0MEOSN	.0.0	.0.0	.0.0	.0.0	.0.0	.0.0	.0.0	Cumulative snowmelt in north open areas (initial values)

2) Initial values of outflows from routing storages:

O0GLRO Glacial outflows for fast flow reservoir(s) (N0GLAC) (cms) =. 00
O0INRN Rainfall outflow for interflow (cms) =. 000
O0INSN Snowmelt outflow for interflow (cms) =. 000
O0FARN Rainfall outflows for fast flow reservoir(s) (N0FASR) (cms) =. 000
O0FASN Snowmelt outflows for fast flow reservoir(s) (N0FASS) (cms) =. 000
O0GWUZ Upper groundwater (cms) =. 11
O0GWDZ Lower groundwater (cms) =. 20

* MONTHLY PARAMETERS *

JAN	FEB	MAR	APR	MAY	JUN	JUL	AUG	SEP	OCT	NOV	DEC	DESCRIPITION OF THE PARAMETER

```
* V0SOTH ,1.00 ,1.00 ,1.00 ,1.00 ,1.00 ,1.00 ,1.00 ,1.00 ,1.00 ,1.00 ,1.00 ,1.00 ,Adjust. factor to solar radiation on S-facing bands (day 21)
*-----------------------------------------------------------------------------------------------------------*
* V0NOTH ,0.40 ,0.40 ,0.40 ,0.70 ,0.90 ,1.0  ,0.90 ,0.70 ,0.40 ,0.40 ,0.4  ,0.40 ,Adjust. factor to solar radiation on N-facing bands (day 21)
*-----------------------------------------------------------------------------------------------------------*
* V0EMOF ,1.00 ,1.00 ,1.00 ,1.00 ,1.23 ,1.29 ,1.16 ,1.09 ,1.00 ,1.00 ,1.00 ,1.00 ,Adjustment factor for the evapotranspiration rate A0EDDF
*-----------------------------------------------------------------------------------------------------------*
* V0EMF1 ,0.00 ,0.00 ,0.00 ,0.00 ,0.00 ,0.00 ,0.00 ,0.00 ,0.00 ,0.00 ,0.00 ,0.00 ,Adjustment factor for snowfall
*-----------------------------------------------------------------------------------------------------------*
* V0EMF2 ,0.00 ,0.00 ,0.00 ,0.00 ,0.00 ,0.00 ,0.00 ,0.00 ,0.00 ,0.00 ,0.00 ,0.00 ,Adjustment factor for rainfall
*************************************************************************************************************
```

6.2 UBC Watershed Parameter File for Model Run Numbers 2 and 3

All parameter data for 2nd and 3rd runs of UBC model using Castle Mountain and Bow Summit weather station data for the continuous time series from 1996 to 1999 are presented below. Main parameter values are those used during the initial statistically optimised calibration. The parameter values used following geochemical optimisation are ***illustrated in bold italics***.

```
*************************************************
*  UBC WATERSHED MODEL - PARAMETER FILE    *
*************************************************


Bow Banff 2207 km2 .05-28-2000
POLATS  Latitude of watershed (degrees) =. 57
J0TIMA!  Start date of run (YYMMDD) =. 951001
J0TIMZ!  End date of run (YYMMDD) =. 990730
J0RLTA!  Start date for detailed BAND output (- for *.CAL) =. 0
J0RLTZ!  End date for detailed BAND output (- for *.CAL) =. 0
J0PARR!  Generation date of FORECAST.WAT file (YYMMDD) =. 0
TSTEP   Time step in hrs =. 24

                        ---------------------------
                        * METEOROLOGICAL AND FLOW DATA *
                        ---------------------------

N0AESS  Number of AES stations  =. 2
AESNAME$  NAMES OF AES FILES USED  =.bowsum2.AES
WSCNAME$  NAME OF WSC FILE USED (TYPE VOID FOR NO DATA)  =.bf6999.WSC
TICAES  Time increment of AES data (daily=24) (hourly=1)  =. 24
TICWSC  Time increment of WSC data (daily=24) (hourly=1)  =. 24
LAPSER  Index for Temp. lapse rate (=1 for algorithm)(=2 AES stations)  =. 1
IGRADP  Index for PP. gradient (=1 for algorithm)(=2 for interpolation)  =. 1
TSNCAP  Temperature below which snow capping at upper stat. may occur (C)  =. 2

            ELEVATIONS AND PARAMETERS OF AES STATIONS
            -----------------------------------------

*************************************************************************************************
* Parameter *  ST. #1 *  ST. #2 *  Description of the parameter                          *
*************************************************************************************************
*  C0ELPT  .  1500   .  2030   .  Elevation of the AES station (m)
*-----------------------------------------------------------------------------------------------*
*  P0SREP  .  0      .  0      .  Adjustment to precipitation when average temperature <0 (snowfall)
*-----------------------------------------------------------------------------------------------*
*  P0RREP  .  0      .  0      .  Adjustment to precipitation when average temperature >A0FORM (rain)
*-----------------------------------------------------------------------------------------------*
*  A0TERM  .  12.0   .         .  Maximum temperature range
*-----------------------------------------------------------------------------------------------*
*  A0FOGY  .  3.0    .         .  Temperature range below which the sky is fully covered with clouds
*-----------------------------------------------------------------------------------------------*
*  A0SUNY  .  12.0   .         .  Temperature range above which the sky is clear of clouds
*-----------------------------------------------------------------------------------------------*
*  A0EDDF  .  0.20   .         .  Potential evapotranspiration factor in mm/day
*************************************************************************************************
```

• DESCRIPTION OF THE WATERSHED •

N0BANS (Number of bands) =. 11

PARAMETER #1	#2	#3	#4	#5	#6	#7	#8	#9	Description of the parameter
C0ELEM	.1371	.1676	.1905	.2133	.2362	.2590	.2895	.3200	.3505 . Mid-elevation (m) of the band
C0ALEM	137	14.433	35.	246.32.	631.85.	389.54.	363.45.	74.57.	6.92 . .51 . Mean area (sq. km.) of the band
C0TREE	.9856	.9579	.8752	.581	.1021	.0078	0.00	.0	.0 . Forested fraction of area in the band
C0CANY	.800	.80	.800	.700	.600	.5	0.00	.0	.0 . Density of the forest canopy
C0RIEN	.0.2	.0.2	.0.5	.0.5	.5	.5	.7	.7	.7 . Orientation index (0=North and 1=South)
C0AGLA	.0 0	.01	.83	.7 05	.11.32	.38.05	.14.08.	1.29	.1 . Glaciated area (sq. km.) in the band
C0AGOR	.0 0	.0 0	.1	.1	.1	.1	.1	.1	.1 . Fraction of glaciated area with south-orientation
C0IMPA	.2	.2	.0.2	.0.25	.3	.5	.5	.0.535.	0.643. Fraction of impermeable area in the band
I0TSTA	.1	.1	.1	.1	.1	.1	.1	.1	.1 . AES selection index for temperature
I0PSTA	.1	.1	.1	.1	.1	.1	.1	.1	.1 . AES selection index for precipitation
P0PADJ	.0 0	.000	.0000	.000	.0 0	.0.0	.0 0	.0	.0 . Precipitation adjustment factor default=0
I0ESTA	.1	.1	.1	.1	.1	.1	.1	.1	.1 . AES selection index for evapotranspiration

• DISTRIBUTION OF METEOROLOGICAL VARIABLES •

1) Temperature distribution (lapse rates):

A0TLZZ Moist adiabatic temperature lapse rate (C/1000m) =.6
A0TLZP Temperature lapse rate (C/1000m) when precipitaion > A0PPTP =.6
A0PPTP Threshold precipitation for temperature lapse rate (mm) =.5.0
A0TLXM Lapse rate of Tmax when elev. of aes. < 2000 m =.6
A0TLNM Lapse rate of Tmin when elev. of aes. < 2000 m =.0.5
A0TLXH Lapse rate of Tmax when elev. of aes. > 2000 m =.6
A0TLNH Lapse rate of Tmin when elev. of aes. > 2000 m =.2.0
P0TEDL Lapse rate of maximum temperature range (C/1000m) for elevations < 2000 m =.6.0
P0TEDU Lapse rate of maximum temperature range (C/1000m) for elevations > 2000 m =.0.0

2) Precipitation distribution:

P0GRADL Precipitation gradient factor (%) for elevations below E0LMID =.4.5
P0GRADM Precipitation gradient factor (%) for elevations below E0LHI =.4.5
P0GRADU Precipitation gradient factor (%) for elevations above E0LHI =.10
E0LMID Elevation at which P0GRADM is effective (m) =.2300
E0LHI Elevation above which P0GRADU is effective (m) =.6000
A0STAB Precipitation gradient modification factor =.0.01 ***(0)***

3) Interception:

P0PINT Fraction of precipitation intercepted in forest =.0.12 ***(0.17)***
P0PINX Maximum value of interception in mm/day =.10

4) Form of precipitation:

P0TASR Added to the temperature before determining the form of precipitation =.0.00
A0FORM Temperature above which all precipitation is rain =.2.0

5) Evapotranspiration:

A0PELA Lapse rate (C/1000 m) for the evapotranspiration rate A0EDDF =.0.90
A0PEFO Multiplier for evapotranspiration in forested area =.1.00
R0SNET If nonzero: snow-covered areas do not contribute any evapotranspiration =.0.0
P0EGEN Determines actual evapotranspiration from potential value =.100.0

* SNOWMELT FUNCTION *

1) Energy method (Activated when R0ERGY is nonzero)

i) Solar incident radiation (shortwave heat input to the snowpack):

F0ERGY Sun exposure factor of forested areas =.0.1 ***(0.15)***
P0CAST Fraction of solar radiation penetrating cloud cover =.0.25
P0BAHT Topographical horizon =.20
P0CLAR Atmospheric turbidity (2 for clear ** 4 to 5 for smog) =.2

ii) Reflectivity (Albedo) of the snowpack:

P0ALBREC Recessional constant for albedo decay of new snow =.0.90 ***(0.1)***
P0ALBSNW Snowfall required to bring albedo to that of new snow (mm) =.15 ***(2)***
P0ALBMAX Albedo of fresh snow =.0.95
P0ALBMIN Albedo of very deep and aged snowpack and of glacier =.0.3
P0ALBMLX Constant of the order of total snowmelt in one year (mm) =.3500
P0ALBASE The albedo initial decay value =.0.65 ***(0.75)***

iii) Wind speed

F0WIND Ratio of wind in forest to wind in open area =.0.70
P0VBMX Maximum wind speed (kmh) =.8.0

iv) Longwave, advective and condective heat transfer to the snowpack and rain melt:

P0BLUE Longwave multiplier for forested area =.0.4
P0LWVF Longwave melt multiplier for forested area =.1.900
P0CONV Convection melt multiplier =.0.18
P0COND Condensation melt multiplier =.0.35

3) Other parameters of the snowmelt function:

i) Glacier

R0GLAC Glacier indicator (1=Glacier 0=No glacier) =.1

ii) Cold content of the snowpack:

P0CTKO Cold content decay factor for snowpack in open areas =.10.0
P0CTKF Cold content decay factor for snowpack in forested areas =.10.0
P0CTKG Cold content decay factor for glacial areas =.10.0

iii) Snowpack distribution across the band:

S0PATS Height of snowpack at which patching occurs in open areas (mm) =.200.0
S0FATS Height of snowpack at which patching occurs in forested areas (mm) =.200.0

iv) Rainfall trapped in the snowpack:

A0WEHO Water holding capacity of snow in open areas =.0.05 ***(0.1)***
A0WEHF Water holding capacity of snow in forested areas =.0.05 ***(0.1)***

* WATER DISTRIBUTION *

1) Water budget allocations:

P0AGEN Impermeable area modification factor (function of soil moisture) =.100.0
V0FLAX Maximum flash factor (mm) =.1600
V0FLAS Flash flood threshold (mm) =.39
P0PERC Groundwater percolation in mm/day =.20
P0DZSH Deep zone share =.0.7

2) Number of routing storages:

N0FASR Number of fast reservoirs for rainfall runoff =.2
N0FASS Number of fast reservoirs for snowmelt runoff =.2
N0GLAC Number of fast reservoirs for glacial runoff =.2

3) Routing (time) constants:

P0FRTK Fast runoff time constant for rain (days) =.2.0
P0FSTK Fast runoff time constant for snowmelt (days) =.2.0
P0GLTK Fast runoff time constant for glacial runoff (days) =.2.0
P0IRTK Interflow time constant for rain (days) =.3.8
P0ISTK Interflow time constant for snowmelt (days) =.4.8
P0UGTK Time constant for upper groundwater runoff (days) =.30
P0DZTK Time constant for deep groundwater runoff (days) =.140

4) Lags:

LAGS Lag in the snowmelt distribution (0 or 1 time steps) =.0
LAGR Lag in the rainfall distribution (0 or 1 time steps) =.0

* INITIAL CONDITIONS *

	BAND #										
* PARAMETER *	#1	#2	#3	#4	#5	#6	#7	#8	#9	#10	#11	* Description of the parameter
S0SWEF	.0.0	.0.0	.0.0	.0.0	.0.0	.0.0	.0.0	.0.0	.0.0	.0.0	.0.0	S.W.E. storage in forested area (initial values)
S0CLDF	.0.0	.0.0	.0.0	.0.0	.0.0	.0.0	.0.0	.0.0	.0.0	.0.0	.0.0	Snowpack cold content storage in forested area (initial values)
S0SWEOS	.0.0	.0.0	.0.0	.0.0	.0.0	.0.0	.0.0	.0.0	.0.0	.0.0	.0.0	S.W.E. storage in south open area (initial values)
S0SWEON	.0.0	.0.0	.0.0	.0.0	.0.0	.0.0	.0.0	.0.0	.0.0	.0.0	.0.0	S.W.E. storage in north open area (initial values)
S0CLDOS	.0.0	.0.0	.0.0	.0.0	.0.0	.0.0	.0.0	.0.0	.0.0	.0.0	.0.0	Snowpack cold content storage in south open area (initial values)
S0CLDON	.0.0	.0.0	.0.0	.0.0	.0.0	.0.0	.0.0	.0.0	.0.0	.0.0	.0.0	Snowpack cold content storage in north open area (initial values)
S0CLDGL	.0.0	.0.0	.0.0	.0.0	.0.0	.0.0	.0.0	.0.0	.0.0	.0.0	.0.0	Glacial cold content storage
S0SOIL	.3.2	.3.0	.2.9	.2.7	.2.6	.2.4	.2.1	.1.1	.0.5			Soil moisture storage deficit (initial values)
S0WEDF	.0.0	.0.0	.0.0	.0.0	.0.0	.0.0	.0.0	.0.0	.0.0	.0.0	.0.0	Snowpack holding storage deficit in forested area (initial values)
S0WEDOS	.0.0	.0.0	.0.0	.0.0	.0.0	.0.0	.0.0	.0.0	.0.0	.0.0	.0.0	Snowpack holding storage deficit in south open area (initial values)
S0WEDON	.0.0	.0.0	.0.0	.0.0	.0.0	.0.0	.0.0	.0.0	.0.0	.0.0	.0.0	Snowpack holding storage deficit in north open area (initial values)
ALBFOR	.0.5	.0.5	.0.5	.0.5	.0.5	.0.5	.0.5	.0.0	.0.0			Albedo in forest (initial values)
S0MEFS	.0.0	.0.0	.0.0	.0.0	.0.0	.0.0	.0.0	.0.0	.0.0	.0.0	.0.0	Cumulative snowmelt in forested areas (initial values)
ALBOPNS	.0.50	.0.50	.0.50	.0.50	.0.50	.0.50	.0.50	.0.00	.0.00			Albedo in south open areas (initial values)
ALBOPNN	.0.50	.0.50	.0.50	.0.50	.0.50	.0.50	.0.50	.0.00	.0.00			Albedo in north open areas (initial values)
S0MEOSS	.0.0	.0.0	.0.0	.0.0	.0.0	.0.0	.0.0	.0.0	.0.0	.0.0	.0.0	Cumulative snowmelt in south open areas (initial values)
S0MEOSN	.0.0	.0.0	.0.0	.0.0	.0.0	.0.0	.0.0	.0.0	.0.0	.0.0	.0.0	Cumulative snowmelt in north open areas (initial values)

2) Initial values of outflows from routing storages:

O0GLRO Glacial outflows for fast flow reservoir(s) (N0GLAC) (cms) =, 0.7 , 0.2
O0INRN Rainfall outflow for interflow (cms) =, 0.0
O0INSN Snowmelt outflow for interflow (cms) =, 0.0
O0FARN Rainfall outflows for fast flow reservoir(s) (N0FASR) (cms) =, 0.0 , 0.0
O0FASN Snowmelt outflows for fast flow reservoir(s) (N0FASS) (cms) =, 0.0 , 0.0
O0GWUZ Upper groundwater (cms) =, 0.00
O0GWDZ Lower groundwater (cms) =, 0.30

MONTHLY PARAMETERS

JAN	FEB	MAR	APR	MAY	JUN	JUL	AUG	SEP	OCT	NOV	DEC	DESCRIPITION OF THE PARAMETER
V0SOTH	.1.00	.1.0	.1.0	.1.0	.1.0	.1.0	.1.0	.1.0	.1.0	.1.0	.1.0	.1.0	.Adjust. factor to solar radiation on South-facing bands (day 21)
V0NOTH	.0.4	.0.4	.0.4	.0.7	.0.9	.1.	.0.9	.0.7	.0.4	.0.4	.0.4	.0.4	.Adjust. factor to solar radiation on North-facing bands (day 21)
V0EMOF	.1.0	.1.0	.1.0	.1.0	.1.2	.1.29	.1.16	.1.09	.1.0	.1.0	.1.0	.1.0	.Adjustment factor for the evapotranspiration rate A0EDDF
V0EMF1	.0.0	.0.0	.0.0	.0.0	.0.0	.0.0	.0.0	.0.0	.0.0	.0.0	.0.0	.0.0	.Adjustment factor for snowfall
V0EMF2	.0.0	.0.0	.0.0	.0.0	.0.0	.0.0	.0.0	.0.0	.0.0	.0.0	.0.0	.0.0	.Adjustment factor for rainfall